

TWO-PHOTON INDUCED PHOTOCHEMISTRY

by

Jing Wang

Copyright © Jing Wang 2007

A Dissertation Submitted to the Faculty of the

DEPARTMENT OF CHEMISTRY

In Partial Fulfillment of the Requirements
For the Degree of

DOCTOR OF PHILOSOPHY

In the Graduate College

THE UNIVERSITY OF ARIZONA

2007

THE UNIVERSITY OF ARIZONA
GRADUATE COLLEGE

As members of the Dissertation Committee, we certify that we have read the dissertation prepared by Jing Wang entitled Two-photon Induced Photochemistry and recommend that it be accepted as fulfilling the dissertation requirement for the Degree of Doctor of Philosophy.

Date: 9/28/07
Dr. Seth R. Marder

Date: 9/28/07
Dr. Dominic V. McGrath

Date: 9/28/07
Dr. Neal R. Armstrong

Date: 9/28/07
Dr. Victor J. Hruby

Date: 9/28/07
Dr. S. Scott Saavedra

Final approval and acceptance of this dissertation is contingent upon the candidate's submission of the final copies of the dissertation to the Graduate College.

I hereby certify that I have read this dissertation prepared under my direction and recommend that it be accepted as fulfilling the dissertation requirement.

Date: 9/28/07
Dissertation Director: Dr. Seth R. Marder

Date: 9/28/07
Dissertation Director: Dr. Dominic V. McGrath

STATEMENT BY AUTHOR

This dissertation has been submitted in partial fulfillment of requirements for an advanced degree at the University of Arizona and is deposited in the University Library to be made available to borrowers under rules of the Library.

Brief quotations from this dissertation are allowable without special permission, provided that accurate acknowledgment of source is made. Requests for permission for extended quotation from or reproduction of this manuscript in whole or in part may be granted by the copyright holder.

SIGNED: Jing Wang

ACKNOWLEDGEMENTS

It is a long journey to be here to write this page. I studied for two and half years at Dr. Seth R. Marder group at the University of Arizona. After Dr. Marder moved to the Georgia Institute of Technology, I conducted Dr. Marder's research in Dr. Dominic V. McGrath's group for another two and half years at the University of Arizona for family reasons. At last, I rejoined Dr. Marder's group for the last one and half years at the Georgia Institute of Technology to finish up. For me, it is not only a scientific training process, but also a pathway of self-discovery and personal improvement. I would like to thank the following people, who have made my thesis possible and enriched my life.

- *Dr. Seth R. Marder*, my thesis advisor: for his determination and insights about science that impacted me deeply; for his enthusiasm and dedication to education that mardered me in both science and other professional skills; for his patience when chemistry did not work; for his understanding for my situation and struggling; for his support all the way through my study.
- *Dr. Dominic V. McGrath*, my co-advisor: for hosting me for the research and giving me scientific guidance.
- *Dr. Joseph W. Perry*: for two-photon studies.
- *Dr. Jean-Luc Brédas*: for quantum chemical calculations.
- *Dr. Steve Barlow*, the senior scientist our group: for his efforts to help me understand the fundamental theory and experiments, and to teach me scientific writing by proofreading the whole thesis.
- All the past and present group members in Dr. Marder and Dr. McGrath groups and people from other groups for scientific discussions and friendship, in particular, Dr. Takashi Okada, Dr. Simon Jones, Dr. Xiaowei Zhan, Dr. Yadong Zhang, Dr. Sungjae Chung, Dr. Raghunath Dasari, Michal Malicki, Chun Huang, Yanrong Shi, Marsha Lamb; Dr. Dave Sisk, Dr. Gemma D'Ambruoso, Xiaochun Chen; Dr. Christina Bauer, Dr. Lisa Dollinger, Dr. Mariacristina Rumi.

DEDICATION

To my father and my mother

Who always encourage me to pursue my dreams.

Who are always there for me whenever I need them.

To Annie, my daughter

Whose happy nature always enlightens my life.

TABLE OF CONTENTS

LIST OF FIGURES.....	12
LIST OF TABLES.....	19
ABSTRACT.....	20
1. INTRODUCTION	21
1.1 Two-photon absorption.....	21
1.1.1 Introduction to two-photon absorption	21
1.1.2 Structure-property relationships.....	26
1.1.3 Two-photon absorbing molecules/materials	27
1.2 Photoinduced electron transfer	33
1.2.1 Introduction to photoinduced electron transfer.....	33
1.2.2 Two-photon induced electron transfer	34
1.2.3 Marcus theory	35
1.2.4 Estimation of free energy of electron transfer	38
1.3 Research goals and organization of the thesis	39
1.3.1 Research goals and design strategy.....	39
1.3.2 The organization of the thesis.....	40
2. ONE-PHOTON ACID GENERATORS.....	42
2.1 Photoacid generators for cationic polymerization	42
2.1.1 Aryldiazonium salts	43
2.1.2 Onium salts	44
2.1.3 Organometallic salts: the iron arene complexes	56
2.2 Photoacid generators via photoinduced electron transfer	57

TABLE OF CONTENTS – *continued*

2.3	Research goals	60
2.3.1	Previous research in our group	60
2.3.2	Research goals	61
2.4	Synthesis of photoacid generators	62
2.4.1	Synthesis of a meta-substituted sulfonium salt	62
2.4.2	Synthesis of para-substituted sulfonium salts	63
2.5	Photochemical studies	64
2.5.1	Absorption spectra	65
2.5.2	Fluorescence quenching	66
2.5.3	Free energy change for electron transfer	67
2.5.4	Quantum yield of acid generation	68
2.6	Quantum-chemical calculations	69
2.7	Discussion and conclusions	73
2.8	Experimental: Quantum yield of acid generation	74
2.9	Experimental: synthetic procedures	78
3.	TWO-PHOTON ACID GENERATORS	89
3.1	Introduction to two-photon induced polymerization	89
3.2	Two-photon acid generators	91
3.2.1	Introduction	91
3.2.2	Negative and positive tone resists	92
3.2.3	Literature review of two-photon acid generators	94
3.2.4	Two-photon acid generator developed by our group	96
3.3	Research goals	101

TABLE OF CONTENTS – *continued*

3.4	Synthesis of short wavelength two-photon acid generators.....	103
3.4.1	Synthesis of the biphenyl two-photon acid generator.....	103
3.4.2	Synthesis of the fluorene two-photon acid generator	104
3.5	One-photon photochemical studies.....	105
3.5.1	Absorption spectra	106
3.5.2	Quantum yield of acid generation.....	106
3.5.3	Polymerization under one-photon conditions	107
3.6	Two-photon induced polymerization studies.....	108
3.7	Conclusions and future work	109
3.8	Experimental: photochemical measurements	110
3.8.1	Quantum yield of acid generation.....	110
3.8.2	Polymerization under one-photon conditions	114
3.8.3	Dose-array measurements of two-photon induced polymerization thresholds	115
3.9	Experimental: synthesis procedures.....	116
4.	TWO-PHOTON RADICAL GENERATORS.....	126
4.1	Two-photon radical polymerization.....	126
4.1.1	Conventional two-photon radical generators and sensitizers.....	126
4.1.2	Two-photon chromophores with large cross-sections	132
4.2	Research goal and molecular design strategy	137
4.3	Study of UV-labile radical generators	139
4.3.1	Literature review	139
4.3.2	Research goal and molecular design.....	142

TABLE OF CONTENTS – *continued*

4.3.3	Synthesis	143
4.3.4	Photochemical studies.....	145
4.3.5	Efficiency of radical polymerization	150
4.3.6	Conclusion	151
4.4	Study of model molecules.....	152
4.4.1	Research goals and molecules design.....	152
4.4.2	Synthesis of model molecules.....	153
4.4.3	Study of anion effects	154
4.4.4	Photochemistry Study.....	155
4.4.5	Conclusion	161
4.5	Long wavelength two-photon radical generators.....	162
4.5.1	Research goal and molecular design.....	162
4.5.2	Synthesis	163
4.5.3	Photochemical study.....	164
4.5.4	Two-photon studies.....	166
4.5.5	Conclusion	167
4.6	Short-wavelength two-photon radical generator.....	168
4.6.1	Research goal and molecular design.....	168
4.6.2	Synthesis	170
4.6.3	Photochemical studies.....	171
4.6.4	Two-photon studies.....	174

TABLE OF CONTENTS – *continued*

4.6.5	Discussion.....	176
4.6.6	Conclusion	177
4.7	Experimental: photochemical experiments.....	178
4.7.1	Fluorescence quenching.....	178
4.7.2	Quantum yield of acid generation.....	180
4.7.3	Polymerization of methyl methacrylate	181
4.7.4	Photoproduct analysis	182
4.7.5	Relative fluorescence quantum yield.....	183
4.7.6	The measurement of two-photon induced polymerization threshold	185
4.8	Experimental: synthetic procedures.....	187
5.	TWO-PHOTON REMOVABLE PROTECTING GROUPS	209
5.1	Historical review.....	209
5.2	Literature review for photoremovable protecting groups.....	212
5.2.1	The o-nitrobenzyl group and its derivatives	213
5.2.2	The benzoin (desyl) group and its derivatives	216
5.2.3	The phenacyl group and its derivatives	222
5.2.4	The coumaryl group and derivatives.....	225
5.3	Photoremoval via photoinduced electron transfer	228
5.4	Research goal.....	231
5.4.1	Literature review of two-photon removable protecting groups	231
5.4.2	Research goal.....	233
5.5	First generation of molecular design.....	235

TABLE OF CONTENTS – *continued*

5.5.1	Molecular design.....	235
5.5.2	Synthesis	236
5.5.3	Photochemical studies.....	238
5.5.4	Discussion and conclusion.....	244
5.6	Second generation of molecular design	246
5.6.1	Molecular design.....	246
5.6.2	Synthesis	247
5.6.3	Photochemical studies.....	249
5.6.4	Conclusions.....	253
5.7	Experimental: photochemical measurements	254
5.7.1	Relative fluorescence quantum yield	254
5.7.2	Photolysis.....	256
5.8	Experimental: synthetic procedures.....	257
6.	CONCLUSIONS AND FUTURE WORK.....	272
	REFERENCES.....	278

LIST OF FIGURES

Figure 1.1	Jablonski diagram for two-photon and one-photon absorption.	21
Figure 1.2	(a) Pinpoint 3D resolution of two-photon absorption. (b) The photograph shows fluorescence from a solution of chromophore excited with wavelength appropriate for TPA (top) and OPA (below).	23
Figure 1.3	Photograph illustrating deeper penetration of light by two-photon absorption (upper spot) as compared to one-photon absorption (lower spot) in a more concentrated solution of the fluorescent chromophore shown in Figure 1.2.	24
Figure 1.4	D- π -D or A- π -A motifs for quadrupolar chromophores.	28
Figure 1.5	Representative D- π -D and D-A-D chromophores. The δ values for 1 – 5 were measured using a two-photon-induced fluorescence method, ^{31,33,36,71} and that of 6 by Z-scan. ⁷⁴	29
Figure 1.6	Representative A- π -A and A-D-A chromophores. The δ value for 7 was measured using a two-photon-induced fluorescence method, ³¹ and that for 8 by Z-scan. ⁷⁵	30
Figure 1.7	D- π -A motif for dipolar chromophores.	30
Figure 1.8	Representative D- π -A chromophores. The δ value for 9 was measured using fs Z-scan method. ⁴⁶ The degenerate δ of 10 was estimated from a non-degenerate δ that was measured by using the WLC pump-probe method. ⁴⁷	31
Figure 1.9	Dipolar 11 , octupolar 12 chromophores and dendritic chromophore 13 . ⁴⁵ ...	32
Figure 1.10	Schematic of oxidative and reductive photoinduced electron transfer.	33
Figure 1.11	State-energy diagram for two-photon induced electron transfer.	34
Figure 1.12	The rate of electron transfer as a function of thermodynamic driving force.	35
Figure 1.13	Relationship between free energy (ΔG) and nuclear motion for diabatic exergonic electron transfer.	37
Figure 1.14	General design strategy of TPA chromophores with photoreactive groups.	39
Figure 2.1	Photodecomposition of aryldiazonium salts.	43

LIST OF FIGURES – *continued*

Figure 2.2	General chemical structures of onium salts.....	44
Figure 2.3	General formula and functions of diaryliodonium salts.....	45
Figure 2.4	Mechanism for photodecomposition of diaryliodonium salts: the cage pathway.....	47
Figure 2.5	Mechanism for photodecomposition of diaryliodonium salts: the escape pathway.....	48
Figure 2.6	Diarylchloronium and diarylbromonium salts.....	48
Figure 2.7	Mechanism for photodecomposition of triarylsulfonium salts: the escape pathway.....	50
Figure 2.8	Mechanism for photodecomposition of triarylsulfonium salts: the cage pathway.....	51
Figure 2.9	Triphenylselenium salts.....	51
Figure 2.10	Dialkylphenacylsulfonium salts and dialkyhydroxyphenylsulfonium salts.....	52
Figure 2.11	Mechanism for photodecomposition of dialkylphenacylsulfonium salts....	53
Figure 2.12	Mechanism for photodecomposition of dialkyl-4-hydroxyphenylsulfonium salts.....	53
Figure 2.13	Mechanism for photodecomposition of phosphonium salts.....	54
Figure 2.14	Phenylacylphenyl arsonium salts.....	54
Figure 2.15	Pyridinium and isoquinonium salts.....	55
Figure 2.16	Mechanism for photodecomposition of isoquinolinium salts.....	55
Figure 2.17	Mechanism for photodecomposition of Irgacure 261.....	56
Figure 2.18	Two classes of sulfonium salts as acid generators.....	57
Figure 2.19	A schematic of the orbital energy diagram for class 1 PAGs.....	58
Figure 2.20	Mechanism for photodecomposition proposed by Saeva.....	59
Figure 2.21	Stabilization of the radical cations by triarylamine substituent.....	60
Figure 2.22	Target molecules of one-photon acid generators.....	61
Figure 2.23	Synthesis of triarylamine sulfonium salt 16	62

LIST OF FIGURES – *continued*

Figure 2.24	Synthesis of the <i>para</i> -substituted triarylamine sulfonium salts 17 – 19	63
Figure 2.25	Absorption spectra of photoacid generators 16 – 19 in acetonitrile.	65
Figure 2.26	Fluorescence spectra of photoacid generators 17 – 19 in acetonitrile.	66
Figure 2.27	Optimized ground state structures of 14 and 17	69
Figure 2.28	HOMO (lower) and LUMO (upper) of 14 in the ground state geometry S_0 (left) and the excited state geometry S_1 (right).	70
Figure 2.29	HOMO (lower) and LUMO (upper) of 17 in the ground state geometry S_0 (left) and the excited state geometry S_1 (right).	70
Figure 2.30	Protonation of Rhodamine B base (RB).	75
Figure 2.31	Measurement of quantum yield of acid generation of the PAGs 14 – 17 . ..	77
Figure 3.1	Initiation reactions typically used for laser 3DLM.	90
Figure 3.2	Negative tone resist approach.	92
Figure 3.3	Positive tone resist approach.	93
Figure 3.4	(a) Chemical structure of CD-1012 . (b) Optical microscopy image of microstructures formed by using CD-1012 . ⁴³	95
Figure 3.5	Isopropylthioxanethone (ITX), a mixture of 2 and 4 isomers.	95
Figure 3.6	Model molecules 27 and 28 for the design of two-photon acid generators. ...	97
Figure 3.7	Chemical structure of BSB-S₂	98
Figure 3.8	SEM image of columnar structures produced with SU-8 and BSB-S₂ . ¹⁹¹	99
Figure 3.9	Decomposition of poly(THPMA- <i>co</i> -MMA) upon acid exposure.	99
Figure 3.10	Two-photon fluorescence microscopy images of three-dimensional microchannel structure fabricated by using BSB-S₂ . ¹⁸⁷	100
Figure 3.11	Target short-wavelength two-photon absorbing chromophores.	101
Figure 3.12	Target molecules of short-wavelength two-photon acid generators 31 and 32	102
Figure 3.13	Synthesis of two-photon acid generator 31	103

LIST OF FIGURES – *continued*

Figure 3.14	Synthesis of two-photon acid generator 32 .	104
Figure 3.15	Absorption spectra of BSB-S₂ , 31 , and 32 in acetonitrile.	106
Figure 3.16	One-photon polymerization of cyclohexene oxide (7.87 M) initiated by 31 (6.60×10^{-3} M) and 32 (6.36×10^{-3} M) irradiated at 300 nm.	107
Figure 3.17	Threshold energies of initiation systems 31 , 32 and CD-1012/ITX .	108
Figure 3.18	Absorbance of PAGs at 555 nm for 31 , 32 and BSB-S₂ , measured over time to determine the concentration of acid generated in acetonitrile.	112
Figure 4.1	(a) Chemical structures of HCPM and BDMP . (b) The mechanism for radical generation.	127
Figure 4.2	Scanning electron microscopic images of a spiral coil made by two-photon radical polymerization. (a) The entire view. (b) The magnified view. ¹⁸⁵	127
Figure 4.3	The SEM images of the micro-bull from the different view angles. ¹³	128
Figure 4.4	Top: structures of H-Nu 470 and DIDMA . Bottom: the micrograph of polymerized microstructure. ³⁹	129
Figure 4.5	Single-photon initiation mechanism proposed by Belfield.	130
Figure 4.6	(a) Structures of DEDC and DIHP . (b) The microstructure of a two-layer log stack with 4 μm period. ²⁰¹	131
Figure 4.7	Molecules for the studies of two-photon initiated radical polymerization.	133
Figure 4.8	Three-dimensional microstructures produced by two-photon initiated radical polymerization. (a) Photonic bandgap structure. (b) Magnified top-view of structure in a. (c) Tapered waveguide structure. (d) Array of cantilevers. ¹²	134
Figure 4.9	Structure of two-photon chromophore 47 .	135
Figure 4.10	SEM magnified images of a single line fabricated at threshold powers. (a) 730 nm excitation of 45 -triacrylate resin. (b) 520 nm excitation of 47 -triacrylate resin. ²⁰³	135

LIST OF FIGURES – *continued*

Figure 4.11 SEM overview images of woodpile-type photonic crystal structures using 47 -triacrylate resin fabricated with 520 nm excitation at (a) 0.60 μW and at (b) 0.45 μW . ²⁰³	136
Figure 4.12 Proposed photolysis mechanism for triarylsulfonium salts	139
Figure 4.13 Target Molecules 48 – 52	142
Figure 4.14 Synthesis of the <i>meta</i> -substituted triarylsulfonium salts 48 and 49	143
Figure 4.15 Synthesis of the <i>para</i> -substituted triarylsulfonium salts 50 and 51	144
Figure 4.16 Absorption spectra for 48 – 52 in acetonitrile	146
Figure 4.17 Fluorescence quenching of 49 and 51	149
Figure 4.18 Radical generators reported in the literature	152
Figure 4.19 Target model molecules 58 – 60	152
Figure 4.20 Synthesis of target molecules 58 – 60	153
Figure 4.21 Synthesis of 61	153
Figure 4.22 Absorption spectra for 58 – 60 in acetonitrile	156
Figure 4.23 Photolysis products of 59	158
Figure 4.24 Photolysis products of 60	159
Figure 4.25 Target molecules for long-wavelength two-photon radical generators	162
Figure 4.26 Synthesis of target molecule 62	163
Figure 4.27 Absorption and fluorescence spectra of 45 , 62 , and 63 in acetonitrile	165
Figure 4.28 Target molecules for short-wavelength two-photon radical generator	168
Figure 4.29 Synthesis of target molecule 69	170
Figure 4.30 Absorption spectra for 47 , 59 , and 69 in acetonitrile	172
Figure 4.31 Two-photon polymerization threshold energies for 47 and 69	174
Figure 4.32 Fluorescence quenching study of 52	179
Figure 4.33 Measurement of acid concentration in acetonitrile	180
Figure 4.34 Measurement of fluorescence quantum yields of 69 and 47	184
Figure 4.35 Threshold measurements of (a) 47 and (b) 69	186

LIST OF FIGURES – *continued*

Figure 5.1	Commonly used <i>o</i> -nitrobenzyl photoremovable protecting groups.	213
Figure 5.2	Norrish type-II photoreaction.	214
Figure 5.3	Photorelease mechanism of <i>o</i> -nitrobenzyl protected acitic acid.	215
Figure 5.4	Commonly used benzoin type photoremovable protecting groups.	216
Figure 5.5	Photorelease mechanism for benzoin protecting group proposed by Sheehan.	217
Figure 5.6	Modified photorelease mechanism proposed by Sheehan.	218
Figure 5.7	Photorelease mechanism of 3',5'-dimethoxybenzoin group	218
Figure 5.8	Photorelease mechanism of 3',5'-bis(carboxymethoxy)benzoin group proposed by Chan.	219
Figure 5.9	Photorelease mechanism of proposed by Givens and Wirz.	220
Figure 5.10	Photorelease mechanism proposed by Sheehan.	222
Figure 5.11	Photorelease mechanism proposed by Givens.	223
Figure 5.12	Photorelease mechanism proposed by Corrie and Wan.	224
Figure 5.13	Coumarin and coumaryl protecting groups.	225
Figure 5.14	Photorelease of carboxylic acids from MCM esters.	226
Figure 5.15	Photorelease mechanism for MCM esters proposed.	226
Figure 5.16	Photorelease mechanism for the dimethylamine-sensitized deprotection proposed by Falvey.	229
Figure 5.17	Photorelease via intramolecular electron transfer.	230
Figure 5.18	Caged compounds with their two-photon cross-sections at the given wavelengths. (*Cross-section of CNB not reported).	232
Figure 5.19	Target molecules of first generation molecular design.	235
Figure 5.20	Synthesis of 78 – 80 for intermolecular electron transfer studies.	236
Figure 5.21	Synthesis of 82	236
Figure 5.22	Synthesis of target molecule 76 and model molecule 77	237
Figure 5.23	Absorption spectra of 45 and 78 – 80 in acetonitrile.	239

LIST OF FIGURES – *continued*

Figure 5.24	Absorption and fluorescence spectra of 45 and 76 in acetonitrile.....	240
Figure 5.25	Photolysis of 76 and the system 45 and 80	242
Figure 5.26	Photolysis of the system 45 and 78	242
Figure 5.27	Photolysis of the system 45 and 79	243
Figure 5.28	Target molecules 85 and 86	246
Figure 5.29	Synthesis of target molecule 85	247
Figure 5.30	Synthesis of target molecule 86	248
Figure 5.31	Absorption and fluorescence spectra of 45 , 85 and 86 in acetonitrile.....	250
Figure 5.32	Photolysis of 85	251
Figure 5.33	Photolysis of 86	252
Figure 5.34	Measurement of fluorescence quantum yield of 77	255
Figure 5.35	Measurement of fluorescence quantum yield of 45	255
Figure 6.1	Future molecular designs for two-photon radical generators.....	275

LIST OF TABLES

Table 2.1	One-photon physical data for photoacid generators 14 – 19 in acetonitrile. ..	64
Table 3.1	One-photon physical data for two-photon acid generators 31 and 32 vs BSB-S₂ in acetonitrile.	105
Table 4.1	One-photon physical data for radical generators 48 – 52	145
Table 4.2	One-photon physical data for radical generators 58 – 60	155
Table 4.3	One-photon physical data for 45, 62, and 63	164
Table 4.4	Two-photon measurement data for 45 and 62	166
Table 4.5	One-photon physical data for 47, 59 and 69	171
Table 5.1	One-photon physical data for 45, 76, and 77 in acetonitrile.	238
Table 5.2	One-photon physical data for 85 and 86 in acetonitrile.	249

ABSTRACT

Two-photon absorption is the process in which a molecule absorbs two photons simultaneously. The two key advantages of two-photon processes over one-photon processes are the possibility of excitation of materials with high three-dimensional spatial resolution and deep light-penetration into absorbing materials. Based on bond-cleavage reactions activated by photon-induced intramolecular electron transfer, two-photon activatable acid and radical initiators and two-photon removable protecting groups have been successfully designed and synthesized for photopolymerization and three-dimensional microfabrication and for biomedical photo-triggers. The optical and chemical properties of synthesized molecules, such as quantum yield of acid generation, initiation efficiency of photopolymerization, and photolysis efficiency, have been studied by using a variety of physical and analytical techniques under one-photon conditions. The two-photon characteristics and applications of these molecules are being investigated in collaboration with other groups.

1. INTRODUCTION

1.1 Two-photon absorption

1.1.1 Introduction to two-photon absorption

One-photon absorption (OPA) occurs when the energy of the incident photon satisfies the Bohr condition (Figure 1.1). In 1931, Maria Goeppert-Mayer established the theoretical framework for two photon absorption (TPA).¹ In this process, a molecule simultaneously (in an order of 10^{-15} seconds) absorbs two individual photons (without populating to a real intermediate state or Eigen state), and is excited to a two-photon excited state at an energy that is equal to the sum of the two-photon energies (Figure 1.1). The energies of the two photons may be equal or differ, and the following discussion will focus on degenerate TPA, wherein the photon energy values are equal because this case is more amenable to theoretical investigations for the structure-property relationships of centrosymmetric molecules, and is relevant to most potential applications.

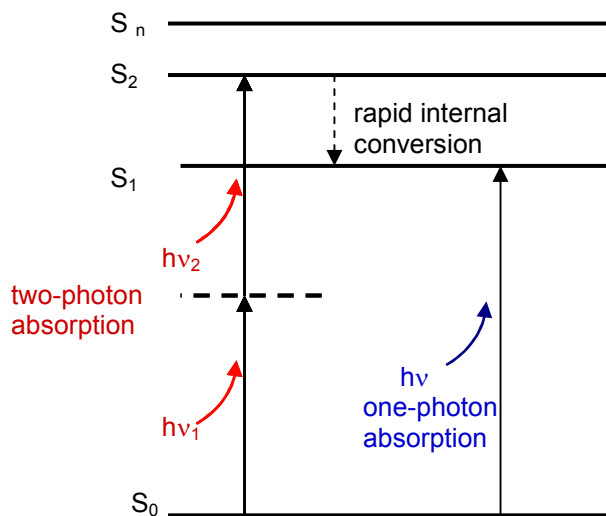


Figure 1.1 Jablonski diagram for two-photon and one-photon absorption.

In case of a centrosymmetric chromophore, the selection rules for OPA and TPA are mutually exclusive; hence, OPA and TPA are shown to access different states (Figure 1.1). However, according to Kasha's rule,² which states that fluorescence almost always occurs from the relaxed S_1 state (i.e. the vast majority of organic compounds), TPA is expected to afford same photochemical and photophysical processes as one-photon absorption, regardless of whether TPA accesses the same state as OPA.

There are three key advantages of two-photon absorption over one-photon absorption that are essential for many of its potential applications. First, the TPA probability has a quadratic dependency on the intensity of the incident irradiation ($TPA \propto I^2$) since two photons are absorbed simultaneously. On the other hand, the probability of one-photon absorption depends linearly on the intensity of the incident irradiation ($OPA \propto I$). Second, two-photon absorption can be spatially controlled with three-dimensional pinpoint resolution (Figure 1.2). The intensity of the incident irradiation in the vicinity of a focused beam falls off as the square of z , the light propagation distance from the focal plane ($I \propto z^{-2}$). Since one-photon absorption depends linearly on I , its light intensity falls off as the square of the distance ($OPA \propto z^{-2}$). On the other hand, the two-photon absorption depends on I^2 , which indicates two-photon absorption decreases much more steeply ($TPA \propto z^{-4}$) in the vicinity of focus. As a result, two-photon absorption can be confined to a small region around the focus, with a volume on the order of λ^3 , where λ is the wavelength of the incident laser light.

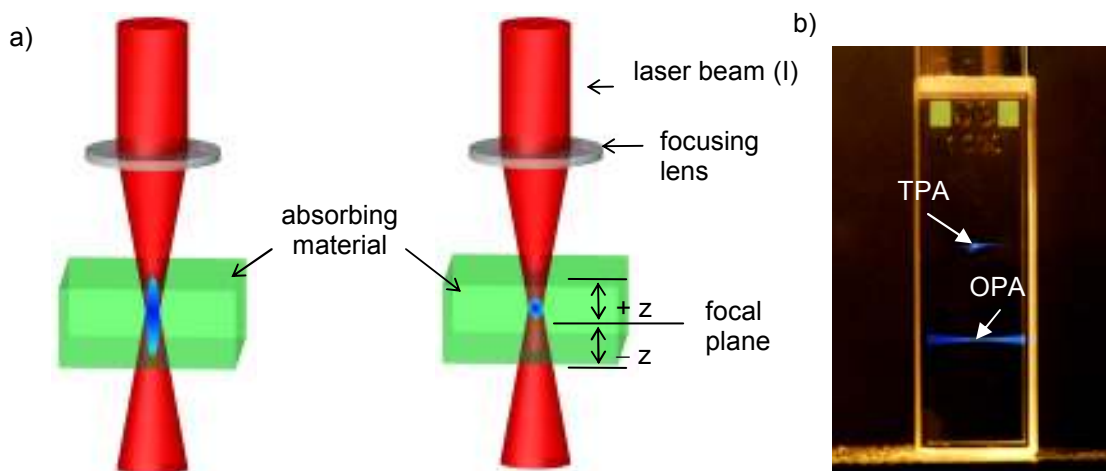


Figure 1.2 (a) Pinpoint 3D resolution of two-photon absorption. (b) The photograph shows fluorescence from a solution of chromophore excited with wavelength appropriate for TPA (top) and OPA (below).

Third, two-photon absorption can be carried out with deeper penetration in materials that would absorb light by one-photon absorption at the same transition energy (Figure 1.3). Since two-photon absorption only occurs at a small region around the focus, materials absorb weakly along the path of the two-photon beam except at the focus. In addition, the wavelength of two-photon excitation is typically roughly twice as that required for one-photon excitation of the same materials. The scattering for light at the TPA wavelength is generally reduced by a factor of 16 since the scattering efficiency is proportional to λ^{-4} . As a result, the optical transparency of materials and decreased light scattering at two-photon excitation wavelengths allow the light penetrate deeper into absorbing materials.

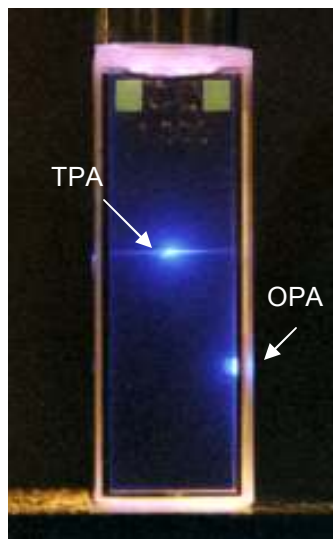


Figure 1.3 Photograph illustrating deeper penetration of light by two-photon absorption (upper spot) as compared to one-photon absorption (lower spot) in a more concentrated solution of the fluorescent chromophore shown in Figure 1.2.

Because the rate of two-photon absorption is only significant at high intensities (typically 10^{20-30} photon/cm²s), this process was not experimentally observed until ruby lasers were invented in 1960.³⁻⁵ Thirty years after Maria Goeppert-Mayer's two-photon theory,¹ Kaiser and Garrett first confirmed laser-induced two-photon fluorescence in CaF₂:Eu²⁺ crystals in 1961.⁶ Shortly thereafter, Peticolas, Goldsborough and Reickhoff monitored two-photon absorption in organic crystals and solutions in 1963.^{7,8} The applications of two-photon absorption were demonstrated for the first time by Rentzepis in optical data storage⁹ in 1989, and Webb in microscopy¹⁰ in 1990. However, the scope of TPA applications was limited by the relatively small cross-sections of two-photon absorbing materials known at that time. Subsequently, there have been considerable efforts made to understand both theoretically and experimentally the structure-property relationships for TPA chromophores, and many new organic chromophores with

enhanced TPA cross-sections have been developed (section 1.2). Over several decades, TPA molecules and materials have been widely applied in both material science and biological science. The major areas include three-dimensional microfabrication and optical storage,¹¹⁻¹⁴ optical power limiting,¹⁵⁻¹⁷ frequency up-converted lasing,¹⁸⁻²⁰ fluorescence microscopy,^{10,21-25} and photodynamic therapy.²⁶⁻²⁸ Two reviews of the TPA applications^{29,30} have been published recently. Literature reviews of two-photon cationic polymerization and two-photon radical polymerization will be presented in Chapter 3 and 4, respectively.

1.1.2 Structure-property relationships

Structure-property relationships for TPA chromophores have been studied with the objective of achieving large TPA cross-sections at a variety of wavelengths. There are two basic design strategies that are widely investigated, which are symmetrical quadrupolar chromophores,³¹⁻³⁶ and asymmetrical dipolar chromophores.^{34,37-47} Different molecule architectures, which are constructed using these two basic motifs, have also been developed, such as octupolar, dendritic, and multi-branched chromophores,^{44,45,48-58} and oligomers and polymers.⁵⁹⁻⁶⁵

In general, large cross-sections of TPA chromophores can be enhanced by extending the conjugation length of π bridge, increasing the strength of donors and/or acceptors, or improving the molecular planarity. However, there is no single design strategy valid for all applications since each has its own requirements in addition to large TPA cross-sections. For example, in the TPA fluorescence microscopy application, a high fluorescence quantum yield is desirable. On the other hand, reduced or quenched emission is required for the power limiting application. Moreover, it is desirable to be able to tune the TPA maximum wavelength as well as the cross-section.

1.1.3 Two-photon absorbing molecules/materials

An ideal two-photon chromophore for a certain application should have a large cross-section at the particular TPA wavelength required for the interest, as well as any other specific requirements for the application. A commonly used unit of TPA cross-section (δ) is GM (the Goeppert-Mayer, where $1 \text{ GM} = 10^{-50} \text{ cm}^4/\text{photon}$). The major measurement techniques for degenerate TPA, where the two photons have the same energy, include non-linear transmission, two-photon excited induced fluorescence,⁶⁶ and open-aperture Z-scan.^{67,68} For non-degenerate TPA, where the two photons have different energies, a pump-probe technique with a white-light continuum (WLC) probe beam⁶⁹ has been developed recently. However, care must be taken to ensure that the data obtained from some techniques reflect the true cross-section, and do not contain contribution from other effects, such as excited state absorption. Two-photon absorbing molecules/materials have been reviewed previously in the literature.⁷⁰ In this section, some representative two-photon chromophores will be briefly reviewed to illustrate the structure-property relationships of two-photon absorbing molecules.

1.1.3.1 Quadrupolar chromophores

Simple quadrupolar chromophores have a conjugated π -bridge with two electron-donors (or electron acceptors) on both ends, i.e. D- π -D or A- π -A motifs (Figure 1.4).



Figure 1.4 D- π -D or A- π -A motifs for quadrupolar chromophores.

Marder and Perry pioneered the study for structure-property relationships of quadrupolar chromophores (Figure 1.5).^{31,33,36,71} Symmetrical attachment of electron-donors in the 4 and 4' positions of *trans*-stilbene **1** (18 GM at 488 nm)^{72,73} afforded **2** (200 GM at 600 nm),³¹ thus increasing the TPA cross-section of **2** relative to that of **1** by an order of magnitude. Chromophore **3** (995 GM at 730 nm) was obtained by extending the π -bridge from stilbene to distyrybenzene, which resulted in an almost five times larger cross-section.^{31,33} Based on the hypothesis that the enhancement of quadrupole moment would increase TPA cross-section, the motif of D-A-D was introduced by attaching electron-acceptors in the center of the π -bridge, for example in chromophore **4**. The result that **4** (1,750 GM at 830 nm)³¹ has almost double the cross-section of **3** demonstrates the strategy is effective in increasing δ . Further studies along this path confirmed that the symmetrical attachment of electron acceptors/donors at the π -bridge to give increased quadrupole moment did indeed enhance the δ values, and chromophore **5** (5,300 GM at 970 nm)^{36,71} is a more extended example. Furthermore, in a recent study

using squaraines as acceptors at the center largely increased the cross-section, such as **6** (33,000 GM at 1050 nm).⁷⁴

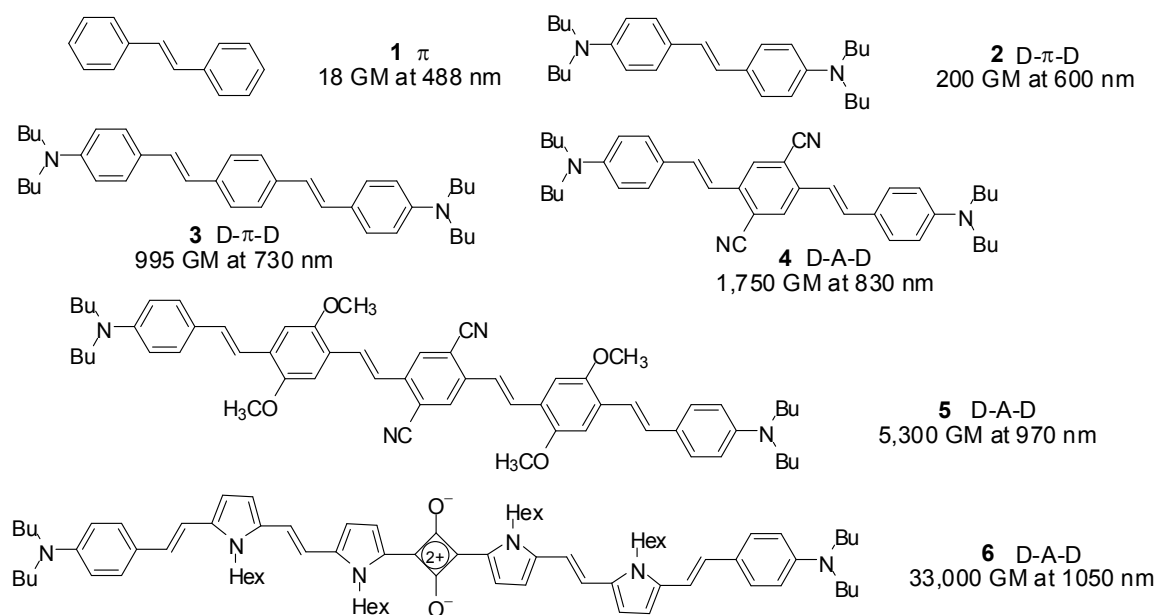


Figure 1.5 Representative D- π -D and D-A-D chromophores. The δ values for **1** – **5** were measured using a two-photon-induced fluorescence method,^{31,33,36,71} and that of **6** by Z-scan.⁷⁴

The A- π -A and A-D-A chromophores have been less widely investigated. Two examples are provided here. Chromophore **7** with a perylene core has a cross-section as high as 8,000 GM at 1050 nm.⁷⁵ Chromophore **8**, which has strong electron acceptors at both ends and electron donors at the center of π -bridge, was also found to show a large TPA cross-section (4,400 GM at 975 nm).³¹

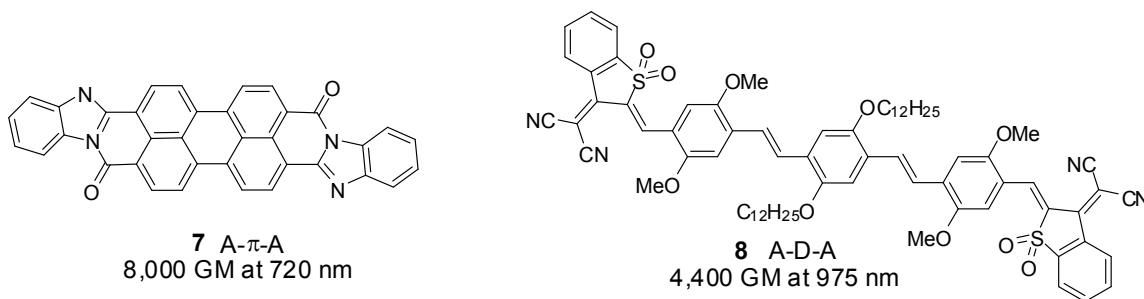


Figure 1.6 Representative A- π -A and A-D-A chromophores. The δ value for **7** was measured using a two-photon-induced fluorescence method,³¹ and that for **8** by Z-scan.⁷⁵

1.1.3.2 Dipolar chromophores

Dipolar D- π -A chromophores containing a conjugated core end-capped by an electron-donor at one side and an electron-acceptor at the other side have also been investigated (Figure 1.7).^{34,37-46}



Figure 1.7 D- π -A motif for dipolar chromophores.

Two examples are shown in Figure 1.8. The cross-section maximum of chromophore **9** (200 GM at 909 nm) obtained from fs Z-scan data is identical to that of D- π -D chromophore **2** (200 GM at 600 nm) using two-photon fluorescence method,⁴⁶ but at a considerably larger two-photon wavelength. The cross-section of chromophore **10** for degenerate TPA (\sim 900 GM at 1440 nm) was estimated from the non-degenerate δ value measured using the WLC pump-probe method.⁴⁷

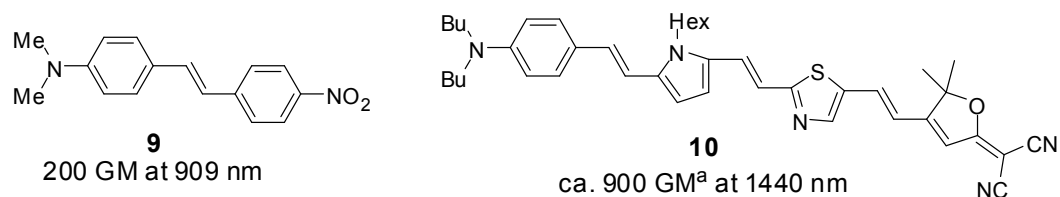


Figure 1.8 Representative D- π -A chromophores. The δ value for **9** was measured using fs Z-scan method.⁴⁶ The degenerate δ of **10** was estimated from a non-degenerate δ that was measured by using the WLC pump-probe method.⁴⁷

1.1.3.3 Octupolar chromophores and other architectures

Octupolar chromophores based on a core attached with three TPA substituents were calculated to have large cross-sections,^{44,51} and significant electronic coupling between the arms can enhance δ .⁴⁴ Some other molecular designs have also been investigated, including dendritic and multibranch chromophores,^{44,45,48-58} and oligomers and polymers.⁵⁹⁻⁶⁵

An example from Spangler's group is shown in Figure 1.9.⁴⁵ The octupolar chromophore **12** and a conjugated dendrimer **13** were synthesized by using 4,4'-bis(diphenylamino)stilbene **11** as building block. The δ_{max} ratio of the δ_{max} over the number of constituent TPA chromophores increases with the chromophore size, which suggests a cooperative enhancement.^{45,53}

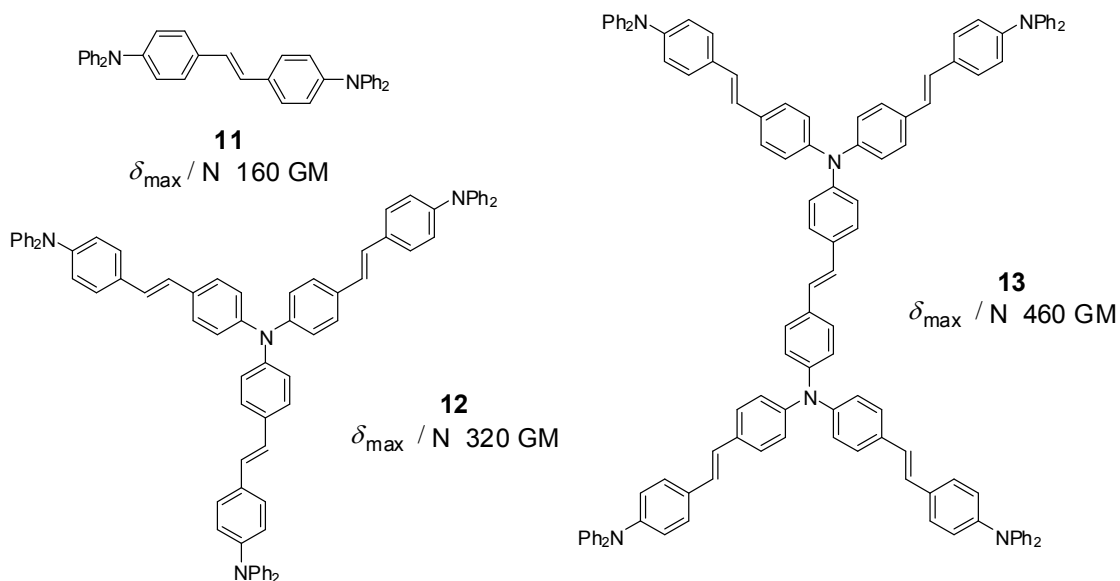


Figure 1.9 Dipolar **11**, octupolar **12** chromophores and dendritic chromophore **13**.⁴⁵

Porphyrin oligomers and polymers also show large TPA cross-sections.⁵⁹⁻⁶⁵ Anderson and co-workers have demonstrated that a porphyrin dimer (11,000 GM at 880 nm) has much higher cross-section than monomeric porphyrin (20 GM at 850 nm) using the TPA fluorescence induced method.^{63,64}

1.2 Photoinduced electron transfer

1.2.1 Introduction to photoinduced electron transfer

Electron transfer is a process by which an electron moves from one atom or molecule to another one. In photoinduced electron transfer (PET), the electron is moved between a photo-excited state and a neighboring ground state. Schematic examples of PET are shown in Figure 1.10. The excited state, marked by the star, can be either an electron-donor (D^*) or an electron-acceptor (A^*). Oxidative electron transfer can occur when the neighboring species (A) has a lower LUMO energy than that of the excited molecule, and the excited electron of D^* can be transferred to the LUMO of the neighboring molecule. On the other hand, reductive electron transfer can occur when the neighboring species has a higher HOMO energy (D) than that of the excited molecule (A^*), and an electron in the HOMO of the neighboring species can be transferred to the HOMO of the excited molecule. As a result, in both cases, a radical ion pair of a radical cation ($D^{\bullet+}$) and a radical anion ($A^{\bullet-}$) is formed, which may separate to give free radical ions or undergo a back electron transfer.

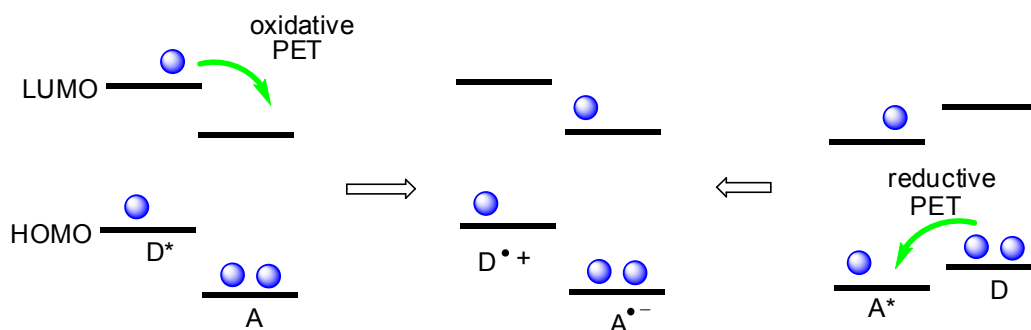


Figure 1.10 Schematic of oxidative and reductive photoinduced electron transfer.

1.2.2 Two-photon induced electron transfer

The proposed state-energy diagram for two-photon induced electron transfer is shown in Figure 1.11. Two-photon excitation promotes an electron from a TPA chromophore either (a) into the excited state S_1 from which electron transfer typically occurs, or (b) into a higher state S_n followed by internal conversion that allows relaxation to S_1 . The efficiency of electron transfer is determined by the rate constant for electron transfer (k_{et}), which competes with the rate constant for back electron transfer (k_{bet}) and the rate constants for radiative (k_{rad}) and non-radiative ($k_{non-rad}$) decay of S_1 .

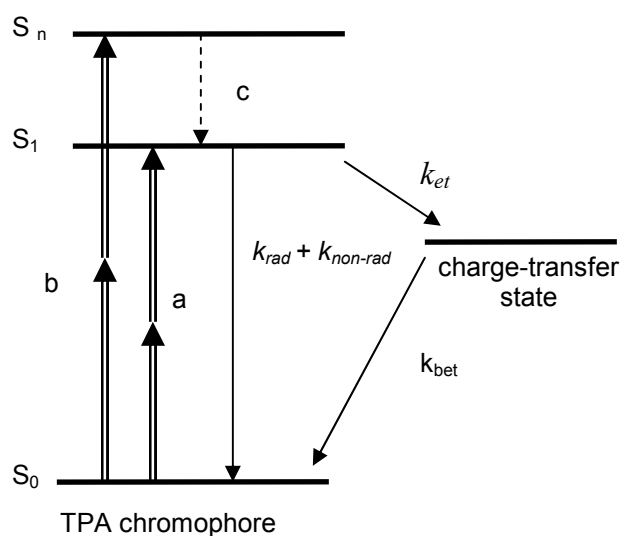


Figure 1.11 State-energy diagram for two-photon induced electron transfer.

1.2.3 Marcus theory

Marcus Theory, originally developed by Rudolph A. Marcus, is currently the dominant theory of electron transfer in chemistry.⁷⁶⁻⁷⁸ There are two key points of the theory. (1) There are two regions, the normal region and the inverted region, along the thermodynamic driving force coordinate ($-\Delta G_0$) (Figure 1.12). In the normal region, the rate constant for electron transfer (k_{et}) increases when driving force increases (ΔG_0 is getting more negative); in the inverted region, when ΔG_0 becomes even more negative, k_{et} decreases. The inverted region was controversial from the time the theory was proposed in 1956⁷⁶ until the experimental observations by Miller over twenty years later.⁷⁹⁻⁸¹ (2) The reorganization energy (λ) is the energy required to move the electron from an electron donor to an electron acceptor without moving the nuclei, which is intimately related to the activation energy for thermal electron transfer process (ΔG^\ddagger) (Figure 1.13).

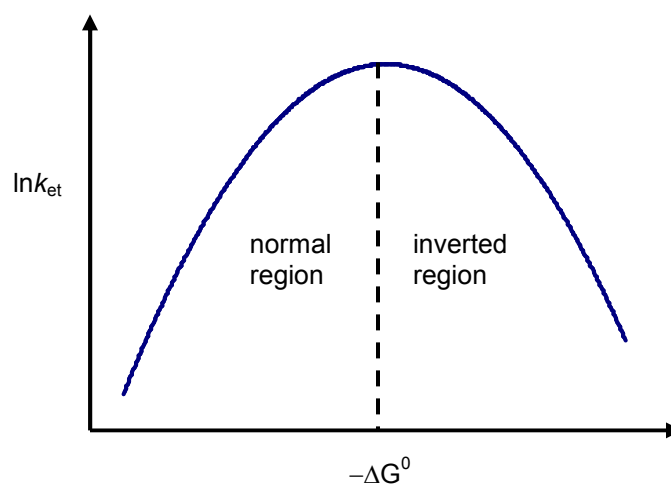


Figure 1.12 The rate of electron transfer as a function of thermodynamic driving force.

The basic relationship of Marcus theory is expressed in Eq 1.1, where k_{et} is the rate of electron transfer, V_{DA} is electronic coupling between donor and acceptor, k_b is the Boltzmann constant, T is thermal temperature, λ is the reorganization energy, and ΔG_0 is the thermodynamic driving force.

$$k_{et} \propto V_{DA}^2 \exp[-(\Delta G_0 + \lambda)^2 / (4 \lambda k_b T)] \quad \text{Eq 1.1}$$

The relationship between the ΔG_0 and λ can be visualized using potential energy surfaces as a function of the nuclear coordinates of the system (Figure 1.13). The left parabola represents the potential energy surface for the nuclear motion of the reactants in the initial state when the electron is still on the donor molecule or group; the right parabola represents the potential energy surface for the nuclear motion of the products in the final state after the electron has been transferred from the donor to the acceptor. The intersection of two parabolas is the point where the energy is the same whether the electron is at the reactant or the product, corresponding to the transition state for thermally activated electron transfer. The free energy required to reach this transition state configuration is the energy of activation (ΔG^\ddagger), which can be calculated by Eq 1.2.

$$\Delta G^\ddagger = (\lambda + \Delta G_0)^2 / 4 \lambda \quad \text{Eq 1.2}$$

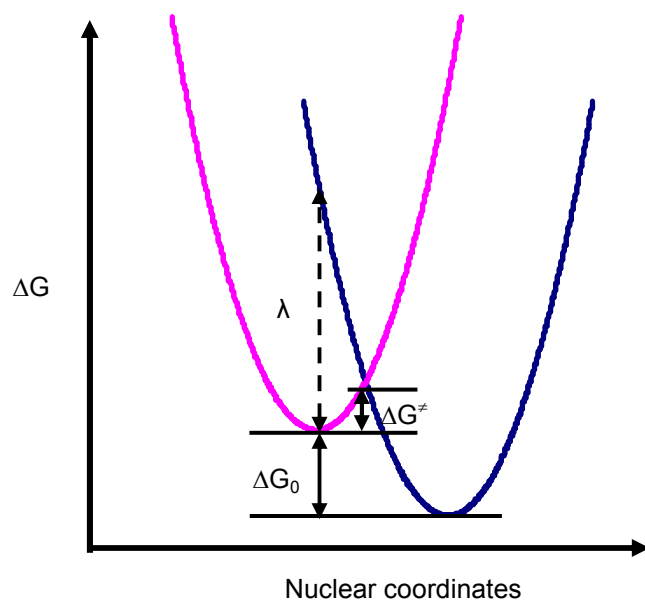


Figure 1.13 Relationship between free energy (ΔG) and nuclear motion for diabatic exergonic electron transfer.

1.2.4 Estimation of free energy of electron transfer

To ensure efficient electron transfer for PET, the charge-transfer state should be at lower energy than the S_1 state, i.e. the free energy of electron transfer (ΔG_0) should be negative. ΔG_0 can be estimated using the Rehm-Weller equation (Eq 1.3).⁸²

$$\Delta G_0 = F [E^{1/2}_{(D/D+\bullet)} - E^{1/2}_{(A\cdot/A)} - E_{(0,0)} - E_{\text{coul}}] \quad \text{Eq1.3}$$

F is the Faraday constant. E_{coul} (a positive value) is the Coulombic stabilization energy that is often neglected based on the assumption of the formation of solvent-separated free ions. $E_{(0,0)}$ is the energy of the relaxed excited state and can be estimated as the energy at which the one-photon absorption onset of the chromophore is seen or at which normalized fluorescence and one-photon absorption spectra intersect. $E^{1/2}_{(D/D+\bullet)}$ is electrochemical half-wave potential corresponding to the oxidation process in which one electron is removed from the electron donor. $E^{1/2}_{(A\cdot/A)}$ is electrochemical half-wave potential corresponding to the reduction process where one electron is put into an electron acceptor group. Eq1.1 shows that k_{et} is larger when ΔG_0 is more negative in the normal Marcus region. Therefore, the ΔG_0 trend obtained from Eq1.3 can be used to estimate the trend of k_{et} . The more negative the ΔG_0 , the larger k_{et} .

1.3 Research goals and organization of the thesis

1.3.1 Research goals and design strategy

Accomplishing photochemically induced processes using two-photon absorption has two advantages over using OPA: high 3D resolution and increased deep penetration. Structure-property relationships for TPA have been investigated, leading to development of many TPA chromophores with large cross-sections which have been utilized in a variety of applications. The research goal of the thesis is to extend their applications in three-dimensional microfabrication and to explore their potential for new biomedical applications using photoinduced electron transfer. The general design strategy consists of a TPA chromophore and a photocleavable group, which are connected via a linker (Figure 1.14). The hypothesis is that the electron is transferred from the excited TPA chromophore to the photocleavable group, which is chosen such that after receiving an electron, it will undergo a bond cleavage process to release the species of interest, such as acids, radicals and protected molecules.

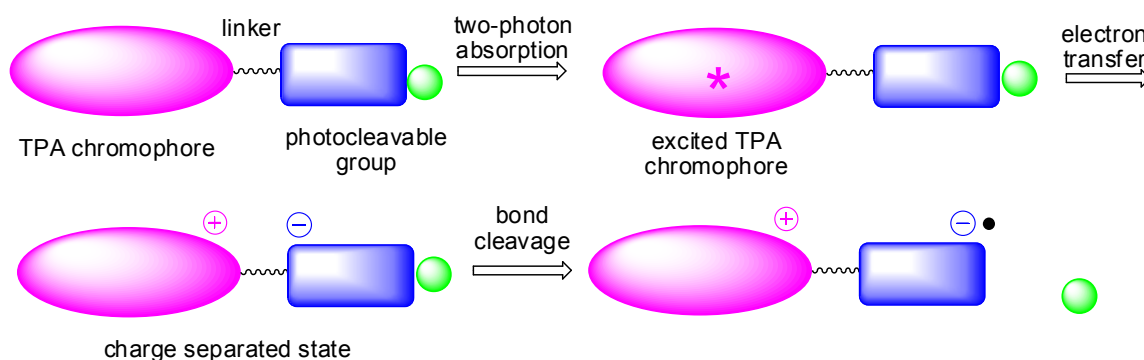


Figure 1.14 General design strategy of TPA chromophores with photoreactive groups.

1.3.2 *The organization of the thesis*

The remainder of the thesis contains the following four chapters.

Chapter 2 describes the study of one-photon acid generators and their mechanism of acid generation for the subsequent design of efficient two-photon acid generators. It includes a literature review of UV-labile photoacid generators, the design and synthesis of target one-photon acid generators, their photochemical properties, and quantum chemical calculations.

Chapter 3 is concerned with developing efficient two-photon acid generators for improvements in the resolution of three-dimensional microfabrication. It contains a literature review of polymerization initiated by two-photon acid generators, the design and synthesis of target two-photon acid generators, studies of their photochemical properties under one-photon conditions, and the preliminary results of two-photon studies.

Chapter 4 is concerned with developing efficient two-photon radical generators for three-dimensional microfabrication applications. It covers the study of UV-labile molecules for the identification of efficient photocleavable molecules, the study of the model molecules with attached UV-labile molecules to understand the linker effects, and the study of two-photon radical generators. For each section, the design, synthesis, and one-photon photochemical studies of target molecules have been performed. The preliminary results of two-photon studies of two-photon radical generators are also presented.

Chapter 5 describes the development of two-photon removable protecting groups for potential biomedical applications. It consists of a literature review of photocleavable protecting groups, the design and synthesis of two-photon removable groups, and their photochemical studies under one-photon conditions.

2. ONE-PHOTON ACID GENERATORS

2.1 Photoacid generators for cationic polymerization

Photoacid generators are molecules that can generate acids upon irradiation by light. Photoacid generators are used extensively to initiate cationic polymerization, which will be reviewed in this section, and are also widely used in photoresist formulations, especially in positive tone resists, which will be discussed in chapter 3.

Over the past twenty years, significant developments have been made in the area of photoinitiated polymerization. Photoinitiated polymerization has been demonstrated to occur through two major routes: photoinitiated free radical polymerization and photoinitiated cationic polymerization. Photoinitiated cationic polymerization (also called cationic photopolymerization) have been applied to photoresists, stereolithography, and holography, and as well as in the curing of coatings and adhesives due to its advantageous characteristics, including insensitivity to the presence of oxygen, the possibility for use of solvent free conditions, and high polymerization rates.

Photoinitiated cationic polymerizations can be initiated by strong Brønsted acids, carbocations, and trialkyloxonium salts. However, the most common usage of the term “cationic photoinitiators”, as defined in most literature papers and books, is essentially limited to that of photoacid generators. Following this convention, in this section, all cationic photoinitiators used are referred to photoacid generators. Their major types and their initiation mechanisms for direct photolysis will be discussed. In the rest of the thesis, photoacid generators will be used.

2.1.2 Onium salts

An onium salt consists of a cationic moiety (R_nO^+) and an anion (MX_n^-), where the cationic moiety (R_nO^+) includes a positively charged heteroatom (O^+) linked to alkyl or aryl groups (R) (Figure 2.2).

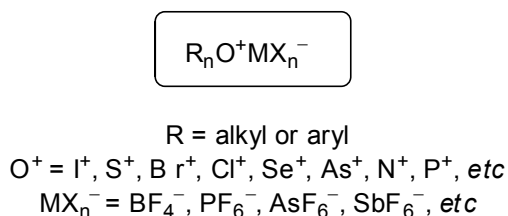


Figure 2.2 General chemical structures of onium salts.

In the past twenty-five years, a large number of onium salts have been synthesized and characterized, and their photodecomposition mechanisms have been investigated. The major onium salts described in the literature will be reviewed in this section, including diaryliodonium, diarylchloronium, and diarylbromonium salts; triarylsulfonium and triphenylselenonium salts; dialkylphenacylsulfonium and dialky-4-hydroxyphenylsulfonium salts; phosphonium and arsonium salts; and pyridium and isoquinonium salts.

2.1.2.1 Diaryliodonium salts

Diaryliodonium salts with counterions SbF_6^- , AsF_6^- , PF_6^- , and BF_4^- , represent an important group of cationic photoinitiators.^{92,95-105} The cation and anion portions of a diaryliodonium salt determine the different critical functions (Figure 2.3).¹⁰⁶

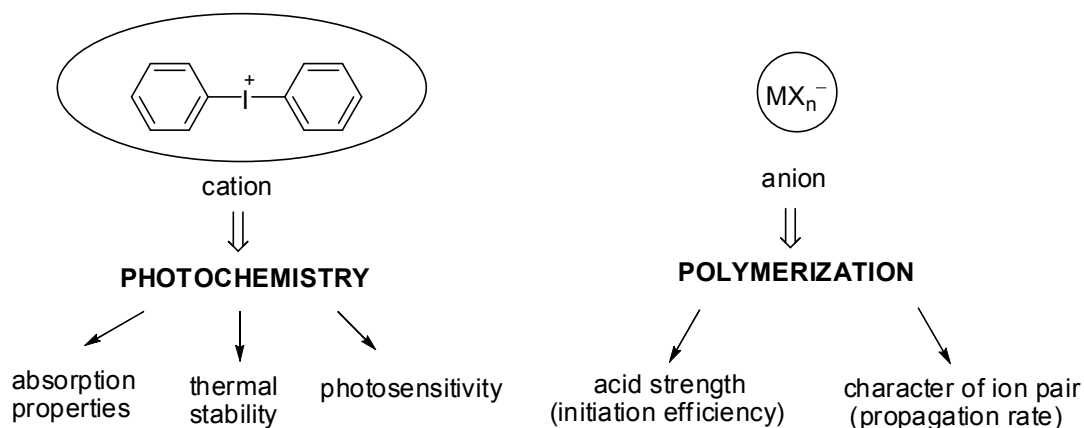


Figure 2.3 General formula and functions of diaryliodonium salts.

The cation is typically the light-absorbing component, and its structure determines the photochemistry, including the absorption characteristics, the photosensitivity (quantum yield), and the ultimate thermal stability. The anion does not affect the decomposition rate of cationic photoinitiators, but it plays important roles in the polymerization, especially propagation. The nature of the anion controls the strength of the acid formed during photolysis, which determines its initiation efficiency, as well as controls the character of the propagating ion pair, which impacts the polymerization kinetics, such as propagation rate. The larger the negatively charged anion, the more loosely it is associated with the propagating cationic species, and the more active the propagating cationic species is in the polymerization. Thus, an order of reactivity ($\text{SbF}_6^- > \text{AsF}_6^- > \text{PF}_6^- > \text{BF}_4^-$) has been observed for the anion.⁹⁴

Simple diaryliodonium salts have limited solubility in non-polar solvents and have shown toxicity. Some modifications have been made to solve these problems. Introduction of long alkyl^{107,108} or alkoxy^{109,110} chains to the aryl ring of diaryliodonium

salts shows improved solubility in various organic solvents, such as toluene.¹⁰⁹ As an additional advantage, the substitution of alkoxy chain with eight or more carbon atoms leads to a biologically non-toxic salt.¹⁰⁹ Diaryliodonium salts with replacement of toxic arsenic and antimony counterions with tetrakis(pentafluorophenyl)borate have demonstrated low toxicity, as well as exceptional solubility in nonpolar media including silicone oils.¹¹¹ Moreover, another approach to increase the solubility and compatibility in formulations of diaryliodonium salts is to incorporate them into either in the backbone of polymers¹¹²⁻¹¹⁴ or as a pendant group of polymers.¹¹⁵

The mechanism for photodecomposition under direct irradiation has been studied by several groups during the past twenty years.^{96,116} The recent re-investigation has led to a better understanding of the mechanistic details. In general, upon irradiation, diaryliodonium salts can undergo either/both homolytic and heterolytic cleavages of the carbon-iodine bond. The final photoproducts could form by following either cage or escape pathways.^{117,118}

The cage pathway is shown in Figure 2.4.¹¹⁷ Both products formed by homolytic or heterolytic cleavages recombine within the primary solvent cage to produce a cyclohexadienyl cation intermediate, which subsequently regains aromaticity upon losing a proton to give iodobiphenyl and the acid. All three possible iodobiphenyl isomers were detected. The 2-substituted isomer was the major product, and the rearranged isomers of 3-iodobiphenyl and 4-iodobiphenyl accounted for 10 – 25%.

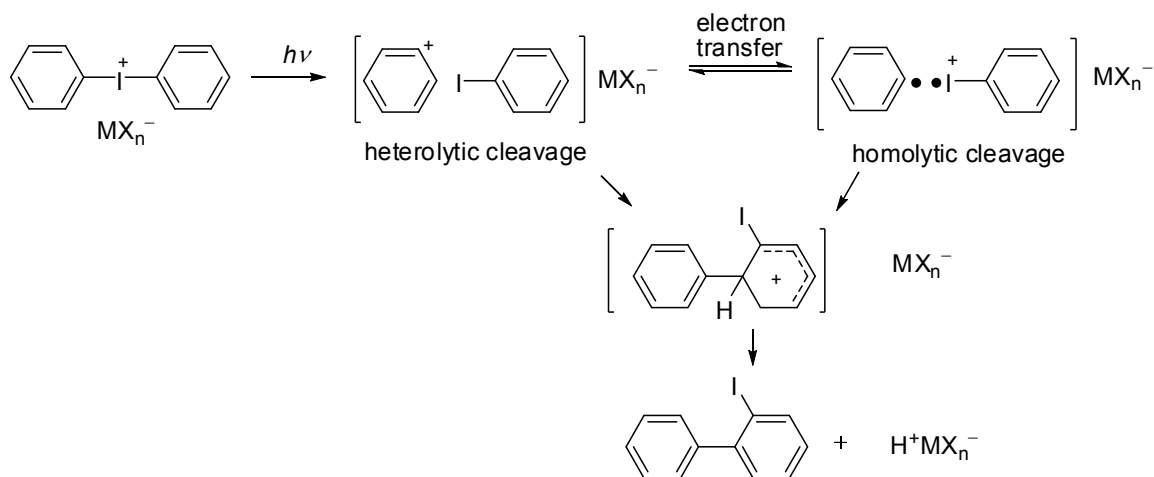


Figure 2.4 Mechanism for photodecomposition of diaryliodonium salts: the cage pathway.

The escape pathway is shown in Figure 2.5. A phenyl cation and iodobenzene pair was obtained by heterolytic cleavage, and a phenyl radical and iodobenzene radical cation pair was obtained by homolytic cleavage. The study of thermodynamic stability for the products of both cleavages showed that the phenyl radical and iodobenzene radical cation pair was slightly more stable. For heterolytic cleavage, the phenyl cation reacts with the solvent via electrophilic attack to generate an aryl compound. For the homolytic cleavage, the phenyl radical abstracts a hydrogen atom from the solvent to form benzene.

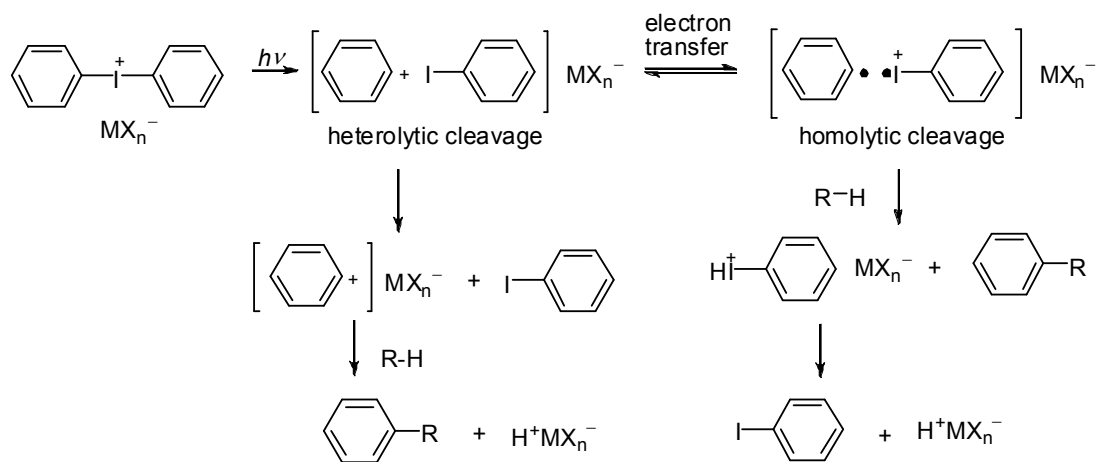


Figure 2.5 Mechanism for photodecomposition of diaryliodonium salts: the escape pathway.

The discovery of diaryliodonium salts as convenient and efficient cationic photoinitiators has led to the development of diarylchloronium and diarylbromonium salts (Figure 2.6).¹¹⁹⁻¹²¹ Diaryliodonium salts have been shown to be highly efficient cationic photoinitiators, but unfortunately they are less thermally stable and more difficult to prepare than diaryliodonium salts.



Figure 2.6 Diarylchloronium and diarylbromonium salts.

2.1.2.2 Triarylsulfonium salts

Triarylsulfonium salts incorporating non-nucleophilic counterions (SbF_6^- , AsF_6^- , PF_6^- , or BF_4^-) are nearly ideal photoinitiators.^{97,110,122-131} The combination of some desirable features, including thermal stability, excellent photosensitivity, solubility in common organic solvents, synthetic accessibility, and low toxicity, has made them very attractive as cationic photoinitiators.

The photodecomposition of triarylsulfonium salts upon direct irradiation is the best understood of all the cationic photoinitiators. Triplet quenching was not observed in either sensitized experiment¹³² or photo-Chemically Induced Dynamic Nuclear Polarization (CIDNP)¹³³ experiments used to investigate radical intermediates,^{134,135} indicating the photolysis occurs predominantly from the excited singlet state. The investigation shows that photoproducts are formed by either cage or escape pathways, which are both significant. The cage/escape ratio increases significantly in solution with the increasing solvent polarity and the increasing viscosity in the resist formulations.

The escape pathway is shown in Figure 2.7. Homolytic cleavage yields a diphenylsulfonyl radical cation, which abstracts a hydrogen atom from the solvent after escape from the solvent cage. The decomposition of the protonated diphenylsulfide produces the diphenylsulfide and a Brønsted acid.¹²³ Heterolytic cleavage generates diphenylsulfide and a phenyl cation that attacks the solvent to give the acid.¹²⁶ The detection of the substituted benzene from the reactions of both the phenyl radical and the phenyl cation with solvent supported the above mechanism.¹³⁶ However, there are two arguments against the proposed mechanism. First, quantitative product analysis showed

the ratio of acid and diphenylsulfide was 3:1 instead of the 1:1 ratio predicted by this mechanism.^{96,116} Second, no heterolysis products were observed, but only a singlet diphenylsulfonyl radical cation/phenyl radical pair formed by homolysis was identified by a CIDNP study.¹³³

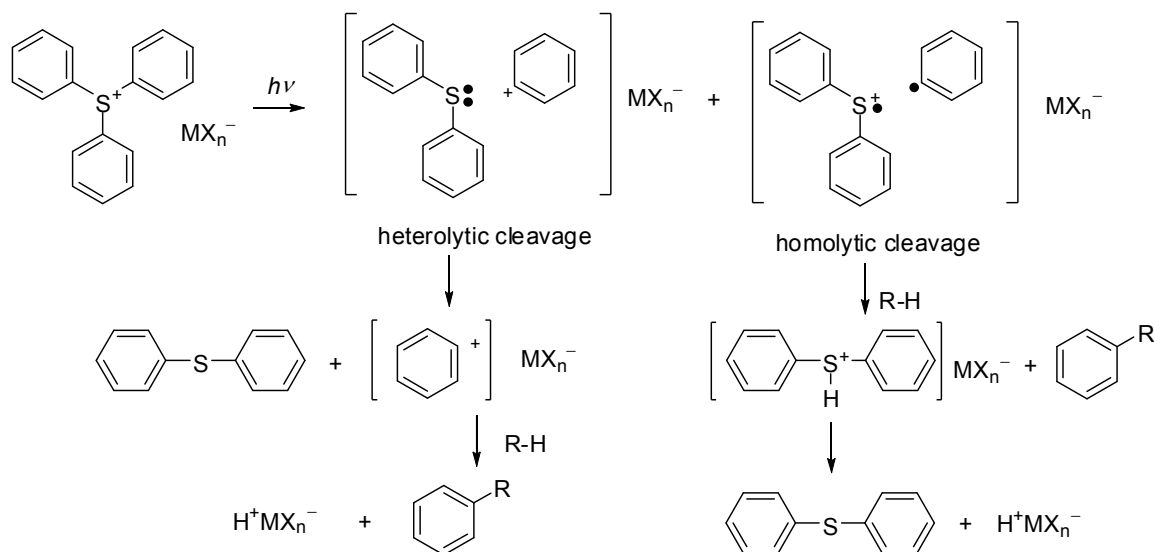


Figure 2.7 Mechanism for photodecomposition of triarylsulfonium salts: the escape pathway.

Later on, studies based on extensive product analysis indicated the cage pathway (Figure 2.8) was dominant.^{136,137} Recombination with rearrangement of both heterolytic and homolytic products in the solvent cage yields three phenylthiobiphenyl isomers and a stoichiometric amount of acid. The rearrangement products, 3- and 4-(phenylthio)-biphenyl, accounted for 60 – 70% of the total products in comparison with 20% for the iodonium analogue. This shows the high reactivity of diphenylsulfide toward electrophilic substitutions.

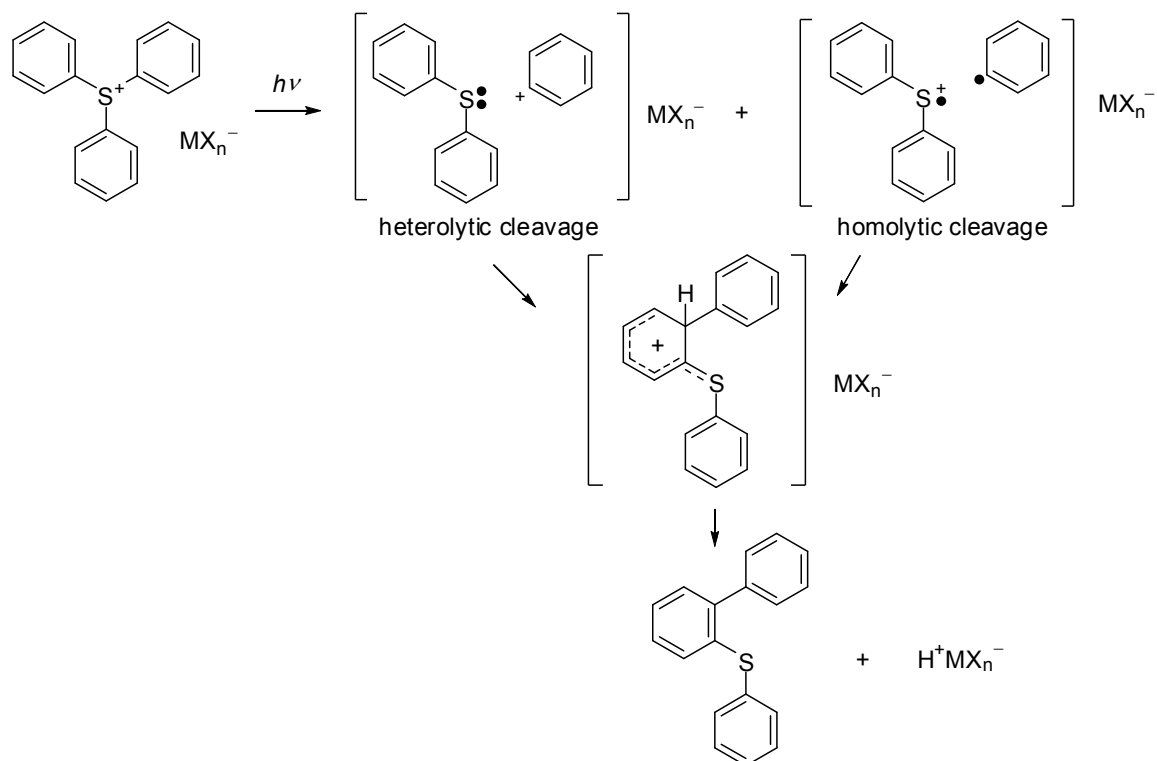


Figure 2.8 Mechanism for photodecomposition of triarylsulfonium salts: the cage pathway.

Like their triarylsulfonium salt analogs, triphenylselenium salts (Figure 2.9) are also efficient cationic photoinitiators although toxic and considerably more costly to prepare.^{122,138}

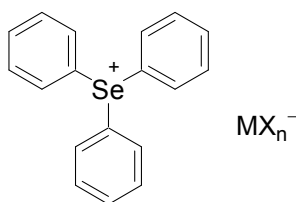


Figure 2.9 Triphenylselenium salts.

2.1.2.3 Dialkylphenacylsulfonium and dialky-4-hydroxyphenylsulfonium salts

As with their triarylsulfonium salt counterparts, dialkylphenacylsulfonium salts^{92,139-145} and dialky-4-hydroxyphenylsulfonium salts^{92,146-148} (Figure 2.10) are found to be attractive cationic photoinitiators due to their excellent thermal stability and high photosensitivity. However, their poor solubility in most cationic monomer systems has limited their practical applications. Recently, dialkylphenacylsulfonium salts bearing long alkyl chains that confer solubility in both polar and nonpolar solvents have been prepared.¹⁴¹

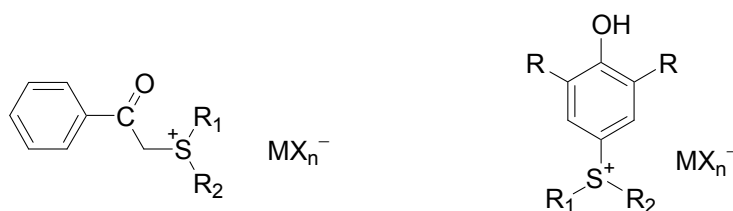


Figure 2.10 Dialkylphenacylsulfonium salts and dialkyhydroxyphenylsulfonium salts.

In contrast to diaryliodonium and triarylsulfonium salts, the photodecomposition of dialkylphenacylsulfonium salts is reversible.^{140,149} The proposed mechanism is shown in Figure 2.11. The first step involves hydrogen abstraction via a typical Norrish II process. The intramolecular radical/radical cation undergoes a facile intramolecular electron transfer to give a carbonium ion, which subsequently loses a proton to generate an ylide and an acid. The ylide is a base, and it could react with the acid formed to regenerate the starting material.

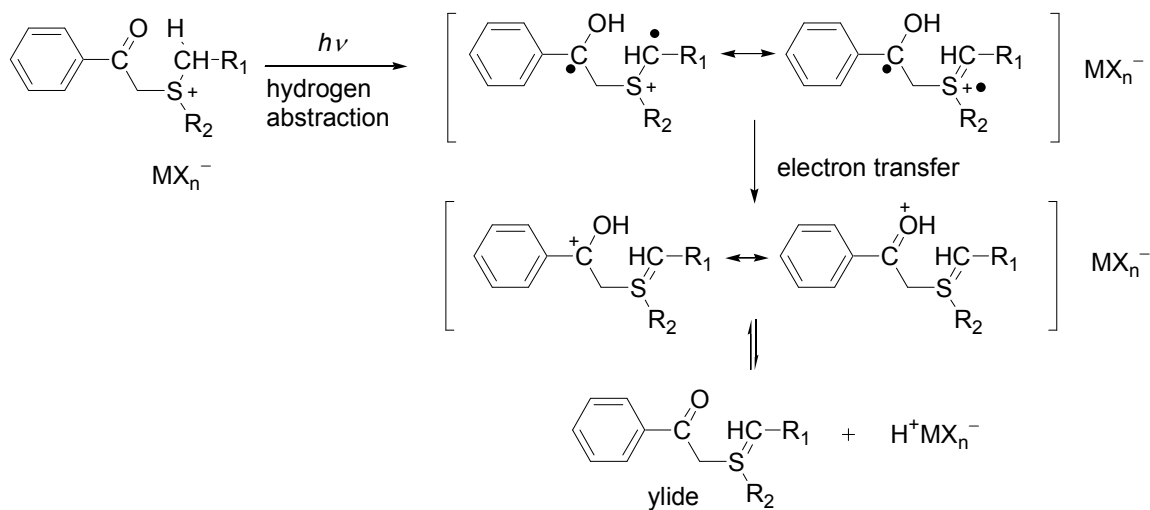


Figure 2.11 Mechanism for photodecomposition of dialkylphenacylsulfonium salts.

The photodecomposition of dialkylphenacylsulfonium salts is also reversible. The rapid dissociation of the excited state generates a strongly solvated Brønsted acid and a slightly basic resonance-stabilized ylide. These two products can recombine to give the starting salt in a thermal process. (Figure 2.12)

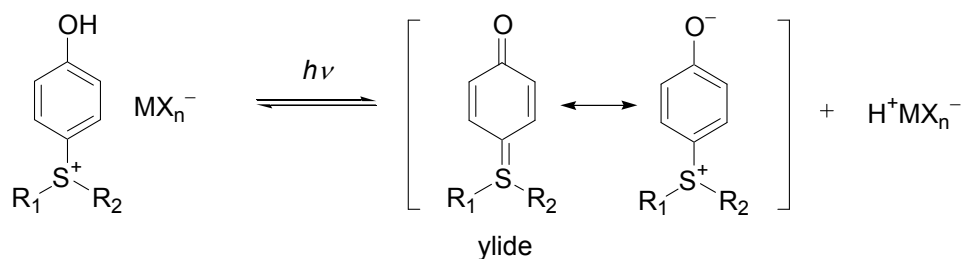


Figure 2.12 Mechanism for photodecomposition of dialkyl-4-hydroxyphenylsulfonium salts.

2.1.2.4 Phosphonium and arsonium salts

Methyl- and phenyl-acylmethyl triphenylphosphonium salts (Figure 2.13) have been reported to initiate cationic polymerization of cyclohexene oxide,^{150,151} styrene,¹⁵² and *p*-methyl styrene efficiently.¹⁵³ Upon irradiation, the phosphonium salts decompose to produce a Brønsted acid and a resonance-stabilized ylide (Figure 2.13).^{150,152}

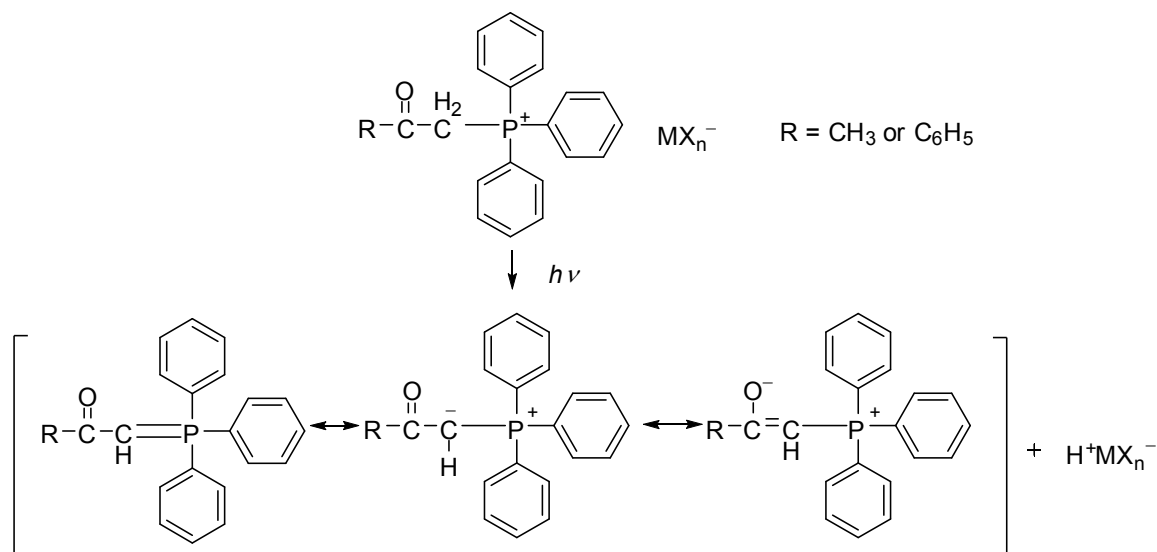


Figure 2.13 Mechanism for photodecomposition of phosphonium salts.

Phenylaclylmethyl triphenylarsonium salts containing SbF_6^- and PF_6^- anions (Figure 2.14) are useful photoinitiators for the cationic polymerization of styrene and cyclohexene oxide.^{151,152}

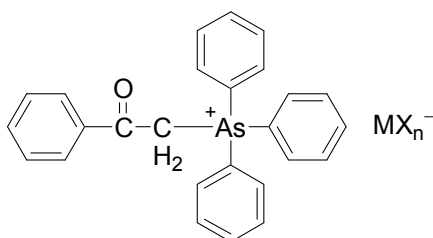


Figure 2.14 Phenylaclylmethyl arsonium salts.

2.1.2.5 Pyridinium and isoquinonium salts

Pyridinium and isoquinonium salts (Figure 2.15)^{148,154-156} have been used to photoinitiate cationic polymerization of various oxirane and vinyl ether monomers.^{155,156}

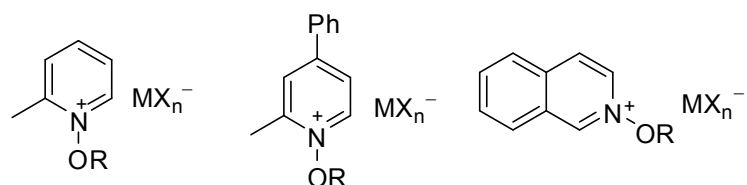


Figure 2.15 Pyridinium and isoquinonium salts.

The photodecomposition mechanism for isoquinonium salts is shown in Figure 2.16.^{154,157} The photolysis of an isoquinonium salt occurs via a rapid N–O bond cleavage, forming a radical cation and a radical. The radical cation abstracts a hydrogen atom from the solvent to generate an acid and another radical. Both radicals could initiate polymerization in the presence of radical monomers. In the absence of radical monomers, they may be quenched by recombination or abstraction from solvent, and the subsequent cleavage of the N–H bond gives an acid initiator.

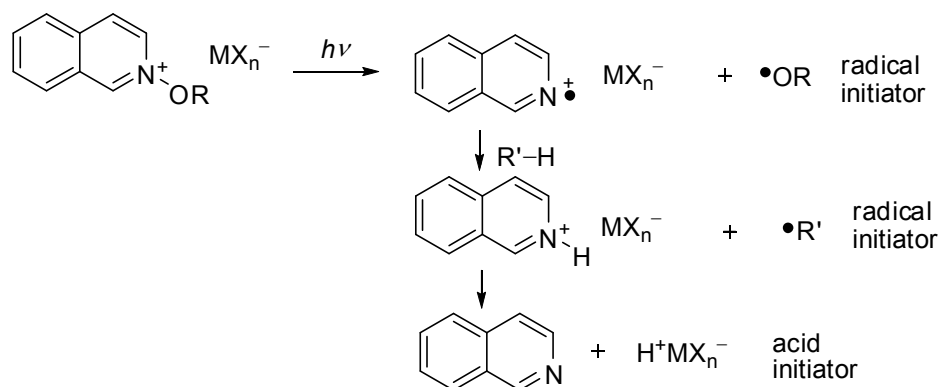


Figure 2.16 Mechanism for photodecomposition of isoquinolinium salts.

2.1.3 Organometallic salts: the iron arene complexes

Organometallic salts were introduced to the family as a new class of cationic photoinitiators in the 1980s. The most widely used organometallic derivatives as cationic photoinitiators are iron arene complexes with weakly nucleophilic anions.¹⁵⁸⁻¹⁶¹ A representative example of this class is Irgacure 261 (Figure 2.17).¹⁵⁸ It has the absorption maximum at 440 nm, and absorbs up to 580 nm,¹⁶⁰ and the varying ligand structures from isopropylbenzene to naphthalene and anthracene causes a further red-shift.^{162,163}

The mechanism for photodecomposition of Irgacure 261 is shown in Figure 2.17.¹⁶⁴ Photolysis of Irgacure 261 results in the removal of the uncharged isopropylbenzene ligand and the formation of the coordinatively unsaturated iron cation, which is a Lewis acid. The subsequent incorporation of three epoxide groups yields a relatively stable iron (II) complex. The cationic species formed in this way is responsible for the cationic polymerization. Since the mechanism involves the essential participation of the monomer, their applications appear restricted to those monomers that can efficiently bond to the coordinatively unsaturated iron center.

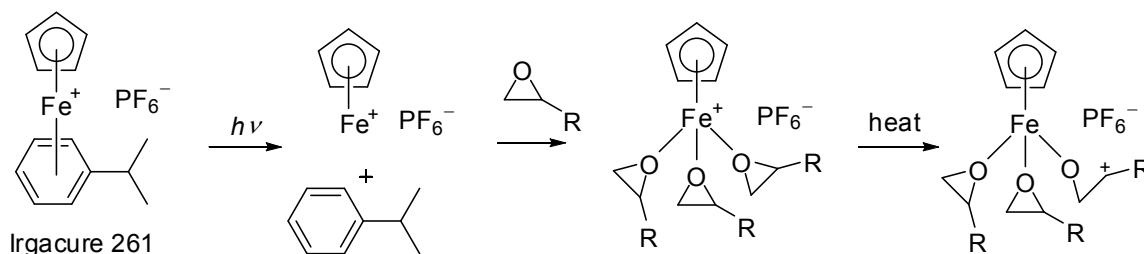


Figure 2.17 Mechanism for photodecomposition of Irgacure 261.

2.2 Photoacid generators via photoinduced electron transfer

Saeva has studied photoacid generation from aryl dialkyl sulfonium salts via photoinduced electron transfer.⁸⁵⁻⁹³ In Saeva's review,¹⁶⁵ the photoacid generators (PAGs) were divided into two classes (Figure 2.18). In class 1, the sulfonium group is directly attached to the light-absorbing chromophore. Due to the strong electron-withdrawing ability of the sulfonium group, the absorption properties of the chromophore are modified in class 1 PAGs. In class 2, the sulfonium group is separated from the light-absorbing chromophore via a linker. As a result, the light-absorbing ability of the chromophore is not significantly affected. In this section, we will focus on the mechanism of class 1.

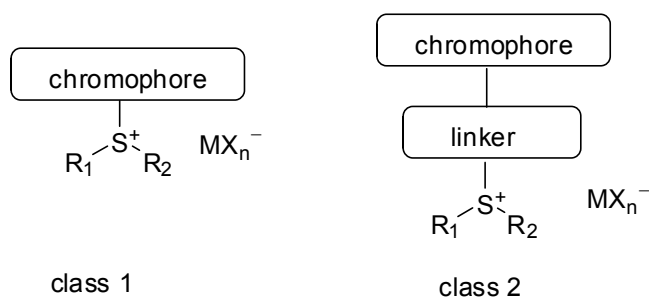


Figure 2.18 Two classes of sulfonium salts as acid generators.

A schematic of the orbital energy diagram described in the Figure 2.19 based on previous studies.¹⁶⁵ The photochemical excitation of the chromophore involves the promotion of an electron from the π -orbital (the local highest occupied orbital of the chromophore moiety) to the π^* -orbital (the local lowest unoccupied molecular orbital of the chromophore moiety). In the case where the energy of the σ^* -orbital of the S–C bond is lower than that of the π^* -orbital, the photoinduced electron transfer occurs from the π^* -

orbital to the σ^* -orbital. Sufficient orbital overlap between the π^* -orbital and the σ^* -orbital can be readily achieved by rotation around an aryl-sulfur single bond, which facilitates the electron transfer. Once the σ^* -orbital is populated, bond cleavage occurs provided the rate constant of bond cleavage (k_{bc}) is faster than the rate constant of the back electron transfer (BET) to the π -orbital to repopulate the molecular ground state (k_{bet}).

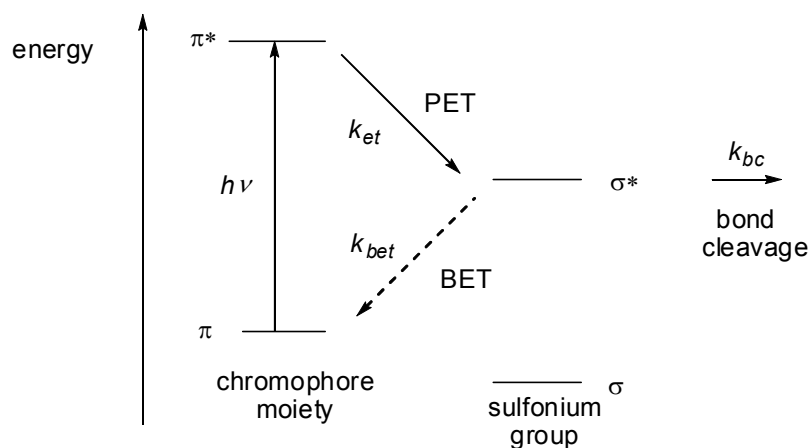


Figure 2.19 A schematic of the orbital energy diagram for class 1 PAGs.

Saeva studied the photoacid generation of naphthyl dialkylsulfonium salts in detail, and proposed a mechanism of σ sulfur-alkyl bond (S–C) breaking concerted with acceptance of an electron.¹⁶⁶ The photoproducts of the photoreaction were investigated to understand the photodecomposition mechanism. The proposed mechanism is shown in Figure 2.20.¹⁶⁷ Homolytic cleavage of the S–C σ -bond leads to a radical fragment/radical cation pair in a solvent cage. Both the recombination of the radical cation with the radical and hydrogen abstraction from the solvent would produce the acid and corresponding

byproducts. The quantum yields of acid generation ranged between 0.10 and 0.24. The stronger the electron-withdrawing ability of the leaving group (R group in the Figure 2.20), the higher quantum yields.

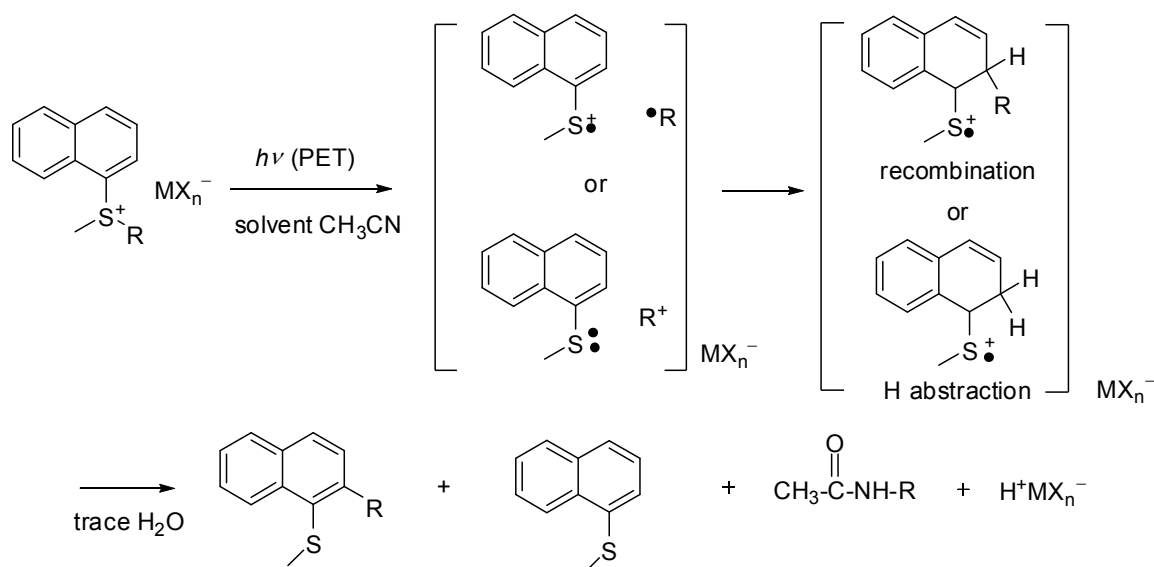


Figure 2.20 Mechanism for photodecomposition proposed by Saeva.

2.3 Research goals

2.3.1 Previous research in our group

Encouraged by the results from Saeva's study, our lab hypothesized that quantum yields of photoacid generation could be enhanced by incorporating functionalities that stabilize the radical cation generated by photolysis of the S–C bond. A triarylamine was selected for this purpose, since the radical cations could be stabilized via electron transfer from amine to the sulfonium to form more stable nitrogen based radical cations (Figure 2.21). Moreover, triarylamine salts are essentially non-basic ($pK_a [\text{Ar}_3\text{N}^+\text{H}] \sim -5$),¹⁶⁸ and thus does not react with the photoacid generated, which could allow for the acid to initiate cationic polymerization efficiently.

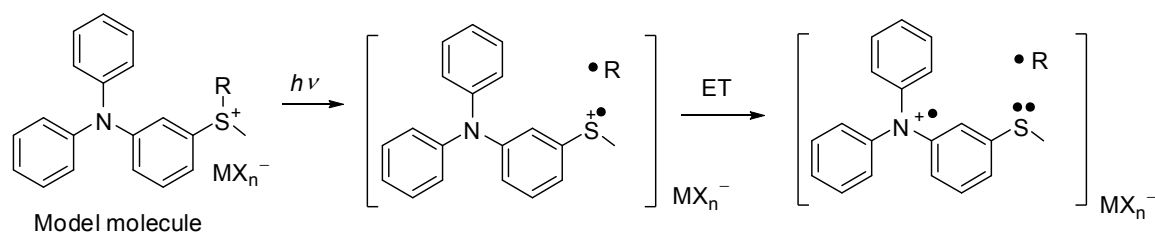


Figure 2.21 Stabilization of the radical cations by triarylamine substituent.

The molecules with both dimethyl **14** and methylbenzyl **15** substituents on the sulfonium at the *meta* position of triarylanimes have been synthesized and investigated by our group (Figure 2.22), and the high quantum yields for acid generation (~ 0.45) have been obtained.¹⁶⁹

2.3.2 Research goals

The goal of this research is to provide further information about this class of photoacid generators for mechanistic studies, and to serve as a simple model system to guide the development of two-photon acid generators. To achieve this goal, the effects of sulfonium substituents with different electron-withdrawing ability at different positions relative to amine on the quantum yield of photoacid generation were planned and studied. The target molecules, including both *meta* and *para* series, are shown on Figure 2.22. An additional example to the *meta* series is **16**, which has a methyl(*p*-cyanobenzyl) substituent that is more electron withdrawing than in **14** and **15**. For the *para* series, the corresponding dimethyl **17**, methylbenzyl **18**, and methyl(*p*-cyanobenzyl) **19** sulfonium salts were the targets. The free energy change of electron transfer, fluorescence quenching of the molecules due to electron transfer, and quantum yields of photoacid generation were also measured and/or calculated.

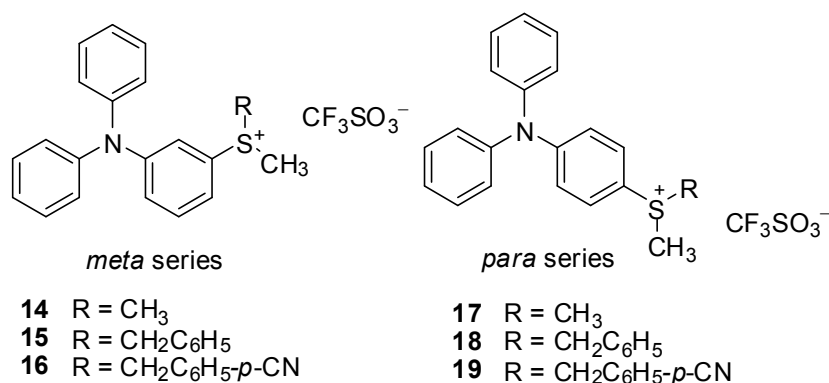


Figure 2.22 Target molecules of one-photon acid generators.

2.4 Synthesis of photoacid generators

2.4.1 Synthesis of a meta-substituted sulfonium salt

To study the electron withdrawing effect on acid generation in the *meta* series, compound **16** was prepared (Figure 2.23). The amination of 1,3-dibromobenzene and diphenylamine catalyzed by the palladium and *bis*(diphenylphosphino)ferrocene (DPPF) complex produced 3-bromo-*N,N*-diphenylaniline **20** in 56% yield. Then compound **20** was lithiated by *tert*-butyl lithium at $-78\text{ }^{\circ}\text{C}$, followed by addition of sulfur after the temperature was raised to room temperature. Once the solid sulfur was completely consumed, α -bromo-*p*-tolunitrile was added. Purification afforded the product **21** in 65% yield. The reaction of methyl trifluoromethanesulfonate and **21** at $-78\text{ }^{\circ}\text{C}$ in the dark gave the desired product **16** in 75% yield.

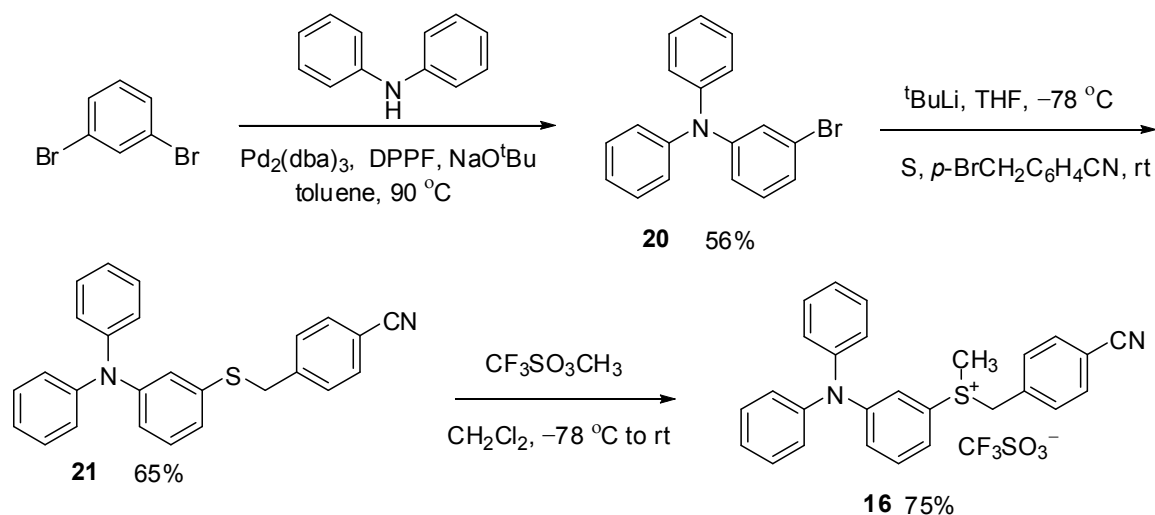


Figure 2.23 Synthesis of triarylamine sulfonium salt **16**.

2.4.2 Synthesis of *para*-substituted sulfonium salts

For the *para*-series, the corresponding dimethyl **17**, methylbenzyl **18**, and methyl(*p*-cyanobenzyl) **19** sulfonium salts were prepared (Figure 2.24). 1,4-Dibromobenzene was reacted with diphenylamine catalyzed by the palladium and DPPF complexes to give 4-bromo-*N,N*-diphenylaniline **22** in 58% yield. By using similar reaction procedures as shown in Figure 2.24, the monoalkylated sulfonium products **23** – **25** were obtained in 80%, 72% and 70% yields respectively, and the dialkyl-substituted sulfonium salts **17** – **19** were obtained in 65%, 49% and 95% yields respectively.

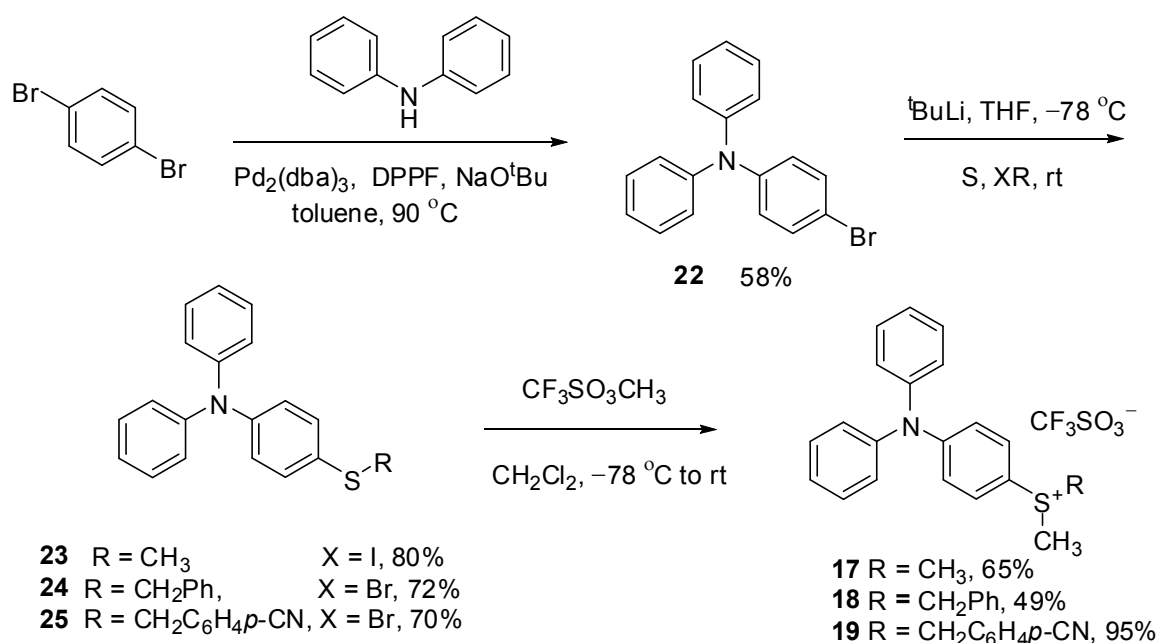


Figure 2.24 Synthesis of the *para*-substituted triarylamine sulfonium salts **17** – **19**.

2.5 Photochemical studies

The absorption and fluorescence spectra, and cyclic voltammetry were measured. Relative fluorescence intensities (I_{fl}) were calculated, the free energy change for electron transfer (ΔG_{et}) was estimated, and quantum yields of acid generation (Φ_{H^+}) were determined. Photochemical results are summarized in Table 2.1.

	<i>Meta</i> substituted salts			<i>Para</i> substituted salts		
	14	15	16	17	18	19
λ_{max}^{abs} nm	293	293	292	321	331	334
ϵ_{max} $10^4 M^{-1} cm^{-1}$	1.69	1.80	1.68	1.81	1.74	1.81
λ_{max}^{flu} nm	379	376	493	439	451	438
Φ_{H^+} ± 0.05	0.48	0.41	0.48	0.23	0.26	0.22
I_{fl}	0.02	0.02	–	0.17	0.08	0.07
ΔG_{et} kJ mol ⁻¹	-57.9	–	–	-21.9	-27.9	–

Table 2.1 One-photon physical data for photoacid generators **14** – **19** in acetonitrile.

2.5.1 Absorption spectra

The absorption spectra for PAGs **16** – **19** are shown in Figure 2.25. The maximum absorption wavelengths of *para* series are somewhat red-shifted relative to those of the *meta* series. This observation suggests a more extensive delocalization of the π system of *para* substitution, which is consistent with stabilization of the π^* -orbital by the sulfonium electron-withdrawing group at the *para*- position.

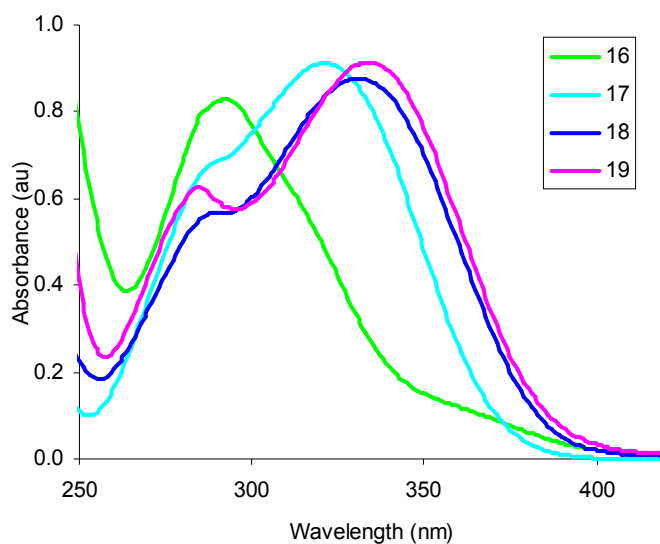


Figure 2.25 Absorption spectra of photoacid generators **16** – **19** in acetonitrile.

2.5.2 Fluorescence quenching

Fluorescence spectra of PAGs **17** – **19** are shown in Figure 2.26. The relative fluorescence intensity (I_{fl}) was defined as the maximum fluorescence intensity of the sulfonium salts relative to that of their parent chromophore, triphenylamine **26**, at the same concentration. For the *meta* series, the dimethyl and methylbenzyl PAGs showed substantially quenched fluorescence with an I_{fl} value of 0.02 for both.¹⁶⁹ For the *para*-substituted series, the I_{fl} values were 0.17 for dimethyl, 0.08 for methylbenzyl, and 0.07 for methyl(*p*-cyanobenzyl) PAGs. The *p*-cyanobenzyl group is the most electron-withdrawing group among the three derivatives, and therefore should stabilize the radical the most efficiently. Thus, the *para*-substituted *p*-cyanobenzyl salt has the lowest I_{fl} value in the series. In general, the I_{fl} -values for *meta*-substituted salts were lower than that for *para*-salts.

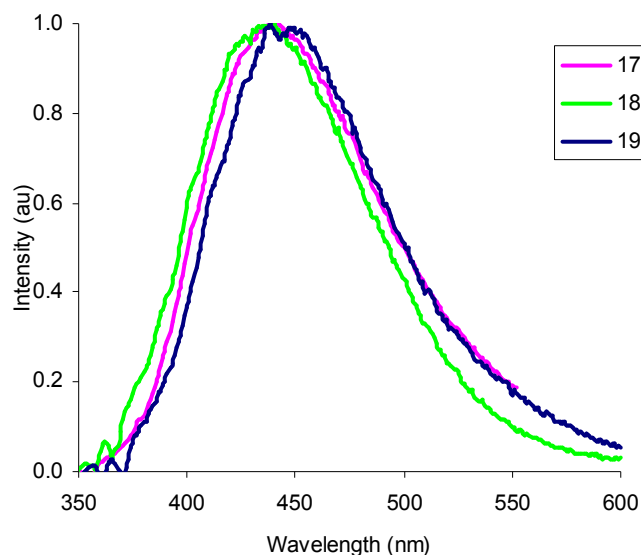


Figure 2.26 Fluorescence spectra of photoacid generators **17** – **19** in acetonitrile.

2.5.3 Free energy change for electron transfer

The free energy change of electron transfer can be estimated by using the Rehm-Weller equation (Eq 1.3, section 1.2.4).⁸² In the case of the electron transfer from the excited state of the triphenylamine moiety to the sulfonium group, the real reduction peak potential $E_{(A\cdot/A)}^{\text{red}}$ is used for the estimation since the reduction peak is irreversible. Both $E_{(D/D+\bullet)}^{1/2}$ and $E_{(A\cdot/A)}^{\text{red}}$ values can be measured from electrochemical data. $E_{(0,0)}$ was estimated as the energy at which the one-photon absorption onset of the chromophore is seen. Considering the neglect of E_{coul} and the conversion of energy units, the free energy change for electron transfer (ΔG_{et}) was estimated by Eq 2.1.

$$\Delta G_{\text{et}} = 23.06 [E_{(D/D+\bullet)}^{1/2} - E_{(A\cdot/A)}^{\text{red}}] - E_{(0,0)} \quad \text{Eq2.1}$$

The ΔG_{et} values of the *para*-substituted PAGs with methyl or benzyl groups are about the same (-21.9 and -27.9 kJ mol^{-1}), which are less negative than its *meta*-substituted analog (-57.9 kJ mol^{-1}). This indicates that the *meta*-dimethyl PAG has more a favorable electron transfer driving force.

2.5.4 Quantum yield of acid generation

The quantum yield of acid generation was determined by using the Scaiano's method,^{170,171} and the measurement details are described in section 2.8.1.

A quantum yield of acid generation for the *meta*-substituted methyl *p*-cyanobenzyl PAG is 0.48, which is the same as those of the dimethyl and methylbenzyl *meta*-substituted PAGs and triphenyl sulfonium triflate in the literature¹⁶⁹ within the uncertainty (± 0.05). The result shows the more stabilization of the radical fragment by more electron-withdrawing *p*-cyanobenzyl group does not enhance the acid generation.

For the *para*-substituted PAGs, the acid generation quantum yields of all three PAGs (~ 0.25) were also identical within the uncertainty (± 0.05), which is almost half as those of their *meta*- analogs.

2.6 Quantum-chemical calculations

Quantum-chemical calculations of *meta*- and *para*-triphenylamine dimethyl sulfonium salts, **14** and **17**, have been conducted by Dr. F. Furche (Universität Karlsruhe, Germany), Dr. E. Zojer and P. Pacher (Technical University of Graz, Austria), and Dr. Brédas (Georgia Technology Institute).

The ground states of **14** and **17** show the expected propeller-type structure (Figure 2.27). The phenyl ring that is attached to the sulfonium group is referred to a Ph', and the other two are called Ph. The Ph' plane forms a 25 – 30 degree angle relative to that of the nitrogen and the ipso carbon atoms of two Phs.

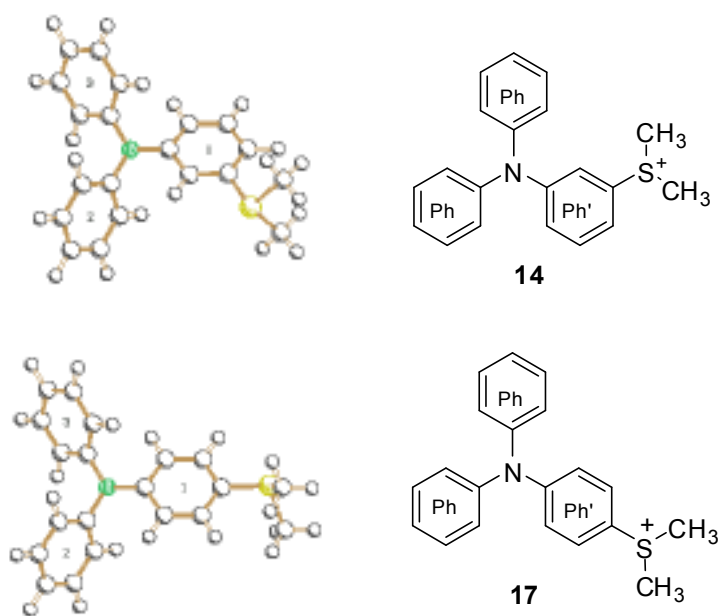


Figure 2.27 Optimized ground state structures of **14** and **17**.

The quantum-chemical calculations are based on time dependent density functional theory, and the contour plots of the frontier orbitals of **14** (Figure 2.28) and **17** (Figure 2.29) are qualitatively similar. The important similarities and differences are highlighted below.

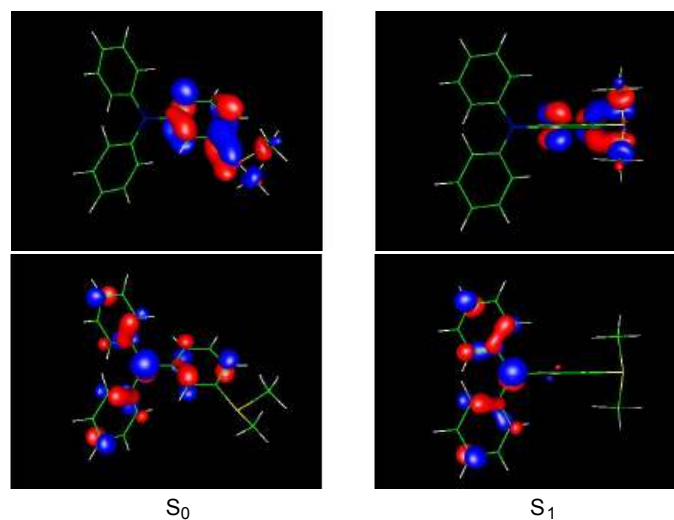


Figure 2.28 HOMO (lower) and LUMO (upper) of **14** in the ground state geometry S_0 (left) and the excited state geometry S_1 (right).

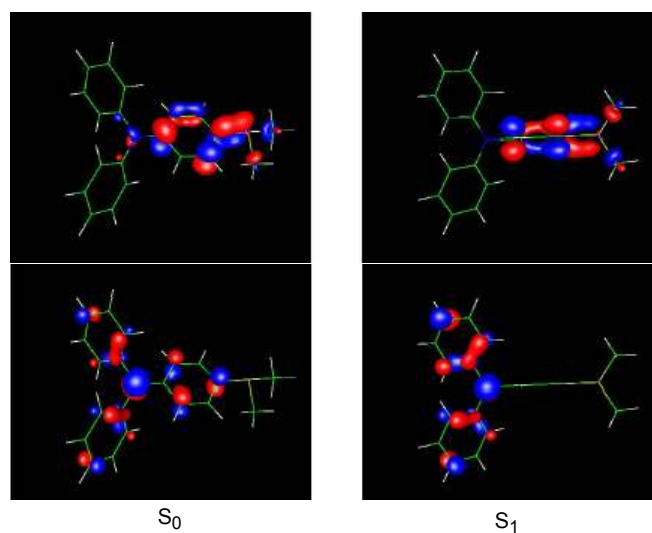


Figure 2.29 HOMO (lower) and LUMO (upper) of **17** in the ground state geometry S_0 (left) and the excited state geometry S_1 (right).

For both PAGs, the first excited state (S_1) may be described as a state in which an electron is promoted from HOMO to LUMO. Once formed, the Franck-Condon S_1 state undergoes a relaxation process to minimize its energy. This leads to the rotation of the least squares plane formed by the sulfur atom and the carbon atoms of Ph' into a position perpendicular to that of the nitrogen and the two ipso carbon atoms of Phs. The orbital distributions indicate the charge transfer from triphenyl amine group to the sulfonium group.

On the other hand, the optimized geometry of the LUMO of S_1 excited state shows some sulfur-methyl (S-CH₃) σ^* character from the contour plots of the frontier orbitals of **14** and **17**. The occupation by an electron of the LUMO weakens, but does not break, the S-CH₃ σ -bonds. The calculated bond lengths show that the S-CH₃ bonds of both **14** and **17** in the S_1 state are longer than that in the S_0 state. The lengthening of the S-CH₃ bond of **14** in the relaxed S_1 state is more extreme than that of **17**. This indicates the S-CH₃ bond breakage of **14** may be easier. The fact that the S-CH₃ bond does not break in the relaxed excited state suggests there is a barrier to bond cleavage. While calculation of the barrier is beyond the scope of the current work, we can compare the barrier of bond cleavage based on the Hammond postulate. Homolytic cleavage is calculated to be exothermic from the relaxed excited state, whereas it is endothermic from the ground state. The Hammond postulate states that in the exothermic reaction, the transition state will resemble the starting material. For both PAGs, it suggests that the structure of transition state resembles that of the relaxed excited state. The bond

lengthening in the relaxed excited state of **14** indicates the greater bond length of the transition state of **14**, which means a lower barrier in **14** versus **17** according to the Hammond postulate. In addition, the calculated oscillator strengths for fluorescence of **14** and **17** are 0.00 and 0.02 respectively, suggesting that fluorescence of **17** may compete to some extent with cleavage. All these results are consistent with the experimental observation that the *meta*-substituted PAGs have higher quantum yields of acid generation than that of *para*-substituted ones.

2.7 Discussion and conclusions

Three substituted groups with different electron-withdrawing ability (methyl, benzyl and *p*-cyanobenzyl) were studied at the both *para* and *meta* positions of the triphenyl sulfonium salts. Within the uncertainties of measurements (± 0.05), the acid generation quantum yields of all three *para*-substituted PAGs were identical (~ 0.25), and those for all their *meta*- analogs were also considered the same (~ 0.45). Thus, functional groups of methyl, benzyl and *p*-cyanobenzyl do not affect the quantum yield of acid generation.

The acid generation quantum yields of PAGs with *meta* sulfonium substituents are almost twice as high as their *para* analogs (0.45 versus 0.25). Other photochemical data also support this result. The free energy change for the electron transfer of the *meta*-dimethyl PAG is more than two times larger than its *para*-substituted analog (-57.9 versus -21.9 kJ mol⁻¹). This indicates that the *meta* PAG has a more favorable electron transfer driving force, and its corresponding lower relative fluorescence intensity (0.02) in comparison with the *para*- analog (0.17) suggests the higher electron transfer probability for the *meta*- PGA. In addition, the quantum-chemical calculations support the sulfur-methyl bond cleavage, and predict the higher quantum yields of acid generation of *meta*-substituted PAGs. Among the three *meta* PAGs, the triphenyl amine dimethyl sulfonium salt was selected for the preparation of two-photon acid generators for its comparably convenient synthesis.

2.8 Experimental: Quantum yield of acid generation

General experimental. Absorption spectra were run on a Hewlett-Packard model 8453 spectrophotometer. The fluorescence spectra were collected on a Jobin Yvon Spex Fluorolog-III fluorimeter. The photon parameters were measured by using a multi-functional optical meter of Newport model 1835-C. All electrochemical experiments were conducted using a BAS Model 100B/W cyclic voltammetry unit. The electrodes used were a glassy-carbon working electrode, a platinum auxiliary wire, and a Ag/AgCl pseudo-reference electrode. The supporting electrolyte was 0.1 M tetrabutylammonium hexafluorophosphate. The spectrophotometric grade acetonitrile (Aldrich) were used as received in all the measurements.

The quantum yield of acid generation is defined as the number of acid molecules created per photon absorbed. In this measurement, the concentration of the test solution was kept sufficiently low to ensure that all the photons that reach the solution are absorbed by the molecules. The monochromatic xenon lamp of Fluorolog-III fluorimeter was used as the irradiation source. The relative intensity of the light reaching the sample was measured as the reference current, which is generated by the internal reference detector of the instrument. The reference current is linearly proportional to the dose rate (number of photon delivered to the cuvette per unit time, photon s^{-1}). The dose rate can be adjusted by changing the slit width of the monochromator. The absolute dose rate over a range of slit widths was determined by Dr. S. Kuebler. The absorption rate (the rate at which photons are absorbed, photon s^{-1}) was determined by using the well-established

ferrioxalate actinometry method.¹⁷² The dose rate measurements were corrected to take into account the reflection loss from the cuvette windows. In this way, a calibration curve was obtained for the dose rate (photon s^{-1}) at the sample as a function of the reference current (μA). Thus, the slope of the dose rate calibration curve determined the power parameter (photon $s^{-1} \mu A^{-1}$) of a certain wavelength within a range of silt widths. The uncertainty of power parameter measurement by this method was 0.3. The absorbed photon number was calculated by the following photon calibration equation (Eq 2.2).

$$\text{absorbed photon number} = \text{power parameters (photon } s^{-1} \mu A^{-1}) \times \text{reference current } (\mu A) \times \text{time (s)} \quad \text{Eq 2.2}$$

The acid number generated by the PAGs was measured by using rhodamine B base (**RB**) as an indicator.^{170,171} The lactone ring opening of **RB** upon protonation generates its acid form (**RB⁺**), which shows a characteristic maximum absorbance at 555 nm (Figure 2.30). The acid concentration was quantitatively determined by using the absorbance at 555 nm of **RB⁺**.

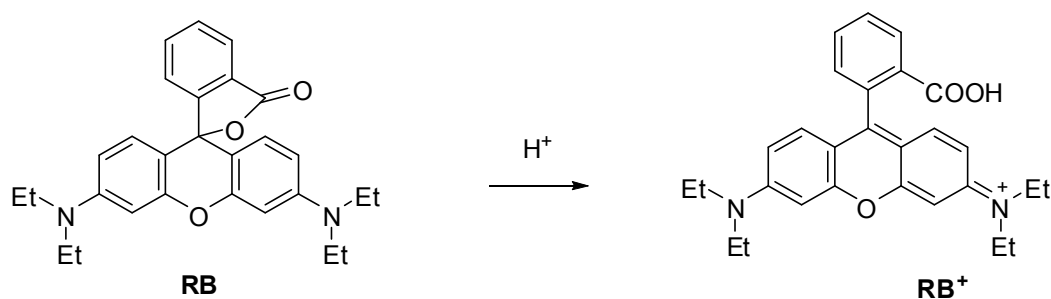


Figure 2.30 Protonation of Rhodamine B base (**RB**).

An acid calibration equation was determined by titration of a solution of **RB** (2.5×10^{-3} M, acetonitrile) with a solution of *p*-toluenesulfonic acid (2.0×10^{-4} M, acetonitrile). Each time, a known amount of the acid solution was added, and the absorbance of **RB**⁺ at 555 nm was recorded. The acid calibration curve was then plotted by absorbance at 555 nm versus acid concentration. The calibration equation of acid concentration versus the absorbance at 555 nm (Eq 2.3) was determined by the average of all six measurements within the uncertainties.

$$\begin{array}{l} \text{acid concentration} \\ (\text{mol L}^{-1}) \end{array} = 9.67 \times 10^6 \times \text{absorbance} + 2.25 \times 10^6 \quad \text{Eq 2.3}$$

The acid number generated by the PAGs is calculated by the product of the acid concentration, the volume of the test solution and the Avogadro's number N_A (Eq 2.4).

$$\begin{array}{l} \text{acid number} \\ \text{generated} \end{array} = \begin{array}{l} \text{acid concentration} \\ (\text{mol L}^{-1}) \end{array} \times \begin{array}{l} \text{volume} \\ (\text{L}) \end{array} \times \begin{array}{l} N_A \\ (\text{H}^+ \text{mol}^{-1}) \end{array} \quad \text{Eq 2.4}$$

For the actual measurements, the irradiation wavelength of the fluorimeter was set to 294 nm for the *meta*-substituted salts and 330 nm for the *para*-substituted derivatives based on their maximum absorption wavelengths. The power parameters were measured to be 4.15×10^{15} photon $\text{s}^{-1} \mu\text{A}^{-1}$ at 294 nm and 3.89×10^{15} photon $\text{s}^{-1} \mu\text{A}^{-1}$ at 330 nm. A sample solution of a PAG (1.5×10^{-4} M, acetonitrile) was prepared, and was irradiated at the excitation wavelength. Immediately after irradiation for a certain time, the reference current was recorded, and the **RB** solution (50.0 μl , 2.5×10^{-3} M, acetonitrile)

was added to the cuvette. The absorption spectrum of the solution was measured and the absorbance at 555 nm was recorded. The photon number absorbed by the PAGs was calculated by the Eq 2.2, and the acid number generated by the PAGs upon irradiation was calculated by the Eq 2.3 and Eq 2.4. A plot of acid number versus photon number was linear, and the slope indicates the value of the quantum yield of acid generation (Figure 2.31). The total uncertainty of the quantum yield of acid generation was 0.05, taking into account of the uncertainties of power parameter and acid concentration.

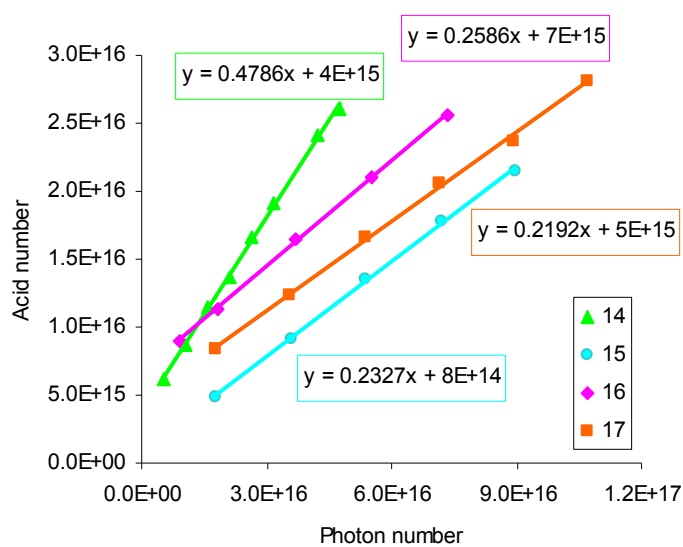
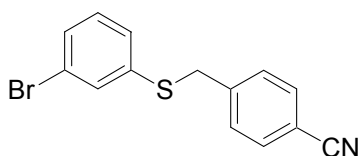


Figure 2.31 Measurement of quantum yield of acid generation of the PAGs 14 – 17.

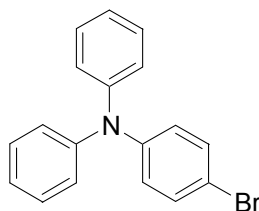
2.9 Experimental: synthetic procedures

General experimental. NMR spectroscopy was performed using either a DRX-500 MHz or Varian Unity Plus-300 MHz spectrometer. Mass spectrometry (MS) was performed by the MS Instrument Facility at the University of Arizona. The combustion experiments for elemental analysis were performed by Desert Analytics, Tucson, Arizona. Flash chromatography was performed using 40 – 63 μm silica gel (EMD Chemical, Inc.). TLC was performed on precoated plates containing a fluorescent indicator (silica gel 60 F₂₅₄, EMD Chemicals, Inc.) All reagents and solvents including dry solvents and anhydrous solvents in Acrosealed bottles were purchased from readily available suppliers (Aldrich, VWR), and were used as received. The general precautions for preparation of light sensitive compounds mentioned in this section include wrapping the reaction flask with aluminum foil and performing the subsequent workup and purification in the dark under the weak red light. These precautions are applied in all cases where it is indicated that the compound is light sensitive.



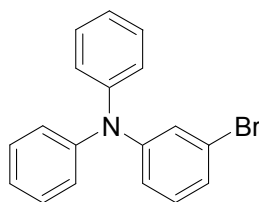
4-((3-Bromophenyl)thio)methylbenzonitrile. To a solution of sodium methoxide prepared from sodium (0.23 g, 10 mmol) in anhydrous methanol (20 ml) was added 3-bromobenzenethiol (1.00 g, 5.02 mmol) at room temperature under nitrogen pressure. After 30 min, a solution of α -bromo-*p*-tolunitrile (0.99 g, 5.1 mmol) in anhydrous methanol (20 mL) was added dropwise, and then the reaction mixture was

stirred overnight. After quenching with an aqueous sodium hydroxide solution (2.0 M) until the solution was basic, the reaction mixture was extracted with diethyl ether (3 × 30 mL). The combined organic layers were washed with aqueous saturated brine and were dried over magnesium sulfate. After filtration and concentration by using rotary evaporation, the pure product (1.25 g) was obtained in 82% yield after flash column chromatography (hexane: ethyl acetate 8:1). ¹H NMR (500 MHz, chloroform-*d*) δ 7.55 (d, *J* = 8.5 Hz, 2H), 7.40 (t, *J* = 2.0 Hz, 1H), 7.35 (d, *J* = 8.0 Hz, 2H), 7.31 (dt, *J* = 7.5 Hz, *J* = 1.5 Hz, 1H), 7.16 (d, *J* = 8.0 Hz, 1H), 7.10 (t, *J* = 7.5 Hz, 1H), 4.10 (s, 2H). ¹³C NMR (125 MHz, chloroform-*d*) δ 142.4, 137.1, 132.4, 132.1, 130.2, 129.8, 129.3, 128.4, 122.6, 118.5, 110.9, 38.5. The data were consistent with the literature data.¹⁷³

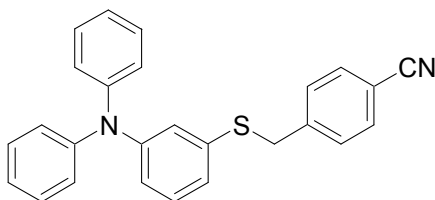


4-Bromo-*N,N*-diphenylaniline. To a solution of *tris*(dibenzylideneacetone) dipalladium(0) (Pd₂(dba)₃) (0.54 g, 0.59 mmol) and *bis*(diphenylphosphino)ferrocene (DPPF) (0.41 g, 0.74 mmol) in dry toluene (100 mL) was added 1,4-dibromobenzene (27.92 g, 118.3 mmol) under nitrogen pressure at room temperature. After 10 min, sodium *tert*-butoxide (13.40 g, 0.14 mol) and diphenylamine (10.32 g, 59.20 mmol) were added. The reaction mixture then was heated to 90 °C, and was stirred for 24 hours under nitrogen pressure. After quenching with water (100 mL), the mixture was extracted with diethyl ether (3 × 100 mL) and the combined organic layers were dried over magnesium

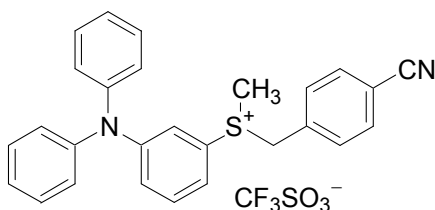
sulfate. The pure product (11.41 g) was obtained in 58% yield after flash column chromatography (1% ethyl acetate in hexane). ^1H NMR (500 MHz, chloroform-*d*) δ 7.32 (d, $J = 8.5$ Hz, 2H), 7.25 (d, $J = 7.5$ Hz, 4H), 7.03 (t, $J = 7.5$ Hz, 8H), 6.94 (d, $J = 9.0$ Hz, 2H). The data were consistent with the literature data.^{174,175}



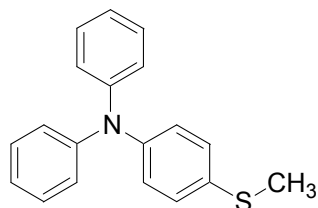
3-Bromo-*N,N*-diphenylaniline. To a solution of *tris*(dibenzylideneacetone) dipalladium(0) ($\text{Pd}_2(\text{dba})_3$) (0.40 g, 0.44 mmol) and *bis*(diphenylphosphino)ferrocene (DPPF) (0.30 g, 0.53 mmol) in dry toluene (100 mL) was added 1,3-dibromobenzene (10.63 g, 43.70 mmol) under nitrogen pressure at room temperature. After 10 min, sodium *tert*-butoxide (6.70 g, 64.3 mmol) and diphenylamine (5.00 g, 29.2 mmol) were added. The reaction mixture then was heated to 90 °C, and was stirred for 24 hours under nitrogen pressure. After quenching with water (100 mL), the mixture was extracted with diethyl ether (3×100 mL) and the combined organic layers were dried over magnesium sulfate. The pure product (5.30 g) was obtained in 56% yield after flash column chromatography (1% ethyl acetate in hexane). ^1H NMR (500 MHz, chloroform-*d*) δ 7.27 (t, $J = 8.0$ Hz, 4H), 7.19 (t, $J = 1.0$ Hz, 1H), 7.11 – 7.04 (m, 8H), 6.97 (dt, $J = 7.0$ Hz, $J = 2.0$ Hz, 1H). The ^1H NMR data were consistent with the literature data.^{176,177}



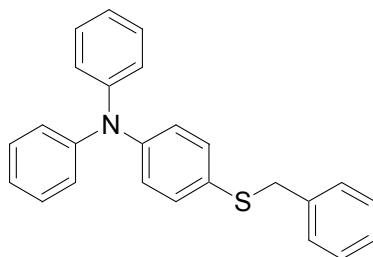
4-(3-(Diphenylamino)phenylthio)methylbenzonitrile. To a solution of 3-bromo-*N,N*-diphenylaniline (3.56 g, 11.0 mmol) in dry tetrahydrofuran (150 mL) at -78 °C, under nitrogen pressure was added *tert*-butyl lithium (14.2 mL, 1.7 M, 24.20 mmol). After 30 min, the reaction mixture was allowed to slowly rise to room temperature. Then sulfur (0.41 g, 12 mmol) was added with a brisk stream of nitrogen passing through the open system to exclude air. When sulfur was consumed, α -bromo-*p*-tolunitrile (2.18 g, 11.0 mmol) was added, and the mixture was stirred at room temperature for 1 hour. The solvent was removed under reduced pressure, and water (100 mL) was added to the residue. The mixture was extracted with diethyl ether (3×100 mL) and the combined organic layers were dried over magnesium sulfate. The pure product (2.78 g) was obtained in 65% yield after flash column chromatography (2% and then 5% ethyl acetate in hexane). ^1H NMR (500 MHz, chloroform-*d*) δ 7.62 (d, $J = 6.5$ Hz, 2H), 7.31 – 7.24 (m, 6H), 7.14 – 7.05 (m, 8H), 6.98 (d, $J = 7.5$ Hz, 1H), 6.89 (d, $J = 6.5$ Hz, 1H), 3.85 (s, 2H). ^{13}C NMR (125 MHz, chloroform-*d*) δ 147.9, 146.6, 141.3, 136.4, 131.5, 129.4, 128.9, 128.7, 123.9, 122.7, 121.1, 120.9, 120.3, 117.9, 110.5, 41.8. MS (EI+) m/z (rel intensity, %) 392 (M^+ , 49), 243 ($\text{M}^+ - \text{SCH}_2\text{PhCN}$, 100). HRMS (FAB+) m/z : Calcd. for $\text{C}_{26}\text{H}_{20}\text{N}_2\text{S}$ (M^+) 392.1347, Found 392.1350. Anal. Calcd. for $\text{C}_{26}\text{H}_{20}\text{N}_2\text{S}$: C, 79.56; H, 5.14; N, 7.14. Found: C, 79.77; H, 5.20; N, 7.23.



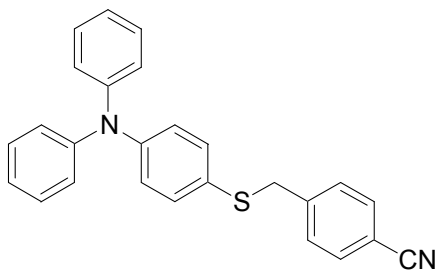
(3-(Diphenylamino)phenyl)(4-cyanobenzyl)methyl sulfonium trifluoromethanesulfonate. To a solution of 4-(3-(diphenylamino)phenylthio)methylbenzonitrile (1.08 g, 2.75 mmol) in dry dichloromethane (30 mL) under nitrogen at $-78\text{ }^{\circ}\text{C}$ was added methyl trifluoromethanesulfonate (0.41 mL, 0.59 g, 3.6 mmol). The reaction mixture was stirred for 30 min at the same temperature, and then it was allowed to slowly rise to room temperature overnight. After the solvent was removed by rotary evaporation, diethyl ether ($2 \times 50\text{ mL}$) was added to wash the product. The oily product was dried under high vacuum, and the solid pure product (1.15 g) was obtained in 75% yield. The product is light sensitive. ^1H NMR (500 MHz, chloroform-*d*) δ 7.58 (d, $J = 8.0\text{ Hz}$, 2H), 7.55 (dd, $J = 8.0\text{ Hz}$, $J = 1.0\text{ Hz}$, 1H), 7.47 (t, $J = 8.0\text{ Hz}$, 1H), 7.35 (d, $J = 8.0\text{ Hz}$, 2H), 7.30 (t, $J = 7.5\text{ Hz}$, 4H), 7.23 (dd, $J = 8.5\text{ Hz}$, $J = 1.5\text{ Hz}$, 1H), 7.15 (t, $J = 7.5\text{ Hz}$, 2H), 6.92 (d, $J = 8.5\text{ Hz}$, 4H), 6.74 (t, $J = 2\text{ Hz}$, 1H), 5.30 (d, $J = 12.5\text{ Hz}$, 1H), 4.92 (d, $J = 12.5\text{ Hz}$, 1H), 3.42 (s, 3H). ^{13}C NMR (125 MHz, chloroform-*d*) δ 149.6, 145.5, 132.8, 132.7, 132.5, 131.5, 129.9, 125.9, 125.4, 125.4, 122.7, 122.0, 120.1, 117.8, 113.8, 50.6, 25.8 (A carbon peak from CF_3 was not observed). HRMS (FAB+) m/z : Calcd. for $\text{C}_{27}\text{H}_{23}\text{N}_2\text{S}$ ($\text{M}^+ - \text{CF}_3\text{SO}_3$) 407.1582, Found 407.1577. Anal. Calcd. for $\text{C}_{28}\text{H}_{23}\text{N}_2\text{O}_3\text{S}_2$: C, 60.42; H, 4.16; N, 5.03. Found: C, 60.04; H, 4.08; N, 4.75.



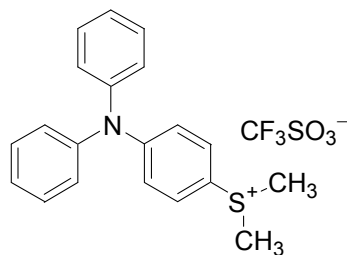
4-(Methylthio)-*N,N*-diphenylaniline. To a solution of 4-bromo-*N,N*-diphenylaniline (1.05 g, 3.24 mmol) in dry tetrahydrofuran (50 mL) at $-78\text{ }^{\circ}\text{C}$ under nitrogen pressure was added *tert*-butyl lithium (4.2 mL, 1.7 M, 7.3 mmol). After 30 min, the reaction mixture was allowed to slowly rise to room temperature. Then sulfur (0.13 g, 3.9 mmol) was added with a brisk stream of nitrogen passing through the open system to exclude air. When sulfur was consumed, methyl bromide (0.61 g, 4.2 mmol) in dry tetrahydrofuran (2 mL) was added, and the mixture was stirred at room temperature for 1 hour. The solvent was removed by rotary evaporation, and water (50 mL) was added to the residue. The mixture was extracted with diethyl ether ($3 \times 60\text{ mL}$) and the combined organic layers were dried over magnesium sulfate. The product (0.75 g) was obtained in 80% yield after flash column chromatography (1% ethyl acetate in hexane). ^1H NMR (500 MHz, chloroform-*d*) δ 7.23 (t, $J = 8.0\text{ Hz}$, 4H), 7.19 (d, $J = 8.5\text{ Hz}$, 2H), 7.09 (d, $J = 9.0\text{ Hz}$, 4H), 7.04 – 7.00 (m, 4H), 2.48 (s, 3H). ^{13}C NMR (125 MHz, chloroform-*d*) δ 147.6, 145.6, 129.2, 128.6, 124.7, 124.6, 124.0, 122.7, 16.9. MS (EI+) m/z (relative intensity, %) 323 (M^+ , 100), 276 ($\text{M}^+ - \text{CH}_3$, 86). HRMS (FAB+) m/z : Calcd. for $\text{C}_{19}\text{H}_{17}\text{NS}$ (M^+) 291.1082, Found 291.1088. Anal. Calcd. for $\text{C}_{19}\text{H}_{17}\text{NS}$: C, 78.31; H, 5.88; N, 4.81. Found: C, 78.39; H, 5.79; N, 4.46.



4-(Benzylthio)-*N,N*-diphenylaniline. To a solution of 4-bromo-*N,N*-diphenylaniline (2.85 g, 8.80 mmol) in dry tetrahydrofuran (100 mL) at $-78\text{ }^{\circ}\text{C}$ under nitrogen flow was added *tert*-butyl lithium (11.4 mL, 1.7 M, 19.4 mmol). After 30 min, the reaction mixture was allowed to slowly rise to room temperature. Then sulfur (0.31 g, 9.7 mmol) was added with a brisk stream of nitrogen passing through the open system to exclude air. When sulfur was consumed, benzyl bromide (1.51 g, 8.80 mmol) was added, and the mixture was stirred at room temperature for 1 hour. The solvent was removed under reduced pressure, and water (100 mL) was added to the residue. The mixture was extracted with diethyl ether ($3 \times 100\text{ mL}$) and the combined organic layers were dried over magnesium sulfate. The pure product (2.31 g) was obtained in 72% yield after flash column chromatography (1% ethyl acetate in hexane). ^1H NMR (500 MHz, chloroform-*d*) δ 7.36 – 7.27 (m, 9H), 7.24 (d, $J = 9.0\text{ Hz}$, 2H), 7.14 (d, $J = 7.5\text{ Hz}$, 4H), 7.08 (t, $J = 7.5\text{ Hz}$, 2H), 7.02 (d, $J = 8.5\text{ Hz}$, 2H), 4.05 (s, 2H). ^{13}C NMR (125 MHz, chloroform-*d*) δ 147.4, 146.9, 137.8, 132.3, 129.2, 128.9, 128.4, 127.0, 124.5, 124.3, 123.9, 122.9, 40.3. MS (EI+) m/z (rel intensity, %): 367 (M^+ , 65), 276 ($\text{M}^+ - \text{CH}_2\text{Ph}$, 100). HRMS (FAB+) m/z : Calcd. for $\text{C}_{25}\text{H}_{21}\text{NS}$ 367.1395 (M^+) Found 367.1393. Anal. Calcd. for $\text{C}_{25}\text{H}_{21}\text{NS}$: C, 81.70; H, 5.76; N, 3.81. Found: C, 81.61; H, 5.73; N, 3.86.

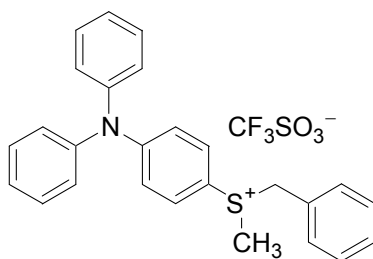


4-(4-(Diphenylamino)phenylthio)methylbenzonitrile. To a solution of 4-bromo-*N,N*-diphenylaniline (5.56 g, 17.2 mmol) in dry tetrahydrofuran (150 mL) at -78 °C under nitrogen pressure was added *tert*-butyl lithium (22.2 mL, 1.7 M, 37.7 mmol). After 30 min, the reaction mixture was allowed to slowly rise to room temperature. Then sulfur (0.62 g, 18 mmol) was added with a brisk stream of nitrogen passing through the open system to exclude air. When sulfur was consumed, α -bromo-*p*-tolunitrile (3.40 g, 17.2 mmol) was added, and the mixture was stirred at room temperature for 1 hour. The solvent was removed under reduced pressure, and water (80 mL) was added to the residue. The mixture was extracted with diethyl ether (3×150 mL) and the combined organic layers were dried over magnesium sulfate. The product (4.71 g) was obtained in 70% yield after flash column chromatography (2% and then 5% ethyl acetate in hexane). ^1H NMR (500 MHz, chloroform-*d*) δ 7.56 (d, $J = 8.5$ Hz, 2H), 7.31 (d, $J = 8.0$ Hz, 2H), 7.27 (t, $J = 7.5$ Hz, 4H), 7.12 (d, $J = 8.5$ Hz, 2H), 7.06 (m, 6H), 6.93 (d, $J = 8.5$ Hz, 2H), 4.02 (s, 2H). ^{13}C NMR (125 MHz, chloroform-*d*) δ 147.6, 147.2, 143.7, 133.3, 132.1, 129.6, 129.3, 126.2, 124.6, 123.3, 123.3, 118.8, 110.7, 40.4. MS (EI⁺) m/z (rel intensity, %): 392 (M^+ , 32), 276 ($\text{M}^+ - \text{CH}_2\text{PhCN}$, 100). HRMS (FAB⁺) m/z : Calcd. for $\text{C}_{26}\text{H}_{20}\text{N}_2\text{S}$ (M^+) 392.1347, Found 392.1350. Anal. Calcd. for $\text{C}_{26}\text{H}_{20}\text{N}_2\text{S}$: C, 79.56; H, 5.76; N, 7.14. Found: C, 79.35; H, 5.07; N, 7.09.



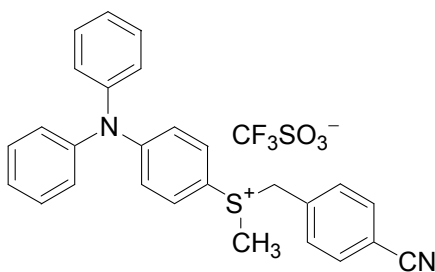
(4-(Diphenylamino)phenyl)dimethylsulfonium trifluoromethanesulfonate. To

a solution of 4-(methylthio)-*N,N*-diphenylaniline (0.51 g, 1.77 mmol) in dry dichloromethane (20 mL) under nitrogen at -78 °C was added methyl trifluoromethanesulfonate (0.15 mL, 0.22 g, 1.8 mmol). The reaction mixture was stirred for 30 min at the same temperature, and then it was allowed to slowly rise to room temperature overnight. After the solvent was removed by rotary evaporation, diethyl ether (60 mL) was added to the residue. White crystals were formed slowly. Filtration followed by washing with diethyl ether (3×30 mL) afforded the pure product (0.77 g) in 96% yield. The product is light sensitive. ^1H NMR (500 MHz, chloroform-*d*) δ 7.67 (d, $J = 8.5$ Hz, 2H), 7.37 (t, $J = 8.0$ Hz, 4H), 7.22 (t, $J = 7.5$ Hz, 2H), 7.17 (d, $J = 8.5$ Hz, 4H), 7.06 (d, $J = 9.5$ Hz, 2H), 3.29 (s, 6H). ^{13}C NMR (125 MHz, chloroform-*d*) δ 153.5, 145.2, 131.1, 129.9, 126.5, 125.9, 120.2, 111.1, 29.9. A carbon peak from CF_3 was not observed. HRMS (FAB+) m/z : Calcd. for $\text{C}_{20}\text{H}_{20}\text{NS}$ ($\text{M}^+ - \text{CF}_3\text{SO}_3$) 306.1316, Found 306.1316. Anal. Calcd. for $\text{C}_{21}\text{H}_{20}\text{F}_3\text{NO}_3\text{S}_2$: C, 55.37; H, 4.43; N, 3.07. Found: C, 54.98; H, 4.43; N, 3.07.



(4-(Diphenylamino)phenyl)methylbenzylsulfonium trifluoromethane-

sulfonate. To a solution of 4-(benzylthio)-*N,N*-diphenylaniline (0.75 g, 2.0 mmol) in dry dichloromethane (20 mL) under nitrogen pressure at $-78\text{ }^{\circ}\text{C}$ was added methyl trifluoromethanesulfonate (0.35 mL, 0.50 g, 3.1 mmol). The reaction mixture was stirred for 30 min at the same temperature, and then it was allowed to slowly rise to room temperature overnight. After the solvent was removed by rotary evaporation, diethyl ether ($2 \times 50\text{ mL}$) was added to wash the product. The oily product was dried under high vacuum, and the solid product (0.53 g) was obtained in 49% yield. The product is light sensitive. ^1H NMR (500 MHz, chloroform-*d*) δ 7.44 (d, $J = 8.5\text{ Hz}$, 2H), 7.36 – 7.26 (m, 9H), 7.20 (t, $J = 7.5\text{ Hz}$, 2H), 7.13 (d, $J = 7.5\text{ Hz}$, 4H), 6.97 (d, $J = 8.5\text{ Hz}$, 2H), 5.07 (d, $J = 12.5\text{ Hz}$, 1H), 4.79 (d, $J = 12.0\text{ Hz}$, 1H), 3.27 (s, 3H). ^{13}C NMR (125 MHz, chloroform-*d*) δ 153.5, 145.1, 132.0, 130.9, 129.9, 129.2, 127.2, 126.5, 126.4, 125.9, 119.9, 108.3, 51.9, 26.0 (A carbon peak from CF_3 was not observed). HRMS (FAB+) m/z : Calcd. for $\text{C}_{26}\text{H}_{24}\text{NS} (\text{M}^+ - \text{CF}_3\text{SO}_3)$ 382.1629, Found 382.1634. Anal. Calcd. for $\text{C}_{27}\text{H}_{24}\text{F}_3\text{NO}_3\text{S}_2$: C, 61.00; H, 4.55; N, 2.63. Found: C, 60.08; H, 4.61; N, 2.65.



(4-(Diphenylamino)phenyl)(4-cyanobenzyl)methyl sulfonium trifluoromethanesulfonate. To a solution of 4-(4-(diphenylamino)phenylthio)methylbenzonitrile (0.92 g, 2.3 mmol) in dry dichloromethane (20 mL) under nitrogen at $-78\text{ }^{\circ}\text{C}$ was added methyl trifluoromethanesulfonate (0.40 mL, 0.58 g, 0.40 mmol). The reaction mixture was stirred for 30 min at the same temperature, and then allowed to slowly rise to room temperature overnight. After the solvent was removed by rotary evaporation, diethyl ether (60 mL) was added to the residue. White crystals were formed slowly. Filtration followed by washing with diethyl ether ($3 \times 30\text{ mL}$) afforded the pure product (1.02 g) in 95% yield. The product is light sensitive. ^1H NMR (500 MHz, chloroform-*d*) δ 7.58 (d, $J = 8.5\text{ Hz}$, 2H), 7.47 – 7.37 (m, 8H), 7.24 (t, $J = 7.0\text{ Hz}$, 2H), 7.14 (d, $J = 9.0\text{ Hz}$, 4H), 6.96 (d, $J = 8.5\text{ Hz}$, 2d), 5.22 (d, $J = 12.5\text{ Hz}$, 1H), 4.95 (d, $J = 12.5\text{ Hz}$, 1H), 3.37 (s, 3H). ^{13}C NMR (125 MHz, chloroform-*d*) δ 153.8, 144.8, 133.1, 132.8, 132.1, 131.5, 130.1, 126.6, 126.3, 119.6, 117.9, 113.8, 106.8, 50.8, 27.1 (A carbon peak from CF_3 was not observed). HRMS (FAB+) m/z : Calcd. for $\text{C}_{27}\text{H}_{23}\text{N}_2\text{S}$ ($\text{M}^+ - \text{CF}_3\text{SO}_3$) 407.1582, found 407.1593. Anal. Calcd. for $\text{C}_{28}\text{H}_{23}\text{F}_3\text{NO}_3\text{S}_2$: C, 60.42; H, 4.16; N, 5.03. Found: C, 60.04; H, 4.23; N, 4.86.

3. TWO-PHOTON ACID GENERATORS

3.1 Introduction to two-photon induced polymerization

Due to the current demand for device miniaturization, particularly in microelectromechanical systems, the development of new fabrication techniques to free-form fabricate three dimensional microstructures, pattern a variety of materials, and couple nano- and micro-scale objects to each other has attracted intense attention.^{178,179} Two-photon induced polymerization has unique merits arising from intrinsic advantages of two-photon absorption. First, the probability of two-photon absorption depends quadratically on light intensity. By using focused laser beams, the excitation can be confined to a volume around the focal point (V) approximately the cube of the two-photon excitation wavelength ($V \propto \lambda^3$).¹⁸⁰ Subsequent photo-induced processes, such as fluorescence or chemical reactions, can therefore also be localized in this small volume. Secondly, the two-photon excitation can potentially be performed in the visible or near-infrared wavelength region, where common monomers and polymers have negligible linear absorption. As a result, laser beams at these wavelengths penetrate more deeply into materials, and directly induce polymerization within the focal volume without affecting the surrounding medium.

Two-photon polymerization was first experimentally reported in 1965 by Pao and Rentzepis.¹⁸¹ They successfully polymerized *p*-isopropyl- and chlorine-styrene through direct two-photon excitation of the monomers using pulsed Ruby laser (694 nm) with a peak power of 3×10^{-5} W. Several subsequent reports in this area are scattered in the literature.¹⁸²⁻¹⁸⁴ In 1997, two-photon induced polymerization was applied in three-

dimension lithographic microfabrication (3DLM),¹¹ which brought two-photon curable resins into the realm of micro-nanofabrication. Since then, high-fidelity micro-nanostructures with complex three-dimensional forms and feature sizes as small as 100 – 200 nm have been produced by two-photon induced polymerization.^{13,43,185,186} These achievements have demonstrated the potential of two-photon induced polymerization for 3DLM.

In general, photoinduced polymerization reactions are classified into two categories: radical photopolymerization and cationic photopolymerization. Their initiation reactions that are typically used for laser 3DLM are shown in Figure 3.1. Resins containing acrylate monomers or oligomers undergo radical type reactions. Most current work in patterning structures using two-photon radical polymerization has utilized commercial acrylate resins and conventional photoinitiators.^{11,185} In Chapter 4, two-photon radical polymerization will be reviewed, and the results from our group on the development of two-photon radical generators will be discussed. Cationic photopolymerization, which is generally based on the ring opening of the oxirane or epoxide group, has been less fully explored than radical polymerization. In this chapter, the application of two-photon cationic polymerization in 3DLM, especially the development of two-photon acid generators, will be presented.

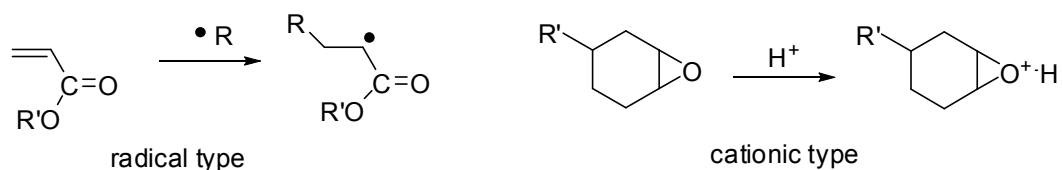


Figure 3.1 Initiation reactions typically used for laser 3DLM.

3.2 Two-photon acid generators

3.2.1 Introduction

Cationic polymerization generally features with high polymerization efficiency upon light irradiation, fast reaction time, low dark polymerization, and less shrinkage after polymerization to facilitate the high 3DLM fidelity.³⁰ As discussed previously in Chapter 2, photoacid generators are the major player for initiation of photon-induced cationic polymerization. In addition, photoacid generators have also been used in positive tone resist approach for 3DLM, as the lower viscosity products produced can be easily washed away during the development, which is important for the fabrication of complicated structures. Thus, current research efforts in this area are largely devoted to synthesis of highly efficient two-photon acid generators and two-photon sensitizers.^{12,31,43,186,187} In this section, the concepts of the negative/positive tone resist 3DLM will be introduced, then the two-photon acid generators and their applications reported in the literature will be reviewed, and finally the contribution from our group to this area will be discussed.

3.2.2 Negative and positive tone resists

Photoresists are light-sensitive materials that are classified into two groups, negative tone resists and positive tone resists. A negative tone resist is a type of photoresist in which the portion that is exposed to light becomes relatively insoluble to the developer, for example by polymerization or cross-linking, and the unexposed portion is soluble in the developer. The developer solution removes only the unexposed portions, leaving behind the structure on the surface wherever it is exposed as shown in the Figure 3.2. If a mask is used for negative tone resists, the final structure contains the inverse (or photographic "negative") of the pattern of the mask.

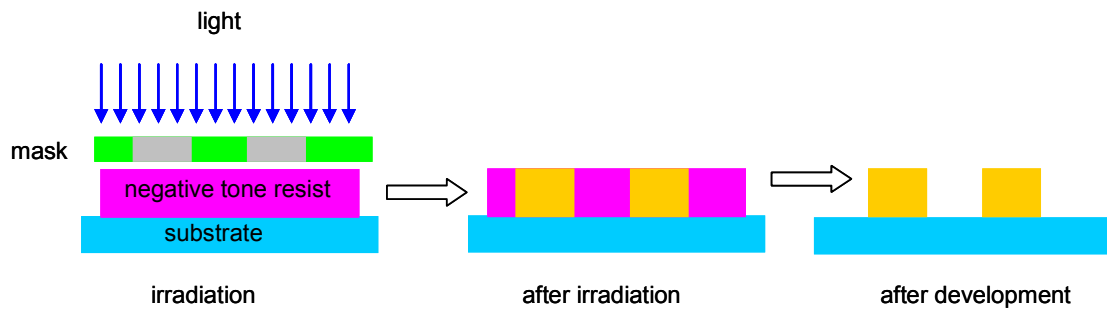


Figure 3.2 Negative tone resist approach.

Positive tone resists behave in just the opposite manner. A positive tone resist is a type of photoresist in which the portion that is exposed to light becomes soluble to the developer, for example by decomposing polymers, and the portion that is unexposed remains insoluble to the developer. The exposed resist is then washed away by the developer solution, leaving the unexposed area on the surface. In other words, "whatever shows, goes." As a result, the final structure is the complement of the exposure pattern. The schematic diagram of the positive tone resist approach for fabrication is shown in the Figure 3.3.

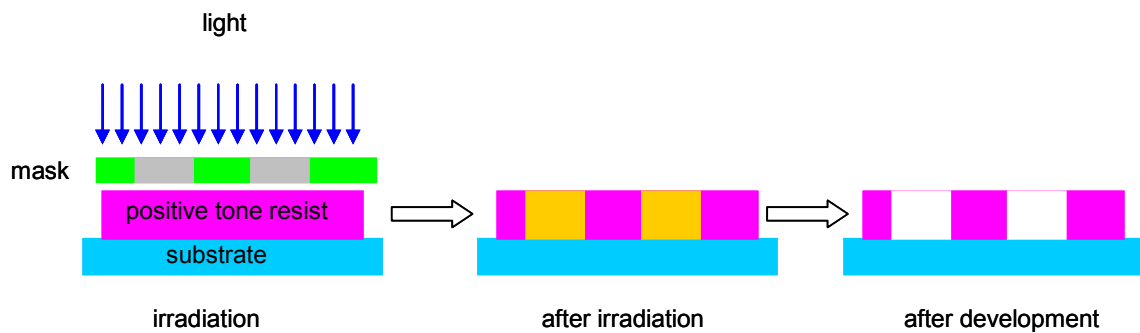


Figure 3.3 Positive tone resist approach.

3.2.3 Literature review of two-photon acid generators

Positive tone resist 3DLM may be useful in manufacturing micro-channel-based structures, such as micro-fluidic devices and waveguide-based micro-optical circuits. It proves to be more efficient for generation of micro-channels within the structure by excavating rather than depositing materials. In addition, positive tone resist 3DLM minimizes the shrinkage and distortion that are normally encountered in negative tone resist 3DLM. Two-photon acid generators could be used with positive tone resist 3DLM and react with a functionality of the insoluble resins, making the exposed region of the resin more soluble in a developer. However, there are few reports of two-photon induced positive tone resist 3DLM published, which are briefly reviewed here.

Belfield have used a commercially available PAG, diaryliodonium (**CD-1012**, Figure 3.4 a) to initiate cationic polymerization of multifunctional epoxide monomers **K126** (a mixture of poly(bisphenolA-co-epichlorohydrin), glycidyl end-capped and 3,4-epoxycyclohexylmethyl 3,4-epoxycyclohexanecarboxylate).⁴³ The resin consisted of **K126** (99%) and **CD-1012** (1%). The two-photon excitation wavelength was 775 nm with an 150 fs pulse width and a repetition rate of 1 kHz. Microstructures of lines were achieved with a linewidth of 18 μm , and a spacing that progressively increased from bottom to top, beginning at 72 μm (Figure 3.4 b). Since the TPA cross-section of **CD-1012** is small (16 GM),¹⁸⁸ it is expected that high excitation powers and long exposure times would be required.

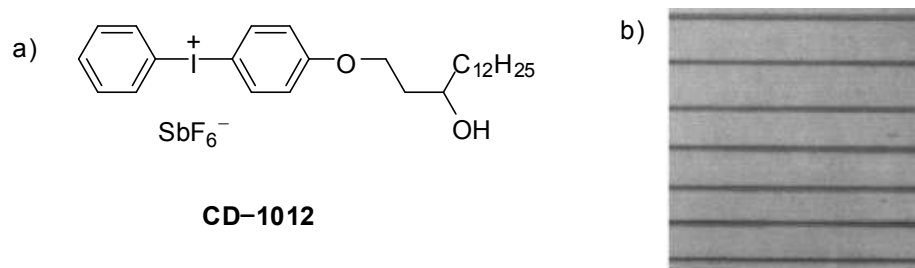


Figure 3.4 (a) Chemical structure of **CD-1012**. (b) Optical microscopy image of microstructures formed by using **CD-1012**.⁴³

Boiko used a resin consisting of isopropylthioxanethone (**ITX**) (Figure 3.5) as a TPA sensitizer, **CD-1012** as an initiator, and **K126** as the monomer. The resin was irradiated at 710 nm with an 150 fs pulse width.¹⁸⁹ A polymerization threshold of 1 GW cm⁻² with a dynamic range bigger than 100 damage-free was reported. **ITX** facilitated the activation of **CD-1012** in the near-IR region, but the low TPA cross-section of **ITX** (5 GM)¹⁸⁸ limited the rate of polymerization.

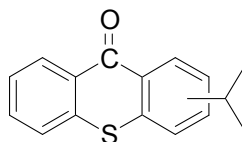


Figure 3.5 Isopropylthioxanethone (**ITX**), a mixture of 2 and 4 isomers.

3.2.4 *Two-photon acid generator developed by our group*

3.2.4.1 Motivation

Two-photon acid generators produce acids subsequent to two-photon absorption of radiation from intense laser pulses. Previous work has shown that two-photon acid generators can be used for both two-photon induced cationic polymerization and 3DLM by a positive tone resist approach. Most current work has used commercially available photoinitiators, which normally have low two-photon sensitivity because they often have small TPA cross-sections, typically less than 20 GM.¹⁸⁸ Due to the low TPA sensitivity results, high excitation power and long exposure time are required, which can lead to optical damage of the structure. These drawbacks limit the scope of two-photon induced 3DLM for widespread applications. To make two-photon induced 3DLM a more widely applicable technique, the development of two-photon acid generators with high TPA cross-section has been explored by our group.

3.2.4.2 Molecular design

For efficient high-fidelity microfabrication of structures, short exposure times and low excitation intensities are highly desirable to avoid optical damage of microstructures. A large TPA cross-section and a high quantum yield for acid generation (Φ_{H^+}) could facilitate these requirements. Therefore, the desired two-photon acid generators would contain a TPA chromophore with a large cross-section,^{31,33} a functionality with a high quantum yield of acid generation,^{165,166,169,190} and a mechanism to ensure that the excitation of the chromophore can lead to activation of the chemical functionality.^{12,180}

The TPA chromophore **27** (Figure 3.6) with a large TPA cross-section (805 GM at 745 nm)³³ was chosen as a good candidate for the TPA chromophore moiety from amongst the pool of molecules with two-photon absorption property that our group has synthesized and studied. Based on Saeva's study on aryl dialkylsulfonium PAGs,^{165,166,190} our group has designed and synthesized triphenylamine dialkylsulfonium PAGs with different alkyl sulfonium substituents at two different positions of triarylamines, and investigated their photochemistry properties and efficiency of quantum yield of acid generation, which has been discussed in Chapter 2. As a result, triphenylamine dimethylsulfonium salt **28** (Figure 3.6) was selected as the model molecule for the design of two-photon acid generators due to its high quantum yield of acid generation (0.48)¹⁶⁹ and synthetic convenience. The mechanism for acid generation has been studied in detail by Saeva,^{165,190} and was discussed in Chapter 2.

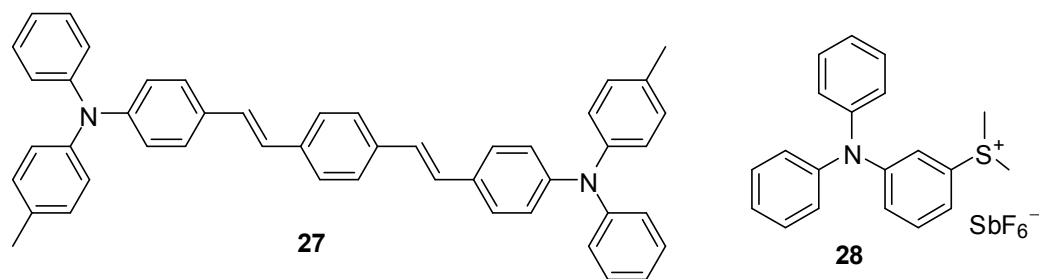


Figure 3.6 Model molecules **27** and **28** for the design of two-photon acid generators.

3.2.4.3 Two-photon acid generator and its applications

According to our design strategy and studies above, a two-photon acid generator with a bis(styryl)benzene TPA core (**BSB-S₂**) (Figure 3.7) was synthesized by replacing the triphenylamine of **28** with the TPA chromophore **27**. **BSB-S₂** has achieved our design strategy, which showed a high TPA cross-section (690 GM at 710 nm) and a high quantum yield for acid generation (0.50 ± 0.05).¹⁸⁷

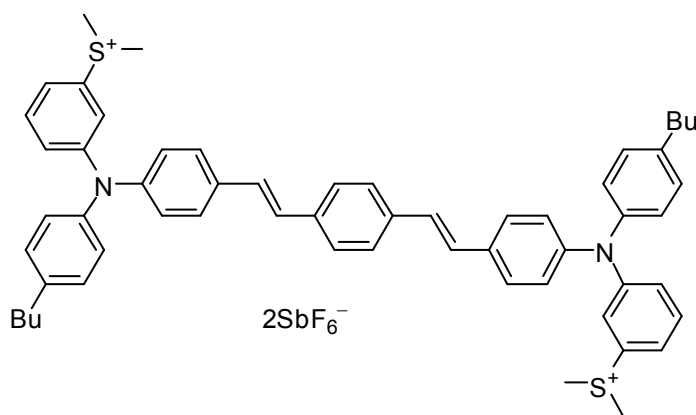


Figure 3.7 Chemical structure of **BSB-S₂**.

BSB-S₂ has been demonstrated to be highly efficient in two-photon induced cationic polymerization.¹⁹¹ **BSB-S₂** (10 mM) was used to initiate the polymerization of the resin, which consists of **SU-8** (80 wt%) and 4-vinyl-1-cyclohexene diepoxide (20 wt%), and irradiated with 5 ns laser pulses at 745 nm in a defined pattern. **SU-8** is a commercially available photoresist for cationic polymerization. Free-standing columns of cross-linked polymers were observed after removal of the monomer (Figure 3.8). The width of the smallest feature is 60 μm.¹⁹¹

A 50- μm -thick film of **BSB-S₂** (4 wt%) in poly(THPMA-*co*-MMA) was exposed at 745 nm with tightly focused pulse laser (80 fs) at an average power of 40 μW and a linear scan speed of 50 $\mu\text{m s}^{-1}$. Acids were released from **BSB-S₂** in the exposed regions, and the tetrahydropyranyl protecting group was hydrolyzed by an acid-catalyzed deprotection reaction to give carboxylic acid groups, which makes the polymer soluble in the base aqueous solution. After exposure, the film was baked for 1 minute at 90 $^{\circ}\text{C}$, and then the exposed resin was dissolved in an aqueous tetramethylammonium hydroxide solution (0.26 M). The final structure, which consisted of twelve parallel channels buried 10 μm below the surface with connecting reservoirs on both ends, was obtained (Figure 3.10).¹⁸⁷

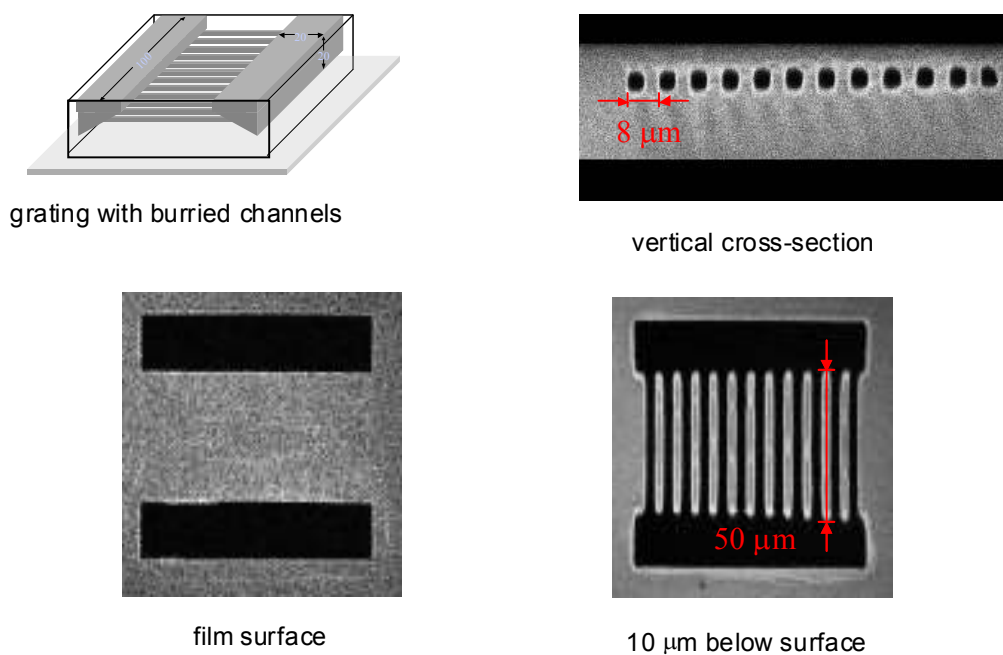


Figure 3.10 Two-photon fluorescence microscopy images of three-dimensional microchannel structure fabricated by using **BSB-S₂**.¹⁸⁷

3.3 Research goals

The diffraction-limited focal volume is proportional to the third power of the excitation wavelength ($V \propto \lambda^3$). Thus, decreasing the excitation wavelength can lead to smaller focal volumes, which, in principle, can result in improvement of the resolution for 3DLM.¹⁸⁰ Bearing this in mind and encouraged by the previous results from **BSB-S₂**, our goal was to develop the short wavelength two-photon acid generators as well.

By using two-photon fluorescence, Perry measured a TPA cross-section of 280 GM at 532 nm for the biphenyl chromophore **29** (Figure 3.11),¹⁹² and Belfield measured a maximum TPA cross-section of 260 GM at 610 nm for the fluorene chromophore **30** (Figure 3.11).¹⁹³ These values are favorably large in comparison with those of commercial photoacid generators, which are typically less than 20 GM.¹⁸⁸ They also have shorter two-photon absorption wavelengths (532 nm for **29** and 600 nm for **30**) than that of **27** (745 nm) due to their shorter conjugation length. In the case of **29**, the significant bond twist (35 degree) between the two central phenyl rings in the core out of plane¹⁹⁴ as determined from both quantum-chemical calculations and the X-ray crystal structure also contributes to the absorption maximum blue-shift.

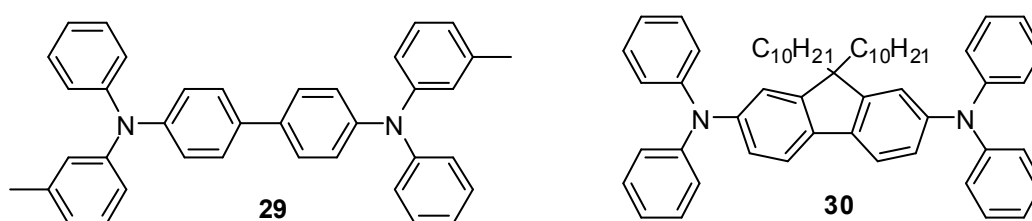


Figure 3.11 Target short-wavelength two-photon absorbing chromophores.

According to the previous molecular design principle, the target biphenyl **31** and fluorene **32** PAGs (Figure 3.12) were designed by replacing triphenylamine of the model molecule of the one-photon acid generator **28** with the TPA chromophores **29** and **30**.

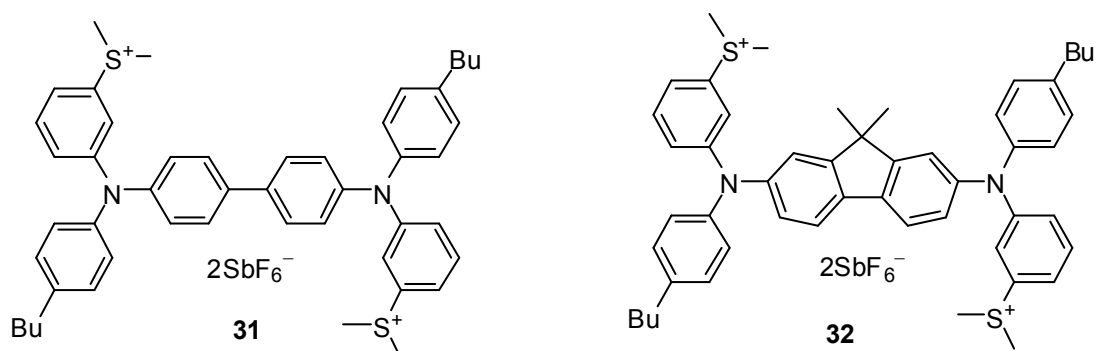


Figure 3.12 Target molecules of short-wavelength two-photon acid generators **31** and **32**.

In this research, the target molecules **31** and **32** were synthesized, their quantum yields of acid generation were measured, and their ability to initiate epoxide polymerization was investigated. Their application to 3DLM by using two-photon initiation is being conducted in collaboration with Dr. Perry's group, and the preliminary results have been obtained.

3.4 Synthesis of short wavelength two-photon acid generators

3.4.1 Synthesis of the biphenyl two-photon acid generator

Synthesis of the biphenyl PAG **31** is shown in Figure 3.13. 3-Bromobenzenethiol was deprotonated by sodium methoxide and further reacted with iodomethane to give 1-bromo-3-(methylsulfanyl)benzene **33** in 94% yield.¹⁶⁹ The coupling of aryl halides with alkyl amines catalyzed by palladium (0) and DPPF complex¹⁹⁵⁻¹⁹⁷ was used first for the reaction between **33** and 4-butylaniline to form **34** in 98% yield, and then was used for the coupling between **34** and 4,4'-dibromo-biphenyl to give product **35** in 44% yield. The alkylation of **35** with methyl triflate gave the corresponding triflate salt **36** in 83% yield.^{166,169} The subsequent anion-exchange to replace the triflate anion with the less nucleophilic hexafluoroantimonate anion afforded the target biphenyl PAG **31**.¹⁶⁹

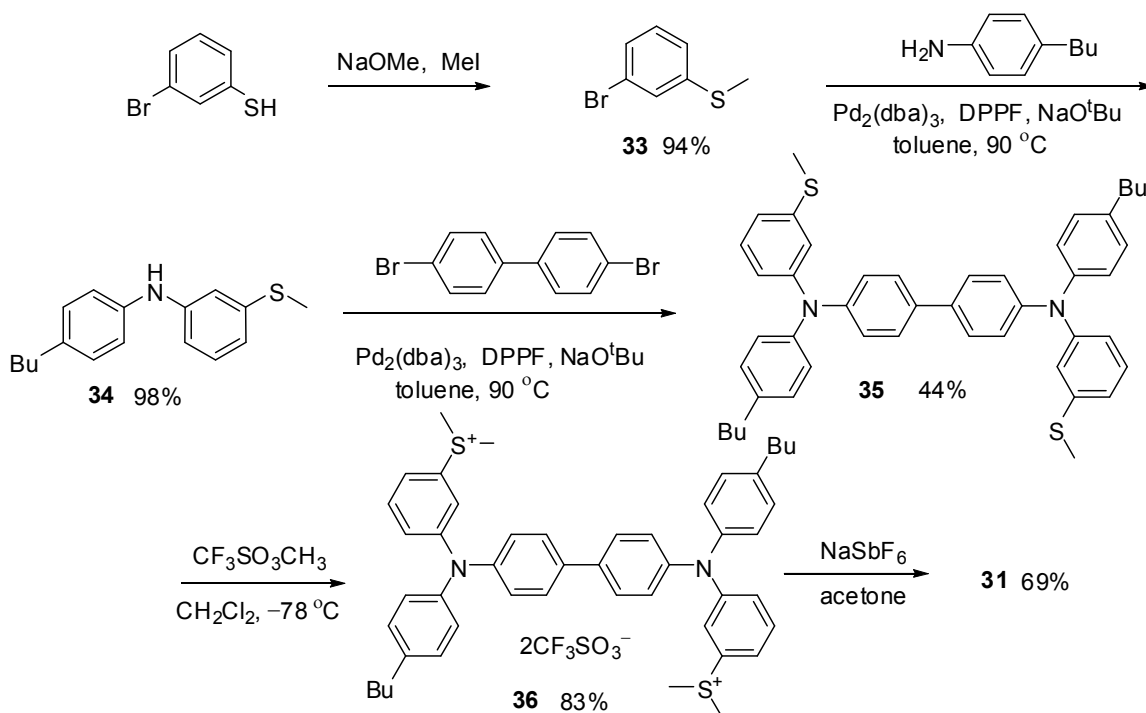


Figure 3.13 Synthesis of two-photon acid generator **31**.

3.4.2 Synthesis of the fluorene two-photon acid generator

Synthesis of the biphenyl PAG **32** is shown in Figure 3.14, and uses a similar procedure shown in Figure 3.13. The 9 position of 2,7-dibromofluorene was first methylated under basic conditions, forming **37** in 90% yield. The following reactions were conducted using similar reaction procedures shown in Figure 3.31. The TPA chromophore with sulfide substitution **38** was obtained by performing the coupling catalyzed by the palladium-DPPF complexes.¹⁹⁵⁻¹⁹⁷ The subsequent S-methylation by methyl triflate gave the triflate salt **39** in 86% yield. The subsequent anion-exchange by using an excess aqueous sodium hexafluoroantimonate provided the fluorene PAG **32** in 80% yield.

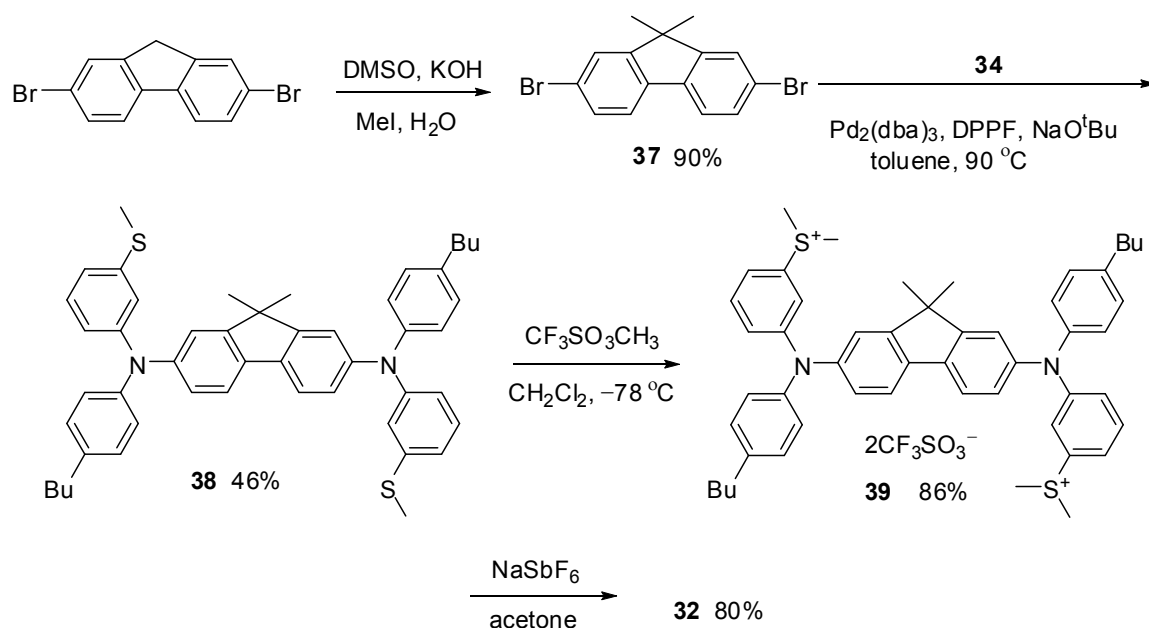


Figure 3.14 Synthesis of two-photon acid generator **32**.

3.5 One-photon photochemical studies

The photochemical properties of the PAGs described above under one-photon irradiation were studied, specifically the quantum yield of acid generation and initiation of epoxide polymerization. The photochemical results are presented in this section, and are summarized in Table 3.1. The discussion of photochemical experiment details will be described in the next section.

Two-photon acid generators	λ_{\max} (nm)	ϵ_{\max} ($10^4 \text{ M}^{-1} \text{ cm}^{-1}$)	$\Phi_{\text{H}^+}^{\text{b}}$ (± 0.05)
BSB-S₂ ¹⁸⁷	392	5.50	0.50
31	340	4.55	0.45
32	355	3.38	0.43

^aAll measurements were conducted in acetonitrile. ^b Φ_{H^+} : quantum yield of acid generation (section 3.8.1).

Table 3.1 One-photon physical data for two-photon acid generators **31** and **32** vs **BSB-S₂** in acetonitrile.

3.5.1 Absorption spectra

The absorption maxima of **31** and **32** are blue-shifted in comparison with **BSB-S₂** as were expected due to the decreased conjugation length (Figure 3.15). The wavelengths of the absorption maxima for **31** (340 nm) and **32** (355 nm) are shorter than that of **BSB-S₂** (392 nm), and as a result, their peak two-photon absorption wavelengths are also expected to be shorter.

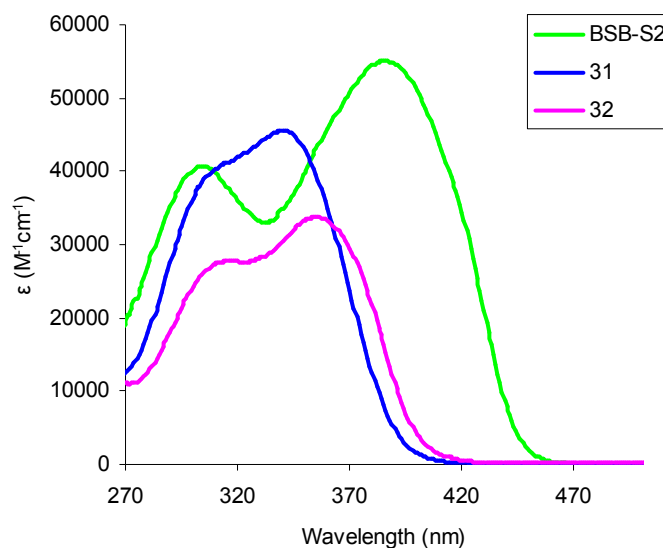


Figure 3.15 Absorption spectra of **BSB-S₂**, **31**, and **32** in acetonitrile.

3.5.2 Quantum yield of acid generation

The quantum yield of acid generation of the known PAG **BSB-S₂** was determined to be 0.49, which was identical to the literature value of 0.50 within the uncertainty (± 0.05).¹⁸⁷ The same measurement was applied to the short wavelength PAGs **31** and **32**, and the Φ_{H^+} of **31** (0.45 ± 0.05) and **32** (0.43 ± 0.05) are considered to be essentially the same to that of **BSB-S₂**.

3.5.3 Polymerization under one-photon conditions

The polymerization of cyclohexene oxide has been investigated, using both biphenyl **31** and fluorene **32** PAGs as initiators under one-photon conditions. The polymerization curve was plotted as conversion versus time (Figure 3.16).

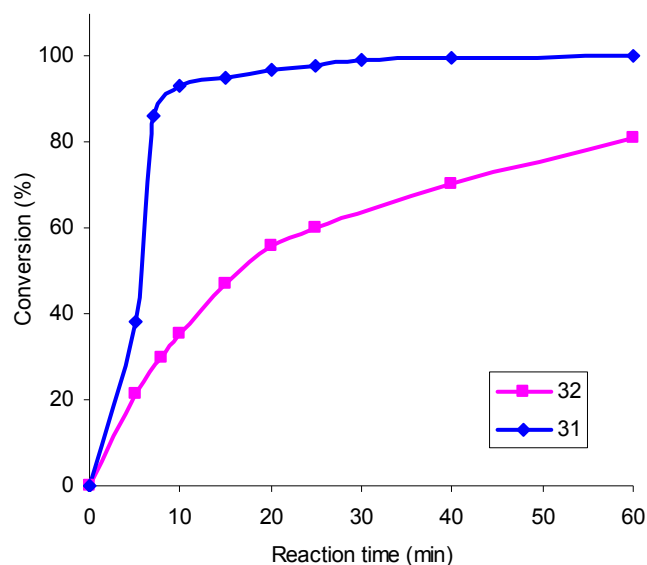


Figure 3.16 One-photon polymerization of cyclohexene oxide (7.87 M) initiated by **31** (6.60×10^{-3} M) and **32** (6.36×10^{-3} M) irradiated at 300 nm.

The conversion curve shows that the biphenyl PAG **31** rapidly initiated cationic polymerization, and the conversion reached 93% after 10 min. The fluorene PAG **32** afforded a reasonable conversion with a lower initiation rate. It may be due to smaller extinction coefficient of the fluorene ($2.45 \times 10^4 \text{ M}^{-1}\text{cm}^{-1}$) than the biphenyl ($3.67 \times 10^4 \text{ M}^{-1}\text{cm}^{-1}$) PAG at 300 nm.

3.6 Two-photon induced polymerization studies

The studies of two-photon induced polymerization were performed by Dr. M. Rumi in Dr. Perry's group. The two-photon induced polymerization of 4-vinyl-1-cyclohexene dioxide at 520 nm was studied using both the literature system (**CD-1012** /**ITX** 1:1.7)¹⁸⁹ and our systems (**31** and **32**) as initiators. For a given exposure time, the polymerization threshold energy can be defined as the average of the lowest and highest pulse energy for which the polymerization was observed and not observed, respectively. The results in Figure 3.17 indicated that at 520 nm, the resins containing **31** and **32** have similar polymerization threshold, whereas the threshold for the **CD-1012/ITX** resin is 1.2 – 1.8 times larger. Therefore, the PAGs **31** and **32** are more efficient than **CD-1012/ITX** to polymerize 4-vinyl-1-cyclohexene dioxide with excitation at 520 nm. Further characterization of the properties of initiators **31** and **32** under two-photon excitation conditions is on the way.

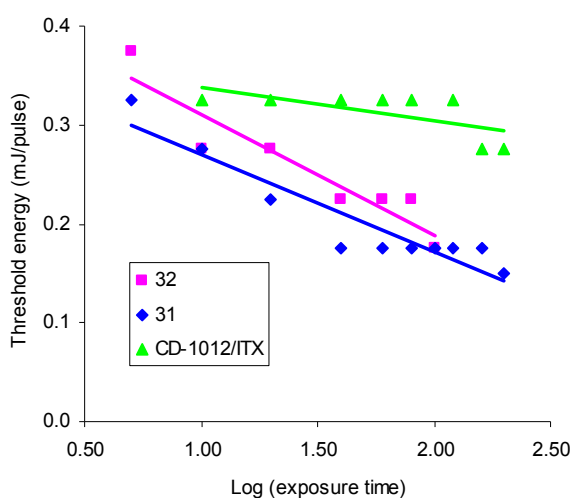


Figure 3.17 Threshold energies of initiation systems **31**, **32** and **CD-1012/ITX**.

3.7 Conclusions and future work

The short-wavelength two-photon acid generators with biphenyl **31** and fluorene **32** cores have been synthesized. Measurements have demonstrated that the maximum one-photon absorption wavelengths of **31** (340 nm) and **32** (355 nm) are shorter than that of the known **BSB-S₂** (392 nm).¹⁸⁷ The acid quantum yields of acid generation of **31** (0.45) and **32** (0.43) are the same as that of **BSB-S₂** (0.50)¹⁸⁷ within the uncertainty (± 0.05). The polymerization of cyclohexene oxide initiated by **31** and **32** under one-photon irradiation showed that they effectively initiated cationic polymerization.

The two-photon maximum absorption wavelengths of **31** and **32** are anticipated to be shorter than that of **BSB-S₂** (710 nm). Their applications in two-photon induced polymerization and positive tone resist 3DLM are being conducted in collaboration with Dr. M. Rumi. The preliminary results show that two-photon induced polymerization of epoxide initiated by **31** and **32** is more efficient than the literature system¹⁸⁹ at 520 nm. More research will be conducted in two-photon induced polymerization. The application of PAGs **31** and **32** with positive tone resist 3DLM will be included in the future directions of this thesis.

3.8 Experimental: photochemical measurements

The absorption spectra were collected on a Hewlett-Packard model 8453 spectrophotometer. The fluorescence spectra were collected on a Jobin Yvon Spex Fluorolog–III fluorometer. A Rayonet photochemical reactor (Model #RPR–100), manufactured by the Southern New England Ultraviolet Company, was used as a light source for photopolymerization studies. Spectrophotometric grade acetonitrile and dichloromethane were purchased from Aldrich or Acros, and were used as received.

3.8.1 *Quantum yield of acid generation*

The quantum yield of acid generation is defined as the rate of acid generation (number of H^+ generated per unit time) by a PAG in a solution upon irradiation divided by the rate of absorption (number of photon absorbed per unit time) by the molecule.

The monochromated xenon lamp of Fluorolog–III fluorometer was used as the irradiation source. The relative intensity of the light reaching the sample was measured (as current) on the internal reference detector of the fluorometer. The reference current is linearly proportional to the dose rate (number of photon delivered to the cuvette per unit time), and the dose rate can be controlled by adjusting the slit width of the monochromator. The absolute dose rate over a range of slit widths was determined by Dr. S. Kuebler. The absorption rate (the rate at which photons are absorbed, photon s^{-1}) was determined by using the well-established ferrioxalate actinometry method.¹⁷² The dose rate measurements were corrected to take into account the reflection loss from the cuvette

windows. In this way a calibration curve was obtained for the dose rate at the sample as a function of the reference current.

The irradiation wavelength was set to 355 nm for the biphenyl **31** and fluorene **32** PAGs and at 400 nm for **BSB-S₂** based on their absorption properties. The slopes of the dose rate calibration curves were found to be 4.05×10^{15} photon $s^{-1}\mu A^{-1}$ at 355 nm and 3.78×10^{15} photon $s^{-1}\mu A^{-1}$ at 400 nm. The transmittance through an empty cuvette was measured at the irradiation wavelength, and the square root of the average transmittance was used to correct for the reflection losses and determine the number of photons that reach the solution in the cuvette. The reference currents were read from the fluorometer. The dose rate (#photon s^{-1}) can then be obtained as the product of the power parameter (photon $s^{-1}\mu A^{-1}$), the average reference current (μA) and the square root of the transmittance (Eq 3.1).

$$\begin{array}{l} \text{dose rate} \\ (\#\text{photon } s^{-1}) \end{array} = \begin{array}{l} \text{power parameters} \\ (\text{photon } s^{-1}\mu A^{-1}) \end{array} \times \begin{array}{l} \text{reference current} \\ (\mu A) \end{array} \times \text{transmittance}^{-1/2} \quad \text{Eq 3.1}$$

Rhodamine B base (**RB**) was used as an acid indicator.¹⁷⁰ As the acid form (**RB⁺**) of **RB** exhibits and absorption maximum at 555 nm changes in absorbance at 555 nm can be used to monitor a change in acid concentration. Solutions of RB (2.5×10^{-3} M), hydrogen chloride (2.0×10^{-4} M), and PAG (2.0×10^{-4} M) in acetonitrile were prepared. The PAG solution (2 mL) was irradiated with stirring in the fluorometer for a certain time, and the reference current was recorded. After irradiation, the **RB** solution (50 μL) and hydrogen chloride solution (40 μL) were added, the absorption spectrum was

measured, and the absorbance at 555 nm was recorded. Figure 3.18 displays the absorbance at 555 nm for the three PAG molecules investigated, as a function of irradiation time. It can be seen that the absorbance increases linearly with time. The lines in the figure are best fits to the data.

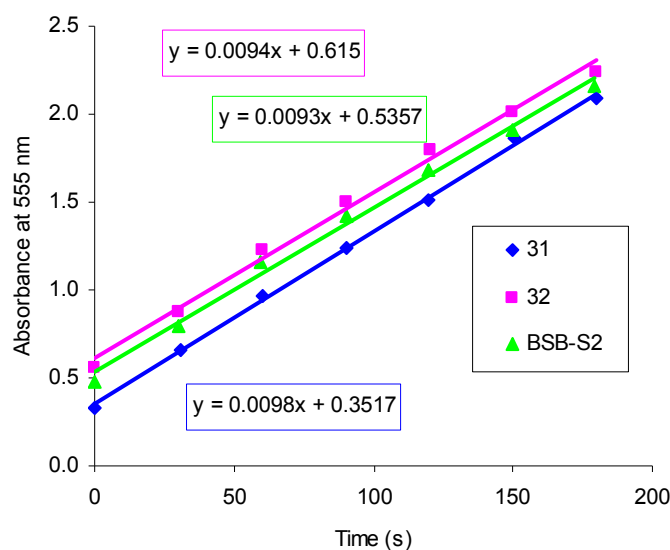


Figure 3.18 Absorbance of PAGs at 555 nm for **31**, **32** and **BSB-S₂**, measured over time to determine the concentration of acid generated in acetonitrile.

The acid rate ($\#\text{H}^+ \text{s}^{-1}$) can then be calculated by Eq 3.2. The slope of the straight line fit divided by the extinction coefficient for RB^+ ($1.19 \times 10^5 \text{ M}^{-1}\text{cm}^{-1}$, as measured by Dr. K. Braun) and the pathlength corresponds to the concentration of acid generated per unit time. This number multiplied by the solution volume and Avogadro's number (N_A) yields the acid rate.

$$\text{acid rate } (\#\text{H}^+\text{s}^{-1}) = \frac{\text{slope } (\text{s}^{-1})}{\epsilon (\text{mol}^{-1}\text{Lcm}^{-1}) l (\text{cm})} \times \text{volume } (\text{L}) \times N_A (\#\text{H}^+ \text{mol}^{-1}) \quad \text{Eq3.2}$$

The quantum yield of acid generation was obtained from the rate of acid generation ($\#H^+ s^{-1}$) divided by the rate of photons absorption ($\#photon s^{-1}$). The uncertainty for the measurement of the acid rate was ± 0.05 , taking into account of the uncertainties of dose rate measurement, acid rate measurement, and transmittance correction.

3.8.2 *Polymerization under one-photon conditions*

A Rayonet photochemical reactor was fitted with a merry-go-round apparatus, and was equipped with eight lamps at 300 nm as light sources for both PAGs. A solution of monomer (7.87 M for both **31** and **32**) and PAGs (6.60×10^{-3} M for **31**, and 6.36×10^{-3} M for **32**) in a vial was prepared in dichloromethane. After the solution was degassed by purging with nitrogen, the vial was put into the photochemical reactor. After a certain irradiation time, the vial was taken out of the photochemical reactor, and ammonia (0.5 mL, 2.0 M in methanol) was added immediately to quench the polymerization. Then the polymers were washed with methanol, cut into small pieces, filtered and dried in the vacuum oven (50 °C) for roughly two days. The weight of the isolated polymers was measured. The conversion was calculated by the weight of the isolated polymer divided by the weight of the monomers. The polymerization curve was plotted by conversion versus time.

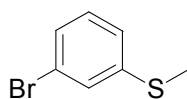
3.8.3 *Dose-array measurements of two-photon induced polymerization thresholds*

The efficiency of our PAG **31** and **32** in polymerizing 4-vinyl-1-cyclohexene dioxide under two-photon excitation conditions was investigated by Dr. Rumi in Prof. Joseph W. Perry's lab. For comparison, a literature PAG system **CD-1012/ITX** was also studied.

The photoresist was prepared by dissolving the initiators (7 mM) in the neat monomer. PAG **31** did not fully dissolve at 7 mM. A cell was made by sandwiching a 500 μm thick o-ring between two glass substrates. The cell was filled with the photoresist. An array of points in the cell was irradiated with focused 6 ns laser pulses at 520 nm (10 Hz repetition rate) to determine the threshold pulse energy for the onset of polymerization for various exposure times. The pulse energy was varied between 0.15 and 0.40 mJ per pulse and the exposure time between 5 s and 200 s. The diameter of the beam at the sample size was about 60 μm . After exposure, the cell was disassembled and rinsed with propylene glycol methylether acetate and ethanol, and imaged with an optical microscope. The occurrence of polymerization was judged by the presence of free-standing columns of cross-linked material on the glass surface after solvent wash.

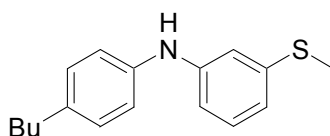
3.9 Experimental: synthesis procedures

General experimental. NMR spectroscopy was performed using either a DRX-500 MHz or Varian Unity Plus 200 MHz and 300 MHz spectrometers. Mass spectrometry (MS) was performed by the MS Instrument Facility at the University of Arizona. The combustion experiments for elemental analysis were conducted by Desert Analytics, Tucson, Arizona. Silica gel (40 – 63 μm , EMD Chemical, Inc.) was used to perform flash column chromatography. TLC was performed on pre-coated plates containing a fluorescent indicator (silica gel 60 F₂₅₄, EMD Chemicals, Inc.) All reagents and solvents including dry solvents and anhydrous solvents in Acrosealed bottles were purchased from Aldrich or Acros, and were used as received. The general precautions for preparation of light sensitive compounds mentioned in this section include wrapping the reaction flask with aluminum foil and performing the subsequent workup and purification in dark under the weak red light. These precautions are applied in all cases where it is indicated that the compound is light sensitive.

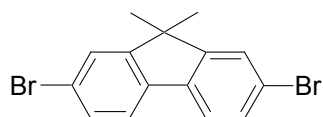


1-Bromo-3-(methylsulfanyl)benzene. To a solution of sodium methoxide prepared from sodium (0.45 g, 43 mmol) in anhydrous methanol (20 ml) was added 3-bromobenzenethiol (1.60 ml, 15 mmol) at room temperature under nitrogen flow. After 30 min, iodiomethane (1.23 ml, 19.5 mmol) was added dropwise, and then the reaction mixture was stirred overnight under nitrogen pressure. After quenching with addition of a 2.0 M aqueous solution of sodium hydroxide until the solution was basic, the mixture was

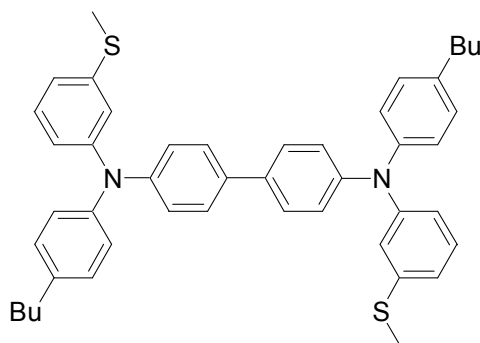
extracted with diethyl ether (3×60 mL). The combined organic layers were washed with brine and dried over magnesium sulfate. The product (2.70 g) was obtained in 89% yield after flash column chromatography (1% and then 3% ethyl acetate in hexane). ^1H NMR (300 MHz, chloroform-*d*) δ 7.25 (m, 4H), 2.42 (s, 3H). The data were consistent with the literature data.¹⁶⁹



***N*-(4'-Butylphenyl)-3-(methylsulfanyl)aniline.** To a solution of *tris*(dibenzylideneacetone)dipalladium (0) ($\text{Pd}_2(\text{dba})_3$) (0.14 g, 0.15 mmol) and *bis*(diphenylphosphino)ferrocene (DPPF) (0.12 g, 0.18 mmol) in dry toluene (20 mL) under nitrogen pressure at room temperature was added 1-bromo-3-(methylsulfanyl)benzene (2.03 g, 10.0 mmol). After 10 min, sodium *tert*-butoxide (2.19 g, 22.0 mmol) and 4-butylaniline (2.4 mL, 2.3 g, 15 mmol) were added. The reaction mixture was then heated to 90 °C, and was stirred for 7 h under nitrogen pressure. After quenching with water (80 mL), the mixture was extracted with diethyl ether (3×60 mL), and the combined organic layers were dried over magnesium sulfate. The product (2.35 g) was obtained in 86% yield after flash column chromatography (2% and then 4% ethyl acetate in hexane). ^1H NMR (300 MHz, chloroform-*d*) δ 7.16 – 6.75 (m, 8H), 2.56 (t, $J = 7.5$ Hz, 2H), 1.58 (quintet, $J = 7.8$ Hz, 2H), 1.36 (sextet, $J = 7.8$ Hz, 4H), 0.93 (t, $J = 7.4$ Hz, 3H). ^{13}C NMR (75 MHz, chloroform-*d*) δ 144.4, 139.9, 139.4, 136.5, 129.6, 129.2, 119.2, 118.1, 114.3, 113.1, 34.9, 33.8, 22.3, 15.7, 14.0. The data were consistent with the literature data.¹⁹¹

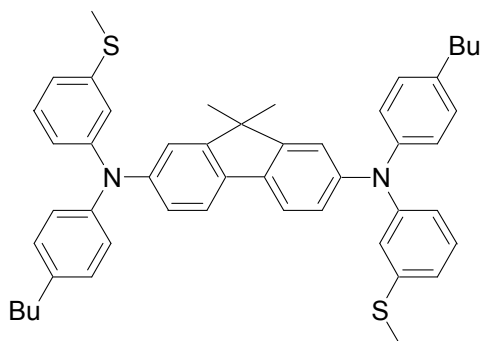


2,7-Dibromo-9,9-dimethyl-9H-fluorene. To a solution of 2,7-dibromofluorene (14.86 g, 44.48 mmol) in DMSO (200 mL) at the room temperature, was added potassium hydroxide (16.64 g, 0.27 mmol). Then iodomethane (8.4 mL, 19 g, 0.13 mmol) was slowly added over 10 min, and water (40 mL) was added dropwise over 2 hours. The reaction was exothermic. After the reaction mixture had returned to room temperature, the mixture was extracted with water (3 × 200 mL), and then the aqueous phase was extracted with dichloromethane (4 × 250 mL). The combined organic layers were dried over magnesium sulfate. The product (14.01 g) was obtained in 90% yield after flash column chromatography (hexane). ¹H NMR (200 MHz, chloroform-*d*) δ 7.56 – 7.47 (m, 6H), 1.46 (s, 6H). ¹³C NMR (50 MHz, chloroform-*d*) δ 155.3, 137.2, 130.3, 126.2, 121.4, 121.2, 47.3, 26.8. The data were consistent with the literature data.^{198,199}



4,4'-Bis((4-butylphenyl)(3-(methylsulfanyl)phenyl)amino)-biphenyl. To a solution of *tris*(dibenzylideneacetone) dipalladium (0) (Pd₂(dba)₃) (0.28 g, 0.30 mmol) and *bis*(diphenylphosphino)ferrocene (DPPF) (0.21 g, 0.36 mmol) in dry toluene (60 mL) under nitrogen pressure at room temperature was added 4,4'-dibromobiphenyl (3.20 g,

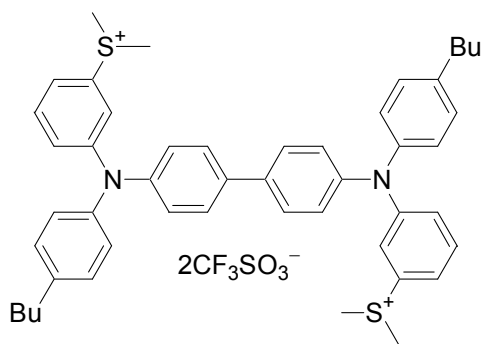
10.1 mmol). After 10 min, sodium *tert*-butoxide (4.39 g, 44.2 mmol) and *N*-(4-butylphenyl)-3-(methylsulfanyl)aniline (6.00 g, 0.12 mmol) were added. The reaction mixture then was heated to 90 °C, and was stirred for 22 h under nitrogen pressure. After quenching with water (100 mL), the mixture was extracted with diethyl ether (3 × 100 mL), and the combined organic layers were dried over magnesium sulfate. The product (2.72 g) was obtained in 44% yield after flash column chromatography (hexane, 0.1%, 0.2% and then 0.4% ethyl acetate in hexane). ¹H NMR (300 MHz, acetone-*d*₆) δ 7.44 (d, *J* = 8.7 Hz, 4H), 7.14 – 6.73 (m, 20H), 2.55 (t, *J* = 7.5 Hz, 4H), 2.31 (s, 6H), 1.57 (quintet, *J* = 7.2 Hz, 4H), 1.34 (sextet, *J* = 7.2 Hz, 4H), 0.90 (t, *J* = 7.2 Hz, 6H). ¹³C NMR (75 MHz, acetone-*d*₆) δ 149.2, 147.4, 145.7, 140.5, 139.1, 135.2, 130.4, 130.2, 127.9, 125.9, 124.6, 121.6, 120.7, 120.6, 35.6, 34.4, 23.0, 15.3, 14.2. HRMS (FAB+) *m/z*: Calcd. for C₄₆H₄₈N₂S₂ (M⁺) 692.3259, Found 692.3241. Anal. Calcd. for C₄₆H₄₈N₂S₂: C, 79.72; H, 6.98; N, 4.04. Found: C, 79.70, H, 7.04, N, 4.05.



2,7-Bis((4-butylphenyl)(3-(methylsulfanyl)phenyl)amino)-9,9-

dimethyl-fluorene. To a solution of *tris*(dibenzylideneacetone) dipalladium (0) (Pd₂(dba)₃) (0.12 g, 0.11 mmol) and *bis*(diphenylphosphino)ferrocene (DPPF) (0.11 g, 0.16 mmol) in dry toluene (25 mL), under nitrogen pressure, at room temperature, was

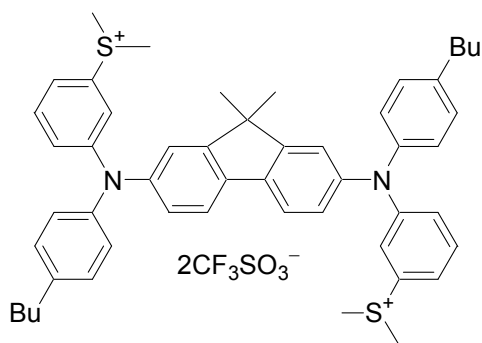
added 2,7-dibromo-9,9-dimethyl-9*H*-fluorene (1.51 g, 4.28 mmol). After 10 min, sodium *tert*-butoxide (1.82 g, 18.8 mmol) and *N*-(4-butylphenyl)-3-(methylsulfanyl)aniline (2.33 g, 8.57 mmol) were added. The reaction mixture then was heated to 90 °C for 23 h under nitrogen pressure. After quenching with water (50 mL), the mixture was extracted with diethyl ether (3 × 50 mL), and the combined organic layers were dried over magnesium sulfate. The product (1.44 g) was obtained in 47% yield after flash column chromatography (hexane, 0.2% and then 0.5% ethyl acetate in hexane). It is a light sensitive compound. ¹H NMR (300 MHz, acetone-*d*₆) δ 7.56 (d, *J* = 8.1 Hz, 2H), 7.23 – 6.74 (m, 20H), 2.57 (t, *J* = 7.5 Hz, 4H), 2.33 (s, 6H), 1.59 (quintet, *J* = 7.5 Hz, 4H), 1.342 – 1.30 (m, 10H), 0.92 (t, *J* = 7.2 Hz, 6H). ¹³C NMR (75 MHz, acetone-*d*₆) δ 156.4, 150.3, 148.1, 146.7, 141.1, 139.5, 135.6, 131.0, 130.8, 126.4, 121.8, 121.0, 120.7, 120.1, 48.1, 36.3, 35.1, 27.9, 23.7, 16.0, 14.9. HRMS (FAB+) *m/z*: Calcd. for C₄₉H₅₂N₂S₂ (M⁺) 732.3572, Found 732.3540. Anal. Calcd. for C₄₉H₅₂N₂S₂: C, 80.28; H, 7.15; N, 3.82. Found: C, 80.22, H, 7.22, N, 3.80.



4,4'-Bis((4-butylphenyl)(3-(dimethylsulfonio)phenyl)amino)-biphenyl

ditrifluoromethanesulfonate. To a solution of 4,4'-bis((4-butylphenyl)(3-(methylsulfanyl)phenyl)amino)-biphenyl (2.43 g, 3.51 mmol) in dry dichloromethane (50

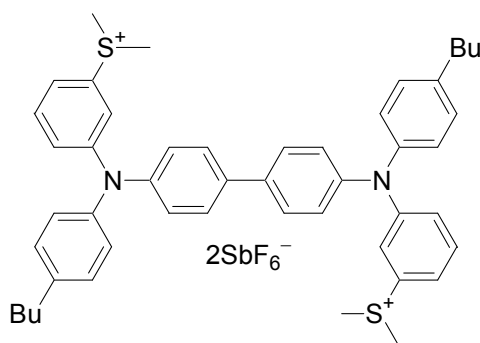
mL) under nitrogen pressure at $-78\text{ }^{\circ}\text{C}$ was added methyl trifluoromethanesulfonate (0.52 mL, 4.6 mmol). The reaction mixture was stirred for 30 min at $-78\text{ }^{\circ}\text{C}$, and then allowed to slowly rise to room temperature overnight under nitrogen pressure. The pure product (2.97 g) was obtained in 83% yield from recrystallization by adding diethyl ether to a dichloromethane solution. The product is light sensitive. ^1H NMR (300 MHz, acetone- d_6) δ 7.73 – 7.85 (m, 10H), 7.32 – 7.12 (m, 14H), 3.43 (s, 12H), 2.64 (t, $J = 7.8\text{ Hz}$, 4H), 1.62 (quintet, $J = 7.5\text{ Hz}$, 4H), 1.41 (sextet, $J = 7.5\text{ Hz}$, 4H), 0.94 (t, $J = 7.5\text{ Hz}$, 6H). ^{13}C NMR (75 MHz, chloroform- d) δ 150.0, 145.0, 143.0, 140.5, 136.6, 132.2, 130.0, 128.2, 125.9, 125.5, 125.4, 125.3, 120.4, 119.6, 35.1, 33.5, 29.1, 22.4, 13.9 (The carbon peak from CF_3SO_3^- was not observed). HRMS (FAB+) m/z : Calcd. for $\text{C}_{48}\text{H}_{53}\text{N}_2\text{S}_2$ ($\text{M}^+ - 2\text{CF}_3\text{SO}_3 - \text{H}$) 721.3650, Found 721.3637. Anal. Calcd. for $\text{C}_{50}\text{H}_{54}\text{F}_6\text{N}_2\text{O}_6\text{S}_2$: C, 58.81; H, 5.33; N, 2.74. Found: C, 59.22; H, 5.39; N, 2.69.



2,7-Bis((4-butylphenyl)(3-(dimethylsulfonio)phenyl)amino)-9,9-

dimethyl-fluorene ditrifluoromethanesulfonate. To a solution of 2,7-bis((4-butylphenyl)(3-(methylsulfany)phenyl)amino)-9,9-dimethyl-fluorene (1.38 g, 1.89 mmol) in dry dichloromethane (20 mL) at $-78\text{ }^{\circ}\text{C}$ under nitrogen atmosphere was added methyl trifluoromethanesulfonate (0.28 mL, 2.5 mmol). The reaction mixture was stirred

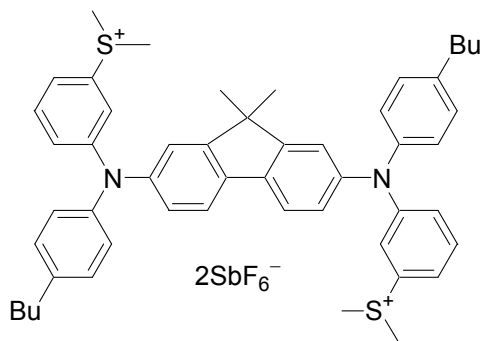
for 30 min at $-78\text{ }^{\circ}\text{C}$, and then it was allowed to slowly rise to room temperature overnight under nitrogen pressure. The product (1.72 g) was obtained in 86% yield from recrystallization by adding diethyl ether to a dichloromethane solution. The product is light sensitive. ^1H NMR (300 MHz, dimethyl sulfoxide- d_6) δ 7.73 (d, $J = 8.1$ Hz, 2H), 7.56 – 7.54 (m, 6H), 7.29 – 6.99 (m, 14H), 3.18 (s, 12H), 2.58 (t, $J = 7.5$ Hz, 4H), 1.57 (quintet, $J = 7.5$ Hz, 4H), 1.39 – 1.27 (m, 10H), 0.91 (t, $J = 7.2$ Hz, 6H). ^{13}C NMR (125 MHz, dimethyl sulfoxide- d_6) δ 155.2, 149.0, 145.6, 143.6, 139.0, 134.5, 131.4, 129.8, 127.6, 125.3, 125.0, 124.0, 121.2, 121.1, 120.9, 119.0, 46.7, 34.3, 33.0, 28.0, 26.6, 21.8, 13.8 (The carbon peak from CF_3SO_3^- was not observed). HRMS (FAB+) m/z : Calcd. for $\text{C}_{51}\text{H}_{57}\text{N}_2\text{S}_2$ ($\text{M}^+ - 2\text{CF}_3\text{SO}_3 - \text{H}$) 761.3963, Found 761.3949. Anal. Calcd. for $\text{C}_{53}\text{H}_{58}\text{F}_6\text{N}_2\text{O}_6\text{S}_2$: C, 59.98; H, 5.51; N, 2.64. Found: C, 59.71; H, 5.51, N, 2.64.



4,4'-Bis((4-butylphenyl)(3-(dimethylsulfonyl)phenyl)amino)-biphenyl

dihexafluoroantimonate. To a solution of 4,4'-bis((4-butylphenyl)(3-(dimethylsulfonyl)phenyl)amino)-biphenyl ditrifluoromethanesulfonate (0.98 g, 0.96 mmol) in acetone (10 mL) was added a solution of sodium hexafluoroantimonate (2.10 g, 8.11 mmol) in water (20 mL). The reaction mixture was stirred for 2 hours at room temperature in the dark. Removal of acetone by evaporation left a solid precipitate in

water, and the water was decanted. The solid was re-dissolved in acetone (10 mL). This procedure was repeated three times. Subsequent to the last ion exchange, the resultant solid was washed with water extensively to remove excess sodium hexafluoroantimonate. Then the solid was dissolved in a minimum amount of acetone. Filtration through Celite gave a clear solution. Precipitation by adding diethyl ether gave an oily product at the bottom of the flask and a white cloudy solution. After the storing the flask at $-30\text{ }^{\circ}\text{C}$ overnight, the clear solution was decanted and the solid was washed by diethyl ether three times. Then the final product (0.79 g) was obtained in 69% yield after drying under vacuum at $50\text{ }^{\circ}\text{C}$ overnight. The product is light sensitive. ^1H NMR (500 MHz, dimethyl sulfoxide- d_6) δ 7.64 – 7.56 (m, 10H), 7.25 – 7.06 (m, 14H), 3.21 (s, 12H), 2.59 (t, $J = 7.5$ Hz, 4H), 1.58 (quintet, $J = 7.5$ Hz, 4H), 1.34 (sextet, $J = 7.0$ Hz, 4H), 0.92 (t, $J = 7.5$ Hz, 6H). ^{13}C NMR (125 MHz, dimethyl sulfoxide- d_6) δ 148.5, 145.3, 143.4, 139.2, 134.8, 131.8, 129.8, 127.7, 127.6, 125.7, 125.5, 124.3, 122.3, 121.2, 34.2, 33.0, 28.1, 21.8, 13.8. HRMS (FAB+) m/z : Calcd. for $\text{C}_{47}\text{H}_{51}\text{N}_2\text{S}_2$ ($\text{M}^+ - 2\text{SbF}_6 - \text{CH}_3$) 707.3494, Found 707.3468; Calcd. for $\text{C}_{46}\text{H}_{48}\text{N}_2\text{S}_2$ ($\text{M}^+ - 2\text{SbF}_6 - 2\text{CH}_3$) 692.3255, Found 692.3253. Anal. Calcd. for $\text{C}_{48}\text{H}_{54}\text{F}_{12}\text{N}_2\text{S}_2\text{Sb}_2$: C, 48.26; H, 4.56; N, 2.35. Found: C, 48.47; H, 4.75; N, 2.32.



2,7-Bis((4-butylphenyl)(3-(dimethylsulfonio)phenyl)amino)-9,9-

dimethyl-fluorene dihexafluoroantimonate. To a solution of 2,7-bis((4-butylphenyl)(3-(dimethylsulfonio)phenyl)amino)-9,9-dimethyl-fluorene ditrifluoromethanesulfonate (1.67 g, 1.57 mmol) in acetone (10 mL) was added a solution of sodium hexafluoroantimonate (2.10 g, 8.11 mmol) in water (20 mL). The reaction mixture was stirred for 2 hours at room temperature in the dark. Removal of acetone by evaporation left a solid product in water and the water was decanted. The solid was re-dissolved in acetone (10 mL). This procedure was repeated three times. Subsequent to the last ion exchange, the resultant solid was washed with water extensively to remove excess sodium hexafluoroantimonate. Then the solid was dissolved in a minimum amount of acetone. Filtration through Celite gave a clear solution. Precipitation by adding diethyl ether gave an oily product at the bottom of the flask and the white cloudy solution. After the storing the flask in $-30\text{ }^{\circ}\text{C}$ overnight, the clear solution was decanted and the solid was washed by diethyl ether three times. Then the final product (1.5 g) was obtained in 80% yield after drying under vacuum at $50\text{ }^{\circ}\text{C}$ overnight. The product is light sensitive.

^1H NMR (500 MHz, dimethyl sulfoxide- d_6) δ 7.73 (d, $J = 7.5$ Hz, 2H), 7.56 – 7.52 (m, 6H), 7.28 (d, $J = 1.5$ Hz, 2H), 7.23 (d, $J = 8.0$ Hz, 4H), 7.13 (dt, $J = 7.0$ Hz, $J = 2.0$ Hz,

2H), 7.07 (d, $J = 8.5$ Hz, 4H), 7.00 (dd, $J = 8.0$ Hz, $J = 2.0$ Hz, 2H), 3.18 (s, 12H), 2.58 (t, $J = 7.5$ Hz, 4H), 1.57 (quintet, $J = 7.0$ Hz, 4H), 1.29 – 1.37 (m, 10H), 0.91 (t, $J = 7.5$ Hz, 6H). ^{13}C NMR (125 MHz, dimethyl sulfoxide- d_6) δ 155.2, 149.0, 145.1, 143.5, 139.0, 134.5, 131.4, 129.8, 127.6, 125.3, 124.9, 124.0, 121.1, 120.9, 119.0, 46.6, 34.2, 33.0, 28.0, 26.5, 21.8, 13.8. HRMS (FAB+) m/z : Calcd. for $\text{C}_{51}\text{H}_{57}\text{N}_2\text{S}_2$ ($\text{M}^+ - 2\text{SbF}_6 - \text{H}$) 761.3963, Found 761.3966; Calcd. for $\text{C}_{50}\text{H}_{55}\text{N}_2\text{S}_2$ ($\text{M}^+ - 2\text{SbF}_6 - \text{CH}_3$) 747.3807, Found 747.3787; Anal. Calcd. for $\text{C}_{51}\text{H}_{58}\text{F}_{12}\text{N}_2\text{S}_2\text{Sb}_2$: C, 49.61; H, 4.73; N, 2.27. Found: C, 49.77; H, 4.85; N, 2.31.

4. TWO-PHOTON RADICAL GENERATORS

4.1 Two-photon radical polymerization

4.1.1 *Conventional two-photon radical generators and sensitizers*

Two-photon induced polymerization was introduced in section 3.1. Based on the types of monomers/oligomers that have been used for polymerization, two-photon induced polymerization can be classified into cationic and radical polymerization. Resins consisting of oxirane or epoxide monomers/oligomers undergo two-photon cationic polymerization, and this has been reviewed in section 3.2. Resins containing acrylate monomers/oligomers are among those that can undergo two-photon radical polymerization. Recently, some high-fidelity microstructures with complex three-dimensional forms and small feature sizes (100 – 200 nm) have been produced by two-photon radical polymerization.^{11,13,43,185,186} These achievements have demonstrated the potential of two-photon radical polymerization in 3DLM, and several representative applications will be presented in this section.

Most current work has been involved patterning structures by using conventional photoinitiators.^{11,185} Kawata used a commercially available resin (**SCR500**) to fabricate the first complex three-dimensional microstructure by two-photon induced polymerization.¹¹ **SCR500** consists of urethane acrylate monomers/oligomers and the two conventional photoinitiators, i.e. (1-hydroxy-cyclohexyl)-phenyl-methanone (**HCPM**) and 2-benzyl-2-dimethylamino-4-methyl-1-(4-morpholin-4-yl-phenyl)-pentan-1-one (**BDMP**) (Figure 4.1 a). The radicals are generated via an α -cleavage process (Figure 4.1 b) upon irradiation at 790 nm by using 200 fs laser. The microstructure obtained was a

spiral coil of 7 μm diameter and 50 μm long with a line cross-section 1.3 μm \times 2.2 μm (Figure 4.2).

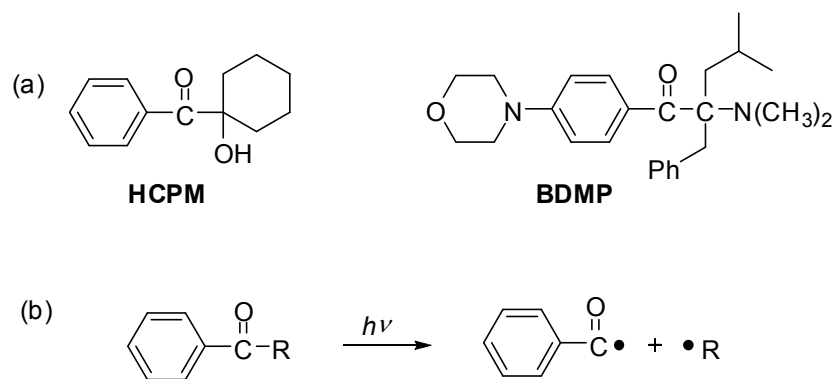


Figure 4.1 (a) Chemical structures of **HCPM** and **BDMP**. (b) The mechanism for radical generation.

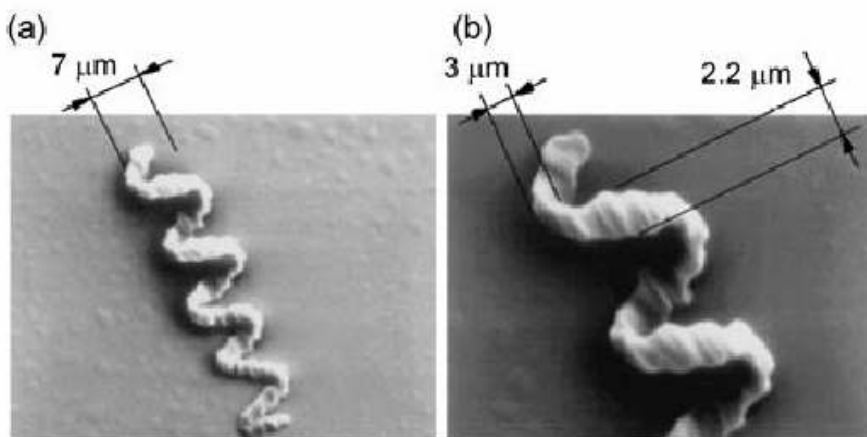


Figure 4.2 Scanning electron microscopic images of a spiral coil made by two-photon radical polymerization. (a) The entire view. (b) The magnified view.¹⁸⁵

Later on, Kawata made further progress using **SCR500**.^{13,185} The resin was irradiated at 780 nm by using 150 fs pulse laser to produce a micro-bull with 7 μm high and 10 μm long (Figure 4.3).

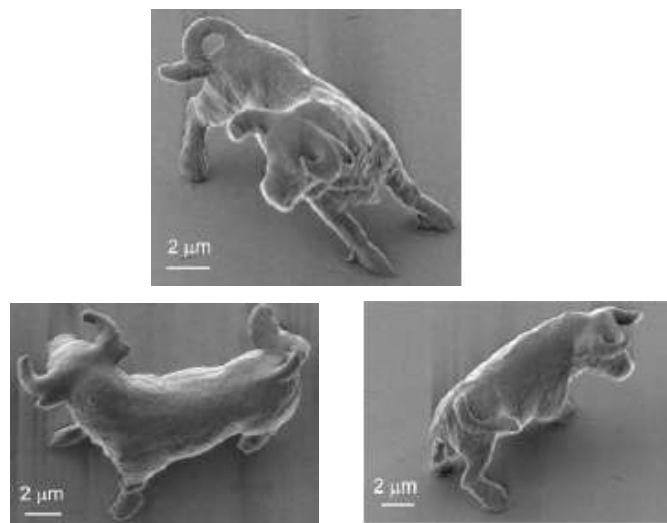


Figure 4.3 The SEM images of the micro-bull from the different view angles.¹³

Belfield reported on two-photon radical polymerization using a different radical generator system.³⁹ The oligomers were commercially available ethoxylated bisphenol A dimethylacrylate (**SR349**). The initiation system comprised of 5,7-diiodo-3-butoxy-6-fluorone (**H–Nu 470**) as a two-photon sensitizer and an electron donor, *N,N*-dimethyl-2,6-diisopropylaniline (**DIDMA**), as a co-initiator (Figure 4.4, top). The resin (**H–Nu 470/ DIDMA/ SR349**) was irradiated at 775 nm with 150 fs pulses, and the microstructure was obtained with features of 9 μm in width separated by 50 μm (Figure 4.4, bottom).

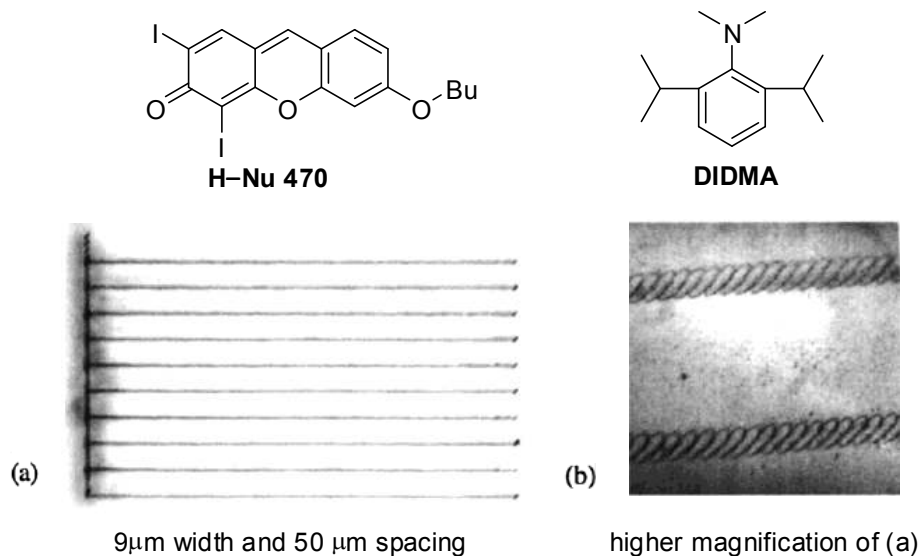


Figure 4.4 Top: structures of **H-Nu 470** and **DIDMA**. Bottom: the micrograph of polymerized microstructure.³⁹

The authors proposed a mechanism^{39,43} based on a single-photon photochemistry study of the initiation system (Figure 4.5):²⁰⁰ **H-Nu 470** was promoted to its excited state by two-photon excitation at 775 nm; an electron was transferred from **DIDMA** to the excited state of **H-Nu 470**; and the subsequent proton transfer resulted in the formation of an arylamine bearing a free radical localized on the α -methylene carbon, which then initiated the radical polymerization.

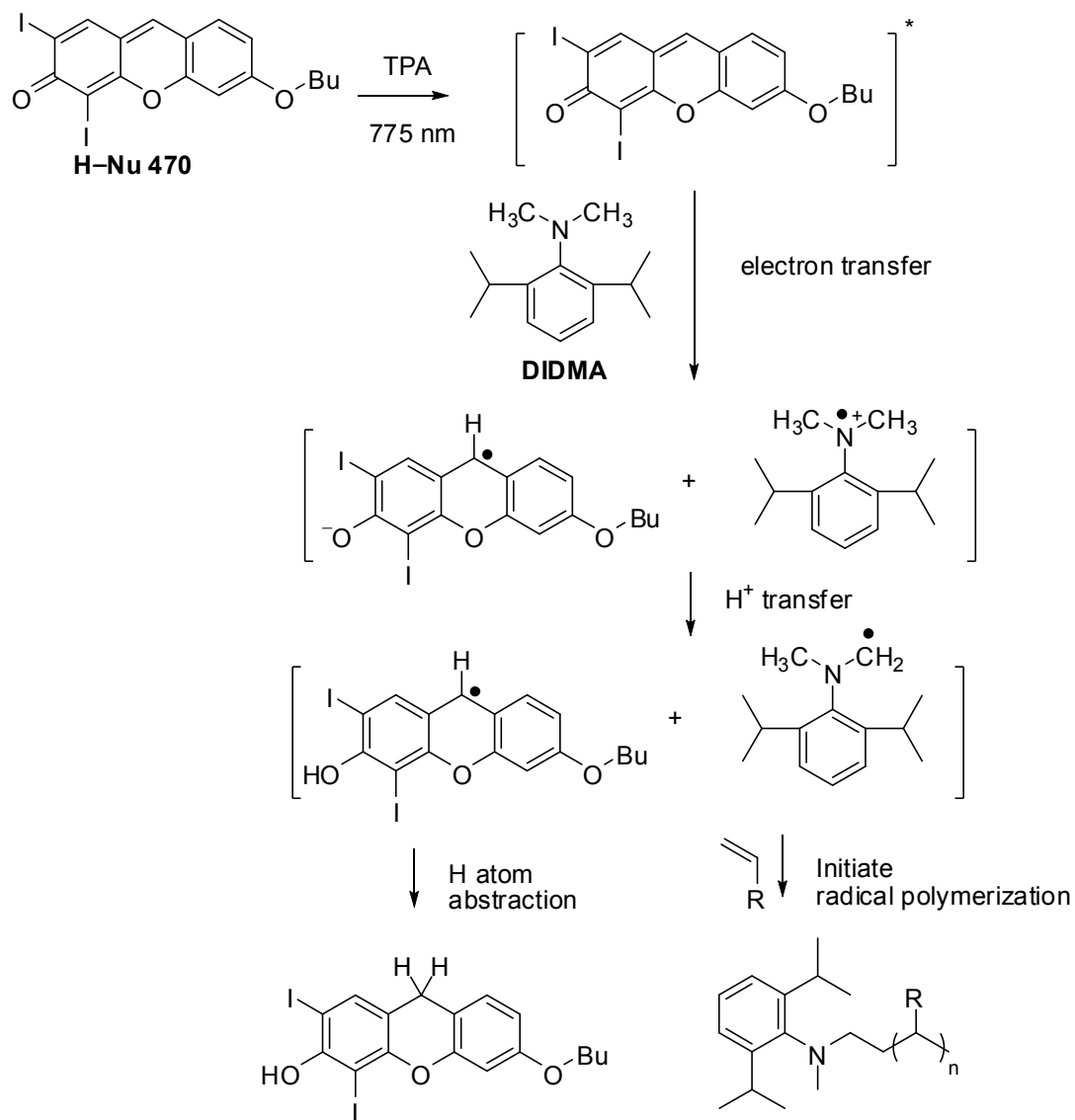


Figure 4.5 Single-photon initiation mechanism proposed by Belfield.

Li used 7-diethylamino-3-(2'-benzimidazolyl)coumarin (**DEDC**) as a sensitizer and diphenyliodonium hexafluorophosphate (**DIHP**) as an initiator (Figure 4.6).²⁰¹ This radical generator system was used to fabricate a microstructure of a two-layer log stack with 4 μm period under the irradiation of 76 MHz, 800 nm and 120 fs laser pulses (Figure 4.6).²⁰¹ The proposed mechanism involves electron transfer from the excited **DEDC** to **DIHP**, generating an active phenyl radical. The cross-section of **DEDC** was determined to be 29.5 GM using two-photon fluorescence measurements.

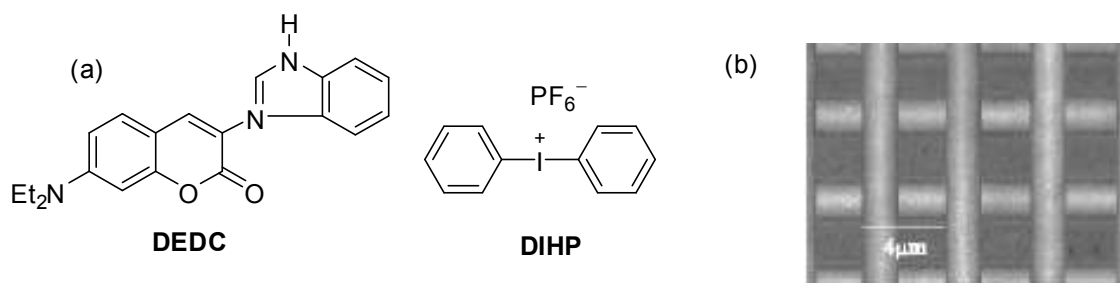


Figure 4.6 (a) Structures of **DEDC** and **DIHP**. (b) The microstructure of a two-layer log stack with 4 μm period.²⁰¹

The conventional radical generators and sensitizers used in these studies typically have small TPA cross-sections (less than 20 GM).¹⁸⁸ Their low two-photon sensitivity requires high excitation power and long exposure time, which may result in optical damage of the structures, which limit the application scope of two-photon radical polymerization in 3DLM.

4.1.2 Two-photon chromophores with large cross-sections

To facilitate the acceptance of two-photon radical polymerization as a commonly applicable technique in 3DLM, efforts have been made to develop two-photon absorbing chromophores with large cross sections. The Perry, Brédas and Marder groups have both theoretically predicted and experimentally investigated the structure-property relationships of two-photon chromophores, and reported many two-photon chromophores with large cross-sections.^{31,33} Furthermore, they have successfully fabricated microstructures by two-photon radical polymerization via direct irradiation of two-photon chromophores.¹² The hypothesis for the initiation mechanism was that electron transfer from the excited chromophores to monomers/oligomers initiated radical polymerization. The intermolecular electron transfer from photoexcited 4,4'-bis(*N,N*-di-*n*-butylamino)-*E*-stilbene **40** (Figure 4.7) to various electron acceptors was experimentally studied and confirmed by steady-state fluorescence quenching, fluorescence lifetime shortening, and appearance of electronic absorption bands due to the formation of the radical cation of **40**. Additionally, the covalently linked chromophore-acceptor systems **41** – **44** were synthesized by replacing one or more of the amino-bound alkyl groups in **40** with different electron acceptors. Efficient intramolecular electron transfer was then confirmed by the same experimental methods. The threshold for photopolymerization of a commercial triacrylate (**SR9008**) initiated by **40** was shown to be only 30% of that using many conventional UV radical photoinitiators,²⁰² such as benzil, 1-[4-(methylthio)phenyl]-2-methyl-2-morpholinopropan-1-one (**MP**) and 4,4-bis(*N,N*-dimethylamino)benzophenone (**DABP**).

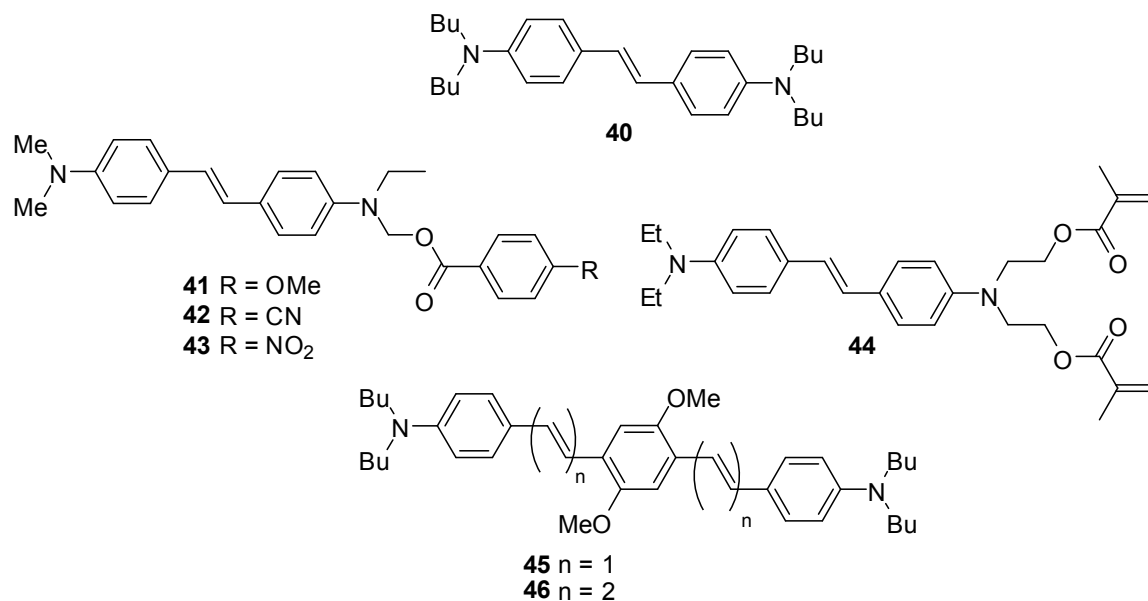


Figure 4.7 Molecules for the studies of two-photon initiated radical polymerization.

Based on the results, two chromophores **45** and **46** (Figure 4.8) with large cross-sections (900 GM at 730 nm for **45**, and 1250 GM at 775 nm for **46**)³³ were selected for 3DLM. The resins consisted of photoinitiators (0.1%, **45** or **46**), triacrylates (70%, **SR9008** and **SR368** in 3:1 ratio), and poly(styrene-*co*-acrylonitrile) (29.9%) as a polymer binder. The resins were irradiated by using laser pulses (50 fs duration, 76 MHz repetition frequency, 0.35 μm radial spot size) at wavelengths near the two-photon absorption peak of the initiators (730 nm for **45** and 775 nm for **46**). The three-dimensional microstructures that were obtained are shown in Figure 4.9. The use of **45** and **46** in photopolymerization resulted in an order-of-magnitude improvement in two-photon sensitivity, relative to benzil, **MP** and **DABP**. These results have opened a path

towards radical polymerization in 3DLM using two-photon chromophores with large cross-sections.

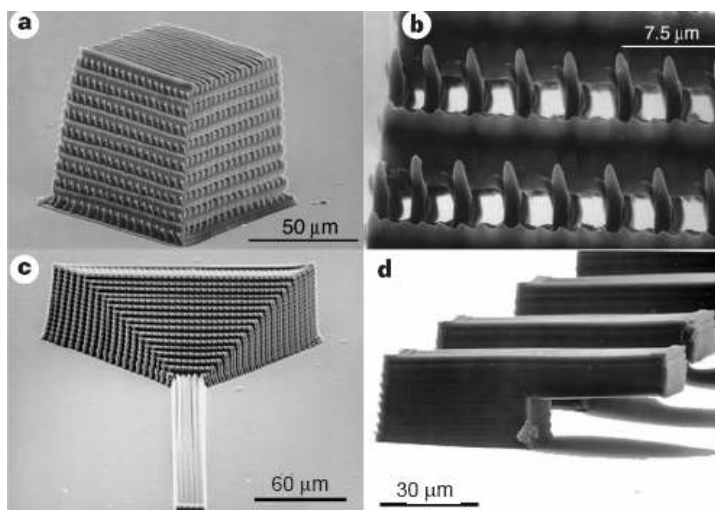


Figure 4.8 Three-dimensional microstructures produced by two-photon initiated radical polymerization. (a) Photonic bandgap structure. (b) Magnified top-view of structure in a. (c) Tapered waveguide structure. (d) Array of cantilevers.¹²

In order to improve the resolution of 3DLM, a subsequent study based on the same initiation mechanism was performed by using a two-photon chromophore with a shorter excitation wavelength, such as 4-4'-bis(di-*n*-butylamino)biphenyl **47** (Figure 4.9).²⁰³ Since the diffraction-limited focal volume is proportional to the third power of the excitation wavelength, decreasing the excitation wavelength can lead to smaller focal volumes, which can improve 3DLM resolution.¹⁸⁰ The molecule **47** has a shorter peak two-photon excitation wavelength (520 nm) than **45** (730 nm) due to its shorter conjugation length, while retaining a reasonably large two-photon cross-section (200 GM

at 520 nm).²⁰⁴ Thus, chromophore **47** was selected as the radical generator for resolution enhancement.

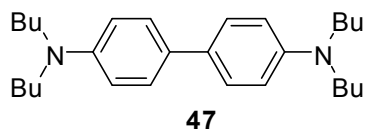


Figure 4.9 Structure of two-photon chromophore **47**.

The resin contained the initiator (0.1%, **45** or **47**) and triacrylates (99.9%, **SR9008** and **SR368** in 1:1 ratio). Two different laser systems were used. The 80 fs pulses (82 MHz repetition rate at 730 nm) were employed for the **45**-triacrylate resin, and the 100 fs pulses (1 kHz repetition rate at 520 nm) were applied for the **47**-triacrylate resin. The width of lines fabricated at threshold powers for both resins are shown in Figure 4.10. A roughly 2.4 times reduction in the feature size was obtained at 520 nm irradiation of **47** in comparison of 730 nm excitation of **45**. The results are consistent with the idea that the resolution is fundamentally tied to the excitation wavelength.

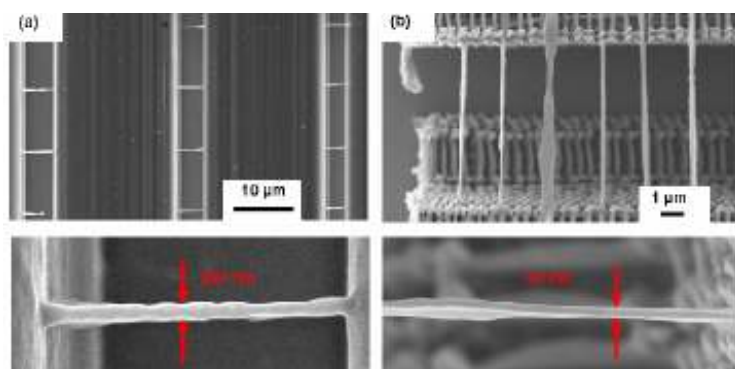


Figure 4.10 SEM magnified images of a single line fabricated at threshold powers. (a) 730 nm excitation of **45**-triacrylate resin. (b) 520 nm excitation of **47**-triacrylate resin.²⁰³

After the microfabrication conditions were optimized, woodpile-type photonic crystal structures were fabricated by using 47-triacrylate resin at 520 nm (Figure 4.11). The lateral line-to-line spacings were (a) 0.85 μm and (b) 0.5 μm , and axial layer to layer spacing was 0.34 μm .

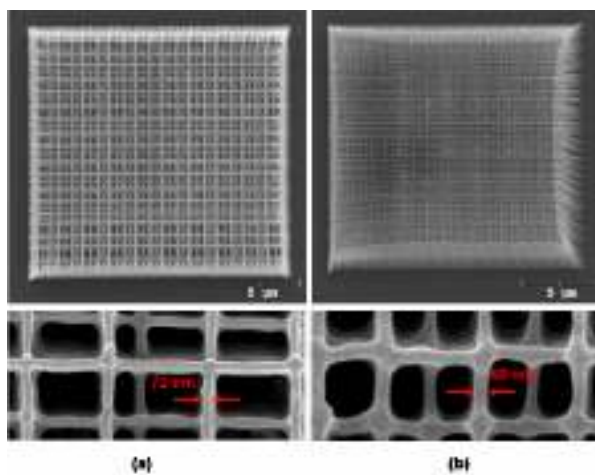


Figure 4.11 SEM overview images of woodpile-type photonic crystal structures using 47-triacrylate resin fabricated with 520 nm excitation at (a) 0.60 μW and at (b) 0.45 μW .²⁰³

4.2 Research goal and molecular design strategy

Our group and collaborators have successfully applied two-photon chromophores with large cross-sections for radical polymerization in 3DLM *via* direct electron transfer from the excited two-photon chromophores to monomers/oligomers.^{12,203} In order to extend the applications, the research goal of this Chapter is to design, synthesize, and characterize two-photon radical generators. The design strategy was to covalently attach a radical generator to a two-photon chromophore via a linker. Upon irradiation, electron transfer from the excited two-photon chromophore to the radical generator moiety might lead to the generation of radicals, which would initiate radical polymerization in 3DLM. Several advantages were expected for this design strategy. First, it provides the flexibility to choose two-photon chromophores according to the excitation wavelength of interest. Second, if radical initiation is faster than initiation through direct electron transfer to the monomer, the polymerization threshold energy would be lower and the microfabrication speed would be faster, which would lead to a decrease in the necessary applied pulse energy and reduction of structural damage. Third, this strategy could be used to explore the polymerization of different monomers. The direct electron transfer mechanism requires that the charge-transfer state formed by electron transfer to the monomer should have a lower energy than the excited state of the two-photon chromophore, which limits the selection of monomers; this would not be the case for radical generators.

Two-photon acid generators were prepared by attaching sulfonium salts to two-photon chromophores, and acids were successfully generated via a mechanism described by electron transfer from the excited two-photon chromophores to the sulfonium

group.^{169,187} In the literature, sulfonium salts were reported to function as both acid generators^{97,110,122,124-127,129,131} and radical generators.²⁰⁵⁻²¹¹ By using the same design strategy, we sought to synthesize two-photon radical generators by covalently attaching sulfonium salts to two-photon chromophores via a linker.

To achieve this goal, the research was divided into three sections. In section 4.3, both radical generation and electron acceptor abilities of triphenylsulfonium salts are determined. In section 4.4, model molecules, designed to study the linker effects on polymerization efficiency, are described. In sections 4.5 and 4.6, synthesis of two-photon radical generators, their behavior under one-photon conditions, and their properties under two-photon conditions, in collaboration with Dr. Perry's group, are also investigated.

4.3 Study of UV-labile radical generators

4.3.1 Literature review

The photolysis mechanism of triarylsulfonium salts upon irradiation has been proposed in the literature (Figure 4.12).²¹² The photoinduced cleavage of a sulfur-carbon bond forms an aryl radical ($\text{Ar}\cdot$) and a diarylsulfonium radical cation ($\text{Ar}_2\text{S}^{+\bullet}$). The subsequent reaction of $\text{Ar}_2\text{S}^{+\bullet}$ with solvent or monomer produces a secondary radical fragment ($\text{Y}\cdot$). The acid (H^+X^-) is then generated following the formation of triarylsulfide. The radicals generated can also recombine. The proposed mechanism suggests that triarylsulfonium salts could generate both acids and radicals, which could initiate either cationic or radical polymerization, or initiate both simultaneously. In addition, it indicates that acid generation and radical generation are two competitive processes.

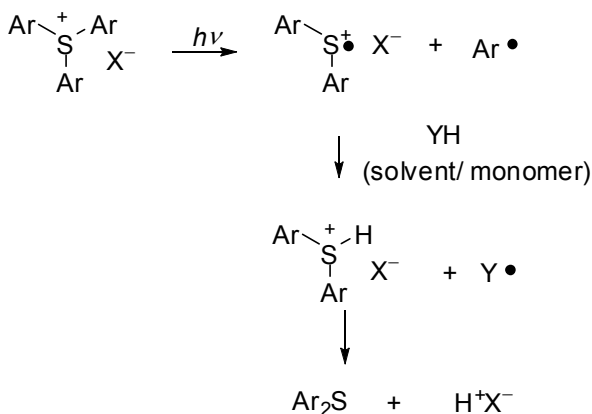


Figure 4.12 Proposed photolysis mechanism for triarylsulfonium salts.

Triarylsulfonium salts exhibit excellent thermal and light stability in the dark compared to conventional free-radical photoinitiators. In fact, they have been used as inhibitors to prevent spontaneous free radical polymerization of unsaturated polyesters.²¹³ However, when they are exposed to light in the presence of vinyl monomers, rapid radical polymerization is observed.²⁰⁵⁻²⁰⁹ In addition, triarylsulfonium salts can initiate simultaneously radical and cationic polymerizations, which can provide a broader spectrum of resist materials whose properties can be modified by choosing combinations of both types of monomers.

Crivello demonstrated that tris(4-methoxyphenyl) sulfonium hexafluoroarsenate and benzoin-*n*-butyl ether both initiated polymerization of methyl methacrylate. The polymerization rate of benzoin-*n*-butyl ether was higher in the beginning due to faster photolysis, but the two rate curves converged at longer irradiation, and their overall rates were comparable at this limit. The simultaneous radical and cationic polymerizations in the presence of both methyl methacrylate and cyclohexene oxide were also been studied for triphenylsulfonium salts with different anions. The BF_4^- salt only gave poly(methyl methacrylate) and no poly(cyclohexene oxide), but the AsF_6^- and PF_6^- salts afforded both poly(cyclohexene oxide) and poly(methyl methacrylate) (96:4 ratio). Thus, they suggested that triarylsulfonium salts bearing non-nucleophilic counterions (SbF_6^- , AsF_6^- , PF_6^-) were efficient acid generators, and those bearing relatively more nucleophilic or basic anions (Cl^- , Br^- , I^- , BF_4^-) were efficient radical generators.²⁰⁵ Kondo reported that benzyl diphenylsulfonium tetrafluoroborate initiated polymerization of both styrene and methyl methacrylate.²⁰⁶ Later on, they studied anion effects (Cl^- , Br^- , I^- , BF_4^-) of

triphenylsulfonium salts on radical polymerization efficiency of both styrene and methyl methacrylate.²⁰⁸ Their results show that the Cl^- , Br^- , and BF_4^- salts initiated radical polymerization for both monomers, but I^- salt did not work for either. Furthermore, the decreasing order of initiation efficiency ($\text{Br}^- > \text{Cl}^- > \text{BF}_4^-$) applied for both radical polymerizations. Timpe studied an initiation system that consisted of various sensitizers and triphenylsulfonium tetrafluoroborate, which initiated photopolymerization of methyl methacrylate.²⁰⁹

4.3.2 Research goal and molecular design

Triarylsulfonium salts were selected as both radical generators and electron acceptors for the design of two-photon radical generators. Triarylsulfonium salts bearing substituents with different electron densities at different positions relative to the sulfonium group were designed and synthesized. The research goal here is to understand the effects of their structures on the efficiency of radical polymerization and on the ability of different sulfonium species to act as acceptors in electron transfer reaction.

The target molecules **48** – **52** are designed for this purpose (Figure 4.13). Butylsulfinyl ($-S\text{Bu}$) is an electron-donating group, and butylsulfonyl ($-\text{SO}_2\text{Bu}$) is an electron-withdrawing group. They were attached at two different positions (*meta*- and *para*-) to the sulfonium group of triarylsulfonium salts to give the target molecules **48** – **51**. The molecular **52** has no substituent at corresponding positions. Br^- was selected as the anion according to the research results in the literature.²⁰⁸ Studies of both the electron transfer aspect and the polymerization aspect were performed.

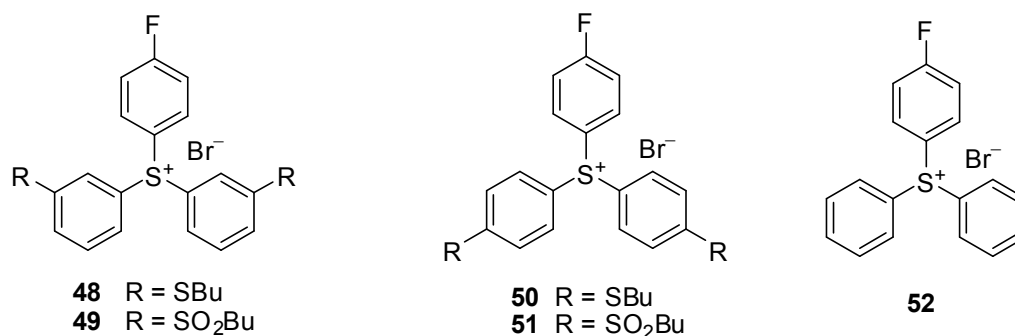


Figure 4.13 Target Molecules **48** – **52**.

4.3.3 Synthesis

The *meta*-substituted triarylsulfonium salts **48** and **49** were synthesized in four steps (Figure 4.14).²¹⁴ 3-Bromobenzenethiol was reacted with 1-bromobutane under basic conditions to form (3-bromophenyl)butylsulfane **53**. The Grignard reagent was prepared by the reaction of **53** and magnesium metal, which was then treated with sulfur dioxide to give sulfoxide **54**. The sulfonium salt with the butylsulfinyl substituent **48** was prepared by the reaction of **54** and the Grignard reagent formed by 4-fluoro-1-bromobenzene and magnesium metal in the presence of chlorotrimethylsilane. The compound **48** was oxidized by oxone to afford the butylsulfonyl substituent sulfonium salt **49**.

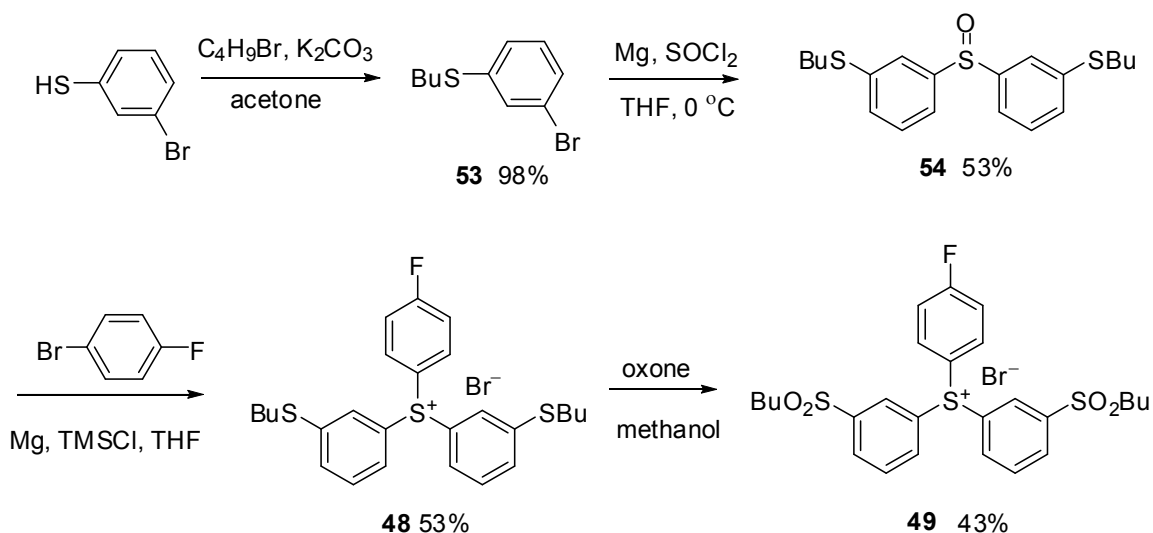


Figure 4.14 Synthesis of the *meta*-substituted triarylsulfonium salts **48** and **49**.

The triarylsulfonium salts with butylsulfinyl **50** and butylsulfonyl **51** substituents at the *para*- position were synthesized by using the same reaction conditions as their *meta*- analogs (Figure 4.15).

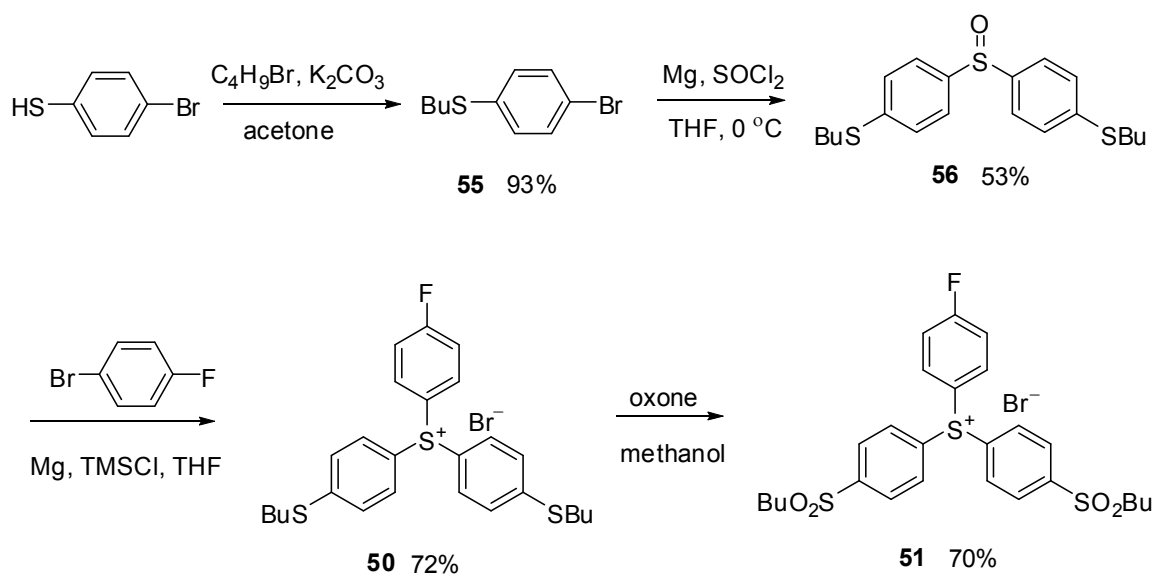


Figure 4.15 Synthesis of the *para*-substituted triarylsulfonium salts **50** and **51**.

4.3.4 Photochemical studies

For **48** – **52**, their absorption spectra, extinction coefficients, and reduction potentials were measured, and their fluorescence quenching was studied. Based on these results, three representative molecules **50** – **52** were selected to study the efficiency of radical polymerization of methyl methacrylate. The photochemical results are summarized in Table 4.1.

	λ_{\max}^a (nm)	ϵ_{\max}^a ($10^4 \text{ M}^{-1} \text{ cm}^{-1}$)	$E_{\text{red}}^{a,c}$ (V)	Fluorescence quenching ^{a,d}	Polymer yield ^{a,e} (%)
48	239, 273, 313	3.54, 2.22, 0.41	-2.03	0.67	–
49	249(sh) ^b	1.27(sh) ^b	-1.71	0.00	–
50	312	2.77	-2.13	0.70	5
51	236	2.81	-1.62	0.00	48
52	234	1.80	-1.95	0.69	25

^aThe measurements were conducted in acetonitrile. ^bsh: shoulder peak and extinction coefficient at shoulder wavelength. ^c E_{red} : reduction peak potentials relative to $\text{FeCp}_2^{+/0}$ (scan rate 50 mV/s). ^dSee details in section 4.3.4.3. ^eThe yield of poly(methylmethacrylate). The solution of MMA (0.067 M) and initiator (1.0 mol% of MMA) in acetonitrile was irradiated at 350 nm. The yield without initiator was 3%.

Table 4.1 One-photon physical data for radical generators **48** – **52**.

4.3.4.1 Absorption spectra

The absorption spectra of **48** – **52** were taken (Figure 4.16). For molecule **49**, only a shoulder peak could be described, and the absorptivity at the shoulder wavelength is reported in the table. The strongest absorption maxima are around 240 nm, except that for **50** while is about 70 nm red-shifted relative to others. The results were consistent with the more extensive delocalization of the π system of **50** due to the electron-donating group ($-S\text{Bu}$) at the *para*-position of the positively charged sulfonium group.

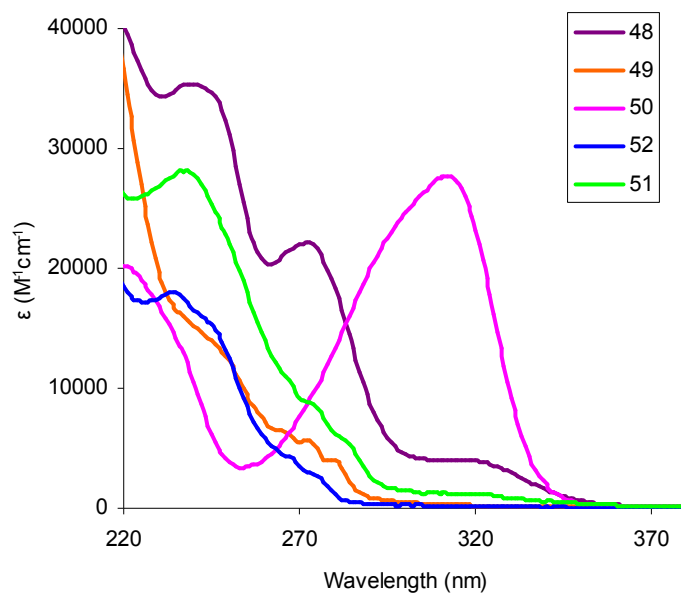


Figure 4.16 Absorption spectra for **48** – **52** in acetonitrile.

4.3.4.2 Reduction potentials

The cyclic voltammetry behavior of all the radical generators **48** – **52** were investigated using ferrocene as an internal standard. For all compounds, only irreversible reduction peaks were found, and no oxidation peaks were observed. The reduction peak potentials (E_{red}) relative to ferrocenium/ferrocene ($\text{FeCp}_2^{+/0}$) are listed in the Table 4.1.

The data show that the same substituent at different positions (*meta*- vs *para*-) does not significantly affect the reduction potentials, and there is only about 0.1 V difference between the effects of $-\text{SBu}$ or $-\text{SO}_2\text{Bu}$ groups at the different positions. For the substituents with different electron density ($-\text{SBu}$ or $-\text{SO}_2\text{Bu}$) at the same position, the difference was relatively larger ($\sim 0.3 - 0.5$ V). Compounds **49** and **51** with the electron-withdrawing group ($-\text{SO}_2\text{Bu}$) are more easily reduced than un-substituted **52**. On the other hand, compounds **48** and **50** with the electron-donating group ($-\text{SBu}$) are less easily reduced in comparison with **52**. The reduction potentials suggest that **51** is the best candidate from the point of view of electron transfer.

4.3.4.3 Fluorescence quenching study

To further investigate the abilities of **48** – **52** to act as electron acceptors, their ability to quench the fluorescence of the two-photon chromophore **45** was investigated. We define the relative fluorescence intensity (I_{fl}) as the maximum fluorescence intensity of **45** at a certain concentration of quencher relative to that of **45** without any quenchers.

At molar ratio of quencher to fluorophore of 4000:1, the I_{fl} values for –SBU compounds **48** and **50**, and the un-substituted compound **52** were about the same (~ 0.70), indicating 30% of fluorescence of **45** was quenched by **48**, **50** and **52**. At the same molar ratio, the I_{fl} values of the –SO₂Bu compounds **49** and **51** were found to be zero, which indicates that the fluorescence quenching was 100% at this ratio. These results suggest molecules with electron-withdrawing groups have higher quenching efficiency than those with electron-donating groups. To compare the quenching efficiency of **49** and **51** (both with the –SO₂Bu group), the dependence of I_{fl} upon the molar ratio of quencher to fluorophore was studied (Figure 4.17). The graph shows that at the same molar ratio, the *para*-substituted **51** is slightly more efficient than the *meta*- substituted **49**.

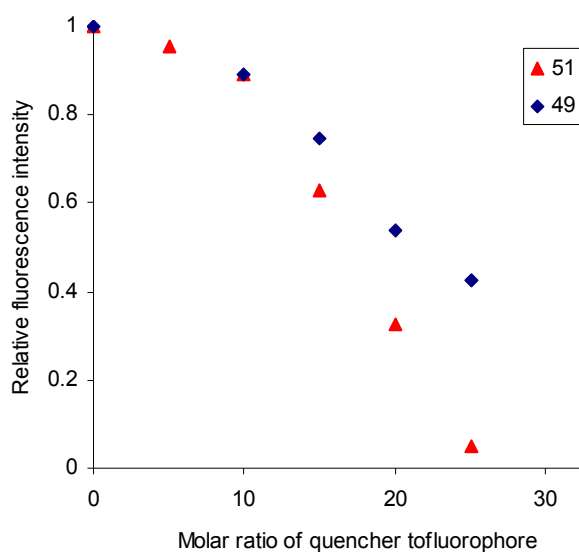


Figure 4.17 Fluorescence quenching of **49** and **51**.

The fluorescence quenching results suggest that the most efficient fluorescence quencher is **51** with an $-\text{SO}_2\text{Bu}$ group at the *para* position of the sulfonium group, which is consistent with the cyclic voltammetry studies. Thus, the molecule **51** has the lowest reduction potential and highest fluorescence quenching efficiency among these five molecules **49** – **52** which indicates that this compound is the best electron acceptor. Compound **51** appears to be the best candidate based on electron transfer considerations.

4.3.5 Efficiency of radical polymerization

The proposed design requires that triarylsulfonium salts function as both electron acceptors and radical generators. In this section, the efficiency of their radical generation of **50** – **52** for a polymerization aspect will be examined.

Radical generators **50** – **52** with different substituents at the *para*-position were selected for the study of polymerization of methyl methacrylate. The solution consisted of methyl methacrylate as a monomer, a triphenylsulfonium salt as a radical generator, and acetonitrile as the solvent. After degassing, the solution was irradiated so that the monomers could polymerize. The isolated polymers were collected by precipitation in methanol. The yields of isolated polymers, normalized for the different light dose received by the different compounds (section 4.7.3), are listed in Table 4.1. The yield of poly(methylmethacrylate) without initiator is 3%, 5% for **50** with an electron-donating substituent (–SBu), 25% for un-substituted **52**, and 48% for **51** with an electron-withdrawing substituent (–SO₂Bu), suggesting that **51** is the most efficient radical generator.

The radical photopolymerizations of different monomers (acrylonitrile, methyl methacrylate, and styrene) photoinitiated by **51** were studied. The activity order of these monomers is acrylonitrile > methyl methacrylate > styrene. The yield of isolated polymers is 95% using **51** vs 0% using no initiator for acrylonitrile, 48% vs 3% for methyl methacrylate, and 2% vs 5% for styrene. The trend of polymer yields is consistent with that of the monomer activity.

4.3.6 Conclusion

The triarylsulfonium salt **51** with an electron-withdrawing group at the *para*-position relative to the sulfonium group is the most easily reduced and has the highest fluorescence quenching efficiency. This suggests that **51** is a good electron acceptor from the point of view of excited-state electron transfer. The study of radical polymerization of methyl methacrylate showed that the polymerization initiated by **51** gave the highest polymerization yield, which suggests that **51** is also an efficient radical generator for the polymerization aspect. Therefore, the molecule **51** was considered as the best candidate building block for incorporation into two-photon radical generators.

4.4 Study of model molecules

4.4.1 Research goals and molecules design

Compounds **57** (Figure 4.18) have been reported to successfully initiate the radical polymerization of pentaerythritol tetraacrylate,²¹¹ however, there have been no other studies on these compounds.

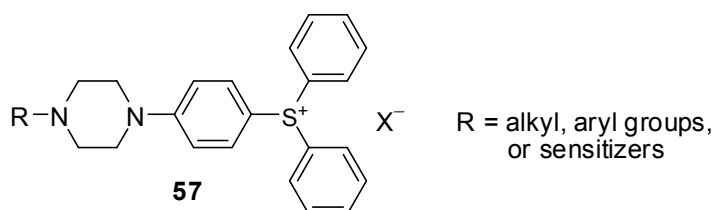


Figure 4.18 Radical generators reported in the literature.

For our design of two-photon radical generators, piperazine was chosen as a linker between the two-photon chromophore and radical generator. To understand the linker effects on the efficiency of radical polymerization, three model molecules **58** – **60** were designed and synthesized by covalently attaching triarylsulfonium salts to 1-phenylpiperazine (Figure 4.19), and their photochemical properties and polymerization efficiencies were studied.

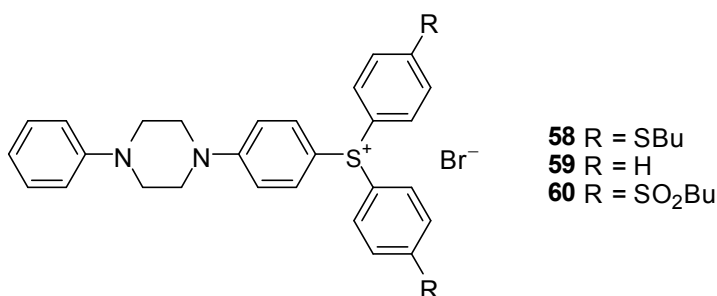


Figure 4.19 Target model molecules **58** – **60**.

4.4.3 Study of anion effects

Triarylsulfonium salts can be used as either acid or radical generators, depending on their anions. The AsF_6^- and PF_6^- salts were reported as effective acid generators, and those bearing relatively more nucleophilic or basic anions (Cl^- , Br^- , I^- , BF_4^-) could be effective radical generators.²⁰⁵ The Br^- salt was reported the most efficient salt among the Cl^- , Br^- , I^- , and BF_4^- salts for initiation of radical polymerization of both styrene and methyl methacrylate.²⁰⁸ To test literature conclusions for our model molecules, the molecules **59** with Br^- and **61** with PF_6^- were employed for radical polymerization of methyl methacrylate. The polymerization solution of methyl methacrylate, a radical generator and acetonitrile was irradiated and was allowed to propagate after the solution was degassed. The isolated polymers were collected by precipitation in methanol. The isolated polymer yield is 5% for **61** with PF_6^- and 12% for **59** with Br^- . The results indicate that Br^- is a more efficient anion than PF_6^- for polymerization of methyl methacrylate, and our result is consistent with the literature conclusions. Thus, Br^- was selected as the anion for the design of two-photon radical generators.

4.4.4 Photochemistry Study

For the three model molecules **58** – **60**, their absorption spectra and quantum yields of acid generation were measured. The photolysis products were analyzed, and their efficiency for radical polymerization was examined. The photochemical results are summarized in Table 4.2.

Initiators	λ_{\max}^a (nm)	ϵ_{\max}^a ($10^4 \text{ M}^{-1} \text{ cm}^{-1}$)	$\Phi_{\text{H}^+}^{a,b}$ (± 0.05)	Polymer yield ^{a, c} (%)
58	305	4.94	0.04	10
59	320	2.29	0.07	14
60	391, 329	1.90, 1.07	0.02	6

^aThe measurements were conducted in acetonitrile. ^b Φ_{H^+} : quantum yield of acid generation (section 4.7.2). ^cThe yield of poly(methylmethacrylate). The solution of MMA (0.067 M) and initiator (1.0 mol% of MMA) in acetonitrile was irradiated at 350 nm. The yield without initiator was 3%.

Table 4.2 One-photon physical data for radical generators **58** – **60**.

4.4.4.1 Absorption spectra

The absorption spectra were measured for **58** – **60** (Figure 4.22). The absorption maxima for **58** (305 nm) and **59** (320 nm) are close. That of **60** is 70 – 85 nm red-shifted with a second absorption maximum (329 nm) close to those of **58** and **59**. The extinction coefficients of **58** and **60** were similar, but that of **59** is doubled.

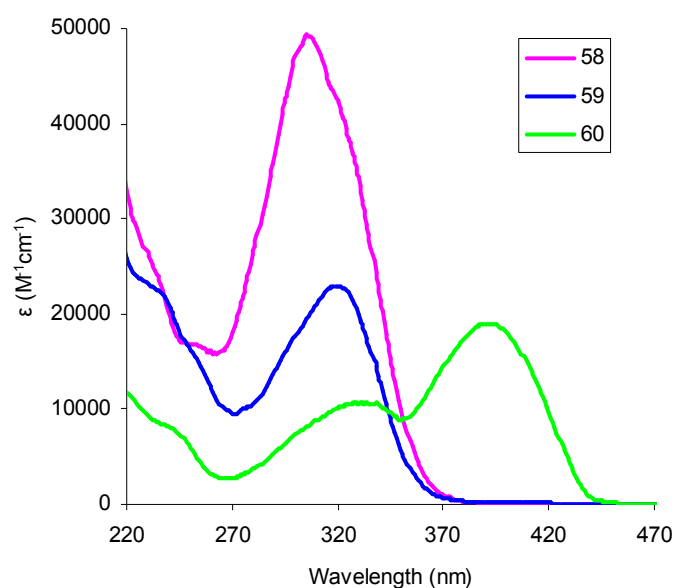


Figure 4.22 Absorption spectra for **58** – **60** in acetonitrile.

4.4.4.2 Quantum yield of acid generation

As discussed in section 4.3.1, it is known that triarylsulfonium salts can function as both acid generators and radical generators. From the proposed mechanism (Figure 4.13), acid generation and radical generation are competitive. Thus, if model compounds **58** – **60** are efficient radical generators, they should have low quantum yields of acid

generation. To confirm this assumption, quantum yields of acid generation were measured for **58** – **60** by using the method that was described in Section 3. It was found that **58** – **60** have very low quantum yields of acid generation (ranged from 0.02 to 0.07), and are identical within uncertainties (± 0.05). Thus, **58** – **60** could be effective radical generators.

4.4.4.3 Photoproduct analysis

The photoproducts of **59** and **60** were analyzed. The molecules were photolyzed in acetonitrile with an immiscible cyclohexane layer on top with continuously purging nitrogen through the acetonitrile layer. The photoproducts in both layers were studied by GS-MS. For **59**, the molecular masses observed in the acetonitrile layer were 186, 237, 314, 317, 347, and 423, while 186 was also observed in the cyclohexane layer. The corresponding molecules are shown in Figure 4.23. The photoproduct results suggest that both possible cleavage pathways (a, b) occurred, and three radical recombination processes were observed. For pathway a, no recombination was observed because the 1,4-diphenylpiperazine radical is stabilized by two nitrogen atoms. For pathway b, recombination between benzene radical and sulfonium radical cation was observed because benzene radical is not very stable. In addition, the recombination of 1,4-diphenylpiperazine radical with bromide anion/radical was also observed.

For **60**, the molecular masses from the acetonitrile layer were observed as 197, 237, 317, 427, and 467, while 427 was also present in the cyclohexane layer. The corresponding molecules are shown in Figure 4.24. Two possible cleavage pathways (a,

b) were observed, and no recombination processes occurred for both pathways. Butylsulfonylbenzene radical is more stable than benzene radical due to the electron-withdrawing ability of the butylsulfonyl group.²¹⁵ So the recombination between butylsulfonylbenzene radical and its corresponding sulfonium radical cation in pathway b was not observed. The recombination between butylsulfonylbenzene radical and 1,4-diphenylpiperazine radical was also not observed. However, the recombination of 1,4-diphenylpiperazine radical with bromide anion/radical was still observed.

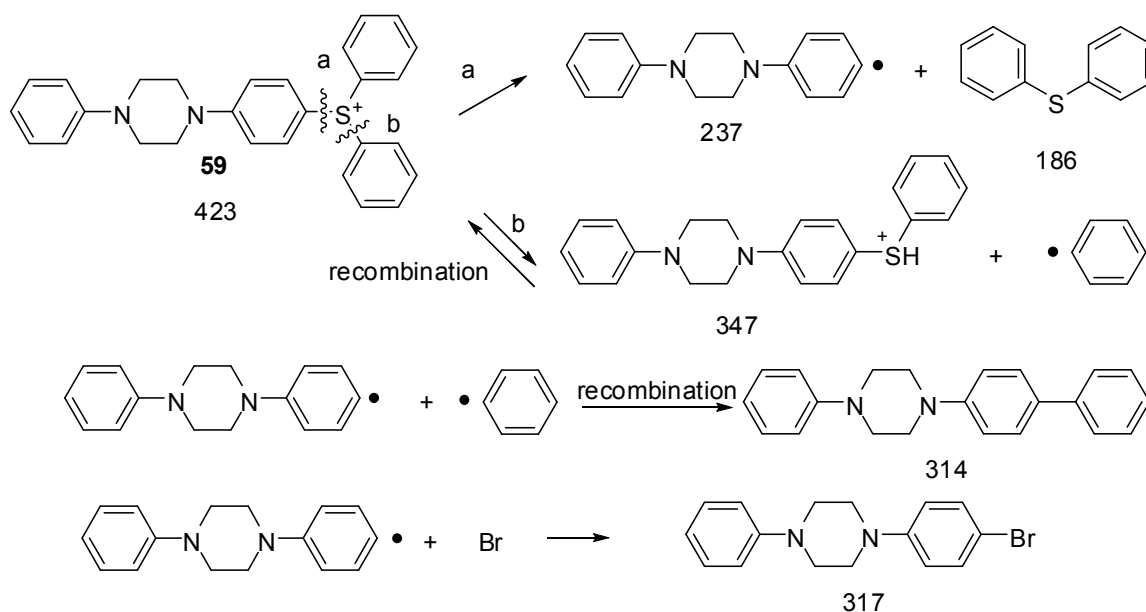


Figure 4.23 Photolysis products of **59**.

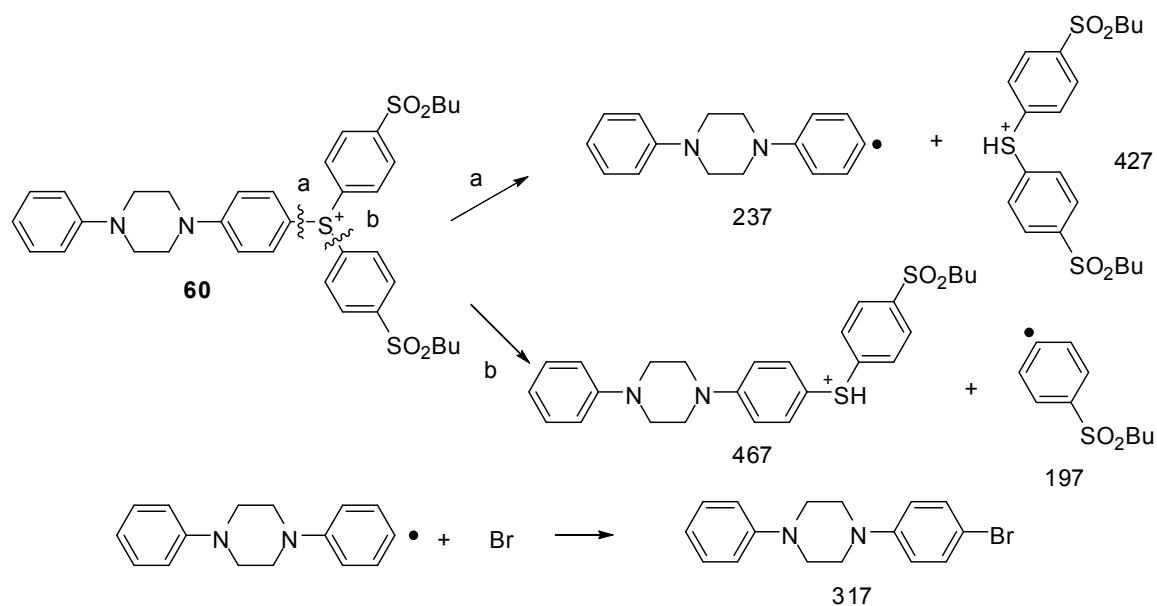


Figure 4.24 Photolysis products of **60**.

The photoproduct analysis suggests that the stabilization of butylsulfonylbenzene radical relative to benzene radical could reduce radical recombination. But on the other hand, it also could reduce the reactivity of butylsulfonylbenzene radical. At this point it is not known which effect plays a more important role in radical polymerization.

4.4.4.4 Polymerization

After degassing a solution of methyl methacrylate and a radical generator in acetonitrile, polymerization was initiated via irradiation. The isolated polymers were collected by precipitation from methanol. The yields of poly(methylmethacrylate) are normalized for the different light dose received by the different compounds (section 4.7.3). The yield without initiator is 3%, 9% for **58** which is functionalized with a $-\text{SBu}$

group, 14% for un-substituted **59**, and 5% for **60** which bears a $-\text{SO}_2\text{Bu}$ group. Compound **60**, with the $-\text{SO}_2\text{Bu}$ group, gave a lower polymer yield than **58** and **59**. This may be due to the stabilization of butylsulfonylbenzene radical by the electron-withdrawing substituent ($-\text{SO}_2\text{Bu}$) in comparison to the benzene radical formed from **58**. The stabilization of this radical could inhibit radical recombination, but also could decrease the activity of the butylsulfonylbenzene radical. Compound **59** gives the highest yield, suggesting that **59** is the most efficient of the model molecules for the radical polymerization of methyl methacrylate.

4.4.5 Conclusion

The model molecules **58** – **60** were synthesized. Their quantum yields of acid generations show that they are poor acid generators, which suggests that they may be good radical generators. The photoproduct analysis suggests both cleavage pathways (a, b) occurred. From the isolated yields of polymerization of methyl methacrylate, the model molecule **58** without any substituent has the highest yield. Thus, model molecule **59** was chosen for the design of a two-photon radical generator.

4.5 Long wavelength two-photon radical generators

4.5.1 Research goal and molecular design

The target molecules for this section are listed in Figure 4.25. Based on the literature and our studies of triarylsulfonium salts, model molecules, and anion effects, the target molecule **62** was designed by covalently attaching triphenylsulfonium bromide to two-photon chromophore **45** through a piperazine linker. Compound **63**^{216,217} was used to study the effects of the piperazine bridge on polymerization. The polymerization ability of **45**, **62** and **63** was tested under one-photon conditions, and the polymerization threshold energies of **62** and **45** were measured under two-photon conditions.

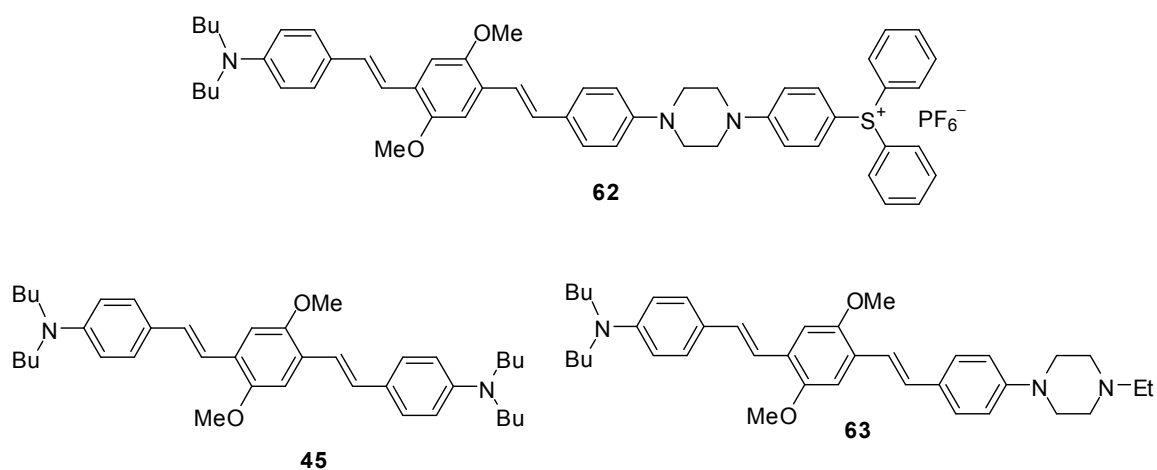
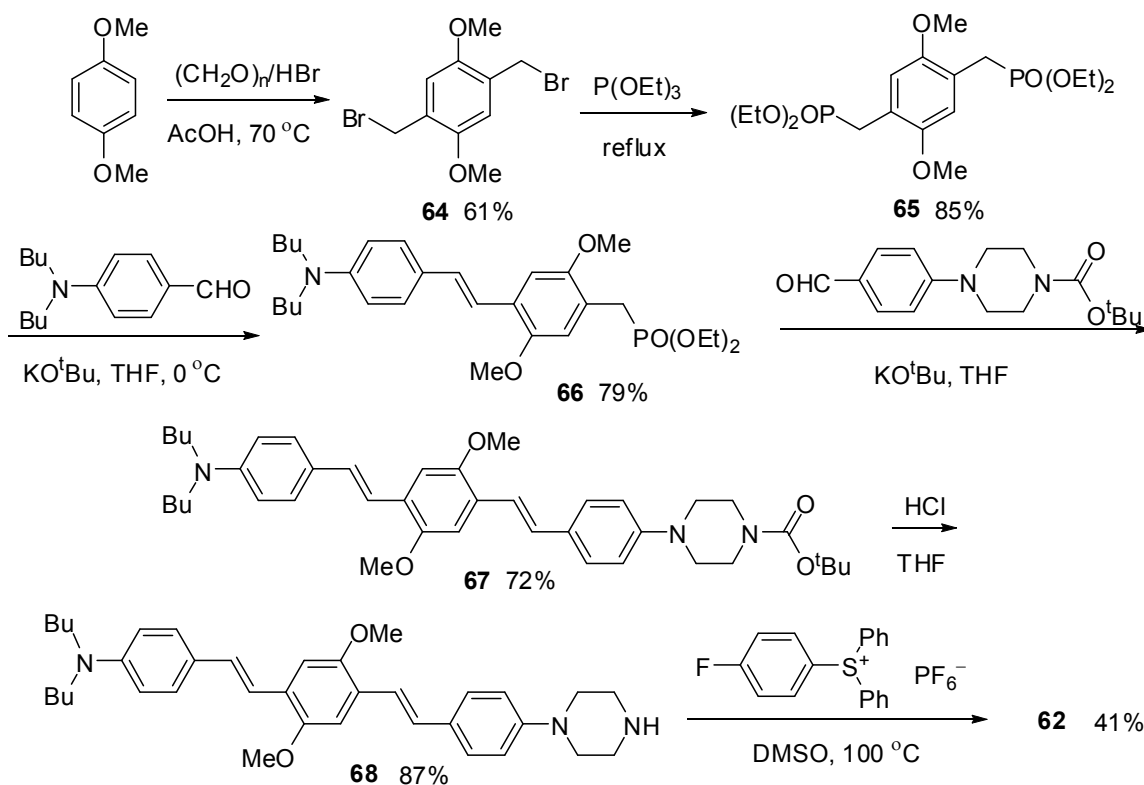


Figure 4.25 Target molecules for long-wavelength two-photon radical generators

4.5.2 Synthesis

The synthesis of **62** is shown in Figure 4.26.²¹⁸ 1,4-Dimethoxybenzene was reacted with formaldehyde in hydrobromic acid to give **64**. The reaction of **64** with triethylphosphite gave **65**. The Horner-Emmons reaction was performed, coupling 4-*N,N*-di-*n*-butylbenzaldehyde to one of the phosphonate groups of **65** to afford **66**. A second Horner-Emmons reaction between **66** and *tert*-butyl 4-(4-formylphenyl)piperazine-1-carboxylate was employed to produce **67**. Deprotection of **67** under acid conditions gave **68**, which has an amine group at one end of the chromophore where the sulfonium salt can be attached. The nucleophilic substitution reaction of **68** and 4-fluorotriphenylsulfonium hexafluorophosphate provided the target molecule **62**.

Figure 4.26 Synthesis of target molecule **62**.

4.5.3 Photochemical study

The absorption spectra and fluorescence spectra were measured for **45**, **62**, and **63**. The fluorescence quantum yields were measured for **45** and **62**.²¹⁹ The efficiencies toward radical polymerization of methyl methacrylate were studied. The photochemical results are summarized in Table 4.3.

	$\lambda_{\max}^{\text{abs}}$ ^a (nm)	ϵ_{\max} ^a ($10^4 \text{ M}^{-1} \text{ cm}^{-1}$)	$\lambda_{\max}^{\text{fl}}$ ^a (nm)	Relative Φ_{Fl} ^{a,b}	Polymer yield ^c (%)
45	429	7.40 ²¹⁹	516	1.00	0
63	422	7.10	534	–	0
62	422, 329	7.60, 3.91 ²¹⁹	537	0.86	4

^aThe measurements were conducted in acetonitrile. ^bRelative fluorescence quantum yields Φ_{Fl} were calculated based on literature data.²¹⁹ ^cThe yield of poly(methylmethacrylate). The solution of the initiator (0.2 mol%) in neat methyl methacrylate was irradiated at 419 nm. The yield without initiator is 2%.

Table 4.3 One-photon physical data for **45**, **62**, and **63**.

Absorption and fluorescence spectra of **45**, **62**, and **63** are shown in Figure 4.30. The absorption spectra show that molecules **62** and **63** with the piperazine linker have the same absorption maximum wavelength (422 nm), which is 7 nm blue-shifted relative to that of chromophore **45** without the piperazine linker (429 nm) (Figure 4.27). A secondary absorption maximum wavelength was only observed for **62** (329 nm), which is consistent with the absorption maximum of the corresponding model molecule **59** (320

nm). The maximum extinction coefficients for these three molecules are very similar. The results suggest that the piperazine linker effectively decouples the chromophore moiety from the triphenylsulfonium group. The fluorescence maxima were 516 nm for **45**, 534 nm for **63**, and 536 nm for **62**.

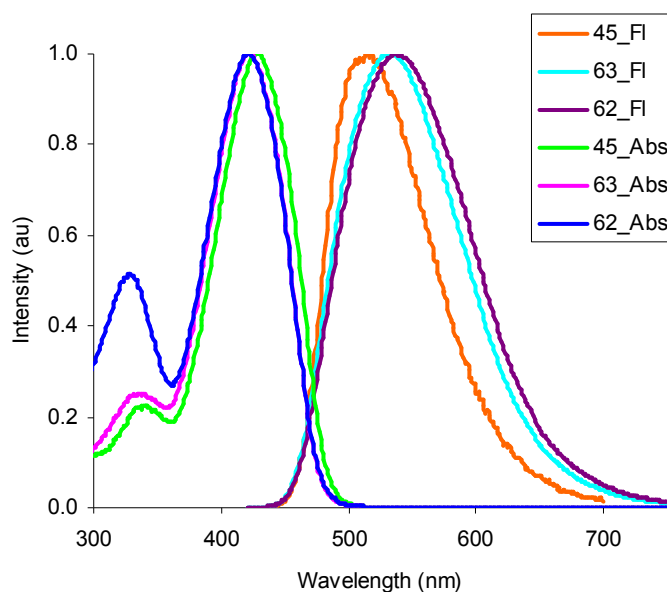


Figure 4.27 Absorption and fluorescence spectra of **45**, **62**, and **63** in acetonitrile.

The fluorescence quantum yield of two-photon radical generator **62** is 0.86 relative to the chromophore **45**, which suggests that probability of electron transfer from the chromophore moiety to the triphenylsulfonium group is low. The polymerization of initiators in neat methyl methacrylate shows that the two-photon radical generator **62** has slightly higher yield, but does not have other substantial advantages.

4.5.4 Two-photon studies

The two-photon studies of **45** and **62** were performed by Dr. Braun in Dr. Perry's group, and the data are shown in the Table 4.4.

	$\lambda_{\max}^{\text{abs}(2)}$ ^a (nm)	δ_{\max} ^b ($10^{-50} \text{ cm}^4 \text{ s photon}^{-1}$)	Threshold ^c (mW)	Threshold ^d (mW)
45	715	740	0.36	0.58
62	705	730	0.46	0.58

^{a,b}The measurements were conducted in acetonitrile. ^bThe TPA cross-sections (δ) were measured using a two-photon-induced fluorescence method with $\pm 15\%$ uncertainty. ^cThe resin of the initiator (12 mM) in neat **SR454** was irradiated at 730 nm. ^dThe resin of the initiator (12 mM) in neat **SR9008** was irradiated at 730 nm.

Table 4.4 Two-photon measurement data for **45** and **62**.

The two-photon absorption maximum of **62** (705 nm) was found to be blue shifted compared to that of **45** (715 nm). For a given exposure time, the polymerization threshold energy can be defined as the average of the lowest and highest pulse energy for which the polymerization was observed and not observed, respectively, which was determined using dose-array measurement that has been described in section 3.8.3. Smaller threshold energy was expected for two-photon radical generator **62** than for chromophore **45**. Both molecules in neat commercial acrylates (**SR454** and **SR9008**) were irradiated at 730 nm, at which the cross-section for **45** and **62** is similar. The thresholds of **62** were slightly higher than (0.46 vs 0.36 in **SR454**) or the same (0.58 in **SR9008**) as those of **45**. The results indicate that two-photon radical generator **62** does not provide an advantage for initiating radical polymerization under these conditions.

4.5.5 Conclusion

The attachment of triphenylsulfonium salts to chromophore **45** has little or no effect on the radical polymerization threshold power under two-photon conditions. The polymerization mechanism of **62** may be inferred to be similar to that of **45**, i.e. through direct electron transfer to the monomers. The key piece of evidence supporting this assumption is a small reduction of the fluorescence quantum yield (14%) of **62** relative to that of **45**. It suggests that probability of electron transfer from the excited state of the chromophore moiety to the charge transfer state of the triphenylsulfonium group is relatively small. Thus, the probability of radical generation is low.

4.6 Short-wavelength two-photon radical generator

4.6.1 Research goal and molecular design

Based on the same molecular design strategy of **62**, a target two-photon radical generator **69** (Figure 4.28) was designed, bearing a two-photon chromophore based on a diaminobiphenyl core with short conjugation, and with bromide as an anion based on the study in section 4.4.3.

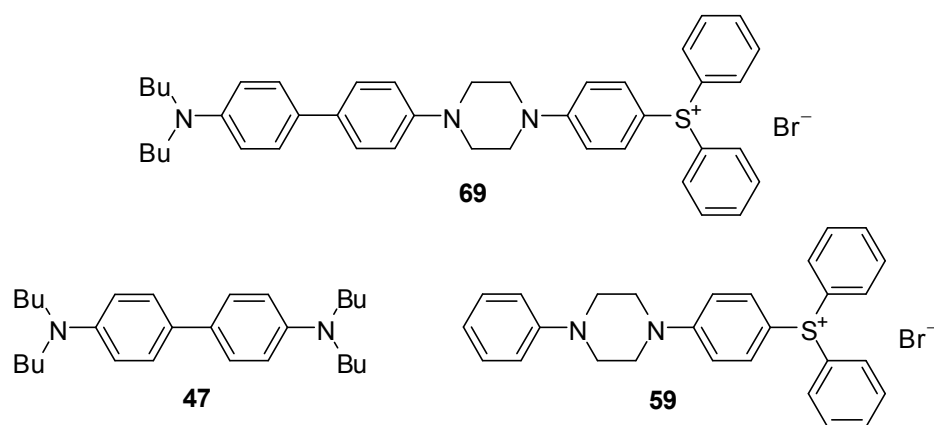


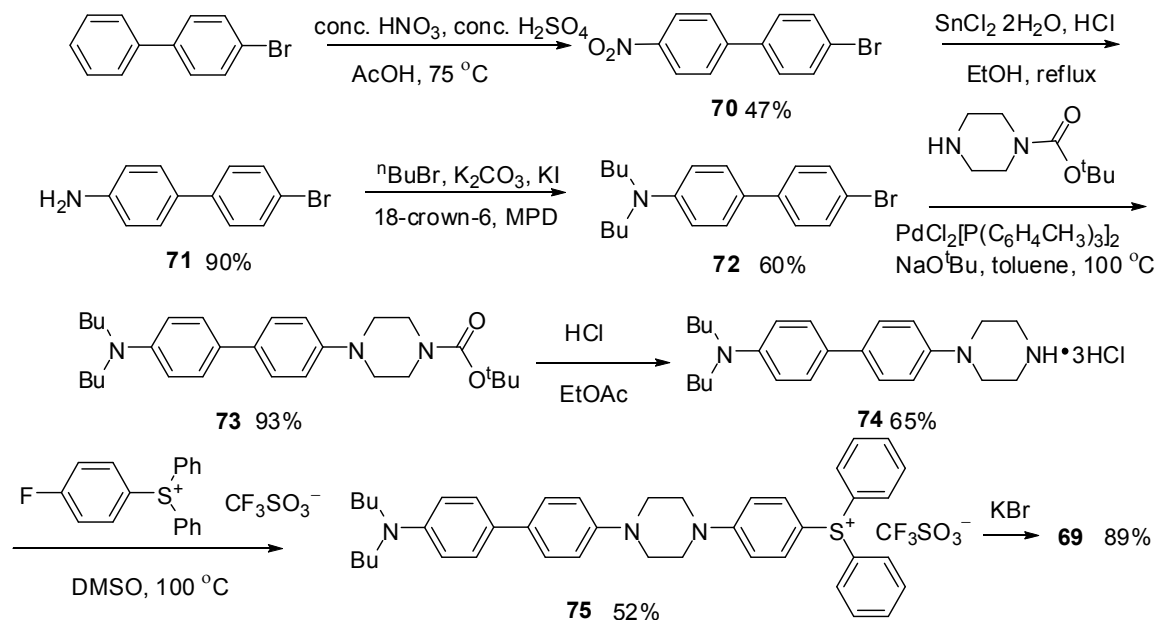
Figure 4.28 Target molecules for short-wavelength two-photon radical generator.

There are two motivations for design of a two-photon radical generator with a shorter conjugation chromophore. First, one possible reason for the poor fluorescence quenching and poor radical generation of compound **62** may be insufficient driving force for electron transfer from the excited state of the chromophore moiety to the sulfonium acceptor. The biphenyl chromophore **47**²²⁰ has shorter conjugation than **62**. The shorter conjugated molecule would be expected to have a higher excited state energy, which would give a larger driving force for electron transfer, leading to an increased rate of

electron transfer from the excited state of the chromophore moiety to the sulfonium acceptor. Secondly, a 2.4 times reduction in feature size has been obtained using 520 nm irradiation of **47** in comparison with 730 nm excitation of **45**, which illustrates that the resolution is fundamentally tied to the excitation wavelength.²⁰³ It indicates that compound **69** could, therefore, similarly be used for shorter wavelength excitation. The biphenyl chromophore **47** and the phenylpiperazine-substituted triphenylsulfonium salt **59** were studied along with the target molecule **69** to understand the contribution from both parts of **69**.

4.6.2 Synthesis

The synthesis of target molecule **69** is shown in Figure 4.29. The nitration of 4-bromobiphenyl was performed in concentrated sulfuric acid and nitric acid to give 4-bromo-4'-nitro-biphenyl **70**. The subsequent reduction was accomplished by tin (II) chloride to afford 4'-bromobiphenyl-4-amine **71**. The alkylation of amine group of **71** under basic conditions afforded (4'-bromo-biphenyl-4-yl)-dibutyl-amine **72**. The coupling between **72** and alkyl amines was catalyzed by palladium (0) to provide **73**. The subsequent deprotection of **73** under acid conditions produced **74**, a corresponding amine salt with 3HCl. The nucleophilic substitution between **74** and 4-fluorophenyl diphenyl sulfonium triflate gave salt **75** with triflate anion. The following anion exchange by washing with potassium bromide provided the target two-photon radical generator target molecule **69**.

Figure 4.29 Synthesis of target molecule **69**.

4.6.3 Photochemical studies

The absorption spectra, fluorescence spectra, and relative fluorescence quantum yields were measured for **47** and **69**. The data for **59** were measured in section 4.4. The efficiency of radical polymerization of methyl methacrylate for **47**, **59** and **69** was studied. The photochemical results are summarized in Table 4.5.

	$\lambda_{\text{max}}^{\text{abs}}$ ^a (nm)	ϵ_{max} ^a ($10^4 \text{ M}^{-1} \text{ cm}^{-1}$)	$\lambda_{\text{max}}^{\text{fl}}$ ^a (nm)	Relative Φ_{Fl} ^{a,b}	Yield ^c (%)
47	320	3.90	407	1.00	2
59	320	2.29	–	–	14
69	324	5.63	401	0.44	15

^aThe measurements were conducted in acetonitrile. ^bRelative fluorescence quantum yield Φ_{Fl} , the corrected value is 0.71 (section 4.7.5) ^cThe yield of poly(methylmethacrylate). The solution of the initiator (0.1 mol%) in neat methyl methacrylate was irradiated at 350 nm.

Table 4.5 One-photon physical data for **47**, **59** and **69**.

The absorption spectra were measured (Figure 4.30). Chromophore **47**, sulfonium salt **59**, and target molecule **69** all absorb at similar wavelength (320 – 324 nm). Under one-photon excitation, it would be difficult to distinguish between radical generation of **69** arising from direct excitation of the sulfonium group and from the excitation of the chromophore moiety followed by electron transfer.

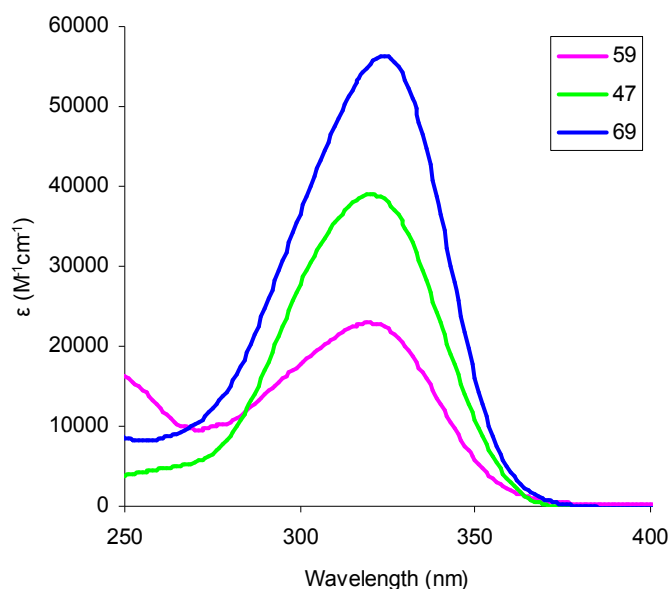


Figure 4.30 Absorption spectra for **47**, **59**, and **69** in acetonitrile.

Although at the first sight, there appears to be more fluorescence quenching in **69** ($\Phi_{\text{Fl}} = 0.44$, Table 4.5) than in the longer system **62** ($\Phi_{\text{Fl}} = 0.86$, Table 4.4), this figure is misleading. The absorption of **69** arises from both the chromophore moiety and the sulfonium group, and its extinction coefficient maximum ($5.63 \times 10^4 \text{ M}^{-1}\text{cm}^{-1}$) is almost equal to the sum of those of **47** ($3.90 \times 10^4 \text{ M}^{-1}\text{cm}^{-1}$) and **59** ($2.29 \times 10^4 \text{ M}^{-1}\text{cm}^{-1}$). Thus only about 63% of the absorbance of **28** can be attributed to the chromophore moiety, assuming $\% \text{ absorbance} = \frac{\epsilon_{\text{max}}(\mathbf{47})}{\epsilon_{\text{max}}(\mathbf{47}) + \epsilon_{\text{max}}(\mathbf{59})} \times 100\%$. This fact suggests that the fluorescence quantum yield of the chromophore moiety in **69** is reduced to 0.71 of that in the free chromophore **47**. Thus, the degree of fluorescence quenching of **69** (29%), potentially attributable to electron transfer, is similar to, but slightly higher than that in **62** (14%).

The solution of the initiator (0.1 mol% of monomers) in neat methyl methacrylate was degassed, irradiated at 350 nm, and was allowed to polymerize. The polymers were isolated and collected by precipitation in methanol. The yields of poly(methylmethacrylate), normalized for the different light dose received by the different compounds (section 4.7.3) are 2% for chromophore **47**, 14% for sulfonium salt **59** and 15% for target molecule **69**. The similar values for **59** and **69** suggest that under one-photon conditions, the polymer yield increase for **69** over **47** can be attributed to direct photo-excitation of the sulfonium group of **69**. Since the absorption spectra of **47**, **59**, and **69** all overlap, only limited conclusions may be drawn from the polymerization results under one-photon conditions. In particular, the yields of **47** and **59** show that polymerization of direct sulfonium excitation is more efficient than that through direct electron transfer from the excited chromophore to monomer. The similarity of the yields of **59** and **69** means that any difference in the efficiencies arising from chromophore excitation is small compared to the role played by direct sulfonium excitation.

4.6.4 Two-photon studies

The initiators for two-photon induced polymerization were excited at 510 nm by using fs pulsed lasers. Under two-photon conditions, the chromophore excitation becomes the dominant mechanism for photoinitiation, assuming negligible triphenylsulfonium excitation at 510 nm. In addition, two-photon studies are, of course, more directly relevant to the intended applications in two-photon polymerization. The measurement of polymerization threshold energies of **47** and **69** under two-photon induced polymerization (Figure 4.31) was performed by V. Chen in Dr. Perry's group.

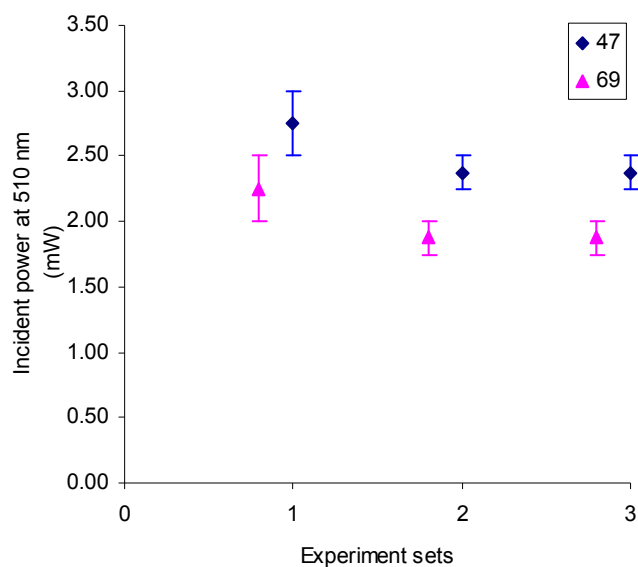


Figure 4.31 Two-photon polymerization threshold energies for **47** and **69**.

For a given exposure time, the polymerization threshold energy can be defined as the average of the lowest and highest pulse energy for which the polymerization was observed and not observed, respectively. The resin for two-photon microfabrication

contained the radical initiator (**47** or **69**, 0.1%) in triacrylates (**SR9008:SR368** in 1:1 ratio), which was excited at 510 nm using laser pulses. Three sets of experiments were performed for both initiators, and each set for both initiators was run on the same day with the same experimental setup. Slight variation of thresholds from day-to-day may be caused by the changes in the optical alignment (for accommodating other experiments). However, over all three sets of experiments, the threshold for **69** is consistently 20% lower than **47** (Figure 4.31). More work is under way to characterize further the properties of initiators **69** under two-photon excitation conditions.

4.6.5 Discussion

Irreversible reduction peaks were observed by cyclic voltammetry spectra for both **62** (−2.04 V) and **69** (−1.99 V). The driving force for electron transfer from the excited chromophore moiety to the sulfonium group (ΔG_{et}) was calculated for both **62** (−61.3 kJ mol^{−1}) and **69** (−142.0 kJ mol^{−1}) based on the equation in section 2.5.3. Compound **62** has a reasonably large electron-transfer driving force, but has a relatively high fluorescence quantum yield ($\Phi_{\text{Fl}} = 0.86$) relative to the corresponding free chromophore **45**, and shows no threshold advantages over **45** under two-photon excitation. The same trends are applied to **69**, which has much larger driving force, but slightly improved fluorescence quenching ($\Phi_{\text{Fl}} = 0.71$) and two-photon thresholds (20% lower) in comparison to chromophore **47**.

The low fluorescence quenching seen for **69**, despite increasing driving force, suggests electron transfer across the piperazine bridge is inherently rather inefficient. It is perhaps due to poor electronic coupling caused by the rigid nature of the bridge, which leads to poor orbital overlap between the local LUMO of sulfonium group and the local LUMO of the chromophore moiety.

4.6.6 Conclusion

The two-photon radical generator with shorter conjugation **69** has slightly lower relative fluorescence quantum yield (0.71 when corrected for both chromophore and sulfonium contribution to the absorbance) compared to the longer system **62** (0.86). Under our one-photon excitation conditions, the radical polymerization yields of **47**, **59**, and **69** suggest that direct excitation of the sulfonium group of **69** dominates. Since the three compounds absorb at similar wavelength (320 – 324 nm), radical generation of **69** arising from direct excitation of the sulfonium group and from the excitation of the chromophore moiety followed by electron transfer is not distinguished under one-photon excitation. However, the two-photon studies of **47** and **69** were performed using irradiation at 510 nm, at which the excitation of the chromophore moiety of **69** is expected to be the dominant mechanism for photoinitiation. The polymerization threshold energy of **69** under two-photon induced polymerization is only 80% high as that of **47**. In comparison with the same thresholds of the longer system **62** and its free chromophore **45** (section 4.5.4), this small but consistent difference in thresholds between **69** and **47** may indicate that the electron transfer mechanism plays a role for **69** to some extent, which is consistent with relative fluorescence quenching results.

4.7 Experimental: photochemical experiments

General experimental. Absorption spectra were run on a Hewlett-Packard model 8453 spectrophotometer. The fluorescence spectra were collected on a Jobin Yvon Spex Fluorolog–III fluorimeter. A Rayonet photochemical reactor (Model #RPR–100), manufactured by the Southern New England Ultraviolet Company, was used for photopolymerization studies. All electrochemical experiments were conducted using a BAS Model 100B/W cyclic voltammetry unit. The electrodes used were a glassy-carbon working electrode, a platinum auxiliary wire, and a Ag/AgCl pseudo-reference electrode. The supporting electrolyte was 0.1 M tetrabutylammonium hexafluorosphonate. The spectrophotometric grade acetonitrile (Aldrich) were used as received in all the measurements.

4.7.1 Fluorescence quenching

The example of the fluorescence quenching study for **52** is described below. Other fluorescence quenching experiments were performed in a similar way. Stock solutions of fluorophore **45** ($\sim 5.5 \times 10^{-6}$ M in acetonitrile) and quencher **52** ($\sim 5.5 \times 10^{-2}$ M in acetonitrile) were prepared. The solution of **45** (2 mL) and a certain amount of solution **52** were added to a volumetric flask, and then diluted to 5 mL by adding acetonitrile. The fluorescence spectra were taken, and the intensities at 504 nm were recorded. The fluorescence intensity at 504 nm of the fluorophore-quencher solution over that of the fluorophore **45** without the quencher was calculated as the relative

fluorescence intensity. The relative fluorescence intensity was plotted against the molar ratio of quencher **52** to fluorophore **45** (Figure 4.32).

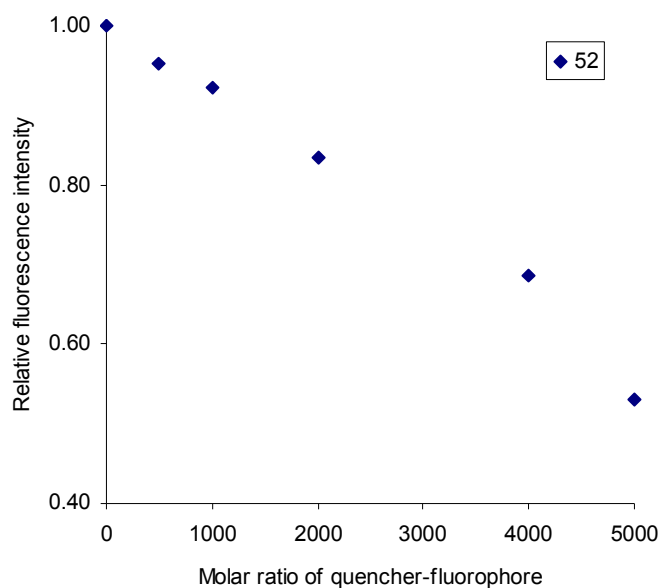


Figure 4.32 Fluorescence quenching study of **52**.

The quencher-fluorophore solutions of molar ratio 4000:1 were prepared for all the quenchers **48** – **52**. Their relative fluorescence intensity at 504 nm was calculated (Table 4.1). For **49** and **51**, their relative fluorescence intensity was zero at this molar ratio (4000:1). By adjusting the concentration and molar ratio, relative fluorescence intensity versus molar ratio were plotted for **49** and **51**.

4.7.2 Quantum yield of acid generation

The quantum yield of acid generation was measured and calculated by using the method that was described in Section 3.8.1. The acid concentrations of **58** – **60** were measured (Figure 4.33), and their quantum yields of acid generation were calculated as 0.04 for **58**, 0.07 for **59**, and 0.02 for **60**.

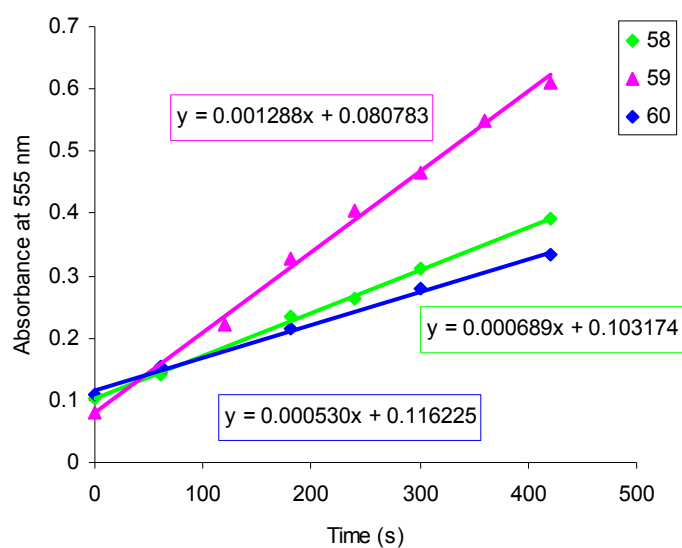


Figure 4.33 Measurement of acid concentration in acetonitrile.

4.7.3 Polymerization of methyl methacrylate

Methyl methacrylate was distilled under vacuum. Solutions of methyl methacrylate (2.5 mL) and initiators (ranged from 0.1 to 1.0 mol% of monomers for different measurements, see each section) in acetonitrile (0.5 – 1.0 mL, see each section) as solvent were prepared in a Schlenk flask. For neat polymerization, no solvent was added. The solutions were degassed by three freeze/pump/thaw cycles. The samples were placed in a “merry-go-around” holder which was rotated continuously to provide even illumination throughout the polymerization period. The entire apparatus was placed into a Rayonet photochemical reactor with six lamps. After 2.5 hours irradiation, the polymer solutions were kept in the dark at room temperature for 17 hours to allow for propagation. The polymers were precipitated by adding the solutions to cold methanol. The polymers were isolated by filtration, washed with methanol, and then dried under vacuum at 60 °C overnight. The yield of isolated polymers was from the ratio of the polymer weight to the monomer weight. ^1H NMR was measured to confirm that the polymer was poly(methyl methacrylate).

The light dose that was absorbed by initiators in the polymerization solution was estimated by the equation $\# \text{photons} \propto \int \phi (1 - 10^{-A}) d\lambda$, where ϕ is photon density of the lamp obtained from the power-density spectrum of lamp. A is the absorbance of the polymerization solution calculated from Beer's Law ($A = \epsilon lc$), where ϵ is the extinction coefficient of initiator in $\text{mol}^{-1} \text{L cm}^{-1}$, l is the diameter of the flask in cm, and c is the initiator concentration in mol L^{-1}).

4.7.4 Photoproduct analysis

Photoproducts analysis were analyzed following the literature procedures of Saeva.²²¹ To a solution of compound **60** (25 mg) in acetonitrile (2 mL) in a quartz cuvette, was added cyclohexane (4 mL) to form two immiscible layers. The solution was placed into a Rayonet photochemical reactor equipped with six lamps (350 nm). The acetonitrile layer was irradiated for 2.5 hours and the cyclohexane layer was wrapped with black tape to avoid irradiation. Nitrogen was continuously purged through the acetonitrile layer during the irradiation. The cyclohexane layer was removed periodically and replaced with fresh cyclohexane. The nonionic photoproducts that were generated in the acetonitrile layer were removed, and the secondary photochemistry was prevented. Both the collected cyclohexane layer and the acetonitrile layer were analyzed using GC-MS. For compound **59**, the concentration of **59** in acetonitrile solution was the same as that of **60**, and the measurement followed the same procedures.

4.7.5 *Relative fluorescence quantum yield*

The excitation wavelength, integration rate, slit width, and data collection wavelength range were the same for both **47** and **69**. The measurement of fluorescence quantum yield **47** is described here.

The dilution solutions of **47** in acetonitrile were prepared, and their absorbance recorded at 320 nm followed by fluorescence spectra with an excitation wavelength at 320 nm. The absorbance at 320 nm of the stock solution A (**47** in acetonitrile) was accurately recorded. The stock solution B was prepared by diluting the stock solution A (2 mL) in a volumetric flask (25 mL). The test solutions (a, b, c) were prepared by diluting the solution A (3, 2, 1 mL) in volumetric flasks (10 mL). The solutions (d and e) were prepared by diluting the solution a (2, 1 mL) to 10 mL. The absorbance at 320 nm of solutions (a – e) were calculated from the absorbance of the initial stock solution A assuming Beer's Law. The fluorescence spectra (a – e) were taken, and the integrations of the area under the spectra were calculated. The fluorescence integration was plotted against the absorbance at 320 nm of the solutions, and the slope of the curve was recorded, as shown in Figure 4.34.

The fluorescence quantum yield of **69** was measured using the same method. Since the molecule **69** (λ_{max} 324 nm, ϵ_{max} $5.63 \times 10^4 \text{ M}^{-1}\text{cm}^{-1}$) contained the chromophore moiety (**47**, λ_{max} 320 nm, ϵ_{max} $3.90 \times 10^4 \text{ M}^{-1}\text{cm}^{-1}$) and the triphenylsulfonium group (**59**, λ_{max} 320 nm, ϵ_{max} $2.29 \times 10^4 \text{ M}^{-1}\text{cm}^{-1}$), the absorbance of **69** has contribution from both the chromophore moiety and the triphenylsulfonium group, which have the same absorption maxima. The extinction coefficient of **69** was almost equal to the sum of those

of **47** and **59**. Our purpose is to measure the fluorescence induced by the absorption of the chromophore moiety of **69** for the electron transfer study. Thus, the absorbance of the chromophore moiety of **69** could be calculated by using the extinction coefficient of **47** divided the sum of those of **47** and **59**, which was 63%. After the correction of absorbance of **69**, the fluorescence integration was plotted against the absorbance of the solution at 320 nm attributable to the chromophore, and the slope of the plot was recorded. The relative fluorescence quantum yield of **69** over **47** was obtained by calculating the slope ratio of **69** to **47**, which is 0.71.

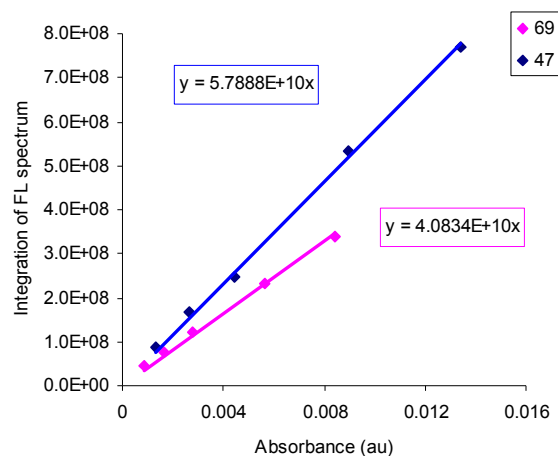


Figure 4.34 Measurement of fluorescence quantum yields of **69** and **47**.

4.7.6 *The measurement of two-photon induced polymerization threshold*

The measurements of the polymerization threshold energies of **47** or **69** were performed by V. Chen in Dr. J. Perry's group. The resin for two-photon microfabrication contained initiator (**47** or **69**, 0.1%) in triacrylates (**SR9008:SR368** in 1:1 ratio). The samples were prepared by sandwiching the resin between a methacrylate modified microscope slide with a 15 micron spacer and a cover slip on the other side. The samples were mounted onto a 3D translation stage (Newport, XPS). Laser excitation at 510 nm was achieved by using frequency-doubling the 1020 nm excitation from MaiTai (Spectra-Physics) using a second-harmonic generation crystal, with the fundamental blocked using two short-pass 550 nm filters. Laser light was delivered into the sample using a 60 × oil-immersion objective (Nikon, 1.4 NA).

Laser exposures were performed at various powers to first determine the polymerization threshold energy, which were approximately 2.5 mW for **47** (Figure 4.35, a) and 2.0 mW for **69** (Figure 4.35, b). Based on the initial thresholds, at least three powers above and three below the thresholds with 0.25 mW increment were applied to the samples to determine the actual thresholds. The test structure for these experiments was a woodpile-type photonic crystal structure with parameters set to 200 nm lateral spacing and 100 nm vertical spacing with writing speed of 1 mm/s.

Three sets of experiments were performed for each initiator. Each set included fabricating one sample of each initiator on the same day with the same experimental setup. Slight variation of thresholds from day-to-day may be caused by the changes in the

optical alignment (for accommodating other experiments). However, over all three set experiments, the threshold for **69** is consistently lower than **47**.

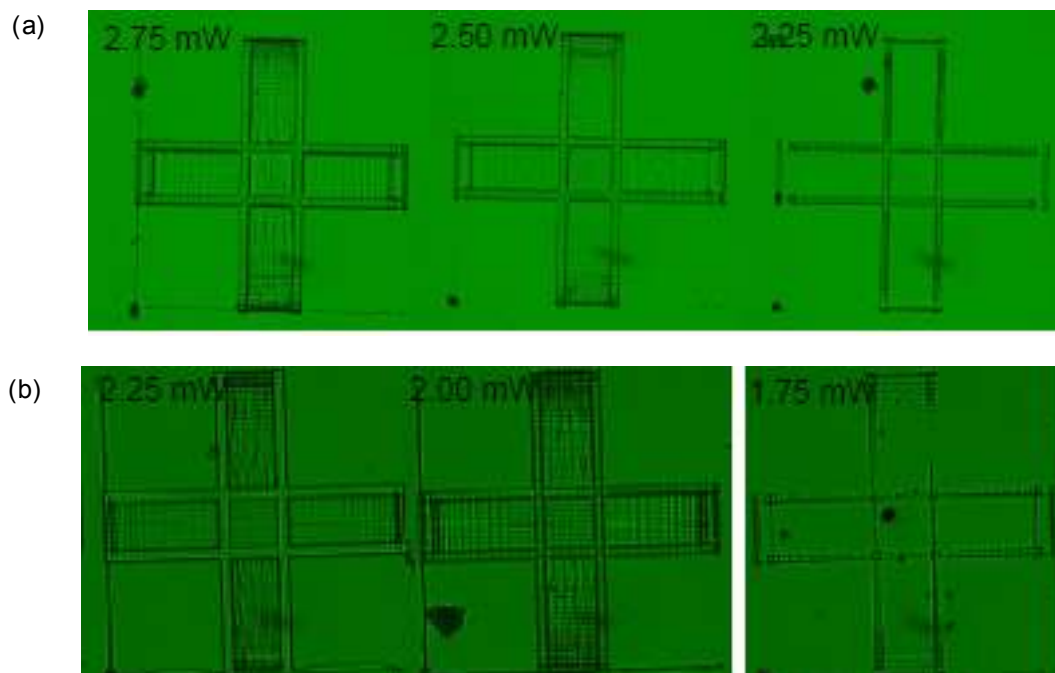
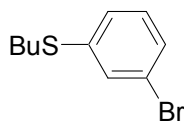


Figure 4.35 Threshold measurements of (a) **47** and (b) **69**.

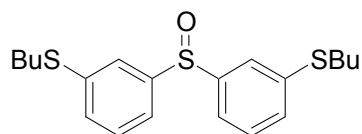
4.8 Experimental: synthetic procedures

General experimental. NMR spectroscopy was performed using either a DRX-500 MHz or Varian Unity Plus-300 MHz spectrometer at the University of Arizona. Mass spectrometry (MS) was performed by the MS Instrument Facility at the University of Arizona. The combustion experiments for elemental analysis were conducted by Desert Analytics. Silica gel (40 – 63 μm , EMD Chemical, Inc.) was used to perform flash column chromatography. TLC was performed on pre-coated plates containing a fluorescent indicator (silica gel 60 F₂₅₄, EMD Chemicals, Inc.) All reagents and solvents including dry solvents and anhydrous solvents in Acroseal bottles were purchased from readily available suppliers (Aldrich and Acros), and were used as received. The general precautions for preparation of light sensitive compounds mentioned in this section include wrapping the reaction flask with aluminum foil and performing the subsequent workup and purification in dark under weak red light. These precautions are applied in all cases where it is indicated that the compound is light sensitive.



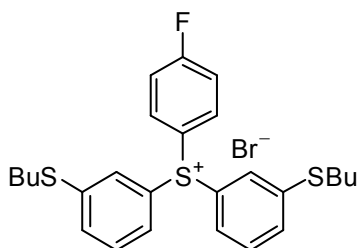
1-Bromo-3-butylsulfanylbenzene. To acetone (50 mL), were added 3-bromothiophenol (5.00 g, 26.4 mmol), 1-bromobutane (4.9 mL, 39.6 mmol), potassium carbonate (7.30 g, 52.8 mmol) and potassium iodide (0.22 g, 1.32 mmol). The reaction mixture was heated to reflux under nitrogen for 2 days. After cooling to room temperature, the mixture was extracted with diethyl ether three times. The combined

organic layers were washed with water, and then dried over magnesium sulfate. After condensation to remove the solvent, 1-bromobutane was removed by using a vacuum pump to remove. The purification by column chromatography (hexane) afforded a colorless liquid (7.00 g) in 98% yield. ^1H NMR (400 MHz, acetonitrile- d_3) δ 7.46 (s, 1H), 7.30 (d, $J = 7.6$ Hz, 1H), 7.26 (d, $J = 7.2$ Hz, 1H), 7.18 (t, $J = 7.8$ Hz, 1H), 2.95 (t, $J = 7.2$ Hz, 2H), 1.57 (quintet, $J = 7.2$ Hz, 2H), 1.42 (sextet, $J = 7.2$ Hz, 2H), 0.90 (t, $J = 7.2$ Hz, 3H). ^{13}C NMR (100 MHz, acetonitrile- d_3) δ 141.0, 131.5, 130.8, 129.1, 127.5, 123.3, 32.9, 31.6, 22.5, 13.8.²¹⁴ The data were consistent with the literature data.²²²



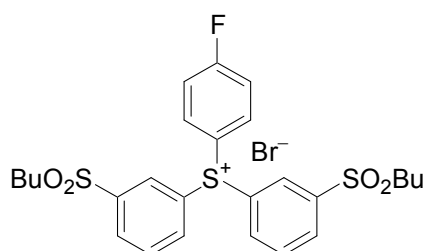
Bis(3-butylthiophenyl) sulfoxide. The Grignard reagent was prepared by the reaction of 1-bromo-3-butylsulfanyl-benzene (6.74 g, 27.5 mmol) and magnesium metal (0.67 g, 27.5 mmol) in THF (35 mL). The reagent was added to the solution of thionyl chloride (0.91 mL, 12.5 mmol) in diethyl ether (10 mL) at 0 °C. The reaction mixture was then stirred overnight. The reaction mixture was extracted with diethyl ether three times. The combined organic layers were washed with aqueous hydrogen chloride solution and then water. After drying over with magnesium sulfate, the purification by column chromatography (dichloromethane: hexane 3:1) afforded a pale brown solid (2.51 g) in 53% yield. ^1H NMR (400 MHz, acetonitrile- d_3) δ 7.55 – 7.53 (m, 2H), 7.44 – 7.36 (m, 6H), 2.96 (t, $J = 7.2$ Hz, 4H), 1.54 (quintet, $J = 7.2$ Hz, 4H), 1.39 (sextet, $J = 7.2$ Hz, 4H), 0.88 (t, $J = 7.2$ Hz, 6H). ^{13}C NMR (100 MHz, acetonitrile- d_3) δ 148.2, 140.7, 131.1, 130.9, 123.3, 121.8, 32.7, 31.6, 22.6, 13.9. HRMS (FAB+) m/z : calcd. for $\text{C}_{20}\text{H}_{27}\text{OS}_3$

(MH⁺) 379.1224, Found 379.1256.²¹⁴ The compound was used for next step without further purification.

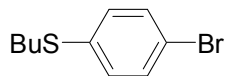


Bis-(3-butylsulfanyl-phenyl)-(4-fluoro-phenyl)-sulfonium bromide. Grignard reagent was prepared from the reaction of 4-fluoro-1-bromobenzene (1.44 g, 8.25 mmol) and magnesium metal (0.20 g, 8.3 mmol) in THF (7.5 mL) in a dark flask. At room temperature, bis(3-butylthiophenyl) sulfoxide (1.26 g, 3.30 mmol) was added to the Grignard reagent, and then trimethylsilyl chloride (1.05 mL, 8.25 mmol) was added. After stirring for 2 h, the aqueous hydrobromic acid solution (5 wt%) was added to quench the reaction, and diethyl ether was added to dilute the organic layer. Then the mixture was extracted with aqueous hydrobromic acid solution (5 wt%) three times. The combined aqueous layers were extracted with dichloromethane three times. All the combined organic layers were dried over magnesium sulfate and concentrated. The white oil was washed with diethyl ether until crystals were formed. The white crystal (0.82 g) was collected by filtration in 53% yield. The product is light sensitive. ¹H NMR (400 MHz, acetonitrile-*d*₃) δ 7.76 (dd, *J* = 8.4 Hz, *J* = 4.4 Hz, 2H), 7.68 (d, *J* = 7.2 Hz, 2H), 7.59 (t, *J* = 8.0 Hz, 2H), 7.49 (t, *J* = 8.4 Hz, 2H), 7.45 (s, 2H), 7.34 (d, *J* = 8.0 Hz, 2H), 2.94 (t, *J* = 7.2 Hz, 4H), 1.54 (quintet, *J* = 7.2 Hz, 4H), 1.36 (sextet, *J* = 7.2 Hz, 4H), 0.87 (t, *J* = 7.2 Hz, 6H). ¹³C NMR (100 MHz, acetonitrile-*d*₃) δ 143.9, 135.6, 135.5,

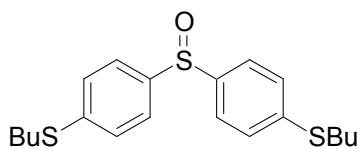
133.6, 132.6, 128.9, 132.6, 128.9, 127.9, 126.3, 120.1, 119.9, 120.1, 119.9, 32.4, 32.1, 22.5, 13.8. HRMS (FAB+) m/z : calcd. for $C_{26}H_{30}FS_3$ (M^+-Br) 457.1494, Found 457.1499. Anal. Calcd. for $C_{26}H_{30}BrFS_3$: C, 58.09; H, 5.62. Found: C, 57.87; H, 5.59.²¹⁴



Bis(3-(butylsulfonyl)phenyl)(4-fluorophenyl)sulfonium bromide. Bis-(3-butylsulfanyl-phenyl)-(4-fluoro-phenyl)-sulfonium bromide (0.179 g, 0.33 mmol) was dissolved in methanol (4 mL). Then a solution of potassium monopersulfate (1.23 g, 1.98 mmol) in water (4 mL) was added to the mixture at 0 °C. After stirring for 4 hours at room temperature, water was added to dilute the mixture, then the solution was extracted with dichloromethane three times. The combined organic layers were washed with water, and were dried over sodium sulfate. After removing solvent, the pale yellow crystal (0.086 g) was collected in 43% yield by filtration. The product is light sensitive. 1H NMR (400 MHz, acetonitrile- d_3) δ 8.30 (d, $J = 7.6$ Hz, 2H), 8.23 (s, 2H), 7.97 (t, $J = 8.0$ Hz, 2H), 7.90 (t, $J = 8.2$ Hz, 2H), 7.85 (dd, $J = 8.4$ Hz, $J = 4.4$ Hz, 2H), 7.53 (t, $J = 8.0$ Hz, 2H), 3.21 (t, $J = 7.6$ Hz, 4H), 1.54 (quintet, $J = 7.6$ Hz, 4H), 1.36 (sextet, $J = 7.6$ Hz, 4H), 0.87 (t, $J = 7.6$ Hz, 6H). ^{13}C NMR (100 MHz, acetonitrile- d_3) δ 143.6, 136.7, 136.2, 136.1, 135.2, 133.9, 131.9, 127.2, 120.4, 120.2, 56.0, 25.2, 22.0, 13.7. HRMS (FAB+) m/z : calcd. for $C_{21}H_{30}FO_4S_3$ (M^+-Br) 521.1290, Found 521.1299.²¹⁴

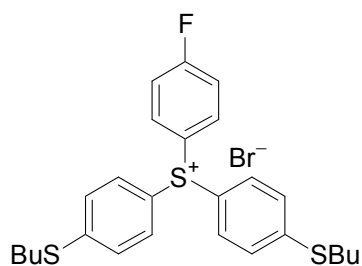


1-Bromo-4-butylsulfanylbenzene. To acetone (200 mL) in a three necked round-bottomed flask equipped with a reflux condenser was added 4-bromothiophenol (20.0 g, 105 mmol), 1-bromobutane (19.6 mL, 158 mmol), potassium carbonate (29.2 g, 210 mmol), and potassium iodide (0.88 g, 5.3 mmol). The reaction mixture was heated under nitrogen to reflux for 3 days. After cooling to room temperature, the mixture was extracted with diethyl ether three times. The combined organic layers were washed with water three times. The organic layer was dried over magnesium sulfate. After concentrated by rotary evaporation, the product (24.02 g) was obtained in 93% yield. ^1H NMR (400 MHz, acetonitrile- d_3) δ 7.41 (d, $J = 8.2$ Hz, 2H), 7.19 (d, $J = 8.4$ Hz, 2H), 2.91 (t, $J = 7.2$ Hz, 2H), 1.52 (quintet, $J = 7.2$ Hz, 2H), 1.44 (sextet, $J = 7.2$ Hz, 2H), 0.89 (t, $J = 7.2$ Hz, 3H). ^{13}C NMR (100 MHz, acetonitrile- d_3) δ 137.7, 132.7, 130.7, 119.4, 33.1, 31.7, 22.5, 13.8.²¹⁴ The data were consistent with the literature data.²²³



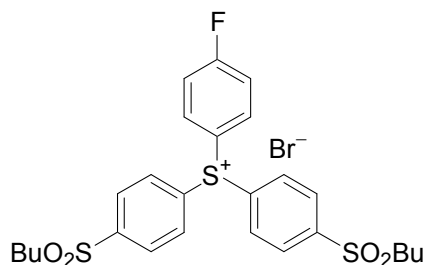
Bis(4-butylthiophenyl) sulfoxide. The Grignard reagent was prepared by the reaction of 1-bromo-4-butylsulfanylbenzene (21.58 g, 88 mmol) and Mg turnings (2.14 g, 88 mmol) in THF (110 mL). The reagent was added to the solution of thionyl chloride (2.9 mL, 40 mmol) in THF (30 mL) at 0 °C, and the reaction mixture was stirred overnight. The reaction mixture was extracted with diethyl ether three times. The combined organic layers were washed with aqueous hydrogen chloride and then water.

The organic layer was dried over magnesium sulfate. The pale brown solid (7.96 g) was obtained in 53% yield after purification by flash column chromatography (dichloromethane: ethyl acetate 20:1). ^1H NMR (400 MHz, acetonitrile- d_3) δ 7.51 (d, $J = 8.4$ Hz, 4H), 7.33 (d, $J = 8.0$ Hz, 4H), 2.94 (t, $J = 7.2$ Hz, 4H), 1.56 (quintet, $J = 7.2$ Hz, 4H), 1.40 (sextet, $J = 7.2$ Hz, 4H), 0.88 (t, $J = 7.2$ Hz, 6H). ^{13}C NMR (100 MHz, acetonitrile- d_3) δ 143.6, 143.1, 128.4, 125.8, 32.3, 31.5, 22.6, 13.8. HRMS (EI+) m/z : calcd. for $\text{C}_{20}\text{H}_{26}\text{OS}_3$ (M^+) 378.1179, Found 378.1176. Anal. Calcd. for $\text{C}_{20}\text{H}_{26}\text{OS}_3$: C, 63.45; H, 6.92. Found: C, 63.16; H, 6.92.²¹⁴



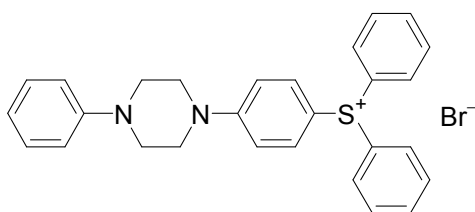
Bis-(4-butylsulfanyl-phenyl)-(4-fluoro-phenyl)-sulfonium bromide. Grignard reagent was prepared from the reaction of 4-fluoro-1-bromobenzene (8.75 g, 50 mmol) and magnesium metal (1.22 g, 50 mmol) in THF (40 mL). Bis(4-butylthiophenyl) sulfoxide (7.66 g, 20 mmol) was added to the Grignard reagent at room temperature, and then trimethyl silyl chloride (6.35 mL, 50 mmol) added to the mixture at 25 °C. After 4 h, the aqueous hydrobromic acid solution (5wt%) was added to quench the reaction, and then diethyl ether was added to dilute the organic layer. The reaction mixture was extracted with aqueous hydrobromic acid solution (5 wt%) three times. The combined aqueous layers were extracted with dichloromethane three times. The combined organic layers were dried over magnesium sulfate and concentrated. The residue was washed

with diethyl ether until the white crystals were obtained. The product (7.49 g) was collected in 72% yield by filtration. The product is light sensitive. ^1H NMR (400 MHz, acetonitrile- d_3) δ 7.77 – 7.73 (m, 2H), 7.58 – 7.51 (m, 8H), 7.46 (t, J = 8.8 Hz, 4H), 3.05 (t, J = 7.2 Hz, 4H), 1.65 (quintet, J = 7.2 Hz, 4H), 1.46 (sextet, J = 7.2 Hz, 4H), 0.92 (t, J = 7.2 Hz, 6H). ^{13}C NMR (100 MHz, acetonitrile- d_3) δ 149.2, 134.9, 134.8, 132.2, 128.9, 120.1, 119.8, 119.6, 31.6, 31.1, 22.6, 13.8. HRMS (ESI+) m/z : calcd. for $\text{C}_{26}\text{H}_{30}\text{FS}_3$ ($\text{M}^+ - \text{Br}$) 457.1493, Found 457.1437. Anal. Calcd. for $\text{C}_{26}\text{H}_{30}\text{FBrS}_3$: C, 58.09; H, 5.62. Found: C, 57.91; H, 5.88.²¹⁴



Bis(4-(butylsulfonyl)phenyl)(4-fluorophenyl)sulfonium bromide. Bis-(4-butylsulfonyl-phenyl)-(4-fluoro-phenyl)-sulfonium bromide (0.538 g, 1.0 mmol) was dissolved in methanol (12 mL) and cooled to 0 °C. A solution of potassium monopersulfate (3.684 g, 6.0 mmol) in water (12 mL) was added to the reaction mixture. After reaction was stirred 4 hours at room temperature, water was added to dilute the reaction mixture. The mixture was then extracted with dichloromethane three times. The combined organic layers were washed with aqueous potassium bromide solution (20 wt%) three times, and water. The organic layer was dried over sodium sulfate. After removing solvent, the oily crude product was washed with diethyl ether, and the pale yellow crystal (0.420 g) was obtained in 70% yield by filtration. The product is light

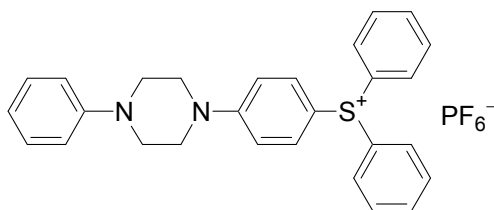
sensitive. ^1H NMR (400 MHz, acetonitrile- d_3) δ 8.16 (d, $J = 8.8$ Hz, 4H), 7.97 – 7.91 (m, 6H), 7.53 (t, $J = 8.8$ Hz, 4H), 3.26 (t, $J = 7.2$ Hz, 4H), 1.61 (quintet, $J = 7.2$ Hz, 4H), 1.39 (sextet, $J = 7.2$ Hz, 4H), 0.87 (t, $J = 7.2$ Hz, 6H). ^{13}C NMR (100 MHz, acetonitrile- d_3) δ 146.1, 136.6, 136.5, 133.4, 131.7, 131.2, 120.4, 120.2, 55.8, 25.1, 22.0, 13.7. HRMS (ESI+) m/z : calcd. for $\text{C}_{26}\text{H}_{32}\text{FO}_4\text{S}_3$ ($\text{M}^+ - \text{Br}$) 521.1290, Found 521.1289.²¹⁴



Diphenyl(4-(4-phenylpiperazin-1-yl)phenyl)sulfonium bromide. The solution of 4-fluorophenyl diphenyl sulfonium triflate (5.16g, 12 mol) and 1-phenylpiperadine (11 mL, 72 mol) in DMSO (150 mL) was heated at 100 °C overnight. The water was added to dilute the reaction mixture, and then the solution was extracted with dichloromethane three times. The combined organic layers were washed with aqueous hydrobromic acid solution (5 wt%), aqueous potassium bromide solution (20 wt%) and water three times respectively. The organic layer was dried over sodium sulfate. After removing solvent, the oily crude product was washed with diethyl ether until the crystals appeared. The yellow solid product (5.40 g) was obtained in 89% yield by filtration. The product is light sensitive. ^1H -NMR (400 MHz, acetonitrile- d_3) δ 7.79 – 7.77 (m, 2H), 7.70 (t, $J = 8.4$ Hz, 4H), 7.61 (d, $J = 8.8$ Hz, 4H), 7.54 (d, $J = 9.2$ Hz, 2H), 7.26 (t, $J = 8.8$ Hz, 2H), 7.16 (d, $J = 9.2$ Hz, 2H), 6.96 (d, $J = 8.0$ Hz, 2H), 6.84 (t, $J = 7.2$ Hz, 1H), 3.58 – 3.56 (m, 4H), 3.31 – 3.28 (m, 4H). ^{13}C NMR (100 MHz, acetonitrile- d_3) δ 155.6, 151.9, 134.9, 134.3,

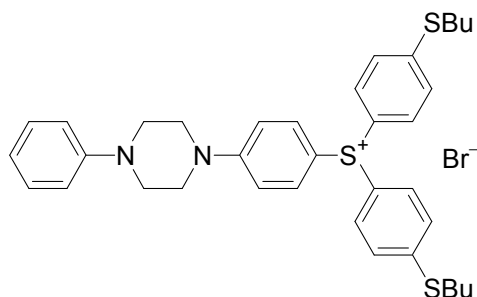
132.2, 131.2, 130.1, 127.5, 120.6, 116.9, 116.4, 107.3, 49.2, 47.3. HRMS (ESI) m/z :

Calcd. for $C_{28}H_{27}N_2S$ ($M^+ - Br$) 423.1895, Found 423.1888.



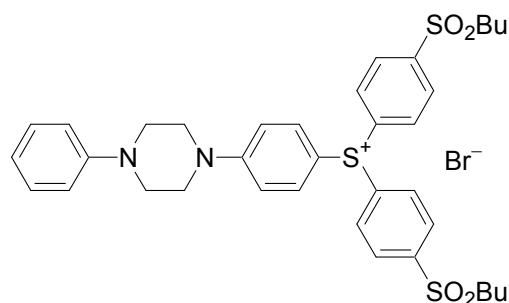
Diphenyl(4-(4-phenylpiperazin-1-yl)phenyl)sulfonium hexafluorophosphate.

diphenyl(4-(4-phenylpiperazin-1-yl)phenyl)sulfonium bromide (1.30 g, 2.58 mmol) was dissolved in dichloromethane (100 mL). The solution was washed with aqueous potassium hexafluorophosphate (20 wt%) and water three times respectively. The organic layer was dried over sodium sulfate. After removing solvent, the oily crude product was washed with diethyl ether, and the yellow solid (1.19 g) was obtained in 81% yield by filtration. The product is light sensitive. 1H -NMR (400 MHz, acetonitrile- d_3) δ 7.79 (t, J = 7.2 Hz, 2H), 7.70 (t, J = 8.0 Hz, 4H), 7.60 (d, J = 7.6 Hz, 4H), 7.54 (d, J = 9.2 Hz, 2H), 7.26 (t, J = 7.2 Hz, 2H), 7.15 (d, J = 9.2 Hz, 2H), 6.97 (d, J = 8.0 Hz, 2H), 6.84 (t, J = 7.2 Hz, 1H), 3.58 – 3.56 (m, 4H), 3.31 – 3.28 (m, 4H). ^{13}C NMR (100 MHz, acetonitrile- d_3) δ 155.7, 152.0, 134.9, 134.3, 132.2, 131.2, 130.1, 127.5, 120.7, 116.9, 116.4, 107.3, 49.2, 47.3. HRMS (ESI+) m/z : Calcd. for $C_{28}H_{27}N_2S$ ($M^+ - PF_6$) 423.1895, Found 423.1880. Anal. Calcd. for $C_{28}H_{27}F_6N_2PS$: C, 59.15; H, 4.79; N, 4.93. Found: C, 59.03; H, 4.80; N, 5.08.²¹⁴



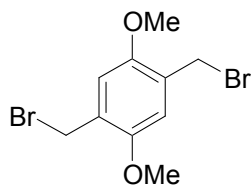
Bis(4-(butylthio)phenyl)(4-(4-phenylpiperazin-1-yl)phenyl)sulfonium

bromide. The solution of bis-(4-butylsulfanyl-phenyl)-(4-fluoro-phenyl)-sulfonium bromide (2.688 g, 5 mmol) and 1-phenylpiperadine (4.6 ml, 30 mmol) in DMSO (30 ml) was heated at 100 °C overnight. After cooling to room temperature, water was added to dilute the reaction mixture, and the solution was extracted with dichloromethane three times. The combined organic layers were washed with aqueous hydrobromic acid solution (5 wt%), aqueous potassium bromide solution (20 wt%) and water three times respectively. The organic layer was dried over sodium sulfate. After removing solvent, the oily crude product was washed with diethyl ether, and a yellow solid (2.69 g) was obtained in 81% yield by filtration. The product is light sensitive. ^1H NMR (400 MHz, acetonitrile- d_3) δ 7.54 – 7.46 (m, 10H), 7.26 (t, J = 8.0 Hz, 2H), 7.14 (d, J = 9.2 Hz, 2H), 6.96 (d, J = 8.0 Hz, 2H), 6.84 (t, J = 7.5 Hz, 1H), 3.56 – 3.54 (m, 4H), 3.29 – 3.27 (m, 4H), 3.04 (t, J = 7.2 Hz, 4H), 1.65 (quintet, J = 7.2 Hz, 4H), 1.46 (sextet, J = 7.2 Hz, 4H), 0.92 (t, J = 7.2 Hz, 6H). ^{13}C NMR (100 MHz, acetonitrile- d_3) δ 155.5, 151.9, 148.1, 133.9, 131.4, 130.1, 128.8, 122.2, 120.6, 116.9, 116.4, 108.4, 49.2, 47.4, 31.7, 31.2, 22.6, 13.8. HRMS (ESI+) m/z : Calcd. for $\text{C}_{36}\text{H}_{43}\text{N}_2\text{S}_3$ ($\text{M}^+ - \text{Br}$) 599.2588, Found 599.2626.

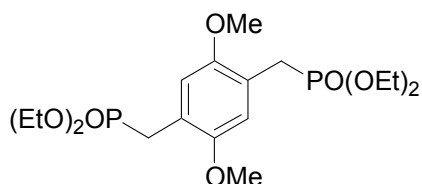


Bis(4-(butylsulfonyl)phenyl)(4-(4-phenylpiperazin-1-yl)phenyl)sulfonium

bromide. The solution of bis(4-(butylsulfonyl)phenyl)(4-fluorophenyl) sulfonium bromide (1.203 g, 2 mmol) and 1-phenylpiperadine (1.8 ml, 12 mmol) in DMSO (10 mL) was stirred at room temperature for 3 h. After cooling to room temperature, water was added to dilute the reaction mixture, and the solution was extracted with dichloromethane three times. The combined organic layers were washed with aqueous hydrobromic acid solution (5 wt%), aqueous potassium bromide solution (20 wt%) and water three times respectively. The organic layer was dried over sodium sulfate. After removing solvent, the oil was washed with diethyl ether, and the yellow solid (1.08 g) was obtained in 73% yield. The product is light sensitive. ^1H NMR (400 MHz, acetonitrile- d_3) δ 8.14 (d, $J = 8.8$ Hz, 4H), 7.88 (d, $J = 8.8$ Hz, 4H), 7.63 (d, $J = 9.2$ Hz, 2H), 7.26 (t, $J = 7.2$ Hz, 2H), 7.18 (d, $J = 9.2$ Hz, 2H), 6.96 (d, $J = 8.0$ Hz, 2H), 6.84 (t, $J = 7.2$ Hz, 1H), 3.63 – 3.60 (m, 4H), 3.32 – 3.29 (m, 4H), 3.26 (t, $J = 7.2$ Hz, 4H), 1.60 (quintet, $J = 7.2$ Hz, 4H), 1.36 (sextet, $J = 7.2$ Hz, 4H), 0.87 (t, $J = 7.2$ Hz, 6H). ^{13}C NMR (100 MHz, acetonitrile- d_3) δ 156.3, 155.9, 151.9, 145.5, 135.4, 133.2, 132.5, 131.4, 130.1, 120.6, 116.8, 116.4, 55.8, 49.1, 47.2, 25.1, 21.9, 13.7. HRMS (ESI+) m/z : Calcd. for $\text{C}_{36}\text{H}_{43}\text{N}_2\text{O}_4\text{S}_3$ ($\text{M}^+ - \text{Br}$) 663.2385, Found 663.2463.



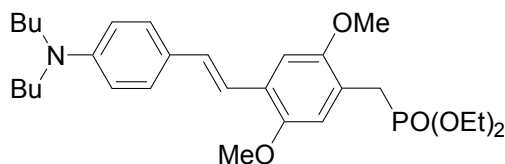
1,4-Bis-bromomethyl-2,5-dimethoxybenzene. To a suspension of 1,4-dimethoxybenzene (15.82 g, 0.11 mol) and paraformaldehyde (7.46 g, 0.24 mol) in acetic acid (220 mL), was added hydrobromic acid (70 mL, 30 wt% in acetic acid). The reaction solution was heated to 70 °C for 4 h. After cooling to room temperature, the reaction mixture was poured to water (1.5 L), and the crude product was collected by filtration. The product (22.32 g) was obtained in 61% yield by washing with hot methanol. ^1H NMR (500 MHz, chloroform-*d*) δ 6.85 (s, 2H), 4.51 (s, 4H), 3.85 (s, 6H). The data were consistent with the literature data.^{224,225}



Tetraethyl (2,5-dimethoxy-1,4-phenylene)bis(methylene)diphosphonate. A solution of 1,4-bis-bromomethyl-2,5-dimethoxybenzene (11.99 g, 12.22 mmol) and triethyl phosphite (50 mL) was refluxed for 18 h. After cooling to room temperature, the reaction solution was stored in the freezer for 2 hours. The product was crystallized from triethyl phosphite. The excess triethyl phosphite was decanted, and the residue was washed with hexane (3 \times 80 mL). The product (13.70 g) was obtained in 85% yield after filtration and dried. ^1H NMR (500 MHz, chloroform-*d*) δ 6.86 (d, J = 1.5 Hz, 2H), 3.98

(dq, $J = 7.5$ Hz, 8H), 3.75 (s, 6H), 3.20 (s, 2H), 3.16 (s, 2H), 1.20 (t, $J = 7.5$ Hz, 12H).

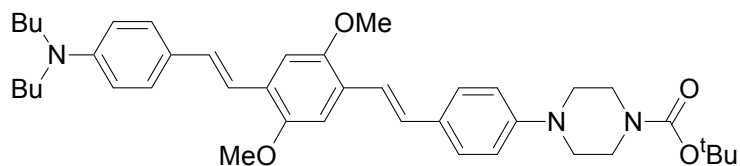
The data were consistent with the literature data.²²⁶



(*E*)-Diethyl 4-(4-(dibutylamino)styryl)-2,5-dimethoxybenzylphosphonate. To

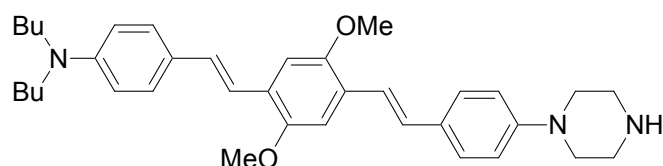
a solution of 4-(dimethylamino)benzaldehyde (0.98 g, 1.0 mL, 4.2 mmol) and tetraethyl (2,5-dimethoxy-1,4-phenylene)bis(methylene)diphosphonate (2.81 g, 6.41 mmol) in dry THF (80 mL), was added potassium *tert*-butoxide (6.5 mL, 6.0 mmol, 1.0 M in 2-methyl-2-propanol) at 0 °C. After stirring at 0 °C for 2 hours, the reaction solution was quenched by adding water (50 mL). THF was removed by evaporation, and the aqueous layer was extracted with dichloromethane until the color of the aqueous layer was only slight yellow or colorless. The combined organic layers were washed with water, and dried over magnesium sulfate. The product (1.52 g) was obtained by flash column chromatography (ethyl acetate) in 79% yield. ¹H NMR (500 MHz, chloroform-*d*) δ 7.39 (d, $J = 8.5$ Hz, 2H), 7.20 (d, $J = 16.5$ Hz, 1H), 7.07 (s, 1H), 6.98 (d, $J = 16.0$ Hz, 1H), 6.90 (d, $J = 2.5$ Hz, 1H), 6.61 (d, $J = 9.0$ Hz, 2H), 4.04 (dq, $J = 7.0$ Hz, 4H), 3.86 (s, 3H), 3.83 (s, 3H), 3.21 – 3.29 (m, 6H, 2NCH₂), 1.58 (quintet, $J = 8.0$ Hz, 4H), 1.36 (sextet, $J = 7.5$ Hz, 4H), 1.26 (t, $J = 7.5$ Hz, 6H), 0.95 (t, $J = 7.5$ Hz, 6H). ¹H NMR (125 MHz, chloroform-*d*) δ 151.4, 150.5, 147.7, 128.9, 127.7, 126.7, 126.7, 124.93, 119.1, 119.0, 118.0, 114.7, 114.7, 111.5, 62.0, 56.4, 50.8, 29.5, 27.2, 26.1, 20.4, 16.4, 14.0. HRMS (FAB+) *m/z*: Calcd. for

$C_{29}H_{44}NO_5P$ (M^+) 517.2957, Found 517.2967. Anal. Calcd. for $C_{29}H_{44}NO_5P$: C, 67.29; H, 8.57; N, 2.71. Found: C, 7.01; H, 8.71; N, 2.68.



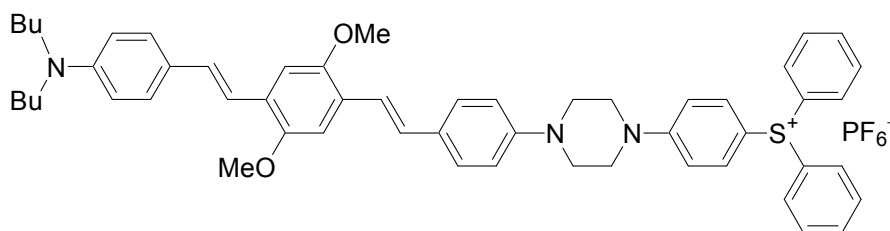
***tert*-Butyl 4-(4-(4-(4-(Dibutylamino)styryl)-2,5-dimethoxystyryl)phenyl)piperazine-1-carboxylate.** To a solution of (*E*)-diethyl 4-(4-(dibutylamino)styryl)-2,5-dimethoxybenzylphosphonate (2.25 g, 4.35 mmol) and 4-*N*-*tert*-butoxycarbonylpiperazinobenzaldehyde (1.26 g, 4.35 mmol) in THF (50 mL), was added potassium *tert*-butoxide solution (4.5 ml, 1.0 M) in THF at 0 °C. The mixture was stirred for 5 hours at 0 °C and allowed to rise to ambient temperature. The reaction was quenched by addition of water (40 mL), and the mixture was extracted with ethyl acetate three times. The combined organic layers were dried over magnesium sulfate. After removal of solvent, the product (2.03 g) was obtained by purification of flash chromatography (ethyl acetate:hexanes 3:7) in 72% yield. 1H NMR (500 MHz, acetone- d_6) δ 7.44 (d, J = 8.5 Hz, 2H), 7.37 (d, J = 9.0 Hz, 2H), 7.34 (d, J = 16.5 Hz, 2H), 7.26 (s, 1H), 7.25 (s, 1H), 7.20 (d, J = 14.0 Hz, 1H), 7.18 (d, J = 18.0 Hz, 1H), 7.15 (d, J = 16.5 Hz, 1H), 6.97 (d, J = 9.0 Hz, 2H), 6.68 (d, J = 9.0 Hz, 2H), 3.91 (s, 1H), 3.90 (s, 1H), 3.54 (t, J = 5.0 Hz, 4H), 3.35 (t, J = 7.5 Hz, 4H), 3.18 (t, J = 5.0 Hz, 4H), 1.59 (quintet, J = 7.5 Hz, 4H), 1.46 (s, 9H), 1.37 (sextet, J = 7.5 Hz, 4H), 0.95 (t, J = 7.5 Hz, 6H). ^{13}C NMR (125 MHz, acetone- d_6) δ 155.0, 152.3, 152.0, 151.7, 148.8, 130.5, 129.8, 128.9, 128.5, 128.1, 127.9, 126.7, 126.1, 121.0, 118.6, 116.9, 112.7, 109.6, 109.3, 79.7, 56.6, 56.5, 51.3,

49.5, 28.6, 20.9, 14.3. HRMS (ESI+) m/z : Calcd. for $C_{41}H_{56}N_3O_4$ (MH^+) 654.4271, Found, 654.4239. Anal. Calcd. for $C_{41}H_{55}N_3O_4$: C, 75.31; H, 8.48; N, 6.43. Found: C, 75.30; H, 8.50, N, 6.62.²¹⁸



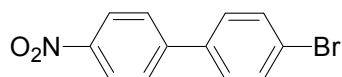
***N,N*-Dibutyl-4-(2,5-dimethoxy-4-(4-(piperazin-1-yl)styryl)styryl)aniline.** To a solution of *tert*-butyl 4-(4-(4-(4-(dibutylamino)styryl)-2,5-dimethoxystyryl)phenyl) piperazine-1-carboxylate (1.53 g, 2.34 mmol) in THF (50 mL) was added hydrochloric acid (15 mL, 2M). The mixture was heated to reflux for 6 hours and allowed to cool to room temperature. The solution was neutralized with aqueous sodium hydroxide solution, and extracted three times with the mixture of diethyl ether and dichloromethane (8:2). The combined organic layers were dried over anhydrous magnesium sulfate. After removal of solvent, the product (1.11 g) was obtained by recrystallization (toluene and hexanes) in 86% yield. 1H NMR (500 MHz, chloroform-*d*) δ 7.47 (d, J = 8.5 Hz, 2H), 7.41 (d, J = 9.0 Hz, 2H), 7.34 (d, J = 16.5 Hz, 1H), 7.25 (d, J = 16.0 Hz, 1H, overlap with solvent peak), 7.11 (s, 1H), 7.10 (s, 1H), 7.04 (d, J = 16.5 Hz, 1H), 7.02 (d, J = 16.5 Hz, 1H), 6.91 (d, J = 9.0 Hz, 2H), 6.63 (d, J = 8.5 Hz, 2H), 3.92 (s, 3H), 3.91 (s, 3H), 3.30 (t, J = 7.5 Hz, 4H), 3.20 (br, 4H), 3.05 (br, 4H), 1.59 (m, 4H), 1.37 (m, 4H), 0.97 (t, J = 7.5 Hz, 6H). ^{13}C NMR (125.7 MHz, chloroform-*d*) δ 151.3, 151.1, 151.0, 129.4, 128.9, 128.0, 127.8, 127.4, 127.1, 125.9, 125.0, 120.4, 118.0, 115.8, 111.5, 108.8, 108.5, 56.5, 56.4, 50.8, 50.1, 46.1, 29.5, 20.3, 14.0. HRMS (ESI+) m/z : Calcd. for $C_{36}H_{48}N_3O_2$ (MH^+)

554.3747, Found, 554.3724. Anal. Calcd. for C₃₆H₄₇N₃O₂: C, 78.08; H, 8.55; N, 7.59. Found: C, 77.71; H, 8.52, N, 7.54.²¹⁸

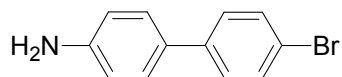


(4-(4-(4-(4-(Dibutylamino)styryl)-2,5-dimethoxystyryl)phenyl)piperazin-1-yl)phenyl)diphenylsulfonium hexafluorophosphate. The solution of *N,N*-dibutyl-4-(2,5-dimethoxy-4-(4-(piperazin-1-yl)styryl)styryl)aniline (0.80 g, 1.5 mmol) and 4-fluorotriphenylsulfonium hexafluorophosphate (0.61 g, 1.5 mmol) in DMSO (5 ml) was heated to 100 °C for 6 hours. After cooling to room temperature, the mixture was poured into an aqueous potassium hexafluorophosphate solution (5 wt%). The yellow solid was filtrated and washed with water. The crude material was washed with methanol two times. The pure product (0.85 g) was obtained by purification of flash column chromatography (hexanes:dichloromethane 1:1, and then dichloromethane) in 41% yield. The product is light sensitive. ¹H NMR (500 MHz, chloroform-*d*) δ 7.69 (t, br, *J* = 7.2 Hz, 2H), 7.65 (t, *J* = 8.0 Hz, 4H), 7.56 (d, *J* = 8.0 Hz, 4H), 7.53 (d, *J* = 9.0 Hz, 2H), 7.46 (d, *J* = 9.0 Hz, 2H), 7.41 (d, *J* = 8.5 Hz, 2H), 7.33 (d, *J* = 16.5 Hz, 1H), 7.25 (d, *J* = 16.5 Hz, 1H), 7.0 – 7.15 (m, 6H), 6.87 (d, *J* = 9.0 Hz, 2H), 6.62 (d, *J* = 8.5 Hz, 2H), 3.91 (s, 3H), 3.89 (s, 3H), 3.56 (t, br, 4H), 3.34 (t, br, 4H), 3.92 (t, *J* = 7.5 Hz, 4H), 1.58 (m, 4H), 1.36 (m, 4H), 0.96 (t, *J* = 7.2 Hz, 6H). ¹³C NMR (125 MHz, chloroform-*d*) δ 154.5, 151.3, 151.1, 149.6, 147.7, 134.1, 133.3, 131.4, 130.1, 129.9, 129.0, 127.8, 127.5, 126.1, 125.7,

125.0, 120.7, 117.9, 115.8, 115.7, 111.5, 108.9, 108.4, 105.7, 56.5, 56.4, 50.7, 48.2, 46.4, 29.5, 20.3, 14.0. HRMS (FAB+) m/z : Calcd. for $C_{54}H_{60}N_3O_2S$ ($M^+ - PF_6$), 814.4406, Found, 814.4418. Anal. Calcd. for $C_{54}H_{60}F_6N_3O_2PS$: C, 67.55; H, 6.30; N, 4.38. Found: C, 67.88; H, 6.36, N, 4.28.²¹⁸

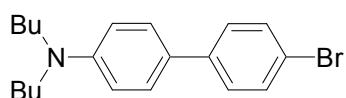


4-Bromo-4'-nitro-biphenyl. To a solution of 4-bromobiphenyl (28.03 g, 0.12 mol) and concentrated sulfuric acid (35.20 g, 98 wt%, 0.35 mol) in acetic acid (220 mL), was added concentrated nitric acid (12.01 g, 70 wt%, 0.13 mol) drop by drop. Then the reaction mixture was heated to 75 °C for 15 hours. After cooling to room temperature, the reaction mixture was filtrated. The product (15.00 g) was obtained from recrystallization (ethanol) in 47% yield. 1H NMR (500 MHz, chloroform-*d*) δ 8.29 (d, $J = 9.0$ Hz, 2H), 7.70 (d, $J = 9.0$ Hz, 2H), 7.63 (d, $J = 8.5$ Hz, 2H), 7.49 (d, $J = 8.5$ Hz, 2H). ^{13}C NMR (125 MHz, chloroform-*d*) δ 142.3, 146.3, 137.6, 132.3, 128.9, 127.6, 124.2, 123.5. The data were consistent with the literature data.²²⁷

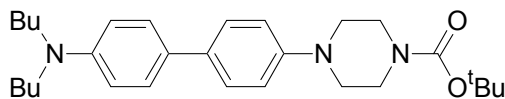


4'-Bromo-biphenyl-4-ylamine. The solution of 4-bromo-4'-nitro-biphenyl (8.56g, 30.8 mmol), concentrated hydrochloric acid (25 mL, 75 wt%), and ethanol (180 mL) was heated to reflux for 10 min. Then tin (II) chloride dihydrate (35.40 g, 0.16 mol) was added during 30 min. The reaction mixture was boiled for 2 h. After cooled to room temperature, the saturated sodium hydroxide aqueous solution was added till the pH was 13. The mixture was extracted with diethyl ether (3×150 mL), and the combined organic

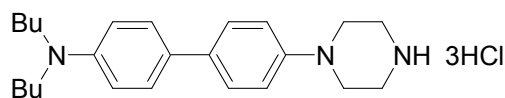
layers were dried over magnesium sulfate, and concentrated. The recrystallization from ethanol afforded the product (15.01 g) in 90% yield. ^1H NMR (500 MHz, chloroform-*d*) δ 7.48 (d, $J = 8.5$ Hz, 2H), 7.37 (d, $J = 8.5$ Hz, 2H), 7.35 (d, $J = 8.5$ Hz, 2H), 6.73 (d, $J = 9.0$ Hz, 2H), 3.69 (br, 2H). ^{13}C NMR (125 MHz, chloroform-*d*) δ 146.1, 139.9, 131.6, 130.1, 127.9, 127.7, 120.2, 115.3. The data were consistent with the literature data.²²⁷



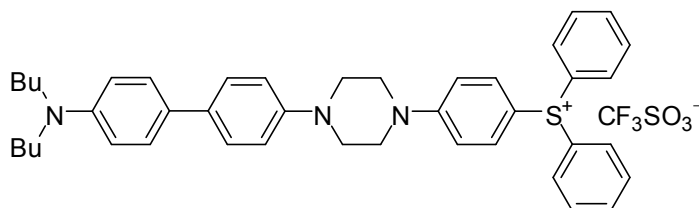
(4'-Bromo-biphenyl-4-yl)-dibutyl-amine. To a solution of 4'-bromo-biphenyl-4-ylamine (0.23 g, 0.93 mmol) in anhydrous 1-methyl-2-pyrrolidinone (10 mL), were added 1-bromobutane (0.30 mL, 0.38 g, 2.9 mmol), potassium carbonate (0.39 g, 2.8 mmol), 18-crown-6-ether (0.23 g, 0.89 mmol), and potassium iodide (0.12 g, 0.72 mmol) at room temperature. After the reaction mixture was heated to reflux for 20 h, the saturate brine solution (30 mL) was added to quench the reaction. The solution was extracted with diethyl ether (3×50 mL). The combined organic layers were dried over magnesium sulfate and concentrated. The product (0.20 g) was isolated by column chromatography (hexane) in 60% yield. ^1H NMR (500 MHz, acetone-*d*₆) δ 7.50 (m, 4H), 7.45 (d, $J = 9.0$ Hz, 2H), 6.73 (d, $J = 9.0$ Hz, 2H), 3.34 (t, $J = 7.5$ Hz, 4H), 1.59 (quintet, $J = 7.5$ Hz, 4H), 1.37 (sextet, $J = 7.5$ Hz, 4H), 0.95 (t, $J = 7.5$ Hz, 6H). ^{13}C NMR (125 MHz, chloroform-*d*) δ 147.8, 140.2, 131.6, 127.6, 127.6, 126.3, 119.6, 111.9, 50.8, 29.5, 20.4, 14.0. The data were consistent with the literature data.²²⁷



tert-Butyl 4-(4'-(dibutylamino)biphenyl-4-yl)piperazine-1-carboxylate. To a solution of (4'-bromo-biphenyl-4-yl)-dibutyl-amine (4.14 g, 11.5 mmol) and *tert*-butyl 1-piperazinecarboxylate (5.52 g, 28.8 mmol) in dry THF (55 mL), were added sodium *tert*-butoxide (2.86 g, 0.13 mmol) and dichlorobis(tri-*o*-tolylphosphine)-palladium (II) PdCl₂[P(C₆H₄CH₃)₂]₂ (0.49 g, 0.63 mmol) at room temperature under nitrogen. The reaction mixture was heated to 100 °C for 18 hours. After cooling to room temperature, the saturate brine solution (100 mL) was added to quench the reaction. The mixture was extracted with diethyl ether (3 × 100 mL). The combined organic layers were dried over magnesium sulfate and concentrated. The product (4.84 g) was isolated by column chromatography (hexane and then 5% ethyl acetate in hexane) in 93% yield. ¹H NMR (500 MHz, acetone-*d*₆) δ 7.44 (d, *J* = 8.5 Hz, 2H), 7.41 (d, *J* = 9.0 Hz, 2H), 6.98 (d, *J* = 8.5 Hz, 2H), 6.72 (d, *J* = 9.0 Hz, 2H), 3.54 (t, *J* = 5.0 Hz, 4H), 3.33 (t, *J* = 7.5 Hz, 4H), 3.12 (t, *J* = 5.0 Hz, 4H), 1.59 (quintet, *J* = 7.5 Hz, 4H), 1.46 (s, 9H), 1.38 (sextet, *J* = 7.5 Hz, 4H), 0.95 (t, *J* = 7.5 Hz, 6H). ¹³C NMR (125 MHz, acetone-*d*₆) δ 155.0, 150.6, 148.0, 133.7, 128.4, 127.6, 127.0, 117.6, 113.0, 79.7, 51.3, 50.1, 44.9 (br), 44.1 (br), 30.3, 28.6, 20.89, 14.3. HRMS (FAB+) *m/z*: Calcd. for C₂₉H₄₃N₃O₂ (M⁺) 465.3355, Found 465.3362. Anal. Calcd. for C₂₉H₄₃N₃O₂: C, 74.80; H, 9.31; N, 9.02. Found: C, 74.96; H, 9.40, N, 9.04.

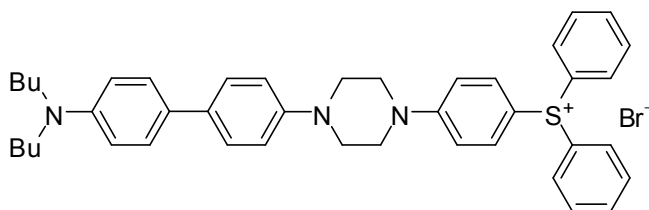


***N,N*-Dibutyl-4'-(piperazin-1-yl)biphenyl-4-amine trihydrochloride.** Hydrogen chloride gas was put through the solution of *tert*-butyl 4-(4'-(dibutylamino)biphenyl-4-yl)piperazine-1-carboxylate (0.18 g, 0.40 mmol) in ethyl acetate (10 mL) for 10 min. The solution was heated to remove the hydrogen chloride gas, and then was concentrated by evaporation. Minimal dichloromethane was added to completely dissolve the solid, and diethyl ether was added until no more white solid was precipitate. After filtration, the solid was collected. The precipitation was repeated three times, and the solid was dried under vacuum to give the product (0.12 g) in 65% yield. ^1H NMR (500 MHz, dimethyl sulfoxide- d_6 and 3 drops of water- d_2) δ 7.78 (d, $J = 8.5$ Hz, 2H), 7.61 (d, $J = 8.5$ Hz, 2H), 7.07 (d, $J = 8.5$ Hz, 2H), 3.48 (t, $J = 7.5$ Hz, 4H), 3.40 (t, $J = 5.0$ Hz, 4H), 3.21 (t, $J = 5.0$ Hz, 4H), 1.35-1.25 (m, $J = 7.5$ Hz, 4H), 1.20 (sextet, $J = 7.5$ Hz, 4H), 0.75 (t, $J = 7.0$ Hz, 6H). ^{13}C NMR (125 MHz, dimethyl sulfoxide- d_6 and 3 drops of water- d_2) δ 150.4, 141.5, 137.1, 130.2, 128.3, 128.1, 123.2, 117.0, 58.1, 45.7, 43.3, 27.2, 19.7, 14.0. HRMS (ESI+) m/z : Calcd. for $\text{C}_{24}\text{H}_{36}\text{N}_3$ ($\text{MH}^+ - 3\text{HCl}$) 366.2909, Found 366.2898. Anal. Calcd. for $\text{C}_{24}\text{H}_{38}\text{Cl}_3\text{N}_3$: C, 60.96; H, 8.06; N, 8.76. Found: C, 61.06; H, 8.41; N, 8.76.



(4-(4-(4'-(Dibutylamino)biphenyl-4-yl)piperazin-1-yl)phenyl)diphenyl sulfonium trifluoromethanesulfonate. A solution of *N,N*-dibutyl-4'-(piperazin-1-

yl)biphenyl-4-amine trihydrochloride (0.79 g, 2.2 mmol) and 4-fluorophenyl diphenyl sulfonium triflate (0.93 g, 2.2 mmol) in DMSO (25 mL) was refluxed at 100 °C for 4 h. The separation by column chromatography (dichloromethane: methanol 30: 1, and then 20: 1) afforded the product (0.87 g) in 52% yield. ^1H NMR (500 MHz, acetone- d_6) δ 7.84 – 7.72 (m, 12H), 7.46 (d, $J = 9.0$ Hz, 2H), 7.42 (d, $J = 9.0$ Hz, 2H), 7.27 (d, $J = 9.0$ Hz, 2H), 7.00 (d, $J = 9.0$ Hz, 2H), 6.72 (d, $J = 9.0$ Hz, 2H), 3.62 (t, $J = 5.0$ Hz, 4H), 3.34 – 3.31 (m, 8H), 1.57 (quintet, $J = 7.5$ Hz, 4H), 1.37 (sextet, $J = 7.5$ Hz, 4H), 0.93 (t, $J = 7.5$ Hz, 6H). ^{13}C NMR (125 MHz, acetone- d_6) δ 155.5, 150.0, 147.8, 134.8, 134.4, 133.4, 132.1, 131.2, 128.2, 127.7, 127.6, 127.0, 117.1, 116.4, 113.0, 107.5, 51.2, 49.3, 47.2, 30.2, 20.8, 14.3. HRMS (FAB+) m/z : Calcd. for $\text{C}_{42}\text{H}_{48}\text{N}_3\text{S}$ ($\text{M}^+ - \text{CF}_3\text{SO}_3$) 626.3569, Found 626.3588. Anal. Calcd. for $\text{C}_{43}\text{H}_{48}\text{F}_3\text{N}_3\text{O}_2\text{S}_2$: C, 66.56; H, 6.23; N, 5.42. Found: C, 66.38; H, 6.08, N, 5.31.



(4-(4-(4'-(Dibutylamino)biphenyl-4-yl)piperazin-1-yl)phenyl)diphenyl

sulfonium bromide. The solution of (4-(4-(4'-(dibutylamino)biphenyl-4-yl)piperazin-1-yl)phenyl)diphenylsulfonium trifluoromethanesulfonate (0.879 g, 1.13 mmol) in dichloromethane (20 mL) was washed by the aqueous potassium bromide solution (20 wt%) three times and then water three times. The solution was dried over magnesium sulfate. The product (0.712 g) was obtained in 89% yield after the solvent was removed by evaporation. ^1H NMR (400 MHz, acetone- d_6) δ 7.88 – 7.77 (m, 12H), 7.46 (d, $J = 8.8$

Hz, 2H), 7.42 (d, $J = 8.8$ Hz, 2H), 7.33 (d, $J = 8.8$ Hz, 2H), 7.00 (d, $J = 8.8$ Hz, 2H), 6.72 (d, $J = 8.8$ Hz, 2H), 3.67 – 3.64 (m, 4H), 3.34 – 3.31 (m, 8H), 1.57 (quintet, $J = 7.6$ Hz, 4H), 1.37 (sextet, $J = 7.6$ Hz, 4H), 0.93 (t, $J = 7.6$ Hz, 6H). ^{13}C NMR (100 MHz, acetone- d_6) δ 155.5, 150.0, 147.9, 134.8, 134.5, 133.5, 132.1, 131.4, 128.2, 127.9, 127.6, 127.0, 117.2, 116.5, 112.9, 107.7, 51.2, 49.4, 47.3, 30.2, 20.8, 14.2. HRMS (FAB+) m/z : Calcd. for $\text{C}_{42}\text{H}_{48}\text{N}_3\text{S}$ ($\text{M}^+ - \text{Br}$) 626.3565, Found 626.3538.

5. TWO-PHOTON REMOVABLE PROTECTING GROUPS

5.1 Historical review

A protecting group (or protective group) is a group introduced into a molecule by chemical modification of a functional group in order to obtain chemoselectivity in a subsequent chemical reaction. Protecting groups are important in multistep organic synthesis and in mechanistic studies of biological processes.^{228,229} Photoremovable protecting groups (also known in the literature as photolabile, photocleavable, photoreleasing, photoactive, or photosensitive protecting groups) are protecting groups that can be removed by irradiation with light. The advantages of photoremovable protecting groups include spatial and temporal control, and mild reaction conditions. For example, in the fabrication of solid-state DNA arrays, the possibility of spatial control allows for surface modification with different patterns.^{230,231} Temporal control has allowed for the first time-resolved image of an enzymatic reaction.²³² A short historical review of the development of photoremovable protecting groups will be described in this section.

In 1962, the first successful development of photoremovable protecting groups was reported by Barltrop.²³³ Free glycine was released from benzyloxycarbonylglycine upon irradiation with ultraviolet light (254 nm). Subsequently, a number of photoremovable protecting groups have been developed for various functional groups, including carboxylic acid, alcohol, amine, ketone, and phosphate residues. In 1970, Sammes briefly mentioned two possible approaches of designing photoremovable protecting groups.²³⁴ One was to use various intramolecular photorearrangement

reactions,²³⁵ and another involved the greater activity of the excited states of aromatic compounds compared to that of their ground states.^{236,237} With a focus on these two approaches, Amit summarized photoremovable protecting groups up to 1973.²³⁸ Until this time, photoremovable protecting groups were still in the developmental stage, and were used predominately in synthetic chemistry.

In the late 1970s, the increased understanding of the nature of photochemical and photophysical processes and the improvement of techniques in the field of photoremovable protecting groups had extended their applications in various biochemical systems. Photoremovable derivatives of natural substrates were first called “caged compounds” by Kaplan,²³⁹ and this terminology has been extensively used. Kaplan²³⁹ and Engels²⁴⁰ successfully achieved rapid photorelease of ATP from *o*-nitrobenzyl caged ATP in intracellular media. In the 1980s, the reviews by Pillai^{241,242} and Zehavi²⁴³ illustrated the applications of photoremovable protecting groups not only in organic synthesis, but also in the synthesis of peptides, polysaccharides, carbohydrates, and nucleotides.

In the last fifteen years, considerable progresses have been made in understanding and improving existing protecting groups, developing new ones, and finding extensive applications. The recently adopted term ‘phototrigger’, which refers to the very rapid release of substrates, has become more acceptable for newer photoremovable protecting groups. In the early 1990s, several excellent reviews by Adams,²⁴⁴ Corrie,²⁴⁵ Trentham^{245,246} and Givens²⁴⁷ have covered the areas of synthesis, physiology and molecular chemistry, and biochemistry. In 1998, a volume of *Methods in Enzymology*

with twenty-seven papers was devoted to caged compounds.²⁴⁸ Since 2000, the reviews by Wirz,²⁴⁹ Bochet,²⁵⁰ Falvey,²⁵¹ and Givens^{252,253} have appeared. In 2005, a book entitled “Dynamic Studies in Biology” was published in this area.²⁵⁴ Some recent applications of photoremovable protecting groups have been found in photorelease of neurotransmitters,^{244,255,256} photorelease of calcium,²⁵⁷⁻²⁶⁰ kinetic study of protein folding,^{261,262} time-resolved X-ray crystallography,^{232,263} two-photon induced photorelease,²⁶⁴⁻²⁶⁸ and synthesis of molecular arrays.^{230,231,269-271}

5.2 Literature review for photoremovable protecting groups

Sheehan²⁷² and Lester²⁷³ have set benchmarks for evaluation of the efficient photoremoval protecting groups: 1) The attachment of a photoremovable protecting group to a substrate should be easily achieved in a very high yield by a general synthetic procedure, especially for synthetic applications. For the biological studies, the substrate, protected substrate, and photoproducts should have good aqueous solubility. 2) The departure of the protecting group from the substrate should be a primary photochemical process. 3) The protected substrate, as well as the photoproducts, should be inert or benign, and stable to the photolysis environment, such as the media, other reagents and products. 4) Excitation wavelengths should be longer than 300 nm, where the absorption of media, substrate, or photoproducts would be weak. 5) The chromophores should have reasonable absorption coefficients at the irradiation wavelength. 6) The quantum yield of photorelease should be high. These six criteria are seldom met in their entirety, but they do serve as excellent guidelines. In this section, representative photoremovable protecting groups in the literature based on *o*-nitrobenzyl, benzoin, phenacyl, and coumaryl groups and their photolysis mechanisms will be reviewed and discussed.

5.2.1 The *o*-nitrobenzyl group and its derivatives

o-Nitrobenzyl groups are the most widely applied photoremovable protecting groups. Barltrop first reported the release of benzoic acid by irradiating *o*-nitrobenzyl benzoate.²³⁵ Kaplan introduced *o*-nitrobenzyl caged ATP into physiological media.²³⁹ Since then, *o*-nitrobenzyl groups have been used to protect a variety of functional groups, such as carboxylic acids, alcohols, amines, and phosphates. Now over 40 nitrobenzyl-protected biomolecules are commercially available.²⁴⁹ The commonly used photoremovable *o*-nitrobenzyl protecting groups are shown in Figure 5.1.²⁴⁹ The most popular one is 6-nitroveratroyloxycarbonyl (**NVOC**), first reported by Patchornik.²⁷⁴

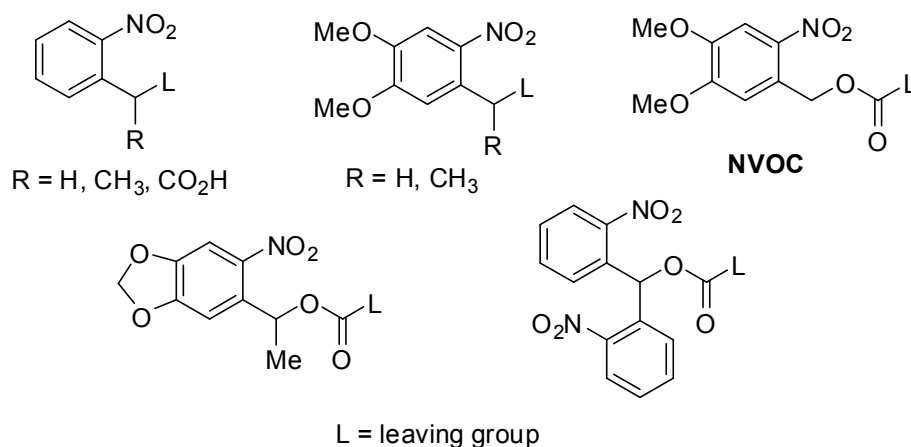


Figure 5.1 Commonly used *o*-nitrobenzyl photoremovable protecting groups.

The photorelease mechanism of *o*-nitrobenzyl groups has been studied and proven to be a Norrish type-II-like reaction (Figure 5.2).²⁷⁵⁻²⁷⁷ The Norrish type-II nomenclature was originally applied to the irradiation of carbonyl compounds, and this process leads to

a highly active 1,2-biradical species, followed by an intramolecular abstraction of a γ -hydrogen atom and formation of a 1,4-biradical as a primary photoproduct.²⁷⁸

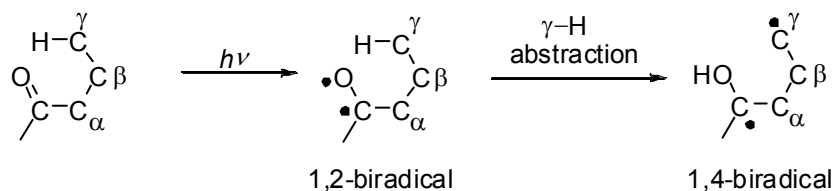


Figure 5.2 Norrish type-II photoreaction.

The mechanism of *o*-nitrobenzyl group cleavage is based on the irradiation of the nitro group instead of the carbonyl group (Figure 5.3). The excited nitro group abstracts a hydrogen atom intramolecularly, and the following electron redistribution leads to the *aci*-nitro form, which rearranges to release the protected group (HOAc) to form *o*-nitrosobenzaldehyde. The generation of a benzylic carbonyl group is the driving force for the release of the protected group. The photoproduct, *o*-nitrosobenzaldehyde, can undergo a secondary photoreaction to generate azobenzene-2,2'-dicarboxylic acid.^{235,274} Hence, the overall efficiency of photodeprotection is reduced. This side-reaction can be eliminated by adding an α -substituent (either an alkyl or an aryl group) to the benzylic methylene group of *o*-nitrobenzyl groups.

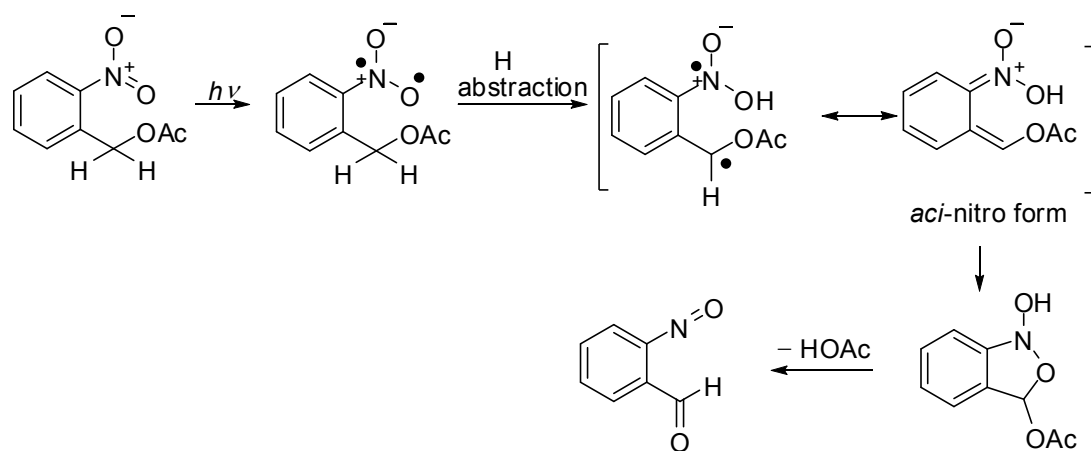


Figure 5.3 Photorelease mechanism of *o*-nitrobenzyl protected acetic acid.

The high quantum yield and the extended absorption at wavelengths longer than 300 nm are the distinctive advantages of using *o*-nitrobenzyl groups. However, there are still several limitations, such as the highly absorbing reactive nitroso byproduct, the slow release rate, and the instability of the caged compounds in biological systems prior to photolysis.^{279,280}

5.2.2 The benzoin (desyl) group and its derivatives

The benzoin (also called desyl) group was first reported as a photoremovable protecting group by Sheehan.²⁸¹ It has been used to protect acids, alcohols, amines, and phosphates. The most common ones in this category are the un-substituted benzoin group^{256,281-286} and the 3',5'-dimethoxybenzoin (**3',5'-DMB**) group (Figure 5.4).^{245,287-293} The studies of the photorelease mechanism are sometimes in apparent contradiction to each other, but have shown that the photorelease strongly depends on the substituents on aromatic rings, solvents, and leaving groups. Several representative mechanisms will be presented in this section.

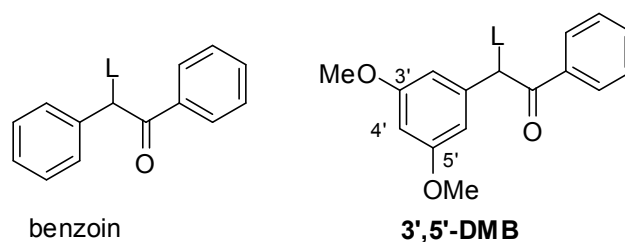


Figure 5.4 Commonly used benzoin type photoremovable protecting groups.

Sheehan first studied the photolysis of benzoin acetate, and the proposed mechanism that is shown in Figure 5.5.²⁸¹ Its mechanism was identified as a biradical process initiated by an $n-\pi^*$ transition of the carbonyl group. The subsequent photolytic cyclization of benzoin acetate yields a 2-substituted benzofuran with concurrent loss of the protected group (HOAc) at the α position of the carbonyl group.

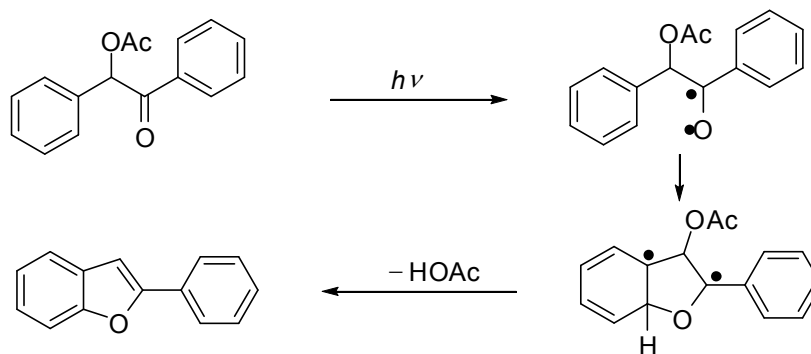


Figure 5.5 Photorelease mechanism for benzoin protecting group proposed by Sheehan.

Later on, Sheehan further studied the effects of substitution on different positions of the benzylic ring on the photorelease efficiency.²⁸⁸ The results show that substitution at the 3' or 5' position significantly accelerated the reaction, but that at the 4' position did not have this effect. They proposed a modified mechanism (Figure 5.6). The electron-donating (methoxy) group matched the electrophilic nature of the $n-\pi^*$ carbonyl singlet excited state, which facilitated the formation of an oxetane intermediate through a Paterno-Büchi reaction, *i.e.* a [2 + 2] olefin and carbonyl photocycloaddition. The loss of the acetate group was assisted by ring opening, and formation of benzofuran was favored by rearomatization. The optimal structure was found to be the 3',5'-dimethoxybenzoin group. The advantages of the near quantitative chemical yield, very high release rate, and high quantum yield made the **3',5'-DMB** group a very attractive member of the benzoin family.

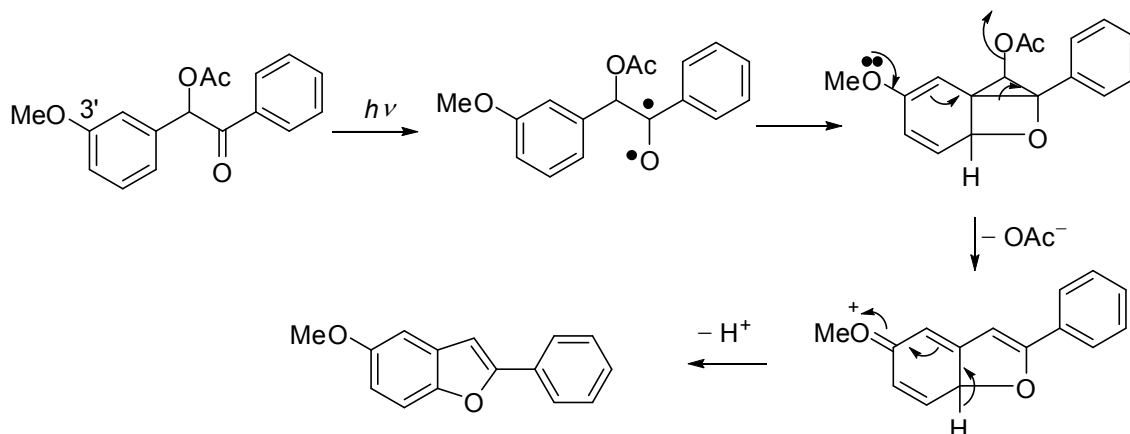


Figure 5.6 Modified photorelease mechanism proposed by Sheehan.

Corrie and Wan proposed a new singlet mechanism from a nanosecond laser flash photolysis study of several 3',5'-dimethoxybenzoin esters.²⁹³ Their data indicate that an intramolecular exciplex was formed between the electron-rich 3',5'-dimethoxy substituted benzene ring and the electron-deficient $n-\pi^*$ singlet excited state of the carbonyl group, and a short-lived cationic intermediate at 485 nm was identified by the laser flash photolysis study supporting this conclusion (Figure 5.7).

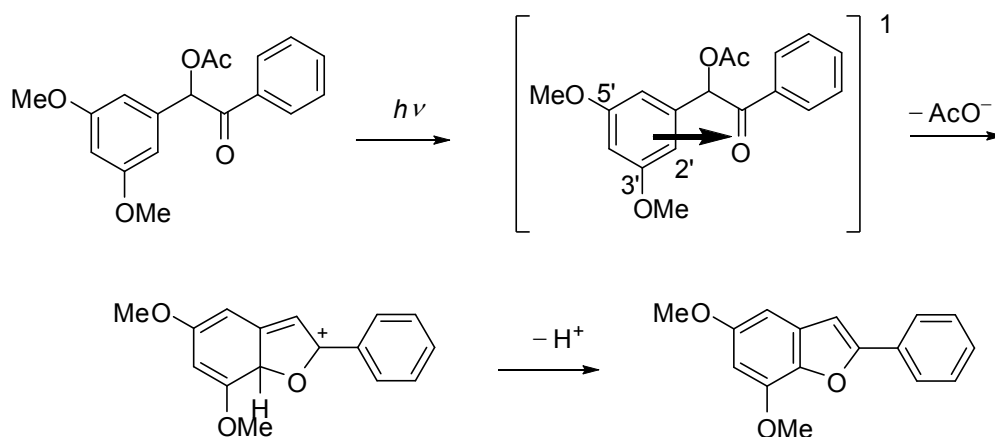


Figure 5.7 Photorelease mechanism of 3',5'-dimethoxybenzoin group.

Chan reported the photochemistry of a water-soluble 3',5'-bis(carboxymethoxy)benzoin (**BCMB**) acetate (Figure 5.8).²⁹⁴ Irradiation of the **BCMB** acetate first generates the biradical intermediate, which further reacts by two pathways: acetoxy migration followed by rearomatization gave benzofuran *via* path **a**, while nucleophilic attack by water produces **BCMB** *via* path **b**. The photoproduct ratio of benzofuran to **BCMB** is 3:7.

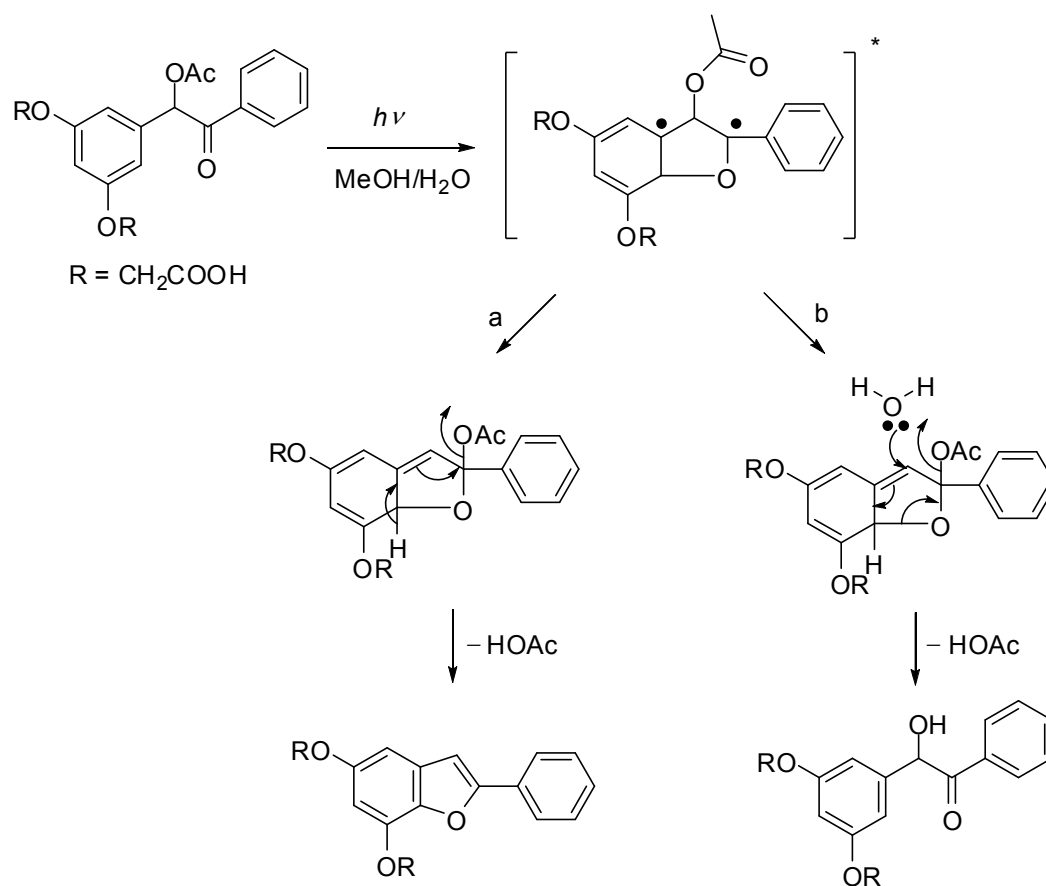


Figure 5.8 Photorelease mechanism of 3',5'-bis(carboxymethoxy)benzoin group proposed by Chan.

Givens and Wirz proposed the photorelease mechanism of benzoin diethyl phosphate (Figure 5.9).²⁸⁵ The lowest triplet excited state was detected by subpicosecond pump-probe spectroscopy, which was formed by two competitive paths. Path a dominated in most solvents except water and fluorinated alcohols, and the 2-phenylbenzofuran was generated with the release of protected group *via* a biradical species. In water or fluorinated alcohols, such as trifluoroethanol, the nucleophilic substitution product, trifluoroethyl benzoin ether, was formed as a major product *via* the path b.

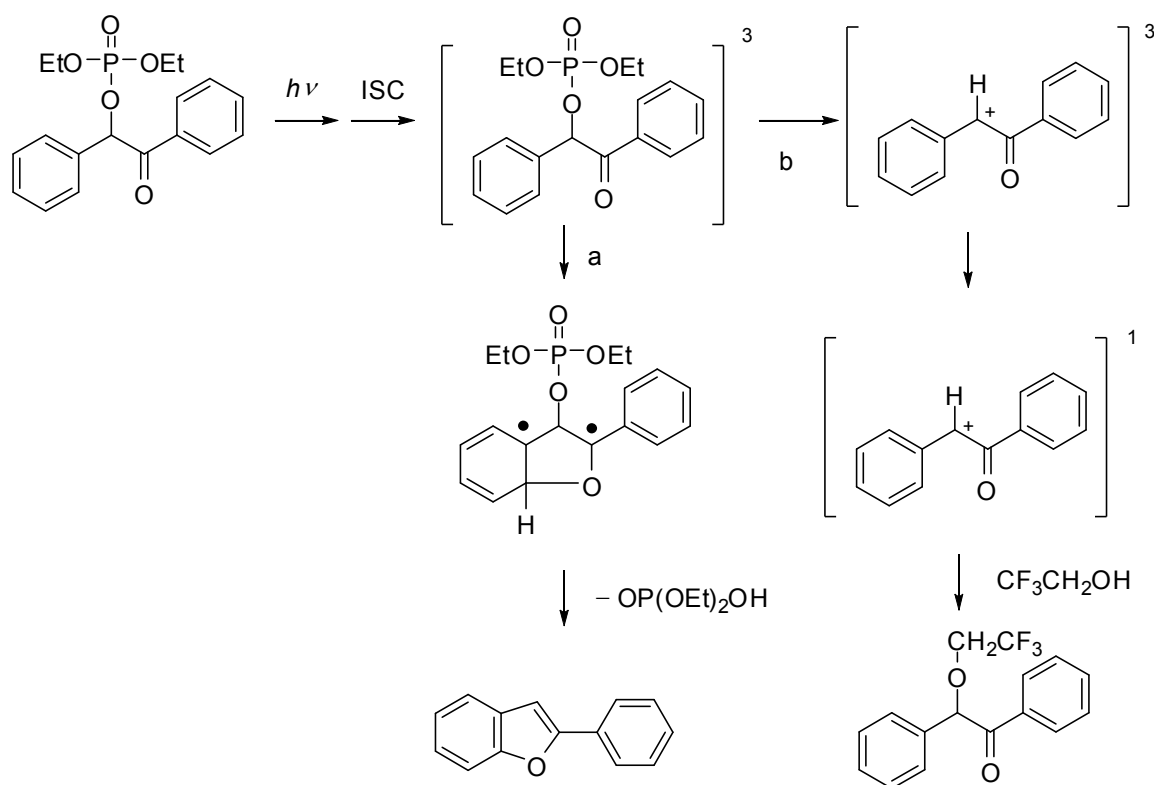


Figure 5.9 Photorelease mechanism of proposed by Givens and Wirz.

The advantages of using benzoin groups as photoremovable protecting groups are high release rates and high chemical and quantum yield. The inert benzofuran photoproduct absorbs light around 300 nm. Thus, the photoreaction can be conveniently monitored by UV spectroscopy. At the same time, benzofuran can also act as an internal light absorber to decrease the photorelease efficiency. The major drawback is the introduction of a new chiral center that would result in a diastereomeric mixture of the protected species when the substrate contains chiral centers.

5.2.3 The phenacyl group and its derivatives

Sheehan first reported the use of *p*-methoxyphenacyl group as a photoremovable protecting group for the release of benzoic acid, several amino acid derivatives, and peptides.²⁷² The continued investigations of *p*-methoxyphenacyl group have been reported by Epstein,²⁹⁵ Baldwin,²⁹⁶ Pirrung,²⁹⁰ Futura,²⁹⁷ and Givens.²⁹⁸⁻³⁰¹ Givens has extensively studied the *p*-hydroxyphenacyl group as a fast release trigger for a variety of bioactive molecules, such as ATP,²⁹⁸ phosphate,²⁹⁹ glutamine,³⁰⁰ GABA,³⁰⁰ the dipeptide Als-Ala,^{300,301} and the nonapeptide Bradykinin.³⁰¹ The photorelease mechanism has been controversial over the years, and is not yet well established. Several representative examples will be discussed in this section.

Sheehan proposed that a direct homolysis of a carbon-oxygen bond yielded two radical species that abstract a hydrogen atom from ethanol to produce *p*-methoxyacetophone and the corresponding protected group (Figure 5.10).²⁷²

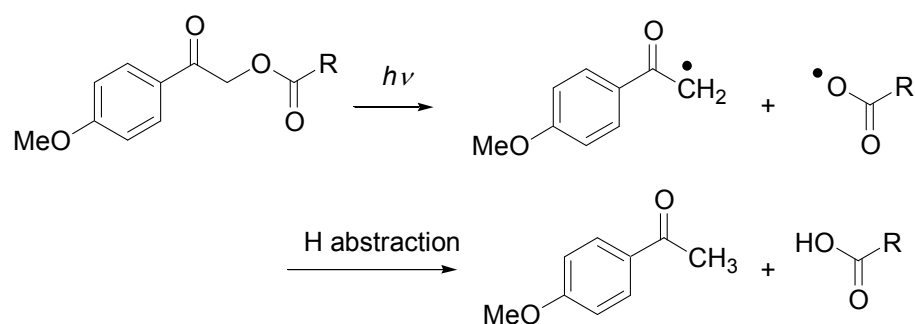


Figure 5.10 Photorelease mechanism proposed by Sheehan.

Givens has comprehensively explored the photorelease efficiency of *p*-substituted phenacyl phosphates (Figure 5.11).³⁰⁰ A short-lived triplet excited state was identified by quenching experiments. The protected group was released and a spiroadienedione was formed with the help of direct neighboring group assistance. The subsequent rearranged photoproduct *p*-hydroxyphenylacetic acid was generated by nucleophilic hydrolysis.

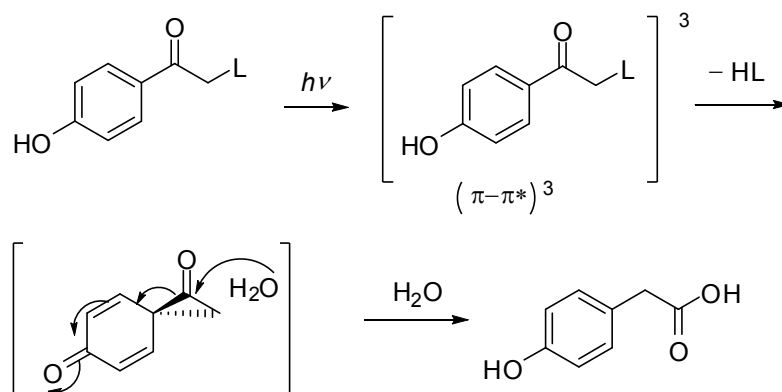


Figure 5.11 Photorelease mechanism proposed by Givens.

The triplet state mechanism proposed by Givens was challenged by a singlet state mechanism proposed by Corrie and Wan based on a photorelease study of *p*-hydroxyphenacyl acetate.³⁰² They suggested that a singlet excited state underwent excited-state intramolecular proton transfer (ESIPT), assisted by solvent, to form its conjugate base (Figure 5.12). Recently, laser flash-photolysis studies by Conrad, Givens and Wirz again confirmed that a very short-lived triplet indeed existed.³⁰³

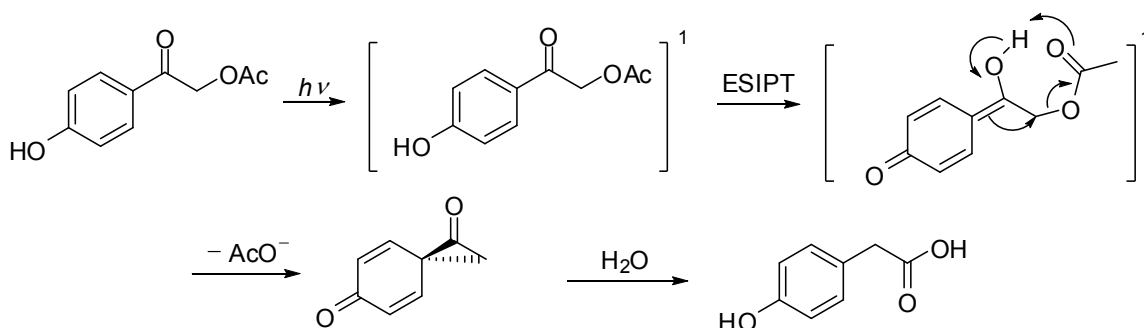


Figure 5.12 Photorelease mechanism proposed by Corrie and Wan.

There are several features that make *p*-hydroxyphenacyl a promising photoremovable protecting group: the *p*-hydroxyphenacyl protected compounds can be synthesized in a straightforward fashion by using commercially available *p*-hydroxyacetophenone, and they are soluble in aqueous media and stable in biological buffers. Unlike the nitrobenzyl groups, the main photo-byproduct, *p*-hydroxyphenacetic acid, is water-soluble and nontoxic, its UV absorption is blue-shifted with respect to its precursor, and the photorelease rate is fast. In contrast to the benzoin groups, the *p*-hydroxyphenacyl group does not have a chiral center, and the formation of diastereomers when attaching to a chiral substrate is avoided. However, the absorption coefficient of the *p*-hydroxyphenacyl group at wavelengths greater than 320 nm is low. Conrad therefore synthesized the 3,5-dimethoxy-*p*-hydroxyphenacyl group to increase the absorption maximum wavelength to 400 nm.³⁰⁴

5.2.4 The coumaryl group and derivatives

Coumaryl groups are relatively new development in this family. Coumarin is the parent compound, and there are four major structures that have been reported as phototriggers, namely 7-alkoxy,^{284,297,305-318} 6,7-dialkoxy,^{314,318-321} 6-bromo-7-alkoxy,^{318,322-329} and 7-dialkyamino^{314,315,318,330,331} groups (Figure 5.13).

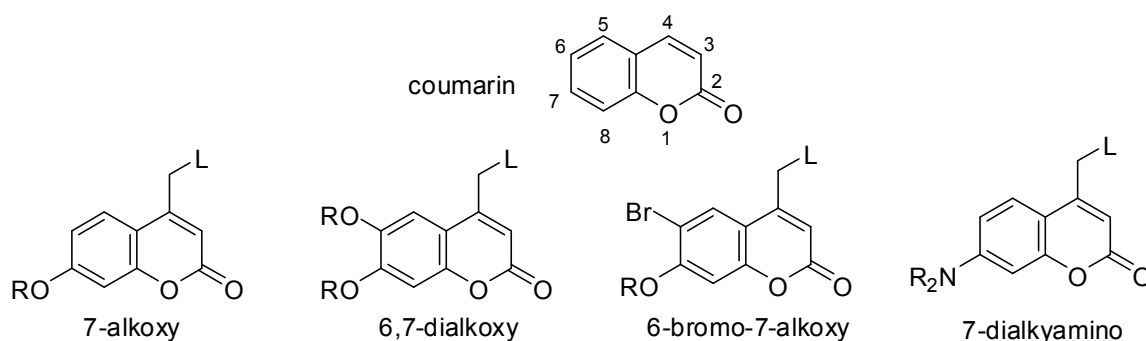


Figure 5.13 Coumarin and coumaryl protecting groups.

About 20 years ago, Givens first reported that 7-methoxycoumarin-4-ylmethanyl (MCM) diethylphosphate ester can be photolyzed to generate a fluorescent electrophile.²⁸⁴ The objective of this study was not to use as a photocleavable group, but to use the fluorescence of the coumaryl group, but did not intend to use it as a photoremovable protecting group. Ten years later, Furuta reinvestigated the MCM group, viewing it as a caged compound, and demonstrated the photorelease of carboxylic acids from MCM esters (Figure 5.14).²⁹⁷ Since then, the applications of the MCM group as a photoremovable protecting group have been studied.^{297,306,307,312-314,322,332}

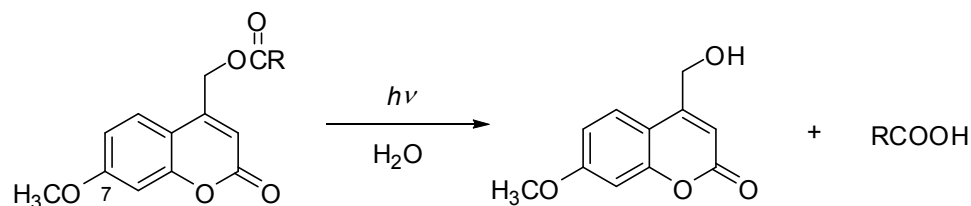


Figure 5.14 Photorelease of carboxylic acids from **MCM** esters.

The photorelease mechanism of **MCM** esters was proposed by Bendig (Figure 5.15).^{313,314} Excitation of the coumaryl chromophore to its singlet excited state is followed by carbon-oxygen bond cleavage to form an ion pair in a solvent cage. The lack of evidence for the cleavage step precluded unambiguous assignment of homolytic vs heterolytic cleavage. The formation of fully solvated ions from the ion pair in the solvent cage competes with the recombination of the ion pair. **MCM** and the deprotected molecule are released from the solvated ions.

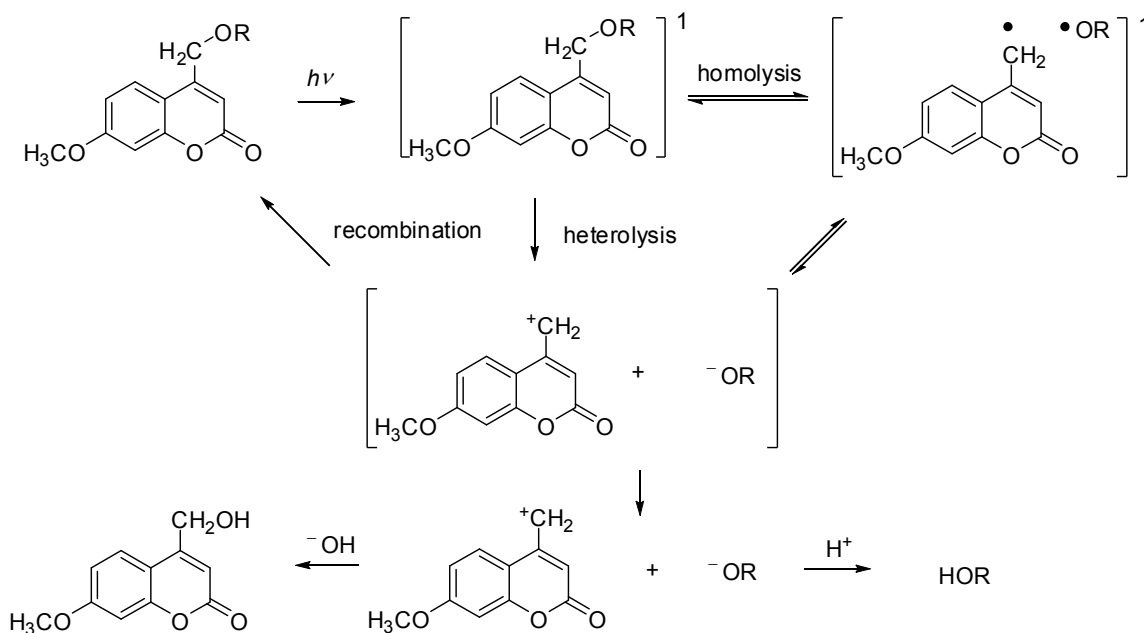


Figure 5.15 Photorelease mechanism for **MCM** esters proposed.

Coumaryl protecting groups have the following advantages over other groups described here: large extinction coefficients at wavelength longer than 350 nm; high photolysis efficiencies upon UV irradiation; fast photolysis kinetics; acceptable stability in the dark; and a practically useful two-photon excitation cross-section (section 5.3.2).

5.3 Photoremoval via photoinduced electron transfer

The absorption maxima of the four most widely used photoremovable protecting groups are normally at wavelengths shorter than 350 nm, but structural modifications can increase the absorption range to around 400 nm. In addition, the species that undergoes bond cleavage is directly photoexcited. Recently, photoinduced electron transfer (PET) has been applied to the design of photoremovable protecting groups. A photoinduced electron-transfer system consists of a sensitizer that controls light absorption and a photoremovable protecting group that determines bond cleavage. The spatial separation of light absorption and bond cleavage allows the two steps to be optimized independently. However, the offset between the energy levels of the sensitizer and the photoremovable group should be optimized to achieve efficient electron transfer. Major investigations in this area include photorelease of amines from tosylamides,^{333,334} ketones and aldehydes from dithianyl,³³⁵⁻³³⁷ secondary amines from 2-bromoethylacetate,³³⁸ and alcohols from benzylic ethers,³³⁹ alcohols, phosphates, and carboxylic acids from phenacyl esters.³⁴⁰⁻³⁴⁴

Among these studies, Falvey's investigation of photorelease of alcohols, phosphates and carboxylic acids from phenacyl esters by photoinduced electron transfer have received the most extensive attention.³⁴⁰⁻³⁴⁴ The proposed sensitized reductive photorelease mechanism is shown in Figure 5.16.³⁴² The electron transfer from the singlet excited state of the sensitizer, *N,N*-dimethylaniline, to the phenacyl ester creates a pair of radical ions. Rapid elimination of carboxylate anion gives a phenacyl radical. The subsequent hydrogen atom transfer from the sensitizer cation radical to the phenacyl

radical provides acetophenone and an iminium ion that is hydrolyzed to *N*-methylaniline.

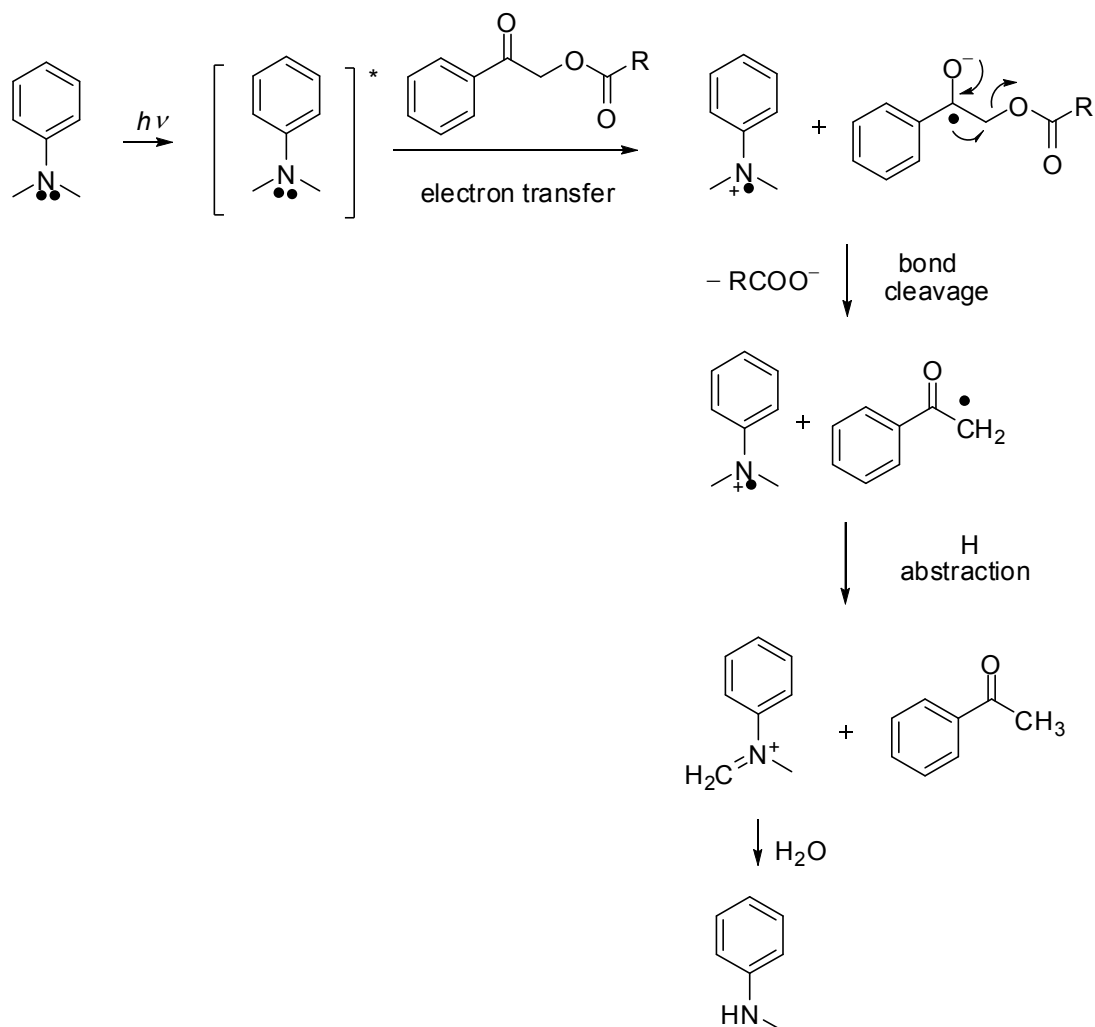


Figure 5.16 Photorelease mechanism for the dimethylamine-sensitized deprotection proposed by Falvey.

Falvey studied photocleavage via intermolecular electron transfer between a sensitizer and a phenacyl protected substrate. The representative sensitizers used in his study were 9,10-dimethylantracene, *N,N,N',N'*-tetramethylbenzene-1,4-diamine, and

N,N-dimethylaniline. They reported 80 – 100% yields of acid release,³⁴² and 60 – 80% release yields for alcohols.³⁴⁵

Encouraged by these results, sensitizers were covalently attached to the phenacyl protected substrates via an ester linker (Figure 5.17).³⁴⁴ The efficiency of photocleavage has been investigated. The aniline system showed moderate quantum yield of acid (0.02), and the anthracene system failed to produce a detectable amount of acetic acid.

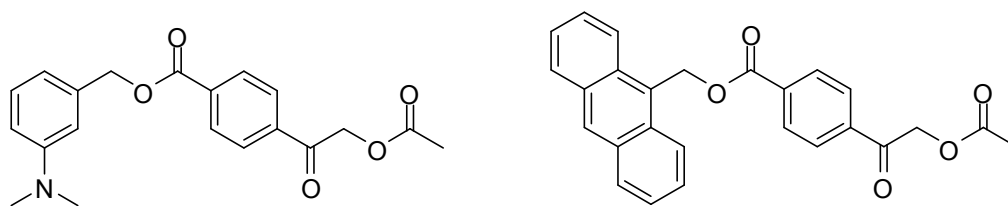


Figure 5.17 Photorelease via intramolecular electron transfer.

5.4 Research goal

5.4.1 Literature review of two-photon removable protecting groups

The two-photon absorption has several advantages (section 1.1) for photoremovable protecting groups. For biological applications, it is desirable to excite chromophores at near-IR wavelength, particularly those in the range 700 – 1100 nm. For tissues without hemoglobin, melanin, or chlorophyll, water is the principal absorber. The transparency window (700 – 1100 nm) exists due to the low extinction coefficient of water in this range. TPA wavelengths are typically roughly twice those required for one-photon excitation of the same materials so many TPA wavelengths can be excited in the biological window, where tissues absorb weakly along the path of the two-photon beam except at the focus where TPA occurs. Light scattering at TPA wavelengths is also generally reduced by a factor of 16 since the scattering efficiency is proportional to λ^{-4} . Consequently, out-of-focus absorption does not occur and near-IR wavelengths reduce light scattering. In addition, two-photon absorption can be spatially controlled to a small region around the focus, which can be as small as $\sim 1 \mu\text{m}^3$. This is approximately similar to the volume of a bacteria cell, and is typically smaller than that of a mammalian cell or neuron. This advantage makes excitation in sub-regions of a cell in a complex tissue conceivable.

Some caged compounds with two-photon sensitivities and their TPA cross-sections are listed in Figure 5.18, including **DMNB**,³²² **CNB**,²¹ **NEP**,³⁴⁶ **MNI**,³⁴⁷ **Bhc**,³²² **Bhc-diol**,³²⁶ and **BHQ**.³⁴⁸

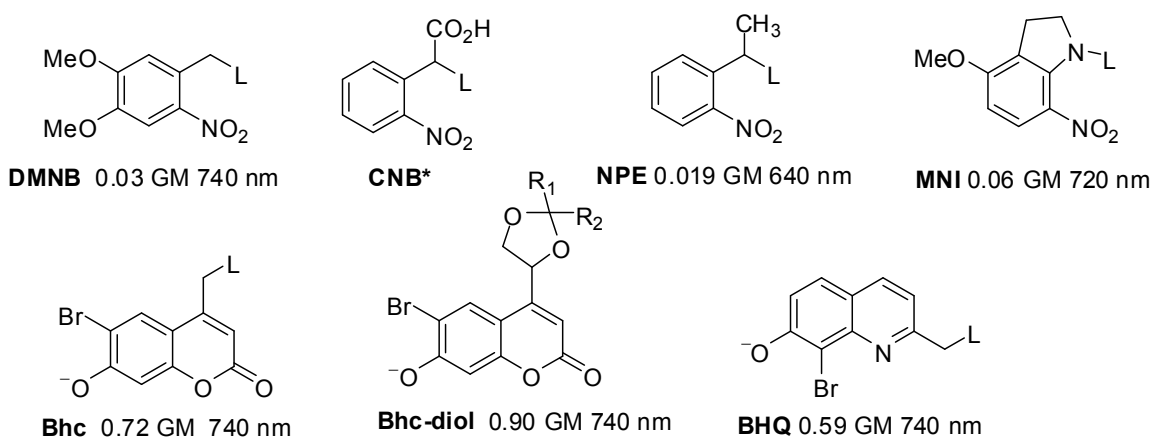


Figure 5.18 Caged compounds with their two-photon cross-sections at the given wavelengths. (*Cross-section of **CNB** not reported).

Tsien has suggested that for caged compounds, their TPA cross-sections should be larger than *ca* 0.1 GM to be biologically useful.³²² Nitrobenzyl-based compounds (**DMNB**, **CNB**, **NEP**, **MNI**) are the most widely used photoremovable protecting groups; however, they are not very sensitive to two-photon excitation. Coumaryl protecting groups, especially **Bhc** and **Bhc-diol**, have better two-photon sensitivity, and have been used to cage neurotransmitters,³²² DNA and RNA,³²³ diols,^{324,349} alcohols,³¹⁸ cyclic nucleotide monophosphates,³²⁸ ketones and aldehydes,³²⁶ an inhibitor of nitric oxide synthase^{325,350} and protein synthesis,³⁵¹ and carboxylates and phosphates.³⁴⁹

5.4.2 Research goal

The research goal of the work described in this chapter is to study a new molecular design strategy for two-photon removable protecting groups. The design strategy reported in the literature has used direct two-photon excitation of photocleavable groups, i.e. photocleavable groups that also act as two-photon absorbers. The disadvantages of this design include (1) the very small TPA cross-sections (typically less than 1 GM) of the known photocleavable groups that have been investigated, which require the use of high laser power and may, in turn, lead to tissue destruction; (2) two-photon excitation wavelengths which are determined by the choice of photocleavable groups. To overcome these disadvantages, a new molecular design strategy is studied in this chapter, wherein a TPA chromophore with large cross-section is covalently attached to a photocleavable group. The hypothesis is that the electron will be transferred from the excited TPA chromophore to the photocleavable group, i.e. two-photon induced electron transfer will occur. After receiving an electron, the photocleavable group undergoes a bond cleavage process to release the protected molecule.

For the *o*-nitrobenzyl groups, the by-product is toxic, and various modifications have been made to trap the by-product or make it less harmful. The major drawback for the benzoin groups are the poor solubility and introduction of a chiral center in protected molecules. The phenacyl groups combine the advantages of the above two groups, and do not suffer these disadvantages. Additionally, photorelease of phenacyl groups using photoinduced inter- and intra-molecular electron transfer has been studied (section 5.3). Therefore, the phenacyl group was selected as the photocleavable group for our

molecular design. Many TPA chromophores with large cross-sections in the near-IR range of interest have been developed (section 1.1 and 1.2). TPA chromophore **45** (900 GM at 730 nm)³³ (Figure 5.19) was selected as a two-photon sensitizer. Acetic acid, a simple acid, was chosen as the protected molecule. The research focuses on the study of the efficient linkage between TPA chromophore **45** and the phenacyl group, and comparing the efficiency of chromophores in which the phenacyl group is attached through two different positions of **45**. The photochemical studies performed in this chapter have all been conducted under one-photon conditions, and the two-photon studies will be conducted by our collaborators.

5.5 First generation of molecular design

5.5.1 Molecular design

According to the design strategy described in the literature for one-photon sensitized phenacyl protected molecules (Figure 5.19),³⁴⁴ target two-photon removable protected molecule **76** is designed by covalently linking TPA chromophore **45** to the photocleavable phenacyl group bearing the protected moiety, acetic acid. The model molecule **77** is designed to attach **45** to a phenacyl group without the protected moiety for fluorescence quenching studies (section 5.5.3.2). Phenacyl esters with substituents of different electron-withdrawing/donating ability at the *para* position, i.e. **78** with electron-donating group ($-\text{OCH}_3$), **79** un-substituted ($-\text{H}$), and **80** with electron withdrawing group ($-\text{CO}_2\text{CH}_3$), are chosen to study the photorelease efficiency via intermolecular electron transfer between **45** and **78** – **80**.

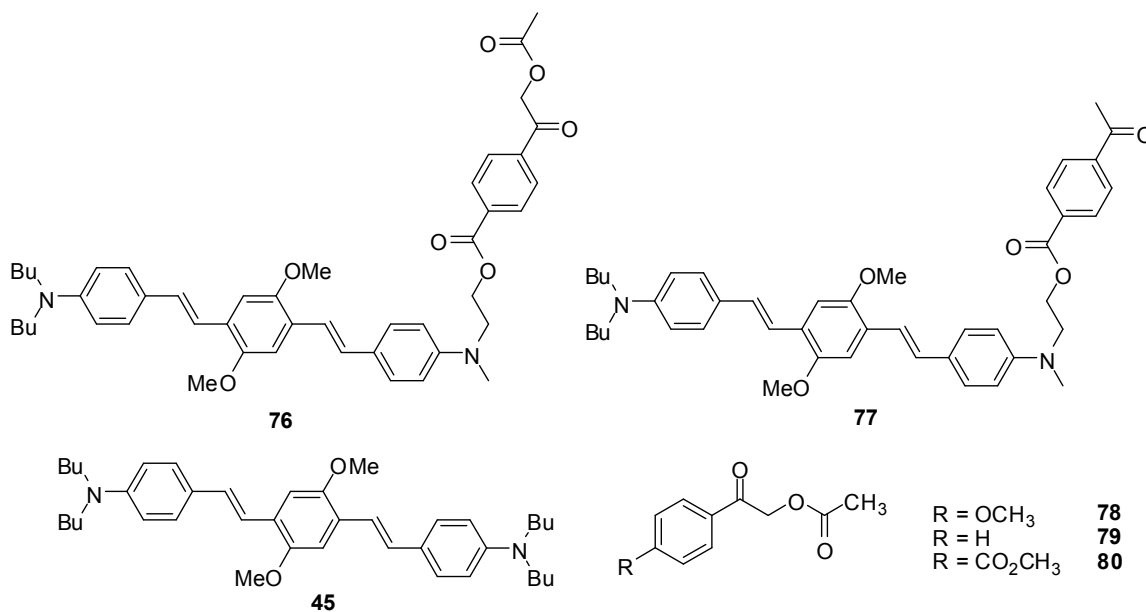


Figure 5.19 Target molecules of first generation molecular design.

Figure 5.22 shows the synthesis of target molecule **76** and model molecule **77**. Synthesis of compound **66** is shown in Figure 4.28 and was discussed in section 4.5.2. The Horner-Emmons coupling between **66** and 4-((2-hydroxyethyl)(methyl)amino) benzaldehyde formed the TPA chromophore **84**, which has a hydroxyl group at one end for subsequent reaction with acetyl chloride. The reactions between chromophore **84** and acetyl chloride derivatives **82** and **83** in benzene gave the target molecule **76** in 66% yield and model molecule **77** in 71% yield, respectively.

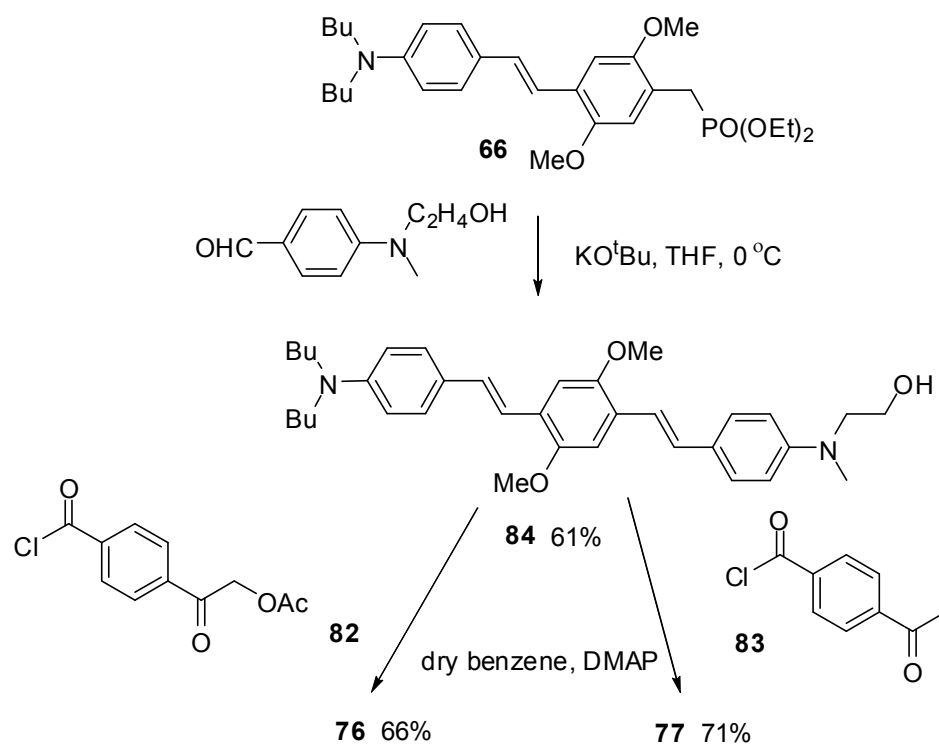


Figure 5.22 Synthesis of target molecule **76** and model molecule **77**.

5.5.3 Photochemical studies

Absorption and fluorescence spectra were measured for chromophores **45**, **76**, and **77**. Fluorescence quantum yields for chromophore **45** and model molecule **77** were measured, and the relative fluorescence quantum yield was calculated based on the measurements. The reduction potentials for **76** and **77** were also measured. The data are summarized in Table 5.1.

	$\lambda_{\text{max}}^{\text{abs}}$ nm	ϵ_{max} $10^4 \text{ M}^{-1} \text{ cm}^{-1}$	$\lambda_{\text{max}}^{\text{fl}}$ nm	Relative $\Phi_{\text{Fl}}^{\text{a}}$
45	429	7.40 ²¹⁹	516	1.00
76	249, 427	7.75	519	–
77	249, 425	7.65	519	0.02

^aRelative fluorescence quantum yields Φ_{Fl} (details in section 5.7.1).

Table 5.1 One-photon physical data for **45**, **76**, and **77** in acetonitrile.

5.5.3.1 Absorption and fluorescence spectra

Absorption spectra of **45** and **78** – **80** are shown in Figure 5.23. The absorption maxima of interest are 272 nm for **78**, 291 nm for **79**, and 249 nm for **80**. Photolysis of chromophore **45** and phenacyl esters **78** – **80** was conducted using lamps with an emission maximum at 419 nm. The lamp emission is seen at wavelength excess of 390 nm, while phenacyl esters only absorb significantly below 320 nm. Thus only the TPA chromophore **45** significantly absorbs light from the lamp.

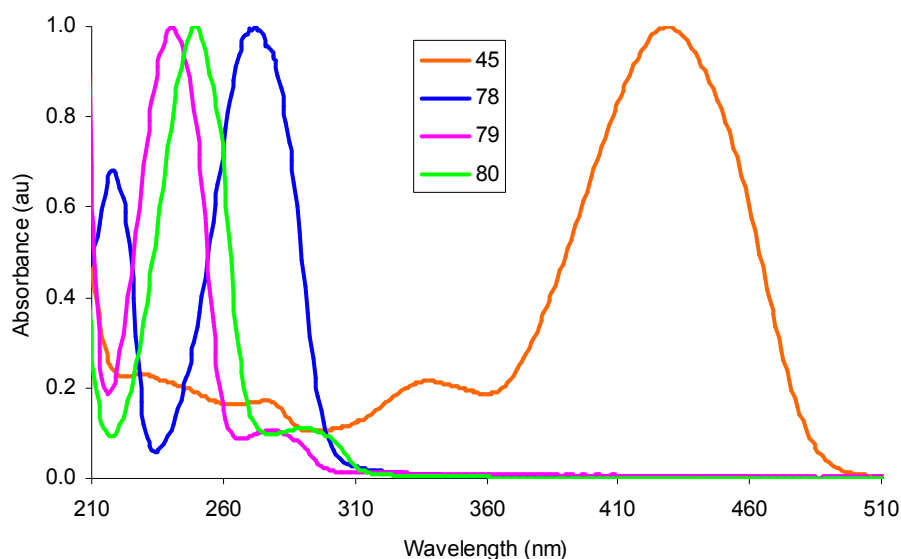


Figure 5.23 Absorption spectra of **45** and **78 – 80** in acetonitrile.

Since absorption and fluorescence spectra for **76** and **77** are almost identical, only those of **76** are shown, together with those of **45**, in Figure 5.24. The absorption spectrum of **76** has peaks (249 and 427 nm), which are similar to those of phenacyl ester **80** (249 nm) and chromophore **45** (429 nm). The maximum of extinction coefficients for **45**, **76**, and **77** are similar, and their fluorescence maxima can be considered the same. These results suggest that the ester linker effectively decouples the chromophore moiety from the phenacyl group of **76**.

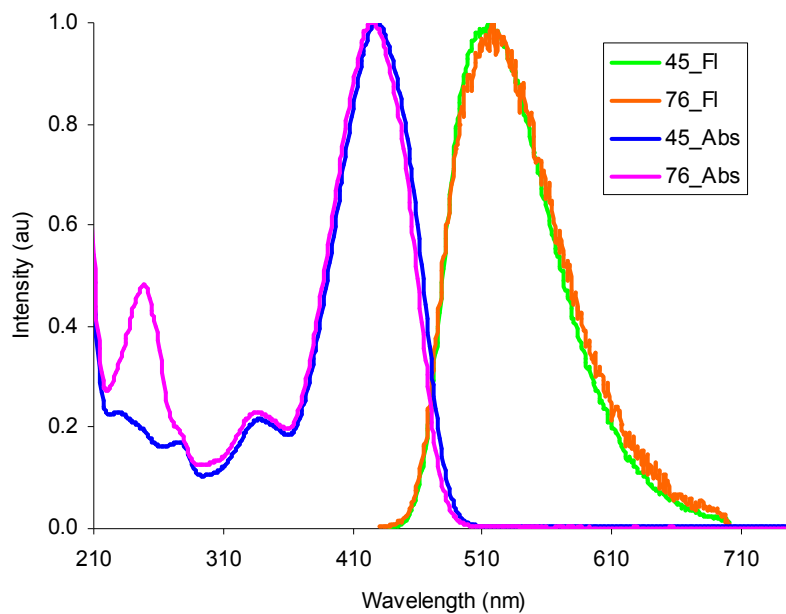


Figure 5.24 Absorption and fluorescence spectra of **45** and **76** in acetonitrile.

5.5.3.2 Relative fluorescence quantum yield

Since the photocleavage of **76** may complicate the measurement of fluorescence quantum yield, model molecule **77** was used for the measurement instead. The relative fluorescence quantum yield of **77** over **45** is 0.02 (section 5.7.1). The significant reduction of the fluorescence quantum yield (98% reduction) of **77** relative to that of **45** suggests that the probability of electron transfer from the excited state of the chromophore moiety to the phenacyl group is high. Thus, assuming the radical anion of phenacyl group to be unstable, the cleavage probability should be high as well.

5.5.3.3 Reduction potentials

An irreversible reduction peak (-1.96 V, vs. $\text{FeCp}_2^{+/0}$, scan rate 50 mV/s) was found for **76**, consistent with the instability of the protected phenacyl moiety with cleavage. The driving force for electron transfer from the excited chromophore moiety to the phenacyl group (ΔG_{et}) for **76** is estimated as -62.4 kJ mol $^{-1}$ based on the calculation discussed in section 2.5.3. The results suggest that target molecule **76** has a reasonably large excited-state electron-transfer driving force.

5.5.3.4 Photolysis

To demonstrate photolysis via intermolecular electron transfer, a solution of chromophore **45** as a sensitizer, a phenacyl ester **78** – **80** as a cleavable compound, and hexamethyldisiloxane as an internal standard was prepared in benzene- d_6 . After the sample was sealed in a NMR tube, degassed, and irradiated at 419 nm for a given time, ^1H NMR spectra were taken to follow the photolysis process. The relative integration of the unconverted phenacyl ester and the photoproduct (acetic acid) was plotted versus the irradiation time. For photolysis for compounds **76** via intramolecular electron transfer, the same method and conditions were applied. The experimental details are described in section 5.7.2.

The photolysis of **76** and the system **45/80** did not produce acetic acid (Figure 2.25). However, the system **45/78** and **45/79** did release acetic acid (Figure 5.26 and Figure 5.27). For these two systems, phenacyl ester (**78** or **79**) disappeared and acetic acid appeared with increasing of irradiation time. Both **76** and **80**, in which photolysis

was not observed, have an electron-withdrawing group ($-\text{CO}_2\text{CH}_3$) at the *para* position of phenacyl group/ester. On the other hand, both **78** and **79**, in which photolysis did proceed, have either no substituent for **79** or an electron-donating group ($-\text{OCH}_3$) for **78** at the same position.

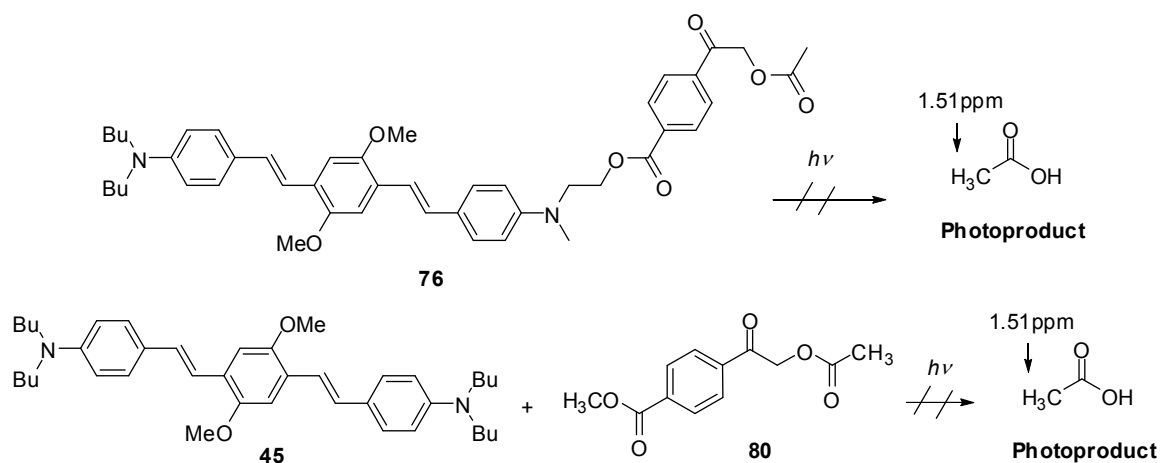


Figure 5.25 Photolysis of **76** and the system **45** and **80**.

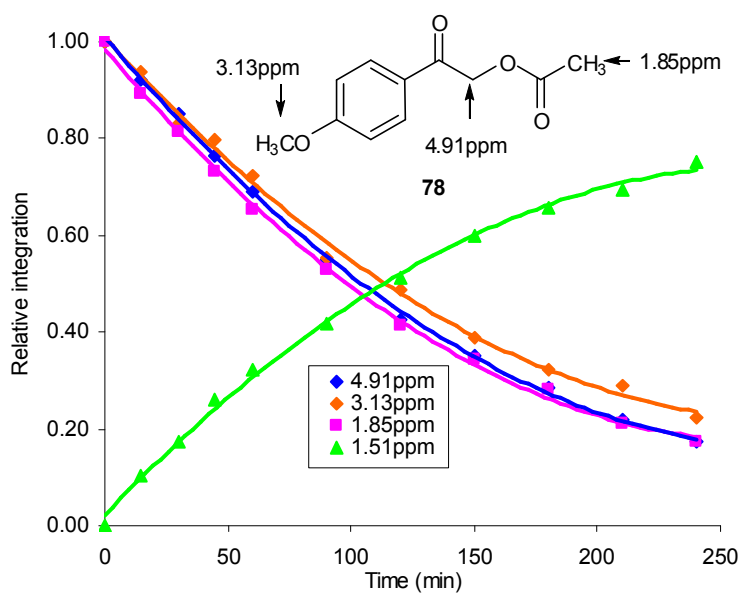


Figure 5.26 Photolysis of the system **45** and **78**.

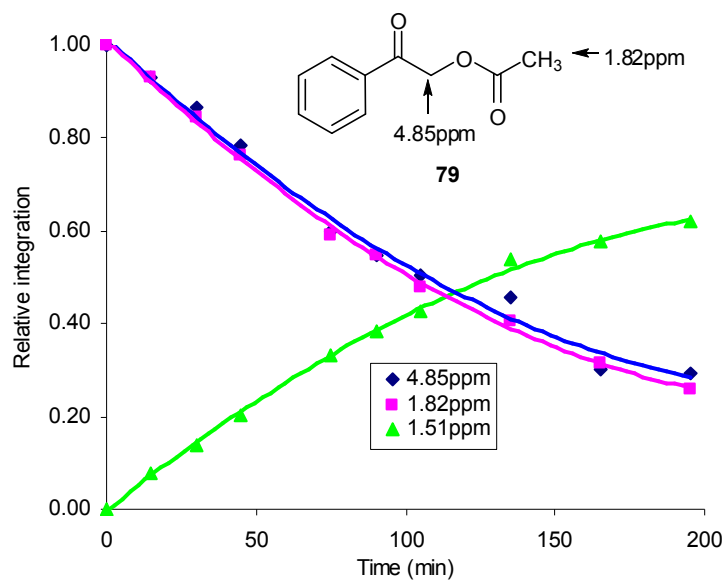


Figure 5.27 Photolysis of the system 45 and 79.

5.5.4 Discussion and conclusion

Based on the molecular design strategy described in the literature for an one-photon removable protected compound,³⁴⁴ a two-photon version **76** was synthesized by attaching TPA chromophore **45** to phenacyl ester via an ester linker. Absorption and fluorescence spectra suggest that the linker effectively decouples the chromophore moiety from the phenacyl group of **76**. Model molecule **77** was synthesized using the same design as that for **76** without the protected group for the measurement of fluorescence quantum yield. The 98% reduction of the fluorescence quantum yield of **77** relative to that of **45** suggests that the rate of electron transfer from the excited state of the chromophore moiety to the phenacyl group is competitive with fluorescence, which is consistent to the reasonably large driving force for electron transfer ($-62.4 \text{ kJ mol}^{-1}$) estimated for **76** from electrochemical and optical data. However, the photolysis of **76** did not release the protected acid under our conditions.

The photolysis mechanisms in Figure 5.10 and 5.11 have been proposed by two different research groups. While these mechanisms differ in the proposed roles of singlet or triplet excited state in the excitation process, they both agreed that the electron donating group at the *para* position ($-\text{OH}$ in these cases) assists the release of the protected groups. In the literature, photolysis via intermolecular electron transfer between a sensitizer, such as 9,10-dimethylantracene and *N,N*-dimethylaniline, and a phenacyl protected acids gave 80 – 100% release yields for acids.³⁴² However, for the literature molecules, in which a sensitizer (anthracene and *N,N*-dimethylaniline) was attached to phenacyl protected acids via an ester linker (Figure 5.17), the photolysis via

intramolecular electron transfer gave low quantum yield of acid release (0.02) for the aniline system, but failed to produce the detectable amount of acids for the anthracene system.³⁴⁴

The failure of **76** to undergo efficient photocleavage may be related to the ester linker, which is electron-withdrawing group at the *para* position of the phenacyl group of **76**. To experimentally prove the hypothesis, phenacyl esters with different substituents at the *para* position, e.g. **78** with an electron-donating group ($-\text{OCH}_3$), **79** with no substituent ($-\text{H}$), and **80** with an electron withdrawing group ($-\text{CO}_2\text{CH}_3$), were designed and synthesized. The photolysis via intermolecular electron transfer from the excited state of chromophore **45** to phenacyl esters **78** – **80** was tested. Photolysis of **45** and **80** ($-\text{CO}_2\text{CH}_3$ substituent) did not release the protected acid, like the compound **76** that has an ester linker at the phenacyl group. However, for **78** (no substituent) and **79** ($-\text{OCH}_3$ substituent), photolysis of **45/78** and **45/79** released the protected acid. Based on the studies in this section, a second generation of two-photon removable system was designed.

5.6 Second generation of molecular design

5.6.1 Molecular design

The hypothesis from the study in section 5.5 is that the ester linker in **76**, an electron-withdrawing group at the *para* position of the phenacyl group is responsible for the failure to achieve photocleavage. A new molecular design strategy was developed to use an electron donating ether linker instead. Target molecules **85** and **86** were designed by attaching the phenacyl group to either the amine donor or π -bridge of chromophore **45** via an ether linker (Figure 5.28). The photolysis efficiency of both compounds will be compared.

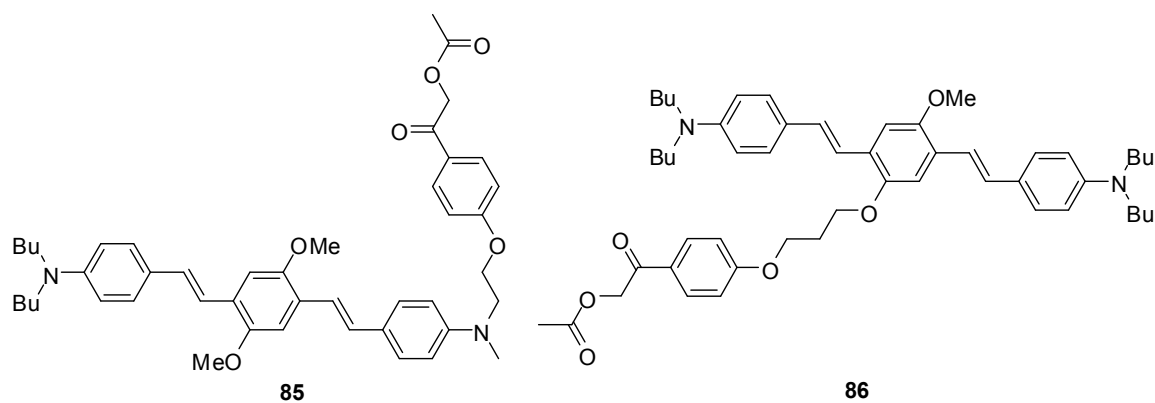


Figure 5.28 Target molecules **85** and **86**.

5.6.2 Synthesis

The synthesis of target molecule **85** is shown in Figure 5.29. TPA chromophore **84** was reacted with 2,3-dichloro-5,6-dicyano-1,4-benzoquinone, triphenylphosphite, and tetrabutyl ammonium bromide, giving the bromide **87**. The reaction of 2-bromo-1-(4-hydroxyphenyl)ethanone and sodium acetate afforded 2-(4-hydroxyphenyl)-2-oxoethyl acetate **88**. The reaction between **87** and **88** gave the target molecule **85**.

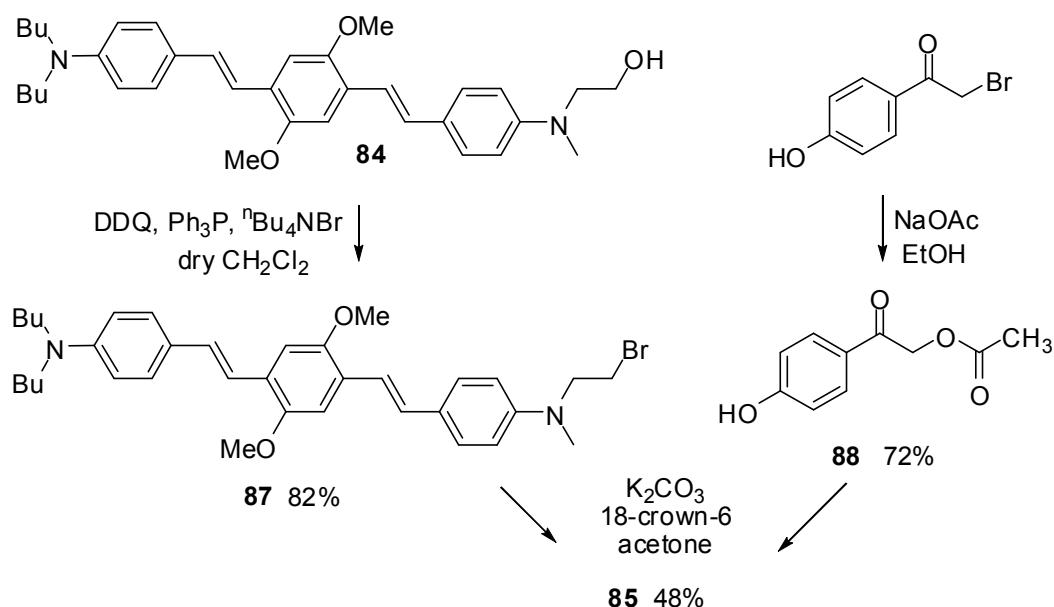


Figure 5.29 Synthesis of target molecule **85**.

The synthesis of target molecule **86** is shown in Figure 5.30. 3-(4-Methoxyphenoxy)propan-1-ol reacted with formaldehyde in hydrobromic acid to give 3-(2,5-bis(bromomethyl)-4-methoxyphenoxy)propyl acetate **89**. The reaction of **89** with triethylphosphite gave 3-(2,5-bis((diethoxyphosphoryl)methyl)-4-methoxyphenoxy)

propyl acetate **90**. Compound **89** was purified washing with water, and compound **90** was purified using vacuum distillation to remove excess triethylphosphite. Both **89** and **90** were used for the reaction of next step without further purification. The Horner-Emmons reaction was performed, coupling 4-(dibutylamino)benzaldehyde to **90** to afford chromophore **91**. Following the same procedures in Figure 5.24, target molecule **86** was obtained.

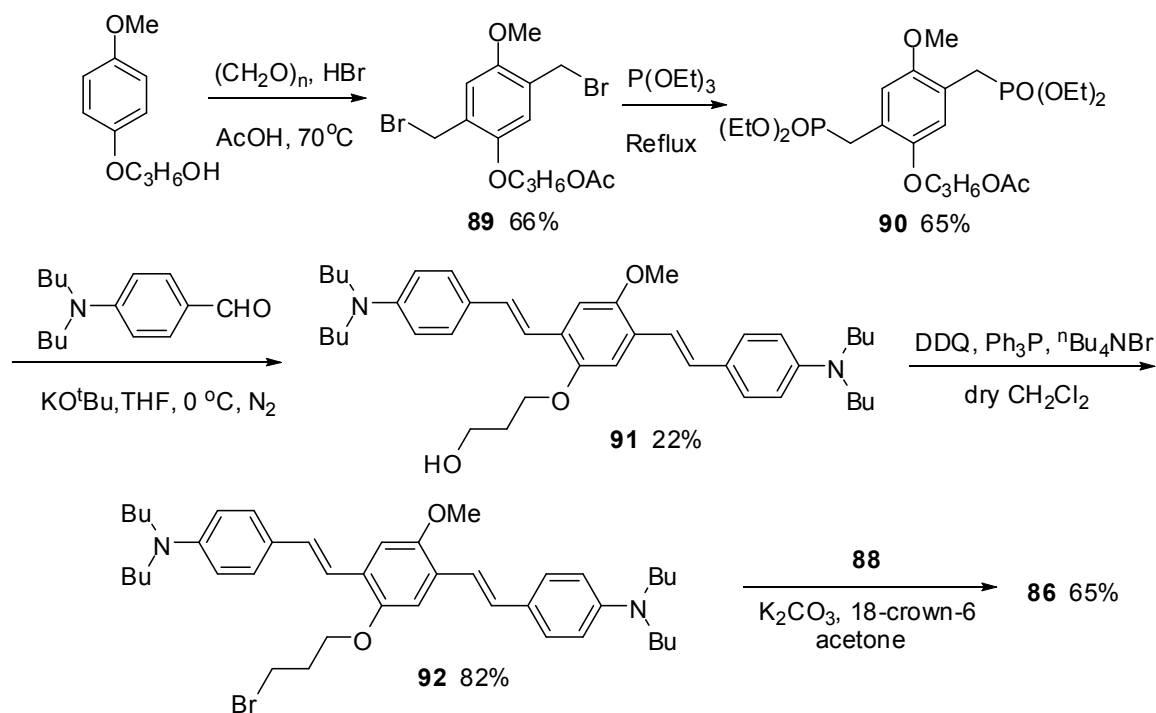


Figure 5.30 Synthesis of target molecule **86**.

5.6.3 Photochemical studies

Absorption and fluorescence spectra were measured for chromophores **85** and **86**.

The photolysis for **85** and **86** were tested. The data were summarized in Table 5.2.

	$\lambda_{\text{max}}^{\text{abs}}$ nm	ϵ_{max} $10^4 \text{ M}^{-1} \text{ cm}^{-1}$	$\lambda_{\text{max}}^{\text{fl}}$ nm
45	429	7.40 ²¹⁹	516
85	272, 429	3.11, 7.76	509
86	274, 431	3.06, 7.37	506

Table 5.2 One-photon physical data for **85** and **86** in acetonitrile.

5.6.3.1 Absorption spectra and fluorescence spectra

The absorption and fluorescence spectra of **45**, **85** and **86** are shown in Figure 5.31. The absorption maxima of interest are 272 and 429 nm for **85**, and 274 and 432 nm for **86**, which are similar to those of phenacyl ester **78** (272 nm) and chromophore **45** (429 nm). The extinction coefficients and the fluorescence spectra of **45**, **85** and **86** are also similar. Therefore, the ether linker effectively decouples the chromophore moiety from the phenacyl group of **76**.

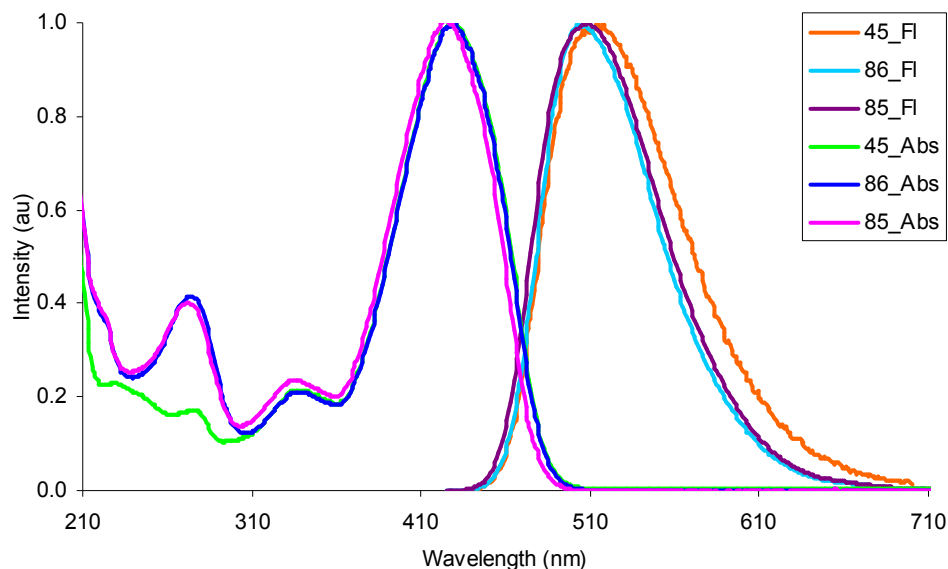


Figure 5.31 Absorption and fluorescence spectra of **45**, **85** and **86** in acetonitrile.

5.6.3.2 Photolysis

The photolysis of **85** and **86** was conducted under the same conditions that of **76** (section 5.5.4). The experiment details are described in section 5.8.2. Both donor-attached molecule **85** and π -bridge-attached molecule **86** underwent successful photolysis with the irradiation of lamps at 419 nm (Figure 5.32 and Figure 5.33). After 90 min irradiation, 92% of **86** disappeared based on NMR results, however, only 47% of **85** was gone. The results indicate that the photolysis of the π -bridge-attached molecule **86** is more efficient than that of the donor-attached molecule **85**.

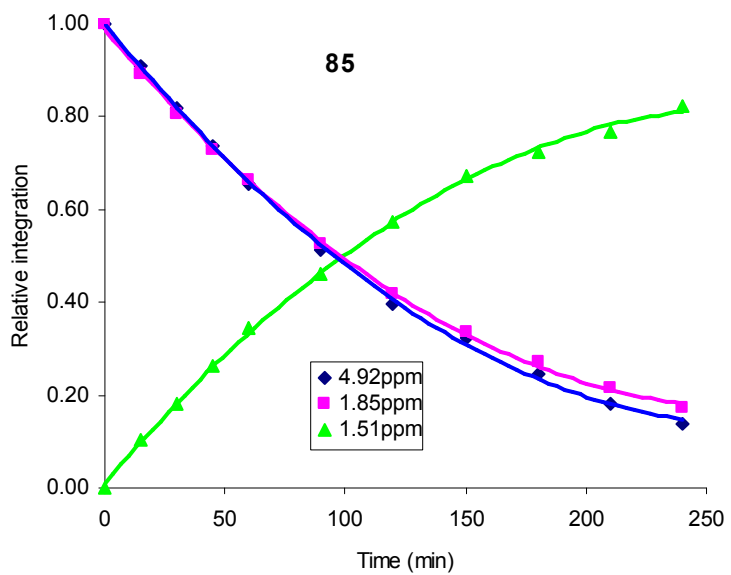
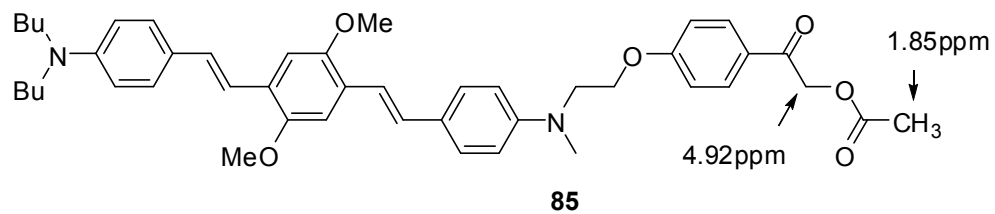
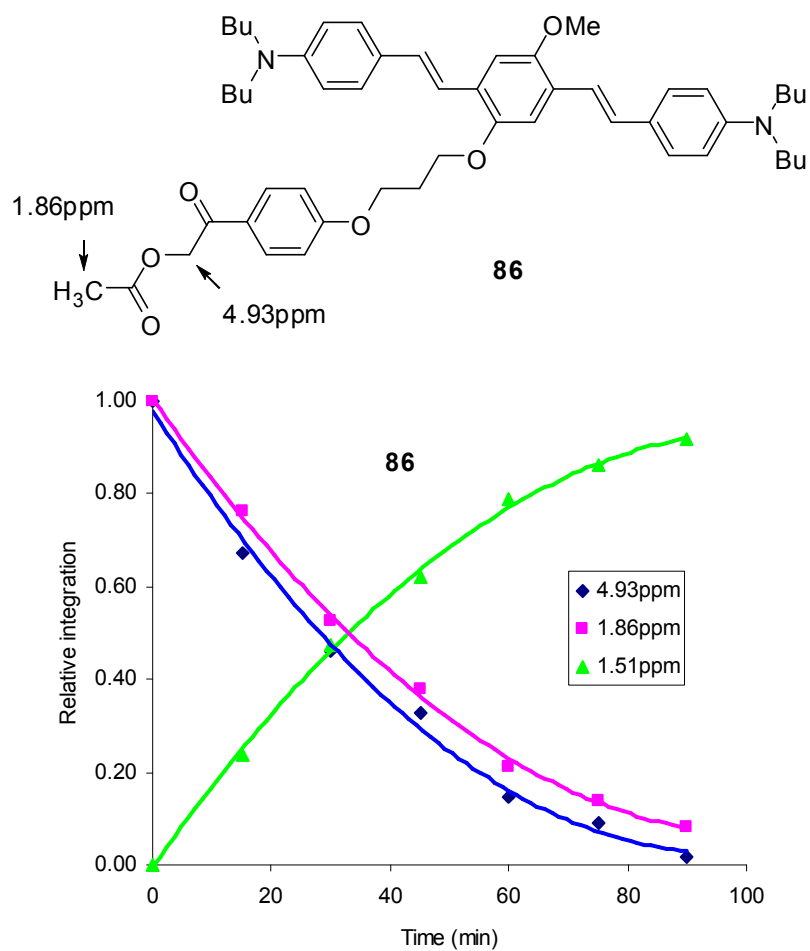


Figure 5.32 Photolysis of **85**.

Figure 5.33 Photolysis of **86**.

5.6.4 Conclusions

New two-photon removable protected compounds were obtained by covalently attaching TPA chromophore **45** to the phancyl ester via an ether linker instead of an ester linker. The donor-attached **85** and the π -bridge-attached **86** were synthesized based on this molecular design. The photolysis results show that both **85** and **86** released the protected acid upon irradiation, and the π -bridge-attached **86** is more efficient than the donor-attached **85**.

5.7 Experimental: photochemical measurements

General experimental. Absorption spectra were run on a Hewlett-Packard model 8453 spectrophotometer. The fluorescence spectra were collected on a Jobin Yvon Spex Fluorolog-III fluorimeter. The photon parameters were measured by using a multi-functional optical meter of Newport model 1835-C. All electrochemical experiments were conducted using a BAS Model 100B/W cyclic voltammetry unit. The electrodes were a glassy-carbon working electrode, a platinum auxiliary wire, and a Ag/AgCl pseudo-reference electrode. The supporting electrolyte was 0.1 M tetrabutylammonium hexafluorophosphate in solution. The spectrophotometric grade acetonitrile and dichloromethane (Aldrich) were used as received in all the measurements.

5.7.1 *Relative fluorescence quantum yield*

The excitation wavelength, integration rate, slit, and data collection wavelength range were set all the same for both TPA chromophore **45** and model molecule **77**. The fluorescence quantum yields of **45** and **77** were measured using the method described in section 4.7.5 (Figure 5.34 for **77** and Figure 5.35 for **45**). The relative fluorescence quantum yield of **77** over **45** was obtained by calculating the slope ratio of **77** to **45**, which was 0.02.

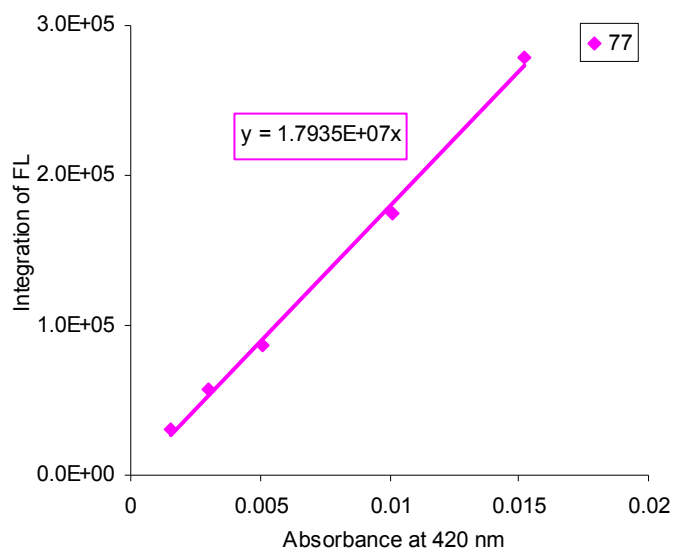


Figure 5.34 Measurement of fluorescence quantum yield of **77**.

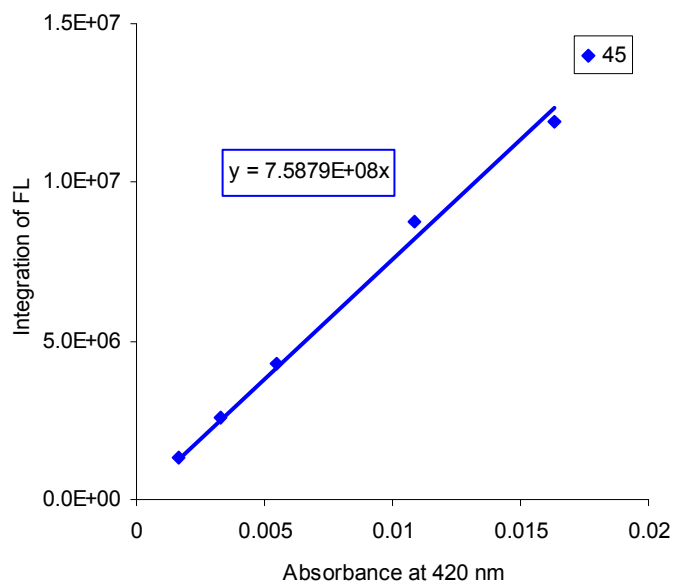


Figure 5.35 Measurement of fluorescence quantum yield of **45**.

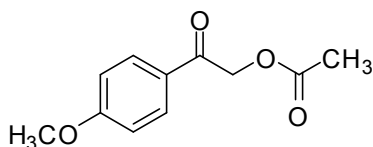
5.7.2 *Photolysis*

The Rayonet photochemical reactor, equipped with fourteen lamps with absorption maximum at 419 nm as light sources, was used for test the photolysis of photoremovable compounds. The lamp emission spectrum starts at 390 nm, and the absorption of phenacyl esters ends at 320 nm. Thus, the lamp emission only irradiated the TPA chromophore **45**, not the phenacyl esters.

¹H NMR spectra were taken to follow the photolysis process. For photolysis via intermolecular electron transfer, a solution of chromophore **45** as a sensitizer (1.5×10^{-2} M), phenacyl ester **78** – **80** (1.5×10^{-2} M), and hexamethyldisiloxane (3 μ L) as an internal standard in benzene-*d*₆ (2 mL) was prepared. The solution (0.5 mL) was transferred to a sealed NMR tube through a mini-filter, and was purged with nitrogen gas for about 15 min. A ¹H NMR spectrum was recorded, and the areas of corresponding peaks relative to hexamethyldisiloxane were determined and recorded. After different irradiation time, the relative peak areas of the unconverted phenacyl ester and the photoproduct (acetic acid) were recorded at different irradiation time. The relative peak area at certain irradiation time is divided by that before the irradiation, and the results were plotted versus the irradiation time. For photolysis of **76**, **85**, or **86** via intramolecular electron transfer, a solution of the chromophore (1.5×10^{-2} M) and hexamethyldisiloxane (3 μ L) as an internal standard in benzene-*d*₆ (2 mL) was prepared, and the rest is the same as above.

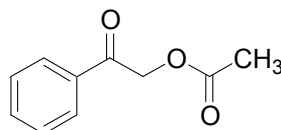
5.8 Experimental: synthetic procedures

General experimental. NMR spectroscopy was performed using either a DRX-500 MHz or Varian Unity Plus 200MHz and 300 MHz spectrometers. Mass spectrometry (MS) was performed by the MS Instrument Facility at the University of Arizona. The combustion experiments for elemental analysis were conducted by Desert Analytics, Tucson, Arizona. Silica gel (40 – 63 μm , EMD Chemical, Inc.) was used to perform flash column chromatography. TLC was performed on pre-coated plates containing a fluorescent indicator (silica gel 60 F₂₅₄, EMD Chemicals, Inc.) All reagents and solvents including dry solvents and anhydrous solvents in Acroseal bottles were purchased from readily available suppliers (Aldrich and Acros), and were used as received. The general precautions for preparation of light sensitive compounds mentioned in this section include wrapping the reaction flask with aluminum foil and performing the subsequent workup and purification in dark under the weak red light. These precautions are applied in all cases where it is indicated that the compound is light sensitive.

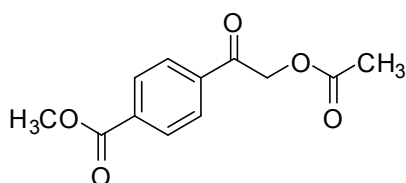


2-(4-Methoxyphenyl)-2-oxoethyl acetate. To a solution of sodium acetate (9.845 g, 0.120 mol) in methanol (100 mL), was added 2-bromo-1-(4-methoxyphenyl)ethanone (4.454 g, 1.94 mmol) in methanol (200 mL) dropwise through a dripping funnel at room temperature. The reaction solution was then heated under reflux for 2 hours. After cooling to room temperature, the reaction solution was removed by evaporation. Water

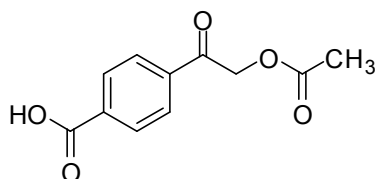
was added, and extracted with ethyl acetate three times. The combined organic layers were dried over magnesium sulfate, and the product (3.32 g) was obtained in 82% yield after purification by column chromatography (hexane : ethyl acetate 4:1 and then 2:1). This compound is light sensitive. ^1H NMR (300 MHz, chloroform-*d*) δ 7.86 (d, $J = 8.7$ Hz, 2H), 6.91 (d, $J = 8.7$ Hz, 2H), 5.27 (s, 2H), 3.85 (s, 3H), 2.20 (s, 3H). ^{13}C NMR (75 MHz, chloroform-*d*) δ 190.5, 170.4, 163.9, 129.9, 127.1, 113.9, 65.7, 55.5, 20.5. The data were consistent with the literature data.³⁵²



2-Oxo-2-phenylethyl acetate. To a solution of acetic sodium acetate (2.081 g, 0.026 mol) in methanol (80 mL), were added 2-bromo-1-phenylethanone (5.20 g, 26.0 mmol) in methanol (50 mL). After 2 hours, the reaction solution was washed with 10% hydrogen chloride aqueous solution three times and then saturated sodium three times. The organic layers were dried over magnesium sulfate. A white solid product (4.08 g) was obtained by recrystallization in diethyl ether in 88% yield. This compound is light sensitive. ^1H NMR (400 MHz, chloroform-*d*) δ 8.09 (d, $J = 8.0$ Hz, 2H), 7.88 (d, $J = 8.0$ Hz, 1H), 7.47 (d, $J = 8.0$ Hz, 2H), 5.32 (m, 2H), 2.20 (s, 2H). ^{13}C NMR (100 MHz, chloroform-*d*) δ 192.1, 170.4, 134.1, 133.9, 128.8, 127.7, 65.9, 20.5. The data were consistent with the literature data.³⁵³

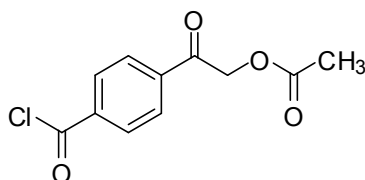


Methyl 4-(2-acetoxyacetyl)benzoate. A solution of sodium acetate (3.40 g, 0.024 mol) and methyl 4-(2-bromoacetyl)benzoate (3.65 g, 14.3 mmol) in methanol (100 mL) was stirred at room temperature for 5 hours. Water was added to quench the reaction. The reaction solution was extracted with ethyl acetate three times, and dried over anhydrous magnesium sulfate. The product (2.56 g) was obtained in 76% yield after column chromatography (hexane: ethyl acetate 4:1). This compound is light sensitive. ^1H NMR (400 MHz, chloroform-*d*) δ 8.13 (d, $J = 8.0$ Hz, 2H), 7.94 (d, $J = 8.0$ Hz, 2H), 5.32 (s, 2H), 3.94 (s, 3H), 2.21 (s, 3H). ^{13}C NMR (100 MHz, chloroform-*d*) δ 191.8, 170.4, 165.9, 137.3, 134.6, 130.0, 127.7, 66.1, 52.6, 20.5. The data were consistent with the literature data.³⁵⁴

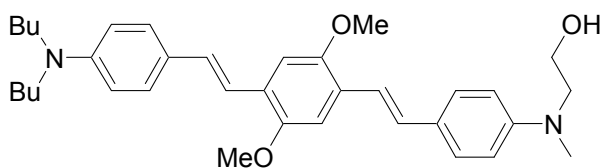


4-(α -Acetoxyacetyl)-benzoic acid. To a solution of sodium acetate (14.78 g, 180.2 mmol) in methanol (200 mL), was added 4-(2-bromoacetyl)benzoic acid (3.12 g, 12.8 mmol) in methanol (400 mL) dropwise through a dripping funnel at room temperature. The reaction solution was then heated under reflux for 1 h. After cooling to room temperature, the reaction solution was removed by evaporation. Water was added to dissolve the white solid, and then aqueous sulfuric acid solution (5% wt%) was added until precipitation completed. The resulting white precipitate was collected by filtration, washed with water, and dried under vacuum. The product (2.13 g) was obtained in 75% yield. ^1H NMR (500 MHz, chloroform-*d*) δ 8.20 (d, $J = 8.0$ Hz, 2H), 7.99 (d, $J = 8.5$ Hz,

2H), 5.34 (s, 2H), 2.23 (s, 3H). ^{13}C NMR (125 MHz, chloroform-*d*) δ 191.8, 170.4, 169.1, 138.0, 133.4, 130.7, 127.8, 66.1, 20.5. The data were consistent with the literature data.^{344,355}

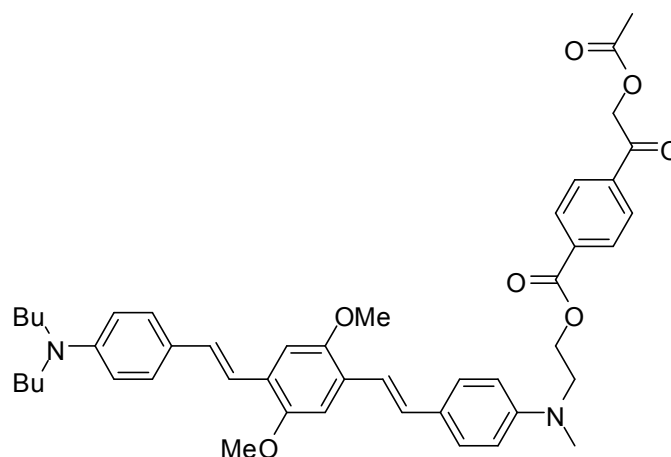


2-(4-(Chlorocarbonyl)phenyl)-2-oxoethyl acetate. The solution of 4-(α -acetoxyacetyl)-benzoic acid (3.27 g, 14.7 mmol) in thionyl chloride (25 mL) was heated to reflux for 17 hours. The thionyl chloride was removed by distillation and decomposed by adding saturated potassium hydroxide aqueous solution. The residue was washed with water, and the product (1.98 g) was obtained in 56% yield after filtration. ^1H NMR (500 MHz, chloroform-*d*) δ 8.21 (d, $J = 8.5$ Hz, 2H), 8.00 (d, $J = 8.5$ Hz, 2H), 5.32 (s, 2H), 2.22 (s, 3H). ^{13}C NMR (125 MHz, chloroform-*d*) δ 191.5, 170.3, 167.7, 138.9, 137.1, 131.6, 128.1, 66.1, 20.5. The compound was used for next reaction without further purification.



2-((4-(4-(4-(Dibutylamino)styryl)-2,5-dimethoxystyryl)phenyl)(methyl)amino)ethanol. To a solution of (*E*)-diethyl 4-(4-(dibutylamino)styryl)-2,5-dimethoxybenzylphosphonate (0.37 g, 0.80 mmol) and 4-((2-hydroxyethyl)methylamino)benzaldehyde (0.15 g, 0.80 mmol) in dry THF (15 mL), was

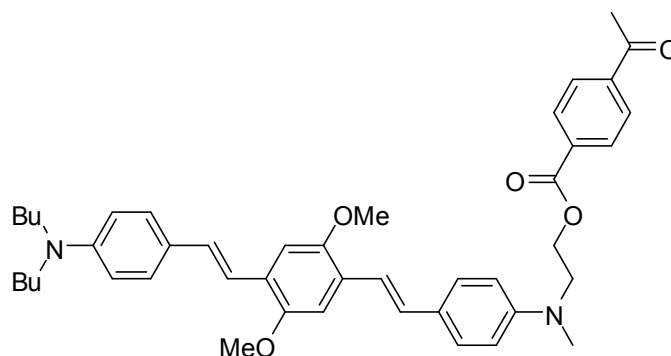
added potassium *tert*-butoxide (2.4 mL, 2.4 mmol, 1.0 M in 2-methyl-2-propanol) at 0 °C. After stirring at 0 °C for 4 hours and at room temperature for 3 hours, the reaction was quenched by adding water, and extracted with ether and dichloromethane until the color of the aqueous layer was only slight yellow or colorless. The combined organic layers were washed with water, and dried over magnesium sulfate. The column chromatography (hexane: ethyl acetate 2: 1) afforded the product (0.26 g) in 61% yield. ¹H NMR (500 MHz, acetone-*d*₆) δ 7.38 (d, *J* = 9.0 Hz, 2H), 7.37 (d, *J* = 9.0 Hz, 2H), 7.25 (d, *J* = 16.5 Hz, 1H), 7.24 (s, 2H), 7.23 (d, *J* = 16.5 Hz, 1H), 7.14 (d, *J* = 16.5 Hz, 1H), 7.13 (d, *J* = 16.5 Hz, 1H), 6.74 (d, *J* = 9.0 Hz, 2H), 6.68 (d, *J* = 9.0 Hz, 2H), 3.90 (s, 6H), 3.73 (t, *J* = 6.5 Hz, 2H), 3.50 (t, *J* = 6.5 Hz, 2H), 3.35 (t, *J* = 7.5 Hz, 4H), 3.02 (s, 3H), 1.59 (quintet, *J* = 7.5 Hz, 4H), 1.38 (sextet, *J* = 7.5 Hz, 4H), 0.95 (t, *J* = 7.5 Hz, 6H). ¹³C NMR (125 MHz, acetone-*d*₆) δ 152.1, 152.0, 149.9, 148.7, 129.5, 129.4, 128.5, 127.3, 127.1, 126.7, 126.1, 118.9, 118.6, 112.8, 112.6, 109.2, 109.1, 59.9, 56.5, 56.4, 55.4, 51.2, 39.2, 20.9, 14.3. HRMS (FAB+) *m/z*: Calcd. for C₃₅H₄₆N₂O₃ (M⁺) 542.3508, Found 542.3525. Anal. Calcd. for C₃₅H₄₆N₂O₃: C, 77.45; H, 8.54; N, 5.16. Found: C, 77.06; H, 8.66; N, 5.16.



2-((4-(4-(4-(Dibutylamino)styryl)-2,5-dimethoxystyryl)phenyl)(methyl)

amino)ethyl 4-(2-acetoxyacetyl)benzoate. A solution of 2-((4-(4-(4-(dibutylamino)styryl)-2,5-dimethoxystyryl)phenyl)(methyl) amino)ethanol (0.21 g, 0.39 mmol), acetic acid 2-(4-chlorocarbonyl-phenyl)-2-oxo-ethyl ester (0.28 mg, 1.2 mmol) and 4-dimethylaminopyridine (DMAP) (0.15 g, 1.2 mmol) in dry benzene (20 mL) was heated to reflux for 2 h. After cooling to room temperature, the reaction mixture was quenched by adding the saturated sodium chloride solution (50 mL), and then was extracted with ethyl acetate (3 × 50 mL). The combined organic layers were dried over magnesium sulfate. The product (0.19 mg) was isolated by column chromatography (hexane: ethyl acetate 8: 1 and then 4:1) in 66% yield. This compound is light sensitive. ^1H NMR (500 MHz, acetone- d_6) δ 8.03 (s, 4H), 7.40 (d, J = 8.0 Hz, 2H), 7.37 (d, J = 9.0 Hz, 2H), 7.27 (d, J = 16.5 Hz, 1H), 7.25 (s, 1H), 7.24 (s, 1H), 7.23 (d, J = 16.5 Hz, 1H), 7.15 (d, J = 16.5 Hz, 1H), 7.14 (d, J = 16.5 Hz, 1H), 6.84 (d, J = 8.5 Hz, 2H), 6.67 (d, J = 9.0 Hz, 2H), 5.40 (s, 2H), 4.55 (t, J = 5.5 Hz, 2H), 3.90 – 3.86 (m, 8H), 3.34 (t, J = 8.0 Hz, 4H), 3.08 (s, 3H), 2.11 (s, 3H), 1.58 (quintet, J = 7.5 Hz, 4H), 1.37 (sextet, J = 7.5 Hz, 4H), 0.95 (t, J = 7.5 Hz, 6H). ^{13}C NMR (125 MHz, acetone- d_6) δ 192.9, 170.4, 165.9,

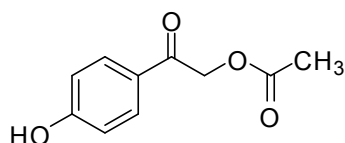
152.1, 152.0, 149.8, 148.7, 138.5, 135.11, 130.6, 129.6, 129.3, 128.6, 128.5, 128.4, 127.5, 127.4, 126.9, 126.1, 119.5, 118.6, 113.3, 112.6, 109.30, 109.1, 67.1, 63.5, 56.5, 56.5, 38.7, 20.9, 20.3, 14.3. HRMS (FAB+) m/z : Calcd for $C_{46}H_{55}N_2O_7$ (MH^+) 747.4009, Found 747.4001. Anal. Calcd. for $C_{46}H_{54}N_2O_7$: C, 73.97; H, 7.29; N, 3.75. Found: C, 73.61; H, 7.19; N, 3.59.



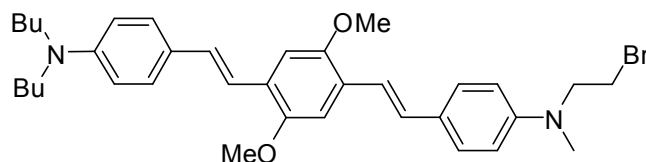
2-((4-(4-(4-(Dibutylamino)styryl)-2,5-dimethoxystyryl)phenyl)(methyl)

amino)ethyl 4-acetylbenzoate. A solution of 2-((4-(4-(4-(dibutylamino)styryl)-2,5-dimethoxystyryl)phenyl)(methyl) amino)ethanol (98 mg, 0.18 mmol), 4-acetyl-benzoyl chloride (41 mg, 0.22 mmol) and 4-dimethylaminopyridine (DMAP) (69 mg, 0.56 mmol) in dry benzene (30 mL) was heated to reflux for 2 h. After cooling to room temperature, the reaction mixture was quenched by adding the saturated sodium chloride solution (50 mL), and then was extracted with ethyl acetate (3×30 mL). The combined organic layers were dried over magnesium sulfate. The product (88 mg) was isolated by column chromatography (hexane: ethyl acetate 4: 1) in 71% yield. 1H NMR (500 MHz, acetone- d_6) δ 8.01 (s, 4H), 7.40 (d, $J = 8.5$ Hz, 2H), 7.37 (d, $J = 8.0$ Hz, 2H), 7.27 (d, $J = 16.5$ Hz, 1H), 7.25 (d, $J = 16.5$ Hz, 1H), 7.24 (s, 2H), 7.15 (d, $J = 16.5$ Hz, 1H), 7.12 (d, $J = 16.5$ Hz, 1H), 6.82 (d, $J = 9.0$ Hz, 2H), 6.67 (d, $J = 9.0$ Hz, 2H), 4.53 (t, $J = 5.5$ Hz, 2H),

3.90 (s, 6H), 3.84 (t, $J = 7.5$ Hz, 2H), 3.33 (t, $J = 7.5$ Hz, 4H), 3.07 (s, 3H), 2.57 (s, 3H), 1.58 (quintet, $J = 7.5$ Hz, 4H), 1.36 (sextet, $J = 7.5$ Hz, 4H), 0.95 (t, $J = 7.5$ Hz, 6H). ^{13}C NMR (125 MHz, acetone- d_6) δ 197.5, 166.1, 152.1, 152.0, 149.8, 148.7, 141.3, 134.5, 130.4, 129.6, 129.3, 128.9, 128.5, 128.4, 127.4, 126.9, 126.1, 119.5, 118.6, 113.3, 112.60, 109.3, 109.1, 63.4, 56.6, 56.5, 51.5, 51.2, 38.8, 30.3, 26.9, 20.9, 14.3. HRMS (FAB+) m/z : Calcd for $\text{C}_{44}\text{H}_{52}\text{N}_2\text{O}_5$ (M^+) 688.3876, Found 688.3893. Anal. Calcd. for $\text{C}_{44}\text{H}_{52}\text{N}_2\text{O}_5$: C, 76.71; H, 7.61; N, 4.07. Found: C, 76.63; H, 7.76; N, 4.11.

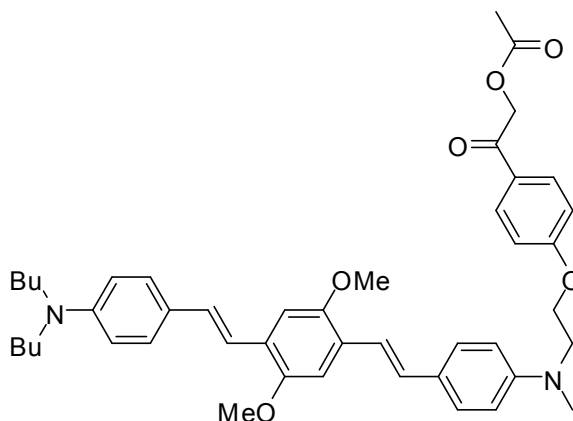


2-(4-Hydroxyphenyl)-2-oxoethyl acetate. A solution of sodium acetate (19.05 g, 0.14 mol) and 2-bromo-1-(4-hydroxyphenyl)ethanone (16.65 g, 0.074 mol) in ethanol (150 mL) was stirred at room temperature for 1 hour. The solvent was removed by evaporation. Water was added to the reaction residue, and the mixture was extracted with ethyl acetate three times. The combined organic layers were dried over anhydrous magnesium sulfate. The product (10.57 g) was obtained in 72% yield after column chromatography (hexane: ethyl acetate 4:1, then 2:1). ^1H NMR (400 MHz, chloroform- d) δ 7.80 (d, $J = 8.0$ Hz, 2H), 6.92 (d, $J = 8.0$ Hz, 2H), 5.27 (s, 2H), 2.22 (s, 3H). ^{13}C NMR (100 MHz, chloroform- d) δ 190.8, 170.9, 161.0, 130.4, 127.0, 115.7, 65.8, 20.7. The data were consistent with the literature data.³⁵²



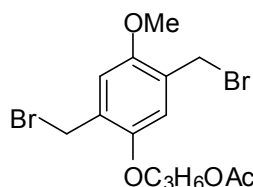
***N*-(2-Bromoethyl)-4-(4-(4-(dibutylamino)styryl)-2,5-dimethoxystyryl)-*N*-**

methylaniline. To the solution of 2,3-dichloro-5,6-dicyano-1,4-benzoquinone (0.641 g, 2.77 mmol) and triphenylphosphite (0.742 g, 2.80 mmol) in dry dichloromethane (15 mL), was added tetrabutyl ammonium bromide (0.936 g, 2.78 mmol) at room temperature. After 10 min, 2-((4-(4-(4-(dibutylamino)styryl)-2,5-dimethoxystyryl)phenyl)(methyl)amino)ethanol (1.021 g, 1.88 mmol) in dry dichloromethane (5 mL) was added to the reaction mixture. After 2 hours, the solvent was removed by evaporation, and the product (0.936 g) was obtained in 82% yield after purification by column chromatography (hexane : ethyl acetate 6:1). ^1H NMR (400 MHz, acetone- d_6) δ 7.42 (d, J = 8.8 Hz, 2H), 7.37 (d, J = 8.8 Hz, 2H), 7.32 – 7.23 (m, 4H), 7.16 (d, J = 16.4 Hz, 1H), 7.13 (d, J = 16.4 Hz, 1H), 6.76 (d, J = 8.8 Hz, 2H), 6.67 (d, J = 8.8 Hz, 2H), 3.90 (s, 6H), 3.80 (t, J = 7.6 Hz, 2H), 3.59 (t, J = 7.2 Hz, 2H), 3.34 (t, J = 7.2 Hz, 4H), 3.06 (s, 3H), 1.56 (quintet, J = 7.6 Hz, 4H), 1.36 (sextet, J = 7.6 Hz, 4H), 0.95 (t, J = 7.6 Hz, 6H). ^{13}C NMR (125 MHz, acetone- d_6) δ 152.1, 151.9, 148.8, 148.7, 129.6, 129.1, 128.5, 127.7, 127.4, 126.9, 126.0, 119.59, 118.5, 112.9, 112.6, 109.3, 109.1, 56.5, 54.7, 51.2, 38.8, 30.2, 20.8, 14.3. HRMS (EI+) m/z : Calcd for $\text{C}_{35}\text{H}_{45}\text{BrN}_2\text{O}_2$ (M^+) 604.2664, Found 604.2698. Anal. Calcd. for $\text{C}_{35}\text{H}_{45}\text{BrN}_2\text{O}_2$: C, 69.41; H, 7.49; N, 4.63. Found C, 69.52; H, 7.71; N, 4.65.

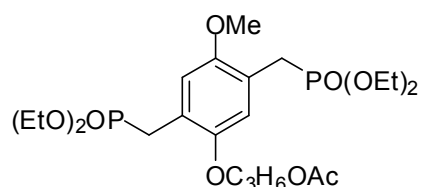


2-(4-(2-((4-(4-(4-(Dibutylamino)styryl)-2,5-dimethoxystyryl)phenyl)(methyl)amino)ethoxy)phenyl)-2-oxoethyl acetate. The solution of *N*-(2-bromoethyl)-4-(4-(4-(dibutylamino)styryl)-2,5-dimethoxystyryl)-*N*-methylaniline (1.120 g, 1.85 mmol), 2-(4-hydroxyphenyl)-2-oxoethyl acetate (0.494 g, 2.54 mmol), potassium carbonate (2.118 g, 15.35 mmol) and 18-crown-6 (0.2 g) in acetone (100 mL) was heated to reflux for 18 hours. After cooling to room temperature, the solid in the reaction mixture was removed by filtration and the solution was removed by evaporation. The product (0.638 g) in 48% yield was obtained after purification by column chromatography (hexane : ethyl acetate 7:1). This compound is light sensitive. ^1H NMR (400 MHz, acetone- d_6) δ 7.92 (d, $J = 8.8$ Hz, 2H), 7.41 (d, $J = 8.8$ Hz, 2H), 7.39 (d, $J = 8.8$ Hz, 2H), 7.32 – 7.25 (m, 4H), 7.16 (d, $J = 16.4$ Hz, 1H), 7.14 (d, $J = 16.4$ Hz, 1H), 7.03 (d, $J = 8.8$ Hz, 2H), 6.77 (d, $J = 8.8$ Hz, 2H), 6.67 (d, $J = 8.8$ Hz, 2H), 5.3 (s, 2H), 4.28 (t, $J = 5.6$ Hz, 2H), 3.90 (s, 6H), 3.82 (t, $J = 5.2$ Hz, 2H), 3.33 (t, $J = 7.2$ Hz, 2H), 3.07 (s, 3H), 2.11 (s, 3H), 1.56 (quintet, $J = 7.6$ Hz, 4H), 1.36 (sextet, $J = 7.6$ Hz, 4H), 0.96 (t, $J = 7.6$ Hz, 6H). ^{13}C NMR (125 MHz, acetone- d_6) δ 191.2, 170.4, 163.9, 152.0, 151.96, 149.4, 148.6, 130.8, 129.5, 129.2, 128.5, 128.4, 128.4, 127.3, 127.2, 126.9, 126.0, 119.3, 118.5, 115.3, 113.0, 112.5, 109.2,

109.0, 66.8, 66.6, 56.5, 56.4, 52.0, 51.2, 39.3, 30.2, 20.8, 20.4, 14.3. HRMS (ESI+) m/z : Calcd for $C_{45}H_{55}N_2O_6$ (MH^+) 719.4006, Found 719.4054.

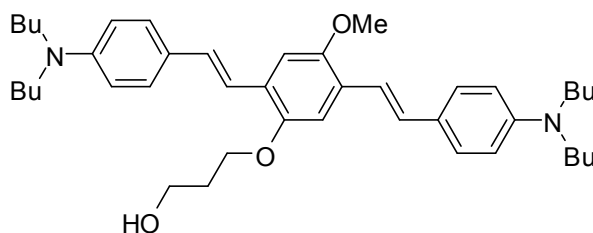


3-(2,5-Bis(bromomethyl)-4-methoxyphenoxy)propyl acetate. To a suspension of 3-(4-methoxyphenoxy)propan-1-ol (5.02 g, 0.027 mol) and paraformaldehyde (14.51 g, 0.48 mol) in acetic acid (60 mL), was added hydrogen bromide (55 mL, 33% wt in acetic acid, 0.31 mol). The reaction solution was heated to 70 °C for 2 h, and then was poured into ice water. The white solid was obtained by filtration, and then washed with water and methanol. The product (7.41 g) was obtained in 66% yield from recrystallization from methanol. 1H NMR (500 MHz, chloroform-*d*) δ 6.85 (s, 1H), 6.84 (s, 1H), 4.50 (s, 2H), 4.49 (s, 2H), 4.30 (t, $J = 6.0$ Hz, 2H), 4.07 (t, $J = 6.0$ Hz, 2H), 3.85 (s, 3H), 2.14 (quintet, $J = 6.0$ Hz, 2H), 2.06 (s, 3H). HRMS (EI+) m/z : Calcd for $C_{14}H_{18}Br_2O_4$ (M^+) 407.9527, Found 407.9547. The compound was used for next reaction without further purification.



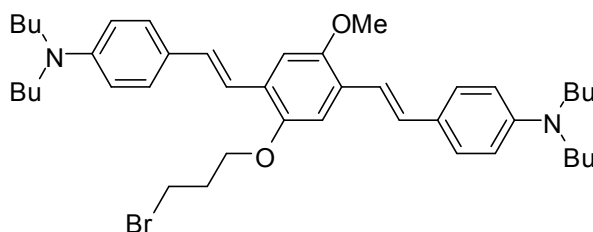
3-(2,5-Bis((diethoxyphosphoryl)methyl)-4-methoxyphenoxy)propyl acetate. A solution of 3-(2,5-bis(bromomethyl)-4-methoxyphenoxy)propyl acetate (3.13 g, 7.63 mmol) and triethyl phosphite (30 mL) was refluxed for 18 h. Triethyl phosphite was

removed by vacuum distillation, and the product (2.59 g) was purified by column chromatography (dichloromethane: methanol 30:1) in 65% yield. ^1H NMR (500 MHz chloroform-*d*) δ 6.89 (s, 1H), 6.87 (s, 1H), 4.23 (t, $J = 6.0$ Hz, 2H), 3.99 – 3.97 (m, 8H), 3.76 (s, 3H), 3.19 (s, 2H), 3.15 (s, 2H), 2.07 (quintet, $J = 7.5$ Hz, 2H), 2.02 (s, 2H), 1.20 (t, $J = 7.5$ Hz, 12H). HRMS (EI+) m/z : Calcd for $\text{C}_{22}\text{H}_{38}\text{P}_2\text{O}_{10}$ (M^+) 524.1940, Found 524.1815. The compound was used for next reaction without further purification.



3-(2,5-Bis(4-(dibutylamino)styryl)-4-methoxyphenoxy)propan-1-ol. To a solution of 3-(2,5-bis((diethoxyphosphoryl)methyl)-4-methoxyphenoxy)propyl acetate (2.59 g, 4.94 mmol) and 4-(dibutylamino)benzaldehyde (2.5 mL, 10 mmol) in dry THF (20 mL), was added potassium *tert*-butoxide (13.0 mL, 13.0 mmol, 1.0 M THF) at 0 °C. After stirring at 0 °C for 2 hours and was allowed to warm to room temperature overnight. The reaction was quenched by adding water, and extracted with dichloromethane three times. The combined organic layers were washed with water, and dried over magnesium sulfate. The column chromatography (hexane : ethyl acetate 7:1 and then 3:1) afforded the product (1.24 g) in 39% yield. ^1H NMR (500 MHz, acetone-*d*₆) δ 7.35 (d, $J = 9.0$ Hz, 4H), 7.25 (s, 1H), 7.24 (d, $J = 16.5$ Hz, 1H), 7.22 (d, $J = 16.5$ Hz, 1H), 7.21 (s, 1H), 7.14 (d, $J = 16.5$ Hz, 1H), 7.11 (d, $J = 16.5$ Hz, 1H), 6.66 (d, $J = 9.0$

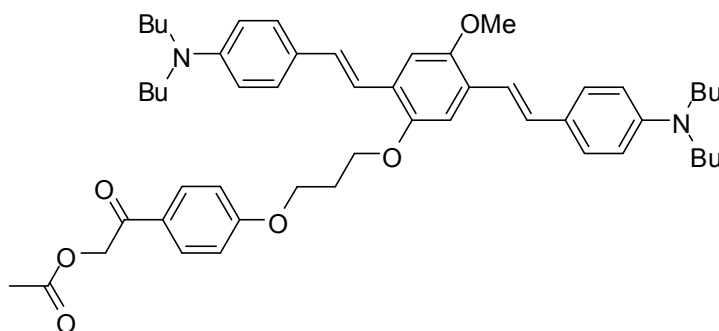
Hz, 4H), 4.17 (t, $J = 6.5$ Hz, 2H), 3.88 (s, 6H), 3.82 (m, 2H), 3.32 (t, $J = 7.5$ Hz, 8H), 2.04 (quintet, $J = 6.0$ Hz, 2H) 1.57 (quintet, $J = 7.5$ Hz, 8H), 1.35 (sextet, $J = 7.5$ Hz, 8H), 0.94 (t, $J = 7.5$ Hz, 12H). ^{13}C NMR (125 MHz, acetone- d_6) δ 152.1, 151.5, 148.7, 129.4, 128.5, 128.4, 127.5, 127.2, 126.2, 126.1, 118.8, 118.6, 112.6, 110, 109.1, 66.9, 59.4, 56.5, 51.3, 51.2, 33.7, 30.3, 20.9, 14.3. HRMS (FAB+) m/z : Calcd for $\text{C}_{42}\text{H}_{61}\text{N}_2\text{O}_3$ (MH^+) 641.4682, Found 641.4690. Anal. Calcd. for $\text{C}_{42}\text{H}_{60}\text{N}_2\text{O}_3$: C, 78.48; H, 9.44; N, 4.37. Found: C, 78.48; H, 9.55; N, 4.39.



4,4'-(1*E*,1'*E*)-2,2'-(2-(3-Bromopropoxy)-5-methoxy-1,4-phenylene)bis

(ethene-2,1-diyl)bis(*N,N*-dibutylaniline). To the solution of 2,3-dichloro-5,6-dicyano-1,4-benzoquinone (1.601 g, 7.05 mmol) and triphenylphosphite (1.854 g, 7.06 mmol) in dry dichloromethane (20 mL), was added tetrabutyl ammonium bromide (2.354 g, 7.08 mmol) at room temperature. After 10 min, 3-(2,5-bis(4-(dibutylamino)styryl)-4-methoxyphenoxy)propan-1-ol (3.011 g, 4.69 mmol) in dry dichloromethane (5 mL) was added to the reaction mixture. After 2 hours, the solvent was removed by evaporation, and the product (2.691 g) was obtained in 82% yield after purification by column chromatography (hexane : ethyl acetate 7:1). ^1H NMR (400 MHz, acetone- d_6) δ 7.39 – 7.35 (m, 4H), 7.29 – 7.22 (m 4H), 7.15 (d, $J = 16.4$ Hz, 1H), 7.12 (d, $J = 16.4$ Hz, 1H),

6.67 (d, $J = 8.8$ Hz, 4H), 4.22 (t, $J = 6.4$ Hz, 2H), 2.49 (s, 3H), 3.78 (t, $J = 6.4$ Hz, 2H), 3.34 (t, $J = 7.6$ Hz, 8H), 2.04 (quintet, $J = 6.0$ Hz, 2H), 1.58 (quintet, $J = 7.6$ Hz, 8H), 1.38 (sextet, $J = 7.6$ Hz, 8H), 0.95 (t, $J = 7.6$ Hz, 12H). ^{13}C NMR (100 MHz, acetone- d_6) δ 152.3, 151.0, 148.6, 129.6, 129.5, 128.5, 128.4, 127.7, 127.3, 126.0, 125.9, 118.4, 112.5, 110.9, 109.0, 67.6, 56.5, 51.2, 33.5, 31.5, 30.2, 20.8, 14.3. HRMS (EI+) m/z : Calcd for $\text{C}_{42}\text{H}_{59}\text{BrN}_2\text{O}_2$ (M^+) 702.3760, Found 702.3723. Anal. Calcd. For $\text{C}_{42}\text{H}_{59}\text{BrN}_2\text{O}_2$: C, 71.67; H, 8.45; N, 3.98. Found C, 71.78; H, 8.47; N, 4.05.



2-(4-(3-(2,5-Bis(4-(dibutylamino)styryl)-4-methoxyphenoxy)propoxy)phenyl)-2-oxoethyl acetate. The solution of 4,4'-(1*E*,1'*E*)-2,2'-(2-(3-bromopropoxy)-5-methoxy-1,4-phenylene)bis(ethene-2,1-diyl)bis(*N,N*-dibutylaniline) (1.051 g, 1.49 mmol), 2-(4-hydroxyphenyl)-2-oxoethyl acetate (0.363 g, 1.87 mmol), potassium carbonate (2.005 g, 14.49 mmol) and 18-crown-6 (0.025 g) in acetone (50 mL) was heated to reflux for 18 hours. After cooling to room temperature, the solid in the reaction mixture was removed by filtration and the solution was removed by evaporation. The product (0.787 g) in 65% yield was obtained after purification by column chromatography (hexane : ethyl acetate 7:1). This compound is light sensitive. ^1H NMR (400 MHz, acetone- d_6) δ 7.92 (d, $J =$

8.8 Hz, 2H), 7.36 – 7.34 (m, 4H), 7.29 – 7.21 (m 4H), 7.16 – 7.08 (m, 4H), 6.67 (dd, $J = 8.8$ Hz, $J = 2.0$ Hz, 4H), 5.33 (s, 2H), 4.40 (t, $J = 6.4$ Hz, 2H), 4.29 (t, $J = 6.4$ Hz, 2H), 3.89 (s, 3H), 3.32 (t, $J = 7.6$ Hz, 8H), 2.36 (t, $J = 6.0$ Hz, 2H), 2.11 (s, 3H), 1.58 (quintet, $J = 7.6$ Hz, 8H), 1.38 (sextet, $J = 7.6$ Hz, 8H), 0.94 (t, $J = 7.6$ Hz, 12H). ^{13}C NMR (100 MHz, acetone- d_6) δ 191.2, 170.4, 164.3, 152.7, 151.2, 148.7, 130.8, 129.6, 129.5, 128.5, 128.4, 128.2, 127.7, 127.3, 126.1, 126.0, 118.5, 118.4, 115.4, 112.6, 110.9, 109.0, 66.6, 66.0, 56.5, 51.2, 30.2, 30.1, 20.9, 20.4, 14.3. HRMS (ESI+) m/z : Calcd for $\text{C}_{52}\text{H}_{69}\text{N}_2\text{O}_6$ (MH^+) 817.5113, Found 817.5159. Anal. Calcd. For $\text{C}_{52}\text{H}_{68}\text{N}_2\text{O}_6$: C, 76.44; H, 8.39; N, 3.43. Found C, 76.29; H, 8.35; N, 3.49.

6. CONCLUSIONS AND FUTURE WORK

The two key advantages of two-photon processes as compared to one-photon processes are that they offer the possibility to excite materials with high three-dimensional spatial resolution and allow light to penetrate more deeply into absorbing materials. These features make two-photon absorbing chromophores attractive to both material and biomedical applications. To achieve the desired properties for any particular application, the right molecular design is the key, which requires an understanding of structure-property relationships, choice of a design strategy, synthesis of the designed molecules, and characterization of their properties using a variety of physical and analytical techniques. This is the path of the thesis. Using photon-induced intramolecular electron transfer, two-photon acid and radical initiators for the applications in three-dimension lithographic microfabrication and two-photon removable protecting groups for potential biomedical applications have been designed, synthesized and characterized under one-photon conditions. Their applications under two-photon conditions are under investigation by our collaborators.

Triphenylamine sulfonium salts **14** and **15** (Figure 2.22) have high quantum yields for acid generation.¹⁶⁹ To further understand the cleavage mechanism of this class of photoacid generators and to guide the development of two-photon acid generators, sulfonium salts **16** – **19** (Figure 2.22) bearing substituents with different electron-withdrawing ability at *para*- and *meta*- positions relative to amine have been designed, synthesized, and characterized. The acid generation quantum yields of PAGs with *meta* sulfonium substituents are almost twice as high as their *para* analogs. Quantum-chemical

calculations of the two representative molecules **14** and **17** performed by our collaborators support the sulfur-methyl bond cleavage, and predict the higher quantum yields of acid generation of *meta*-substituted PAGs, which are the first examples of quantum-chemical calculations for this type of molecules in the literature.

The efficient two-photon acid generator **BSB-S₂** (Figure 3.7) with a bis(styryl)benzene TPA core has been used to fabricate buried parallel microchannels (Figure 3.10).¹⁸⁷ To improve the resolution of this type microfabrication, short-wavelength two-photon acid generators **31** and **32** (Figure 3.12) have been designed and synthesized. Their quantum yields of acid generation are the same as that of **BSB-S₂**. The polymerization of cyclohexene oxide initiated by **31** and **32** under one-photon irradiation showed that they effectively initiated cationic polymerization. The preliminary results show that two-photon induced polymerization of epoxide initiated by **31** and **32** is more efficient than the literature system¹⁸⁹ at 520 nm (Figure 3.17), and further studies under two-photon conditions are ongoing by our collaborators.

In order to improve the efficiency of two-photon radical polymerization, two-photon radical generator **62** (Figure 4.25) was designed and synthesized. However, its threshold energy is not more efficient than TPA chromophore **45** for two-photon induced radical polymerization.²¹⁹ A small reduction of the fluorescence quantum yield (14%) of **62** relative to that of **45** suggests that rate of electron transfer from the excited state of the chromophore moiety to the charge transfer state of the triphenylsulfonium group is relatively small.²¹⁹ A possible solution would be to attach electron-withdrawing groups on the aryl ring of triarylsulfonium group to increase the driving force for electron

transfer and thereby increase the rate. First, trarylsulfonium salts substituted by groups with different electron-withdrawing ability at different positions **48** – **52** (Figure 4.13) were designed and studied. The results shows that compound **51** with an electron-withdrawing group at the *para*- position relative to the sulfonium group is both a good electron acceptor from the point of view of excited-state electron and also an efficient radical generator for initiation of polymerization. Second, the model molecules **58** – **60** (Figure 4.19) were designed to study the piperazine linker effects on radical polymerization. The results show that the compound **59** with electron-withdrawing group has lower isolated yield of radical polymerization than **58** without any substituent. The photoproduct analysis suggests that the radical stabilization by electron-withdrawing group may reduce its reactivity. Another solution was made to increase the energy level of excited state of TPA chromophore, which would facilitate the electron transfer. Two-photon acid generator **69** (Figure 4.28) was designed and studied for this purposes by attaching a short-wavelength TPA chromophore to the sulfonium group. The polymerization threshold energy for **69** is consistently 20% lower than that for **47** under two-photon induced polymerization (Figure 4.31). More work is under way to characterize further the properties of initiators **69** under two-photon excitation conditions. However, the slightly improved fluorescence quenching (29%) of **69** relative to its corresponding TPA chromophore **47** suggests electron transfer across the piperazine bridge is inherently rather inefficient. It is perhaps due to poor electronic coupling caused by the rigid nature of the bridge, which leads to poor orbital overlap between the local LUMO of sulfonium group and the local LUMO of the chromophore moiety. Encouraged

by the molecular design of two-photon removable groups (Chapter 5), for future study, a new molecular design strategy is suggested to attach the TPA chromophores to the sulfonium group by using a flexible chain, for example the compounds **93** and **94** (Figure 6.1).

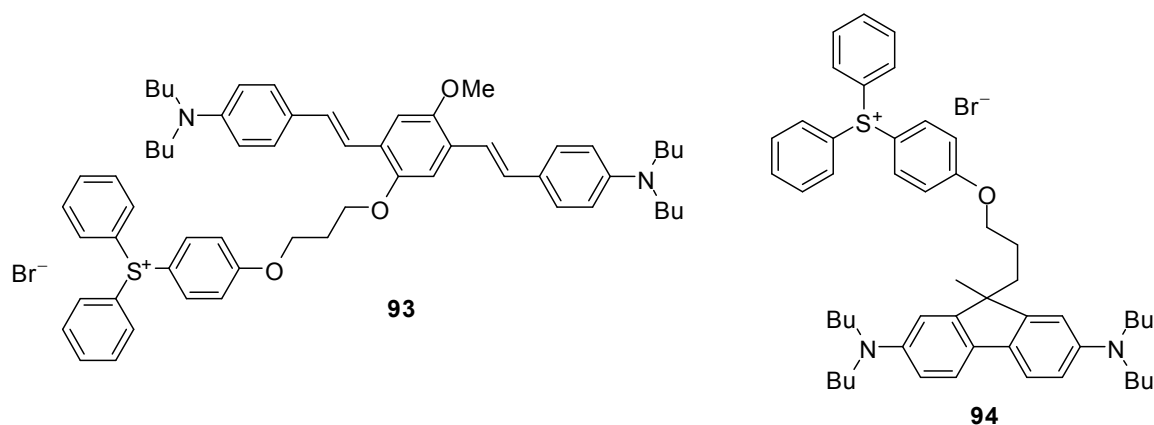


Figure 6.1 Future molecular designs for two-photon radical generators.

In the literature, the most biologically useful two-photon removable protecting groups are coumarin based molecules (Figure 5.18), which have the largest two-photon cross section ($\sim 0.1 \text{ GM}$) among the existing photoremovable groups. In addition, both light-absorbing and cleavage occur at the same coumaryl molecules for two-photon studies. Falvey's design strategy of photoinduced electron transfer under one-photon conditions has used a sensitizer that is responsible for light absorption and a photoremovable protecting group that facilitates bond cleavage.^{342,343} A lot of cleavage examples via intermolecular electron transfer have been demonstrated, but there are very limited investigations for the cleavage via intramolecular electron transfer.³⁴⁴ Building on Falvey's design concept, the design strategy in this thesis was to attach efficient TPA

chromophores with large cross-sections to photocleavable groups using a covalent linker to achieve two-photon induced cleavage via intramolecular electron transfer. First, the two-photon removable protecting molecule **76** (Figure 5.19) was designed using the ester linker in the literature,³⁴⁴ but the photocleavage of **76** did not occur under our conditions. The direct photolysis mechanisms (Figure 5.12, Figure 5.11) show that the electron donating group at the ester position of compound **76** assists the release of the protected groups. The failure of **76** to undergo efficient photocleavage may be related to the ester linker. Second, to experimentally prove the hypothesis, molecules **78** with electron-donating group ($-\text{OCH}_3$), **79** un-substituted ($-\text{H}$), and **80** with electron withdrawing group ($-\text{CO}_2\text{CH}_3$) (Figure 5.19) were designed, and the photolysis via intermolecular electron transfer from the excited state of chromophore **45** to phenacyl esters **78** – **80** show that photolysis of **45/80** did not release the protected acid, but photolysis of **45/78** and **45/79** released the protected acid efficiently. Third, based on the intermolecular photolysis studies, a new molecular design of **85** and **86** (Figure 5.28) was developed by attaching the photocleavage group to either the amine donor or π -bridge of chromophore **45** via an ether linker. The photolysis results show that both **85** and **86** released the protected acid, but the π -bridge-attached **86** is more efficient than the donor-attached **85**. Therefore, the attachment of the photocleavable group to π -bridge of the TPA chromophore using an ether linker efficiently releases acid via intramolecular electron transfer under one-photon conditions. The future directions of this research are to further understand the photolysis of **85** and **86**, to extend the photorelease of amines, alcohols,

and phosphates by using the same molecular design, and to conduct the photorelease under two-photon condition, and eventually to develop the biomedical applications.

Overall, two-photon activatable acid and radical initiators and two-photon removable protecting groups have been successfully designed and synthesized for photopolymerization and three-dimensional microfabrication and for biomedical photo-triggers, based on bond-cleavage reactions activated by photon-induced intramolecular electron transfer. The optical and chemical properties of synthesized molecules have been studied by using a variety of physical and analytical techniques under one-photon conditions, and their two-photon characteristics and applications are being investigated in collaboration with other groups.

REFERENCES

- (1) Goppert-Mayer, M. *Annalen der Physik (Berlin, Germany)* **1931**, 9, 273.
- (2) Kasha, M. *Discussions of the Faraday Society* **1950**, No. 9, 14.
- (3) Collins, R. J.; Nelson, D. F.; Schawlow, A. L.; Bond, W.; Garret, C. G. B.; Kaiser, W. *Phys. Rev. Lett.* **1960**, 5, 303.
- (4) Maiman, T. H. *Brit. Commun. Electron.* **1960**, 7, 674.
- (5) Javan, A.; Bennett, W. R., Jr.; Herriott, D. R. *Phys. Rev. Lett.* **1961**, 6, 106.
- (6) Kaiser, W.; Garrett, C. G. B. *Phys. Rev. Lett.* **1961**, 7, 229.
- (7) Peticolas, W. L.; Goldsborough, J. P.; Rieckhoff, K. E. *Phys. Rev. Lett.* **1963**, 10, 43.
- (8) Peticolas, W. L.; Rieckhoff, K. E. *J. Chem. Phys.* **1963**, 39, 1347.
- (9) Parthenopoulos, D. A.; Rentzepis, P. M. *Science* **1989**, 245, 843.
- (10) Denk, W.; Strickler, J. H.; Webb, W. W. *Science* **1990**, 248, 73.
- (11) Maruo, S.; Nakamura, O.; Kawata, S. *Opt. Lett.* **1997**, 22, 132.
- (12) Cumpston, B. H.; Ananthavel, S. P.; Barlow, S.; Dyer, D. L.; Ehrlich, J. E.; Erskine, L. L.; Heikal, A. A.; Kuebler, S. M.; Lee, I. Y. S.; McCord-Maughon, D.; Qin, J.; Rockel, H.; Rumi, M.; Wu, X.-L.; Marder, S. R.; Perry, J. W. *Nature* **1999**, 398, 51.
- (13) Kawata, S.; Sun, H.-B.; Tianaka, T.; Takada, K. *Nature* **2001**, 412, 697.
- (14) Dvornikov, A. S.; Rentzepis, P. M. *Opt. Commun.* **1995**, 119, 341.
- (15) He, G. S.; Bhawalkar, J. D.; Zhao, C. F.; Prasad, P. N. *Appl. Phys. Lett.* **1995**, 67, 2433.
- (16) Ehrlich, J. E.; Wu, X. L.; Lee, I. Y. S.; Hu, Z. Y.; Rockel, H.; Marder, S. R.; Perry, J. W. *Opt. Lett.* **1997**, 22, 1843.
- (17) Fleitz, P. A.; Brant, M. C.; Sutherland, R. L.; Strohkendl, F. P.; Larsen, R. J.; Dalton, L. R. *Proc. SPIE-Int. Soc. Opt. Eng.* **1998**, 3472, 91.

- (18) He, G. S.; Zhao, C. F.; Bhawalkar, J. D.; Prasad, P. N. *Appl. Phys. Lett.* **1995**, *67*, 3703.
- (19) Zhao, C. F.; He, G. S.; Bhawalkar, J. D.; Park, C. K.; Prasad, P. N. *Chem. Mater.* **1995**, *7*, 1979.
- (20) Bhawalkar, J. D.; He, G. S.; Prasad, P. N. *Rep. Prog. Phys.* **1996**, *59*, 1041.
- (21) Denk, W. *Proc. Natl. Acad. Sci. U. S. A.* **1994**, *91*, 6629.
- (22) Mertz, J.; Xu, C.; Webb, W. W. *Opt. Lett.* **1995**, *20*, 2532.
- (23) Xu, C.; Zipfel, W.; Shear, J. B.; Williams, R. M.; Webb, W. W. *Proc. Natl. Acad. Sci. U. S. A.* **1996**, *93*, 10763.
- (24) Denk, W.; Svoboda, K. *Neuron* **1997**, *18*, 351.
- (25) Kohler, R. H.; Cao, J.; Zipfel, W. R.; Webb, W. W.; Hanson, M. R. *Science* **1997**, *276*, 2039.
- (26) Bhawalkar, J. D.; Kumar, N. D.; Zhao, C. F.; Prasad, P. N. *J. Clin. Laser Med. Surg.* **1997**, *15*, 201.
- (27) Fisher, W. G.; Partridge, W. P., Jr.; Dees, C.; Wachter, E. A. *Photochem. Photobiol.* **1997**, *66*, 141.
- (28) Spangler, C. W.; Starkey, J. R.; Meng, F.; Gong, A.; Drobizhev, M.; Rebane, A.; Moss, B. *Proc. SPIE-Int. Soc. Opt. Eng.* **2005**, *5689*, 141.
- (29) Lin, T.-C.; Chung, S.-J.; Kim, K.-S.; Wang, X.; He, G. S.; Swiatkiewicz, J.; Pudavar, H. E.; Prasad, P. N. *Adv. Polym. Sci.* **2003**, *161*, 157.
- (30) Sun, H.-B.; Kawata, S. *Adv. Polym. Sci.* **2004**, *170*, 169.
- (31) Albota, M.; Beljonne, D.; Bredas, J.-L.; Ehrlich, J. E.; Fu, J.-Y.; Heikal, A. A.; Hess, S. E.; Kogej, T.; Levin, M. D.; Marder, S. R.; McCord-Maughon, D.; Perry, J. W.; Rockel, H.; Rumi, M.; Subramaniam, G.; Webb, W. W.; Wu, X.-L.; Xu, C. *Science* **1998**, *281*, 1653.
- (32) Kim, O.-K.; Lee, K.-S.; Woo, H. Y.; Kim, K.-S.; He, G. S.; Swiatkiewicz, J.; Prasad, P. N. *Chem. Mater.* **2000**, *12*, 284.
- (33) Rumi, M.; Ehrlich, J. E.; Heikal, A. A.; Perry, J. W.; Barlow, S.; Hu, Z.; McCord-Maughon, D.; Parker, T. C.; Roeckel, H.; Thayumanavan, S.; Marder, S. R.; Beljonne, D.; Bredas, J.-L. *J. Am. Chem. Soc.* **2000**, *122*, 9500.

- (34) Ventelon, L.; Charier, S.; Moreaux, L.; Mertz, J.; Blanchard-Desce, M. *Angew. Chem., Int. Ed. Engl.* **2001**, *40*, 2098.
- (35) Mongin, O.; Porres, L.; Moreaux, L.; Mertz, J.; Blanchard-Desce, M. *Org. Lett.* **2002**, *4*, 719.
- (36) Pond, S. J. K.; Rumi, M.; Levin, M. D.; Parker, T. C.; Beljonne, D.; Day, M. W.; Bredas, J.-L.; Marder, S. R.; Perry, J. W. *J. Phys. Chem. A* **2002**, *106*, 11470.
- (37) Reinhardt, B. A.; Brott, L. L.; Clarson, S. J.; Dillard, A. G.; Bhatt, J. C.; Kannan, R.; Yuan, L.; He, G. S.; Prasad, P. N. *Chem. Mater.* **1998**, *10*, 1863.
- (38) Belfield, K. D.; Hagan, D. J.; Van Stryland, E. W.; Schafer, K. J.; Negres, R. A. *Org. Lett.* **1999**, *1*, 1575.
- (39) Belfield, K. D.; Schafer, K. J.; Mourad, W.; Reinhardt, B. A. *J. Org. Chem.* **2000**, *65*, 4475.
- (40) Abbotto, A.; Beverina, L.; Bozio, R.; Facchetti, A.; Ferrante, C.; Pagani, G. A.; Pedron, D.; Signorini, R. *Org. Lett.* **2002**, *4*, 1495.
- (41) Hess, S. E.; Yuan, L.; Chen, N.; Bhawalkar, J. D.; Prasad, P. N. *Opt. Soc. Am. B* **1997**, *14*, 1079.
- (42) Kannan, R.; Hess, S. E.; Yuan, L.; Xu, F.; Prasad, P. N. *Chem. Mater.* **2001**, *13*, 1896.
- (43) Belfield, K. D.; Schafer, K. J.; Liu, Y.; Liu, J.; Ren, X.; Van Stryland, E. W. *J. Phys. Org. Chem.* **2000**, *13*, 837.
- (44) Beljonne, D.; Zojer, E.; Shuai, Z.; Vogel, H.; Wenselleers, W.; Pond, S. J. K.; Perry Joseph, W.; Marder, S. R.; Bredas, J.-L. *Adv. Funct. Mater.* **2002**, *12*, 631.
- (45) Drobizhev, M.; Karotki, A.; Rebane, A.; Spangler, C. W. *Opt. Lett.* **2001**, *26*, 1081.
- (46) Antonov, L.; Kamada, K.; Ohta, K.; Kamounah, F. S. *Phys. Chem. Chem. Phys.* **2003**, *5*, 1193.
- (47) Beverina, L.; J., F.; Lecercq, A.; Zojer, E.; Pacher, P.; Barlow, S.; Van Stryland, E. W.; Hagan, D. J.; Bredas, J.-L.; Marder, S. R. *J. Am. Chem. Soc.* **2005**, *127*, 7282.
- (48) Adronov, A.; Frechet, J. M. J.; He, G. S.; Kim, K.-S.; Chung, S.-J.; Swiatkiewicz, J.; Prasad, P. N. *Chem. Mater.* **2000**, *12*, 2838.

- (49) Chung, S.-J.; Kim, K.-S.; Lin, T.-C.; He, G. S.; Swiatkiewicz, J.; Prasad, P. N. *J. Phys. Chem., B* **1999**, *103*, 10741.
- (50) Wang, Y.; He, G. S.; Prasad, P. N.; Goodson, T. *J. Am. Chem. Soc* **2005**, *127*.
- (51) Lee, W.-H.; Lee, H.; Kim, J.-A.; Choi, J.-H.; Cho, M.; Jeon, S.-J.; Cho, B. R. *J. Am. Chem. Soc.* **2001**, *123*, 10658.
- (52) Cho, B. R.; Son, K. H.; Lee, S. H.; Song, Y. S.; Lee, Y. K.; Jeon, S. J.; Choi, J. H.; Lee, H.; Cho, M. *J. Am. Chem. Soc.* **2001**, *123*, 10039.
- (53) Drobizhev, M.; Karotki, A.; Dzenis, A.; Rebane, Z.; Spangler, C. W. *Phys. Chem. B* **2003**, *107*, 7540.
- (54) Cho, B. R.; Piao, M. J.; Son, K. H.; Lee, S. H.; Yoon, S. J.; Jeon, S.-J.; Cho, M. *Chem. Eur. J.* **2002**, *8*, 3907.
- (55) Yoo, J.; Yang, S. K.; Jeong, M.-Y.; Ahn, S.-J.; Cho, B. R. *Org. Lett.* **2003**, *5*, 645.
- (56) Zhang, B. J.; Jeon, S.-J. *Chem. Phys. Lett.* **2003**, *377*, 210.
- (57) Bartholomew, G. P.; Rumi, M.; Pond, S. J. K.; Perry Joseph, W.; Tretiak, S.; Bazan, G. C. *J. Am. Chem. Soc.* **2004**, *126*, 11529.
- (58) Macak, P.; Luo, Y.; Norman, P.; Agren, H. *J. Chem. Phys.* **2000**, *113*, 7055.
- (59) Screen, T. E. O.; Thorne, J. R. G.; Denning, R. G.; Bucknall, D. G.; Anderson, H. L. *J. Am. Chem. Soc* **2002**, *124*, 9712.
- (60) Thorne, J. R. G.; Kuebler S., M.; Denning, R. G.; Blake, I. M.; Taylor, P. N.; Anderson, H. L. *Chem. Phys.* **1999**, *248*, 181.
- (61) Kuebler S., M.; Denning, R. G.; Anderson, J. C. *J. Am. Chem. Soc* **2000**, *122*, 339.
- (62) Screen, T. E. O.; Lawton, K. B.; Wilson, G. S.; Dolney, N.; Ispasoiu, R.; Goodson, T.; Martin, S. J.; Bradley, D. D. C.; Anderson, H. L. *J. Mater. Chem.* **2001**, *11*, 312.
- (63) Drobizhev, M.; Stephanenko, Y.; Dzenis, Y.; Karotki, A.; Rebane, A.; Taylor, P. N.; Anderson, H. L. *J. Am. Chem. Soc.* **2004**, *126*, 15352.

- (64) Drobizhev, M.; Stephanenko, Y.; Dzenis, Y.; Karotki, A.; Rebane, A.; Taylor, P. N.; Anderson, H. L. *J. Phys. Chem. B* **2005**, *109*, 7223.
- (65) Inokuma, Y.; Ono, N.; Uno, H.; Kim, D. Y.; Noh, S. B.; Kim, D.; Osuka, A. *Chem. Commun.* **2005**, 3782.
- (66) Xu, C.; Webb, W. W. *J. Opt. Soc. Am.* **1996**, *B13*, 955.
- (67) Sheik-Bahae, M.; Said, A. A.; Hagan, D. J.; Van Stryland, E. W. *IEEE J. Quantum Electron.* **1990**, *26*, 760.
- (68) Sheik-Bahae, M.; Said, A. A.; Van Stryland, E. W. *Opt. Lett.* **1989**, *14*, 955.
- (69) Negres, R. A.; Hales, J. M.; Kobayakov, A.; Hagan, D. J.; Van Stryland, E. W. *Opt. Lett.* **2002**, *27*, 270.
- (70) Barlow, S.; Marder, S. R. *Nonlinear Optical Properties of Organic Materials* Wiley-VCH: Weinheim, 2007.
- (71) Chung, S.-J.; Rumi, M.; Barlow, S.; Perry Joseph, W.; Marder Seth, R. *J. Am. Chem. Soc.* **2005**, *127*, 10844.
- (72) Stacheleck, T. M.; Pazoha, T. A.; M., M. W. *J. Chem. Phys.* **1977**, *66*, 4540.
- (73) Anderson, R. J. M.; Holtom, G. R.; McClain, W. M. *J. Chem. Phys.* **1979**, *70*, 4310.
- (74) Chung, S.-J.; Zheng, S.; Odani, T.; Beverina, L.; Fu, J.; Padilha, L. A.; Biesso, A.; Hales, J. M.; Zhan, X.; Schmidt, K.; Ye, A.; Zojer, E.; Barlow, S.; Hagan, D. J.; Van Stryland, E. W.; Yi, Y.; Shuai, Z.; Pagani, G. A.; Bredas, J.-L.; Perry, J. W.; Marder, S. R. *J. Am. Chem. Soc.* **2006**, *128*, 14444.
- (75) Oliverira, S. L.; Correa, D. S.; Misoguti, C. J. L.; Constantino, R. F.; Aroca, S. C.; Zilio, S. C.; Mendonca, C. R. *Adv. Mater.* **2005**, *17*, 1890
- (76) Marcus, R. A. *J. Chem. Phys.* **1956**, *24*, 966
- (77) Marcus, R. A. *Can. J. Chem.* **1959**, *37*, 155.
- (78) Marcus, R. A. *Rev. Mod. Phys.* **1993**, *65*, 599
- (79) Beitz, J. V.; Miller, J. R. *J. Chem. Phys.* **1979**, *71*, 4579.
- (80) Miller, J. R.; Beitz, J. V. *J. Am. Chem. Soc.* **1984**, *106*, 5057.

- (81) Closs, G. L.; Calcaterra, L. T.; Green, N. J.; Penfield, K. W.; Miller, J. R. *J. Phys. Chem.* **1986**, *90*, 3673
- (82) Rehm, D.; Weller, A. *Isr. J. Chem.* **1970**, *8*, 259.
- (83) Fischer, E. US 3,236,784, 1966.
- (84) Schlesinger, S. I. *Polym. Eng. Sci.* **1974**, *14*, 513.
- (85) Green, G. E.; Stark, B. P.; Zahir, S. A. *J. Macromol. Sci., Rev. Macromol. Chem. Phys.* **1981**, *C21*, 187.
- (86) Smets, G.; Aerts, A.; Van Erum, J. *Polym. J.* **1980**, *12*, 539.
- (87) Schlesinger, S. I. *Photograph. Sci. Eng.* **1974**, *18*, 387.
- (88) Pobiner, H. *Anal. Chim. Acta* **1978**, *96*, 153.
- (89) Watt, W. R. *ACS Symp. Ser.* **1979**, *114*, 17.
- (90) Ito, H.; Willson, C. G. *ACS Symp. Ser.* **1984**, *242*, 11.
- (91) Ito, H.; Willson, C. G. *Org. Coat. Appl. Polym. Sci. Proc.* **1983**, *48*, 60.
- (92) Crivello, J. V. *Adv. Polym. Sci.* **1984**, *62*, 1.
- (93) Scaiano, J. C.; Nguyen, K. T.; Leigh, W. J. *J. Photochem.* **1984**, *24*, 79.
- (94) Crivello, J. V.; Lam, J. H. W.; Volante, C. N. *J. Radiat. Curing* **1977**, *4*, 2.
- (95) Crivello, J. V.; Lam, J. H. W. *J. Polym. Sci., Polym. Symp.* **1976**, *56*, 383.
- (96) Crivello, J. V.; Lam, J. H. W. *Macromolecules* **1977**, *10*, 1307.
- (97) Crivello, J. V.; Conlon, D. A. *Makromol. Chem., Macromol. Symp.* **1988**, *13-14*, 145.
- (98) Pappas, S. P.; Pappas, B. C.; Gatechair, L. R.; Jilek, J. H. *Polym. Photochem.* **1984**, *5*, 1.
- (99) Pappas, S. P.; Gatechair, L. R.; Jilek, J. H. *J. Polym. Sci., Part A: Polym. Chem.* **1984**, *22*, 77.
- (100) Devoe, R. J.; Sahyun, M. R. V.; Serpone, N.; Sharma, D. K. *Can. J. Chem.* **1987**, *65*, 2342.

- (101) Castellanos, F.; Fouassier, J. P.; Priou, C.; Cavezzan, J. *J. Appl. Polym. Sci.* **1996**, *60*, 705.
- (102) Fouassier, J. P.; Burr, D.; Crivello, J. V. *J. Macromol. Sci., Chem.* **1994**, *A31*, 677.
- (103) Gu, H.; Zhang, W.; Feng, K.; Neckers, D. C. *J. Org. Chem.* **2000**, *65*, 3484.
- (104) Hartwig, A.; Harder, A.; Luhning, A.; Schroder, H. *Eur. Polym. J.* **2001**, *37*, 1449.
- (105) Schnurpfeil, G.; Harder, A.; Schroder, H.; Wohrle, D.; Hartwig, A.; Hannemann, O.-D. *Macromol. Chem. Phys.* **2001**, *202*, 180.
- (106) Crivello, J. V. *J. Polym. Sci., Part A: Polym. Chem.* **1999**, *37*, 4241.
- (107) Eckberg, R. P.; LaRochelle, R. W. US 4,780,511, 1983.
- (108) Crivello, J. V. US 5,079,378, 1992.
- (109) Crivello, J. V.; Lee, J. L. *J. Polym. Sci., Part A: Polym. Chem.* **1989**, *27*, 3951.
- (110) Akhtar, S. R.; Crivello, J. V.; Lee, J. L.; Schmitt, M. L. *Chem. Mater.* **1990**, *2*, 732.
- (111) Priou, C.; Soldat, A.; Cavezzan, J.; Castellanos, F.; Fouassier, J. P. *J. Coat. Technol.* **1995**, *67*, 71.
- (112) Yamada, Y.; Okawara, M. *Makromol. Chem.* **1972**, *152*, 163.
- (113) Crivello, J. V.; Lee, J. L. US 4,780,511, 1988.
- (114) Ciardelli, F.; Ruggeri, G.; Aglietto, M.; Angiolini, D.; Carlini, C.; Bianchini, G.; Siccardi, G.; Bigogno, G.; Cioni, L. *J. Coat. Technol.* **1989**, *61*, 77.
- (115) Crivello, J. V.; Lam, J. H. W. *J. Polym. Sci., Part A: Polym. Chem.* **1979**, *17*, 3845.
- (116) Pappas, S. P.; Pappas, B. C.; Gatechair, L. R.; Schnabel, W. *J. Polym. Sci., Part A: Polym. Chem.* **1984**, *22*, 69.
- (117) Dektar, J. L.; Hacker, N. P. *J. Org. Chem.* **1990**, *55*, 639.
- (118) Hacker, N. P.; Dektar, J. L. *ACS Symp. Ser.* **1990**, *417*, 82.

- (119) Dektar, J. L.; Hacker, N. P. *J. Org. Chem.* **1991**, *56*, 1838.
- (120) Crivello, J. V.; Lam, J. H. W. *J. Polym. Sci., Part A: Polym. Chem* **1978**, *16*, 563.
- (121) Hacker, N. P.; Dektar, J. L. *Polym. Mater. Sci. Eng.* **1989**, *60*, 22.
- (122) Crivello, J. V.; Lam, J. H. W. *J. Org. Chem.* **1978**, *43*, 3055.
- (123) Crivello, J. V.; Lam, J. H. W. *J. Polym. Sci., Part A: Polym. Chem* **1979**, *17*, 977.
- (124) Crivello, J. V.; Lam, J. H. W. *J. Polym. Sci., Part A: Polym. Chem.* **1980**, *18*, 2697.
- (125) Crivello, J. V.; Lam, J. H. W. *J. Polym. Sci., Part A: Polym. Chem.* **1980**, *18*, 2677.
- (126) Davidson, R. S.; Goodin, J. W. *Eur. Polym. J.* **1982**, *18*, 589.
- (127) Egger, N.; Schmidt-Rohr, K.; Bluemich, B.; Domke, W. D.; Stapp, B. *J. Appl. Polym. Sci.* **1992**, *44*, 289.
- (128) Knapczyk, J. W.; McEwen, W. E. *J. Am. Chem. Soc.* **1969**, *91*, 145.
- (129) Watt, W. R.; Hoffman, H. T., Jr.; Pobiner, H.; Schkolnick, L. J.; Yang, L. *S. J. Polym. Sci., Part A: Polym. Chem.* **1984**, *22*, 1789.
- (130) Smith, G. H.; Olofson, P. M. DE 2,904,626, 1979.
- (131) Crivello, J. V. *Org. Coat.* **1983**, *5*, 35.
- (132) Dektar, J. L.; Hacker, N. P. *J. Org. Chem.* **1988**, *53*, 1833.
- (133) Welsh, K. M.; Dektar, J. L.; Hacker, N. P.; Turro, N. J. *Polym. Mater. Sci. Eng.* **1989**, *61*, 181.
- (134) Bargon, J.; Fischer, H.; Johnsen, U. *Z. Naturforsch. A: Phys. Sci.* **1967**, *22*, 1551.
- (135) Kaptein, R. *J. Am. Chem. Soc.* **1972**, *94*, 6251.
- (136) Dektar, J. L.; Hacker, N. P. *J. Chem. Soc., Chem. Commun.* **1987**, 1591.
- (137) Hacker, N. P.; Dektar, J. L. *Polym. Mater. Sci. Eng.* **1989**, *61*, 76.

- (138) Crivello, J. V.; Lam, J. H. W. *J. Polym. Sci., Part A: Polym. Chem* **1979**, *17*, 1047.
- (139) Crivello, J. V.; Lee, J. L. *Macromolecules* **1983**, *16*, 864.
- (140) Crivello, J. V.; Kong, S. *Macromolecules* **2000**, *33*, 833.
- (141) Crivello, J. V.; Kong, S. *Macromolecules* **2000**, *33*, 825.
- (142) Crivello, J. V.; Kong, S. *J. Polym. Sci., Part A: Polym. Chem.* **2000**, *38*, 1433.
- (143) Kong, S.; Crivello, J. V. *Polym. Prepr. (Am. Chem. Soc., Div. Polym. Chem.)* **1999**, *40*, 569.
- (144) Williams, H.; Laird, T. *J. Chem. Soc., Sec. C: Org.* **1971**, 1863.
- (145) Toba, Y.; Saito, M. *J. Polym. Sci., Part A: Polym. Chem.* **1998**, *5*, 111.
- (146) Everett, J. P.; Schmidt, D. L.; Rose, G. D.; Argritis, P.; Aidinis, C. J.; Hatzakis, M. *Polymer* **1997**, *38*, 1719.
- (147) Crivello, J. V.; Lam, J. H. W. *J. Polym. Sci., Part A: Polym. Chem.* **1980**, *18*, 1021.
- (148) Toba, Y.; Saito, M.; Usui, Y. *Macromolecules* **1999**, *32*, 3209.
- (149) McKinney, P. S.; Rosenthal, S. *J. Electroanal. Chem. Interfacial Electrochem.* **1968**, *16*, 261.
- (150) Abu-Abdoun, I. I.; Ali, A. *Eur. Polym. J.* **1992**, *28*, 73.
- (151) Abu-Abdoun, I. I.; Aale, A. *Eur. Polym. J.* **1993**, *29*, 1445.
- (152) Abu-Abdoun, I. I.; Aale, A. *Macromol. Rep.* **1993**, *A30*, 327.
- (153) Abu-Abdoun, I. I.; Aale, A. *Eur. Polym. J.* **1993**, *29*, 1439.
- (154) Yagci, Y.; Kornowski, A.; Schnabel, W. *J. Polym. Sci., Part A: Polym. Chem.* **1992**, *30*, 1987.
- (155) Yagci, Y.; Schnabel, W. *Macromol. Rep.* **1993**, *A30*, 175.
- (156) Boettcher, A.; Schnabel, W.; Yagci, Y. EP 441,232, 1991.
- (157) Yagci, Y.; Schnabel, W. *Macromol. Symp.* **1994**, *85*, 115.

- (158) Zweifel, H.; Meier, K. *Polym. Prepr. (Am. Chem. Soc., Div. Polym. Chem.)* **1985**, 26, 347.
- (159) Roloff, A.; Meier, K.; Riediker, M. *Pure Appl. Chem.* **1986**, 58, 1267.
- (160) Meier, K.; Zweifel, H. *J. Radiat. Curing* **1986**, 13, 26.
- (161) Lohse, F.; Zweifel, H. *Adv. Polym. Sci.* **1986**, 78, 61.
- (162) Meier, K.; Buehler, N.; Zweifel, H.; Berner, G.; Lohse, F. EP 094,915, 1983.
- (163) Chrisope, D. R.; Park, K. M.; Schuster, G. B. *J. Am. Chem. Soc.* **1989**, 111, 6195.
- (164) Gill, T. P.; Mann, K. R. *Inorg. Chem.* **1980**, 19, 3007.
- (165) Saeva, F. D. *Advances in Electron Transfer Chemistry* **1994**, 4, 1.
- (166) Saeva, F. D.; Morgan, B. P. *J. Am. Chem. Soc.* **1984**, 106, 4121.
- (167) Saeva, F. D.; Morgan, B. P.; Luss, H. R. *J. Org. Chem.* **1985**, 50, 4360.
- (168) March, J. *Advanced Organic Chemistry*; 3rd ed.; John Wiley & Sons: New York, 1985.
- (169) Zhou, W. K., S. M.; Carrig, D.; Perry, J. W.; Marder, S. R. *J. Am. Chem. Soc.* **2002**, 124, 1897.
- (170) Pohlers, G.; Scaiano, J. C.; Sinta, R. *Chem. Mater.* **1997**, 9, 3222.
- (171) Ortica, F.; Scaiano, J. C.; Pohlers, G.; Cameron, J. F.; Zampini, A. *Chem. Mater.* **2000**, 12, 414.
- (172) Hatchard, C. G.; Parker, C. A. *Proc. Roy. Soc. Ser. A* **1956**, 518.
- (173) Dann, O.; Fernbach, R.; Pfeifer, W.; Demant, E.; Bergen, G.; Lang, S.; Luerding, G. *Justus Liebigs Annalen der Chemie* **1972**, 760, 37.
- (174) Pudzich, R.; Salbeck, J. *Synth. Met.* **2003**, 138, 21.
- (175) Suh, S. C.; Suh, M. C.; Shim, S. C. *Macromol. Chem. Phys.* **1999**, 200, 1991.
- (176) Hanna, S. Y. *Spectrochim. Acta, Part A* **1992**, 48A, 1397.

- (177) Grimley, E.; Collum, D. H.; Alley, E. G.; Layton, B. *Org. Magn. Reson.* **1981**, *15*, 296.
- (178) Madou, M. J. *Fundamentals of Microfabrication: The Science of Miniaturization*; 2nd ed.; CRC: New York, 2002.
- (179) Lyshevski, S. E. *MEMS and NEMS: Systems, Devices and Structures*; CRC: New York, 2002.
- (180) Kuebler, S. M.; Rumi, M.; Watanabe, T.; Braun, K.; Cumpston, B. H.; Heikal, A. A.; Erskine, L. L.; Thayumanavan, S.; Barlow, S.; Marder, S. R.; Perry, J. W. *J. Photochem. Photobiol.* **2001**, *14*, 657.
- (181) Pao, Y.-h.; Rentzepis, P. M. *Appl Phys Lett* **1965**, *6*, 93.
- (182) Chin, S. L.; Bedard, G. *Phys. Lett. A* **1971**, *36*, 271.
- (183) Papouskova, Z.; Pola, J.; Bastl, Z.; Tlaskal, J. *J. Macromol. Sci., Chem.* **1990**, *A27*, 1015.
- (184) Morita, H.; Sadakiyo, T. *J. Photochem. Photobiol. A* **1995**, *87*, 163.
- (185) Maruo, S.; Kawata, S. *J. Microelectromech. Syst.* **1998**, *7*, 411.
- (186) Belfield, K. D.; Ren, X.; Van Stryland, E. W.; Hagan, D. J.; Dubikovsky, V.; Miesak, E. J. *J. Am. Chem. Soc.* **2000**, *122*, 1217.
- (187) Zhou, W.; Kuebler Stephen, M.; Braun Kevin, L.; Yu, T.; Cammack, J. K.; Ober Christopher, K.; Perry Joseph, W.; Marder Seth, R. *Science* **2002**, *296*, 1106.
- (188) Schafer, K. J.; Hales, J. M.; Balu, M.; Belfield, K. D.; Van Stryland, E. W.; Hagan, D. J. *J. Photochem. Photobiol., A* **2004**, *162*, 497.
- (189) Boiko, Y.; Costa, J. M.; Wang, M. M.; Esener, S. C. *Opt. Express* **2001**, *8*, 571.
- (190) Saeva, F. D.; Breslin, D. T.; Martic, P. A. *J. Am. Chem. Soc.* **1989**, *111*, 1328.
- (191) Kuebler, S. M.; Braun, K. L.; Zhou, W.; Cammack, J. K.; Yu, T.; Ober, C. K.; Marder, S. R.; Perry, J. W. *J. Photochem. Photobiol., A* **2003**, *158*, 163.
- (192) Ehrlich, J. E.; Ananthavel, S. P.; Barlow, S.; Mansour, K.; Mohanalingam, K.; Marder, S. R.; Perry, J. W.; Rumi, M.; Thayumanavan, S. *Mol. Cryst. Liq. Cryst. Sci. Technol. Sect. B: Nonlinear Optics* **2001**, *27*, 121.

- (193) Belfield, K. D.; Morales, A. R.; Hales, J. M.; Hagan, D. J.; Van Stryland, E. W.; Chapela, V. M.; Percino, J. *Chem. Mater.* **2004**, *16*, 2267.
- (194) Low, P. J.; Paterson, M. A. J. P.; Horst; Geota, A. E.; Howard, A. K.; Lambert, C.; Cherryman, J. C.; Tackley, D. R.; Leeming, S.; Brown, B. *Chem. Eur. J.* **2004**, *10*, 83.
- (195) Driver, M. S.; Hartwig, J. F. *J. Am. Chem. Soc.* **1996**, *118*, 7217.
- (196) Wolfe, J. P.; Rennels, R. A.; Buchwald, S. L. *Tetrahedron* **1996**, *52*, 7525.
- (197) Wolfe, J. P.; Wagaw, S.; Buchwald, S. L. *J. Am. Chem. Soc.* **1996**, *118*, 7215.
- (198) Hreha, R. D.; George, C. P.; Haldi, A.; Domercq, B.; Malagoli, M.; Barlow, S.; Bredas, J.-l.; Kippelen, B.; Marder, S. R. *Adv. Funct. Mater.* **2003**, *13*, 967.
- (199) Hallas, G.; Hepworth, J. D.; Waring, D. R. *J. Chem. Soc., Sec. B: Phys. Org.* **1970**, 975.
- (200) Hassoon, S.; Neckers, D. C. *J. Phys. Chem.* **1995**, *99*, 9416.
- (201) Li, C.; Luo, L.; Wang, S.; Huang, W.; Gong, Q.; Yang, Y.; Feng, S. *Chem. Phys. Lett.* **2001**, *340*, 444.
- (202) Odian, G. *Principles of Polymerization*; 2nd ed.; Wiley: New York, 1981.
- (203) Haske, W.; Chen, W. V.; Hales, M. J.; W., D.; Barlow, S.; Marder, R. S.; Perry, W. J. *Optics Express* **2007**, *15*, 3426
- (204) Rumi, M. *School of Chemistry and Biochemistry, Georgia Institute of Technology, Atlanta, Georgia 30332* **2006**, unpublished results
- (205) Crivello, J. V.; Lam, J. H. W. *J. Polym. Sci., Poly. Sci. Ed.* **1979**, 759.
- (206) Kunieda, A.; Kondo, S.; Tsuda, K. *Polym. Lett. Ed.* **1974**, *12*, 395
- (207) Crivello, J. V. *Polym. Eng. Sci.* **1983**, *23*, 953
- (208) Kondo, S.; Muramatsu, M.; Tsuda, K. *J. Macromol. Sci-Chem.* **1983**, 999.
- (209) Timpe, H.-J.; Bah, A. *Makromol. Chem., Rapid Commun.* **1987**, *8*, 353.
- (210) Kalgutkar, S. R. US 2005/0070621 A1, 2005.
- (211) Wright, B. B.; Devoe, R. J. US 287909, 1989.

- (212) Crivello, J. V.; Lam, J. H. W.; Moore, J. E.; Schroeter, S. H. *J. Radiat. Curing* **1978**, *5*, 2.
- (213) Adams, M. J.; Benezra, L. L.; Goold, D. R. US 3,028,361, 1962.
- (214) The compound was synthesized by Dr. T. Okada and was characterized by J. Wang.
- (215) Itagaki, Y.; Lund, A.; Shiotani, M.; Hasegawa, A. *Trends in Chemical Physics* **1999**, *7*, 277.
- (216) The compound was synthesized and characterized by Dr. T. Okada.
- (217) Szoszkiewicz, R.; Okada, T.; Jones, S. C.; Li, T.-D.; King, W. P.; Marder, S. R.; Riedo, E. *Nano Letters* **2007**, *7*, 1064.
- (218) The compound was synthesized by Dr. W. Zhou and was characterized by J. Wang.
- (219) Braun, K. L., University of Arizona, 2005.
- (220) The compound was synthesized and characterized by Dr. S. Barlow.
- (221) Saeva, F. D.; Breslin, D. T. *J. Org. Chem.* **1989**, *54*, 712.
- (222) Saeva, F. D. WO 9,407,183, 1994.
- (223) Bates, C. G.; Gujadhur, R. K.; Venkataramau, D. *Org. Lett.* **2002**, *4*, 2803
- (224) Irgartinger, H.; Herich, R. *Eur. J. Org. Chem.* **1998**, *4*, 595
- (225) Meochowski, L. S.; Kloc, K. *Tetrahedron* **1983**, *39*, 781
- (226) Iwase, Y.; Kamada, K.; Kondo, K. *J. Mater. Chem.* **2003**, *13*, 1575
- (227) Delmond, S.; Letard, J.-F.; Lapouyade, R.; Rettig, W. *J. Photochem. Photobiol. A* **1997**, *105*, 135
- (228) Kocienski, P. J. *Protecting Groups*; 3rd ed.; Georg Thieme Verlag (The Americas): Stuttgart, 2003.
- (229) Greene, T. W.; Wuts, P. G. M. *Protective Groups in Organic Synthesis*; 3rd ed.; John Wiley: New York, 1999.
- (230) Pirrung, M. C.; Chen, J. *J. Am. Chem. Soc.* **1995**, *117*, 1240.

- (231) Pirrung, M. C.; Bradley, J.-C. *J. Org. Chem.* **1995**, *60*, 6270.
- (232) Schlichting, I.; Almo, S. C.; Rapp, G.; Wilson, K.; Petratos, K.; Lentfer, A.; Wittinghofer, A.; Kabsch, W.; Pai, E. F.; et al. *Nature* **1990**, *345*, 309.
- (233) Barltrop, J. A.; Schofield, P. *Tetrahedron Lett.* **1962**, 697.
- (234) Sammes, P. G. *Q. Rev., Chem. Soc.* **1970**, *24*, 37.
- (235) Barltrop, J. A.; Plant, P. J.; Schofield, P. *Chem. Commun.* **1966**, 822.
- (236) Havinga, E.; De Jongh, R. O.; Kronenberg, M. E. *Helv. Chim. Acta* **1967**, *50*, 2550.
- (237) Havinga, E.; Kronenberg, M. E. *Pure Appl. Chem.* **1968**, *16*, 137.
- (238) Amit, B.; Zehavi, U.; Patchornik, A. *Isr. J. Chem.* **1974**, *12*, 103.
- (239) Kaplan, J. H.; Forbush, B., 3rd; Hoffman, J. F. *Biochemistry* **1978**, *17*, 1929.
- (240) Engels, J.; Schlaeger, E. J. *J. Med. Chem.* **1977**, *20*, 907.
- (241) Pillai, V. N. R. *Synthesis* **1980**, 1.
- (242) Pillai, V. N. R. *Org. Photochem.* **1987**, *9*, 225.
- (243) Zehavi, U. *Adv. Carbohydr. Chem. Biochem.* **1988**, *46*, 179.
- (244) Adams, S. R.; Tsien, R. Y. *Annu. Rev. Physiol.* **1993**, *55*, 755.
- (245) Corrie, J. E. T.; Trentham, D. R. *J. Chem. Soc., Perkin Trans. 1* **1992**, 2409.
- (246) McCray, J. A.; Trentham, D. R. *Annu. Rev. Biophys. Biophys. Chem.* **1989**, *18*, 239.
- (247) Givens, R. S.; Kueper, L. W., III *Chem. Rev.* **1993**, *93*, 55.
- (248) Marriott, G. *Meth. Enzymol.* **1998**, 291.
- (249) Pelliccioli Anna, P.; Wirz, J. *Photochem. Photobiol. Sci.* **2002**, *1*, 441.
- (250) Bochet, C. G. *J. Chem. Soc., Perkin Trans. 1* **2002**, 125.
- (251) Falvey, D. E.; Sundararajan, C. *Photochem. Photobiol. Sci.* **2004**, *3*, 831.

- (252) Givens, R. S.; Lee, J.-I. *J. Photosci.* **2003**, *10*, 37.
- (253) Givens, R. S.; Conrad, P. G., II; Yousef, A. L.; Lee, J.-I. *Handbook of Organic Photochemistry and Photobiology*; 2nd ed.; CRC 2004.
- (254) Geoldner, M.; Givens, R. S. *Dynamic Studies in Biology*; WILEY-VCH: Weinheim, 2005.
- (255) Corrie, J. E. T.; Trentham, D. R. *Bioorg. Photochem.* **1993**, *2*, 243.
- (256) Gee, K. R.; Kueper, L. W., III; Barnes, J.; Dudley, G.; Givens, R. S. *J. Org. Chem.* **1996**, *61*, 1228.
- (257) Adams, S. R.; Kao, J. P. Y.; Grynkiewicz, G.; Minta, A.; Tsien, R. Y. *J. Am. Chem. Soc.* **1988**, *110*, 3212.
- (258) Kaplan, J. H.; Ellis-Davies, G. C. *Proc. Natl. Acad. Sci. U. S. A.* **1988**, *85*, 6571.
- (259) Adams, S. R.; Lev-Ram, V.; Tsien, R. Y. *Chem. Biol.* **1997**, *4*, 867.
- (260) DelPrincipe, F.; Egger, M.; Ellis-Davies, G. C. R.; Niggli, E. *Cell Calcium* **1999**, *25*, 85.
- (261) Eaton, W. A.; Munoz, V.; Thompson, P. A.; Henry, E. R.; Jas, G.; Hofrichter, J. *Book of Abstracts, 216th ACS National Meeting, Boston, August 23-27 1998*, PHYS.
- (262) Hansen, K. C.; Rock, R. S.; Larsen, R. W.; Chan, S. I. *J. Am. Chem. Soc.* **2000**, *122*, 11567.
- (263) Schlichting, I.; Rapp, G.; John, J.; Wittinghofer, A.; Pai, E. F.; Goody, R. S. *Proc. Natl. Acad. Sci. U. S. A.* **1989**, *86*, 7687.
- (264) Brown, E. B.; Shear, J. B.; Adams, S. R.; Tsien, R. Y.; Webb, W. W. *Biophys. J.* **1999**, *76*, 489.
- (265) Brown, E. B.; Webb, W. W. *Methods Enzymol.* **1998**, *291*, 356.
- (266) Kiskin, N. I.; Chillingworth, R.; McCray, J. A.; Piston, D.; Ogden, D. *Eur. Biophys. J.* **2002**, *30*, 588.
- (267) Lipp, P.; Niggli, E. *J. Physiol.* **1998**, *508 (Pt 3)*, 801.
- (268) Hopt, A.; Neher, E. *Biophys. J.* **2001**, *80*, 2029.

- (269) Fodor, S. P. A.; Read, J. L.; Pirrung, M. C.; Stryer, L.; Lu, A. T.; Solas, D. *Science* **1991**, *251*, 767.
- (270) Chee, M.; Yang, R.; Hubbell, E.; Berno, A.; Huang, X. C.; Stern, D.; Winkler, J.; Lockhart, D. J.; Morris, M. S.; Fodor, S. P. A. *Science* **1996**, *274*, 610.
- (271) Pease, A. C.; Solas, D.; Sullivan, E. J.; Cronin, M. T.; Holmes, C. P.; Fodor, S. P. *Proc. Natl. Acad. Sci. U. S. A.* **1994**, *91*, 5022.
- (272) Sheehan, J. C.; Umezawa, K. *J. Org. Chem.* **1973**, *38*, 3771.
- (273) Lester, H. A.; Nerbonne, J. M. *Annu. Rev. Biophys. Bioengi.* **1982**, *11*, 151.
- (274) Patchornik, A.; Amit, B.; Woodward, R. B. *J. Am. Chem. Soc.* **1970**, *92*, 6333.
- (275) De Mayo, P. *Adv. Org. Chem.* **1960**, *2*, 367.
- (276) Morrison, H. A. *The Chemistry of the Nitro and Nitroso Groups* Feuer, Henry, Ed; John Wiley and Sons: New York, 1969; Vol. Part I, Chapter 4, 165.
- (277) Schupp, H.; Wong, W. K.; Schnabel, W. *J. Photochem.* **1987**, *36*, 85.
- (278) Bamford, C. H.; Norrish, R. G. W. *J. Chem. Soc.* **1935**, 1504.
- (279) Walker, J. W.; Reid, G. P.; McCray, J. A.; Trentham, D. R. *J. Am. Chem. Soc.* **1988**, *110*, 7170.
- (280) Walker, J. W.; Reid, G. P.; Trentham, D. R. *Methods Enzymol.* **1989**, *172*, 288.
- (281) Sheehan, J. C.; Wilson, R. M. *J. Am. Chem. Soc.* **1964**, *86*, 5277.
- (282) Givens, R. S.; Athey, P. S.; Kueper, L. W., III; Matuszewski, B.; Xue, J. *J. Am. Chem. Soc.* **1992**, *114*, 8708.
- (283) Givens, R. S.; Athey, P. S.; Matuszewski, B.; Kueper, L. W., III *J. Am. Chem. Soc.* **1993**, *115*, 6001.
- (284) Givens, R. S.; Matuszewski, B. *J. Am. Chem. Soc.* **1984**, *106*, 6860.
- (285) Rajesh, C. S.; Givens, R. S.; Wirz, J. *J. Am. Chem. Soc.* **2000**, *122*, 611.
- (286) Peach, J. M.; Pratt, A. J.; Snaith, J. S. *Tetrahedron* **1995**, *51*, 10013.

- (287) Cameron, J. F.; Wilson, C. G.; Frechet, J. M. J. *J. Am. Chem. Soc.* **1996**, *118*, 12915.
- (288) Sheehan, J. C.; Wilson, R. M.; Oxford, A. W. *J. Am. Chem. Soc.* **1971**, *93*, 7222.
- (289) Pirrung, M. C.; Fallon, L.; Lever, D. C.; Shuey, S. W. *J. Org. Chem.* **1996**, *61*, 2129.
- (290) Pirrung, M. C.; Shuey, S. W. *J. Org. Chem.* **1994**, *59*, 3890.
- (291) Pirrung, M. C.; Huang, C.-Y. *Tetrahedron Lett.* **1995**, *36*, 5883.
- (292) Pirrung, M. C.; Bradley, J.-C. *J. Org. Chem.* **1995**, *60*, 1116.
- (293) Shi, Y.; Corrie, J. E. T.; Wan, P. *J. Org. Chem.* **1997**, *62*, 8278.
- (294) Rock, R. S.; Chan, S. I. *J. Am. Chem. Soc.* **1998**, *120*, 10766.
- (295) Epstein, W. W.; Garrossian, M. *J. Chem. Soc., Chem. Commun.* **1987**, 532.
- (296) Baldwin, J. E.; McConnaughie, A. W.; Moloney, M. G.; Pratt, A. J.; Shim, S. B. *Tetrahedron* **1990**, *46*, 6879.
- (297) Furuta, T.; Torigai, H.; Sugimoto, M.; Iwamura, M. *J. Org. Chem.* **1995**, *60*, 3953.
- (298) Givens, R. S.; Park, C.-H. *Tetrahedron Lett.* **1996**, *37*, 6259.
- (299) Park, C.-H.; Givens, R. S. *J. Am. Chem. Soc.* **1997**, *119*, 2453.
- (300) Givens, R. S.; Jung, A.; Park, C.-H.; Weber, J.; Bartlett, W. *J. Am. Chem. Soc.* **1997**, *119*, 8369.
- (301) Givens, R. S.; Weber, J. F. W.; Conrad, P. G., II; Orosz, G.; Donahue, S. L.; Thayer, S. A. *J. Am. Chem. Soc.* **2000**, *122*, 2687.
- (302) Zhang, K.; Corrie, J. E. T.; Munasinghe, V. R. N.; Wan, P. *J. Am. Chem. Soc.* **1999**, *121*, 5625.
- (303) Conrad, P. G., II; Givens, R. S.; Hellrung, B.; Rajesh, C. S.; Ramseier, M.; Wirz, J. *J. Am. Chem. Soc.* **2000**, *122*, 9346.
- (304) Conrad, P. G., II; Givens, R. S.; Weber, J. F. W.; Kandler, K. *Org. Lett.* **2000**, *2*, 1545.

- (305) Furuta, T.; Torigai, H.; Osawa, T.; Iwamura, M. *Chem. Lett.* **1993**, 1179
- (306) Furuta, T.; Monotake, A.; Sugimoto, M.; Iwamura, M. *Biochem. Biophys. Res. Commun.* **1996**, 228, 193
- (307) Furuta, T.; Iwamura, M. *Methods Enzymol.* **1998**, 129, 50
- (308) Sarker, A. M.; Kaneto, Y.; Nikolaitchik, A. V.; Neckers, D. C. *J. Phys. Chem. A* **1998**, 102, 5375
- (309) Sarker, A. M.; Kaneto, Y.; Neckers, D. C. *J. Photochem. Photobiol. A* **1998**, 117, 67
- (310) Wiesner, B.; Wiesner, J.; Middendorff, R.; Hagen, V.; Kaupp, U. B.; Weyand, I. *J. Cell. Biol.* **1998**, 142, 473
- (311) Wiesner, B.; Hagen, V. *J. Photochem. Photobiol. B* **1999**, 49, 112
- (312) Hagen, V.; Bendig, J.; Frings, S.; Wiesner, B.; Schade, B.; Helm, S.; Lorenz, D.; Kaupp, U. B. *J. Photochem. Photobiol., B* **1999**, 53, 91
- (313) Schade, B.; Hagen, V.; Schmidt, R.; Herbrich, R.; Krause, E.; Eckardt, T.; Bendig, J. *J. Org. Chem.* **1999**, 64, 9109
- (314) Hagan, D. J.; Bendig, J.; Frings, S.; Eckardt, T.; Helm, S.; Reuter, D.; Kaupp, U. B. *Angew. Chem. Int. Ed.* **2001**, 40, 1045
- (315) Eckardt, T.; Hagen, V.; Schade, B.; Schmidt, R.; Schweitzer, C.; Bendig, J. *J. Org. Chem.* **2002**, 67, 703
- (316) Takaoka, K.; Tatsu, Y.; Yumoto, N.; Nakajima, T.; Shimamoto, K. *Bioorg. Med. Chem. Lett.* **2003**, 13, 703
- (317) Schoenleber, R. O.; Giese, B. *Synlett.* **2003**, 501
- (318) Suzuki, A. Z.; Watanabe, T.; Kawamoto, M.; Nishiyama, K.; Yamashita, H.; Ishii, M.; Iwamura, M.; Furuta, T. *Org. Lett.* **2003**, 5, 4846
- (319) Bradley, J.; Reuter, D.; Frings, S. *Science* **2001**, 294, 2176
- (320) Kaupp, U. B.; Solzin, J.; Hildebrand, E.; Brown, J. E.; Helbig, A.; Hagen, V.; Beyermann, M.; Pampaloni, F.; Weyand, I. *Nat. Cell. Biol.* **2003**, 5, 109
- (321) Matsumoto, M.; Solzin, J.; Helbig, A.; Hagen, V.; Ueno, S.; Kawase, O.; Maruyama, Y.; Kaupp, U. B.; Hoshi, M.; Weyand, I. *Dev. Biol.* **2003**, 260, 314

- (322) Furuta, T.; Wang, S. S. H.; Dantzker, J. L.; Dore, T. M.; Bybee, W. J.; Callaway, E. M.; Denk, W.; Tsien, R. Y. *Proc. Natl. Acad. Sci. U. S. A.* **1999**, *96*, 1193.
- (323) Ando, H.; Furuta, T.; Tsien, R. Y.; Okamoto, H. *Nat. Genet.* **2001**, *28*, 317
- (324) Lin, W.; Lawrence, D. S. *J. Org. Chem.* **2002**, *67*, 2723
- (325) Montgomery, H. J.; Perdikakis, B. R.; Fishlock, D.; Lajoie, G. A.; Jervis, E.; Guillemette, J. G. *Bioorg. Med. Chem. Lett.* **2002**, *10*, 1919
- (326) Lu, M.; Fedoryak, O. D.; Moister, B. R.; Dore, T. M. *Org. Lett.* **2003**, *5*, 2119
- (327) Robu, V. G.; Pfeiffer, E. S.; Robia, R. C.; Balijepalli, R. C.; Pi, Y. *J. Biol. Chem.* **2003**, *278*, 48154
- (328) Furuta, T.; Takeuchi, H.; Isozaki, M.; Takahashi, Y.; Kanehara, M.; Sugimoto, M.; Watanabe, T.; Noguchi, K.; Dore, T. M.; Kurahashi, T.; Iwamura, M.; Tsien, R. Y. *Chem. Bio. Chem.* **2004**, *5*, 1119.
- (329) Nishigaki, T.; Wood, C. D.; Tatsu, Y.; Yumoto, N.; Furuta, T. *Dev. Biol.* **2004**, *272*, 376.
- (330) Schoenleber, R. O.; Bendig, J.; Hagen, V.; Giese, B. *Bioorg. Med. Chem.* **2002**, *10*, 97
- (331) Geisler, D.; Kresse, W.; Wiesner, B.; Bendig, J.; Kettenmann, H.; Hagen, V. *ChemBioChem* **2003**, *4*, 162
- (332) Bendig, J.; Helm, S.; Schade, B.; Hagen, V. *J. Inf. Rec.* **1998**, *24*, 165
- (333) Hamada, T.; Nishida, A.; Yonemitsu, O. *Journal of the American Chemical Society* **1986**, *108*, 140.
- (334) Hamada, T.; Nishida, A.; Yonemitsu, O. *Tetrahedron Letters* **1989**, *30*, 4241.
- (335) Mitkin, O. D.; Kurchan, A. N.; Wan, Y.; Schiwal, B. F.; Kutateladze, A. G. *Organic Letters* **2001**, *3*, 1841.
- (336) Vath, P.; Falvey, D. E.; Barnhurst, L. A.; Kutateladze, A. G. *Journal of Organic Chemistry* **2001**, *66*, 2887.
- (337) McHale, W. A.; Kutateladze, A. G. *Journal of Organic Chemistry* **1998**, *63*, 9924.

- (338) Cossy, J.; Rakotoarisoa, H. *Tetrahedron Letters* **2000**, *41*, 2097.
- (339) Pandey, G.; Krishna, A. *Synthetic Communications* **1988**, *18*, 2309.
- (340) Banerjee, A.; Lee, K.; Yu, Q.; Fang, A. G.; Falvey, D. E. *Tetrahedron Letters* **1998**, *39*, 4635.
- (341) Banerjee, A.; Falvey, D. E. *Journal of the American Chemical Society* **1998**, *120*, 2965.
- (342) Banerjee, A.; Falvey, D. E. *Journal of Organic Chemistry* **1997**, *62*, 6245.
- (343) Banerjee, A.; Falvey, D. E. *Book of Abstracts, 214th ACS National Meeting, Las Vegas, NV, September 7-11 1997*, ORGN.
- (344) Lee, K.; Falvey, D. E. *J. Am. Chem. Soc.* **2000**, *122*, 9361.
- (345) Banerjee, A.; Lee, K.; Falvey, D. E. *Tetrahedron* **1999**, *55*, 12699.
- (346) Kiskin, N. I.; Chillingworth, R.; McCray, J. A.; Piston, D.; Ogden, D. *Eur. Biophys. J.* **2002**, *30*, 588.
- (347) Matsuzaki, M.; Ellis-Davies, G. C.; Nemoto, T.; Miyashita, Y.; Iino, M.; Kasai, H. *Nat. Neurosci.* **2001**, *4*, 1086.
- (348) Fedoryak, O. D.; Dore, T. M. *Org. Lett.* **2002**, *4*, 3419.
- (349) Zhu, Y.; Pavlos, C. M.; Toscano, J. P.; Dore, T. M. *J. Am. Chem. Soc.* **2006**, *128*, 4267
- (350) Perdikakis, B. R.; Montgomery, H. J.; Abbott, G. L.; Fishlock, D.; Lajoie, G. A.; Jervis, E.; Guillemette, J. G. *Bioorg. Med. Chem. Lett.* **2005**, *13*, 47
- (351) Goard, M.; Aakalu, G.; Fedoryak, O. D.; Quinonez, C.; St. Julien, J.; Poteet, S. J.; Schuman, E. M.; Dore, T. M. *Chem. Biol.* **2005**, *12*, 685
- (352) Kaila, N.; Janz, K.; DeBernardo, S.; Bedard, P. W.; Camphausen, R. T.; Tam, S.; Tsao, D. H. H.; Keith, J. C., Jr.; Nickerson-Nutter, C.; Shilling, A.; Young-Sciame, R.; Wang, Q. *J. Med. Chem.* **2007**, *50*, 21.
- (353) Paizs, C.; Tosa, M.; Majdik, C.; Bodai, V.; Novak, L.; Irimie, F.-D.; Poppe, L. *J. Chem. Soci, Perkin Trans.1* **2002**, 2400.
- (354) Liebeskind, L. S.; Srogl, J. *J. Am. Chem. Soc.* **2000**, *122*, 11260.

(355) Moffett, R. B.; Tiffany, B. D.; Aspergren, B. D.; Heinzelman, R. V. *J. Am. Chem. Soc.* **1957**, *79*, 1687.